# Exploring Microglial Activation And Neurodegeneration Following Traumatic Brain Injury

**Dr Gregory Scott**

The Computational, Cognitive and Clinical Neuroimaging Laboratory

Imperial College London

This thesis is submitted for the degree of Doctor of Philosophy

## Abstract

Traumatic brain injury (TBI) patients may deteriorate months and years after injury, developing unforeseen consequences such as dementia. However, the mechanisms relating acute injury to later neurodegeneration are unclear. The positron emission tomography (PET) ligand [11C]-Pittsburgh compound B ([11C]PIB) detects Aβ plaques, a hallmark of Alzheimer's disease. I found [11C]PIB binding in long-term survivors of moderate-severe TBI was increased in posterior cingulate cortex (PCC) and cerebellum. PCC binding increased with damage in white matter (WM) tracts connected to the region, measured using diffusion MRI. These findings suggest a link between TBI and development of dementia. Previously, using [11C]PK11195 PET, which binds the translocator protein (TSPO) up-regulated by activated microglia, we observed increased thalamic binding years after TBI. I found [11C]PK11195 binding in the thalamus was correlated with damage in thalamo-cortical WM tracts, supporting a link between axonal damage and microglial activation. In fifteen patients at least six months after injury, I found binding of [11C]PBR28, a second-generation TSPO ligand, was increased in WM. WM damage was higher in areas of increased [11C]PBR28 binding. The antibiotic minocycline is neuroprotective in models of acute TBI, through microglial inhibition. Patients received either minocycline 100mg twice daily or no drug for 12 weeks, followed by repeat PET. [11C]PBR28 binding post-minocycline was reduced (WM VT=-23.3%) compared to no drug. Neurofilament light chain (NFL) is a neuronal protein, elevated in the CSF acutely after TBI. I found plasma NFL was increased in patients, negatively correlated with time since injury, and positively correlated with [11C]PBR28 WM binding. These findings suggest NFL has promise as a marker of progressive damage in chronic TBI. However, minocycline increased NFL levels and reduced corpus callosal WM integrity. Together, these findings suggest minocycline inhibits chronic microglial activation, which is greater in areas of WM damage, but may impede recovery after brain trauma.

## Acknowledgements

I thank Professor David Sharp for his supervision and support, his clinical insight, and for his work in creating a research environment which fosters collaboration and innovation.

I also thank Professor Paul Matthews for his supervision and insight. Our discussions are invariably stimulating and constructive.

I am grateful to everyone at The Computational, Cognitive and Clinical Neuroimaging Laboratory, who have helped me in ways too numerous to list.

I am grateful to all the people who volunteered to take part in the studies presented here, and to the Wellcome Trust, GSK, Medical Research Council and National Institute of Health Research, who funded the research.

Finally, I thank my wife Carina and three children, Oliver, Alexis and Elliott, for their love and support.

## Statement of Publications

The data presented in Chapters 2 and 3 have been published in Neurology and The Journal of Neuroinflammation and Neurology, respectively:

Scott, G., Ramlackhansingh, A., Edison, P., Hellyer, P.J., Cole, J., Veronese, M., Leech, R., Greenwood, R.J., Turkheimer, F., Gentleman, S., Heckemann, R.A., Matthews, P.M., Brooks, D., Sharp, D.J., 2016, Amyloid pathology and axonal injury after brain trauma, Neurology, Vol:86, ISSN:0028-3878, pp:821-828

Scott, G., Hellyer, P.J., Ramlackhansingh, A.F., Brooks, D.J., Matthews, P.M., Sharp, D.J., 2015. Thalamic inflammation after brain trauma is associated with thalamo-cortical white matter damage. Journal of neuroinflammation, 12(1), pp:1-5

The data presented in Chapters 4 and 5 are being submitted to Science Translational Medicine.

Many of the topics covered in Chapters 1, 2 and 3 have been published as a review in Nature Reviews Neurology:

Sharp, D.J., Scott, G., Leech, R., 2014. Network dysfunction after traumatic brain injury. Nature Reviews Neurology 10(3), pp:156-166

In addition, the following work relevant to the thesis, regarding white matter damage and brain function, has been published in The Journal of Neuroscience:

Hellyer., P.J.*, Scott, G.*, Shanahan, M., Sharp, D.J., Leech, R. Cognitive Flexibility through Metastable Neural Dynamics Is Disrupted by Damage to the Structural Connectome. The Journal of Neuroscience, 35(24), pp:9050-9063 (*joint first authorship)

## Declaration of Originality

The data presented in Chapter 2 and 3 were collected jointly by Dr Anil Ramlackhansingh and Professor David Sharp, as part of a previous study in traumatic brain injury.

Part of the data from healthy controls presented in Chapters 4 and 5, were collected jointly by Dr Peter Bloomfield, Dr David Owen and Dr Nicola Kalk, as part of other studies. Data from other healthy controls presented in Chapters 4 and 5 were collected by Dr Peter Jenkins, Dr Claire Feeney and Dr Joel Raffel, as part of other current studies in traumatic brain injury. Data from fifteen healthy controls were collected by Dr James Cole.

The collection of data presented in Chapters 4 and 5 was supported by Amy Jolly, a research assistant.

All other work contained in this thesis is my own and conforms to the rules and guidelines set out for PhD theses by Imperial College London. The work of others is appropriately referenced.

## Copyright Declaration

The copyright of this thesis rests with the author and is made available under a Creative Commons Attribution Non-Commercial No Derivatives licence. Researchers are free to copy, distribute or transmit the thesis on the condition that they attribute it, that they do not use it for commercial purposes and that they do not alter, transform or build upon it. For any reuse or redistribution, researchers must make clear to others the licence terms of this work.

# Table of contents

List of tables ..... 11

List of figures ..... 12

List of abbreviations ..... 14

1. Introduction ..... 18

1.1. Aim and objectives ..... 18

1.2. Hypotheses ..... 19

1.3. Chapter summary ..... 19

1.4. Traumatic brain injury (TBI) ..... 20

Definition of TBI ..... 20

Public health and socioeconomic consequences of TBI ..... 20

The need for drug treatments in TBI ..... 21

The Mayo classification of TBI severity ..... 21

Use of the Mayo classification in this thesis ..... 23

1.5. Long-term consequences of TBI ..... 24

Clinical consequences of TBI ..... 24

Cognitive impairment after TBI ..... 24

Long-term clinical deterioration after TBI ..... 24

The risk of dementia after TBI ..... 25

Long-term brain atrophy after TBI ..... 27

Long-term mortality after TBI ..... 27

1.6. Pathophysiology of TBI ..... 29

Primary and second injury ..... 29

Traumatic axonal injury (TAI) ..... 30

TAI and cognitive impairment ..... 30

TAI and long-term WM degeneration ..... 30

1.7. Microglial activation after TBI ..... 31

Neuroinflammation after TBI ..... 31

The role of microglia in response to brain injury ..... 32

Microglial activation phenotypes ..... 33

Factors influencing microglial activation phenotype....34
Early time course of and phenotype of microglial activation after TBI....35
Post-acute and chronic microglial activation after experimental TBI....37
Chronic microglial activation after TBI in humans....40
1.8. *In vivo* imaging of chronic microglial activation....43
TSPO positron emission tomography (PET)....43
TSPO imaging of chronic microglial activation after TBI....44
1.9. Neurodegenerative pathologies after TBI....46
Aβ pathology after TBI....46
Mechanisms of acute and chronic Aβ plaque genesis after TBI....48
Microglia and Aβ plaque pathology after TBI....50
NFT pathology after TBI....50
*In vivo* imaging of Aβ and NFT pathology....50
Fluid biomarkers of TBI and neurodegeneration....51
1.10. Translational prospects of minocycline after TBI....52
Chronic neuroinflammation as a therapeutic target after TBI....52
Minocycline....52
Mechanisms of minocycline neuroprotection....53
Experimental studies of minocycline administered in acute TBI....54
Experimental studies of minocycline in neurodegenerative disease....55
Clinical trials of minocycline in CNS disorders....56
Pharmacology of minocycline....60
Safety and tolerability of minocycline....61
2. Amyloid pathology and axonal injury after brain trauma....63
2.1. Abstract....63
2.2. Introduction....64
2.3. Methods....65
Study design and participants....65
Procedures....66
Procedure for automatic reference region extraction....68
PET and T1 processing....70
Region of interest analysis....71

Manual segmentation and sampling of lesions ..... 71
Diffusion tensor image acquisition ..... 72
Diffusion tensor imaging analysis ..... 72
Statistical analysis ..... 73
2.4. Results ..... 74
Neuropsychological impairment after TBI ..... 75
Amyloid pathology after TBI detected by [$^{11}$C]PIB binding ..... 78
[$^{11}$C]PIB binding is decreased around focal lesions ..... 80
[$^{11}$C]PIB binding after TBI is correlated with WM damage and time since injury ..... 80
[$^{11}$C]PIB binding is not correlated with cognitive impairment in TBI ..... 81
Distinct distributions of [$^{11}$C]PIB binding in TBI and AD ..... 81
Exploring regional PIB binding and time since injury ..... 83
2.5. Discussion ..... 85
3. Thalamic inflammation after brain trauma is associated with thalamo-cortical white matter damage ..... 89
3.1. Abstract ..... 89
3.2. Introduction ..... 90
3.3. Methods ..... 91
3.4. Results ..... 92
3.5. Discussion ..... 94
4. Chronic microglial activation and the effect of minocycline after brain trauma ..... 99
4.1. Abstract ..... 99
4.2. Introduction ..... 100
4.3. Methods ..... 103
Study design ..... 104
Recruitment, eligibility criteria and screening ..... 104
Study procedures ..... 106
[$^{11}$C]PBR28 PET image analysis ..... 108
Lesion segmentation ..... 110
VBM and longitudinal registration ..... 110

DTI ..... 111
Statistical analyses ..... 112
4.4. Results ..... 115
[$^{11}$C]PBR28 binding in TBI patients is increased in WM and subcortical regions ..... 119
Cognitive impairment in TBI patients is associated with increased thalamic [$^{11}$C]PBR28 binding ..... 121
WM damage in TBI patients is greater in areas of high [$^{11}$C]PBR28 binding ..... 123
Increased plasma NFL levels in TBI patients are associated with time since injury and [$^{11}$C]PBR28 WM binding ..... 126
Minocycline in TBI patients reduces [$^{11}$C]PBR28 binding ..... 127
5. Neurodegeneration and the effect of minocycline after brain trauma . 130
5.1. Results ..... 130
Longitudinal WM atrophy in TBI patients is greater in areas of high baseline [$^{11}$C]PBR28 binding ..... 130
Minocycline in TBI patients has no effect on longitudinal WM atrophy ..... 132
Minocycline in TBI patients increases plasma NFL levels, associated with reduction in [$^{11}$C]PBR28 binding ..... 132
Plasma NFL levels predict longitudinal WM atrophy in TBI patients ..... 134
Minocycline in TBI patients has a negative effect on WM tract integrity ... 134
Minocycline in TBI patients is associated with a borderline worsening of information processing speed ..... 135
Minocycline was generally well tolerated in TBI patients ..... 136
5.2. Discussion ..... 136
Further discussion on TSPO PET ..... 142
6. Discussion ..... 146
6.1. Summary of findings ..... 146
Chapter 2 ..... 147
Chapter 3 ..... 147
Chapter 4 ..... 148
Chapter 5 ..... 149

6.2. Interpretation ..... 149
A multi-modal investigation of chronic disease processes after TBI ..... 149
Importance of WM damage in the chronic pathophysiology of TBI ..... 150
Biomarkers of chronic neurodegeneration after TBI ..... 150
Does a reduction in [$^{11}$C]PBR28 binding after minocycline imply a direct action on microglia? ..... 151
Increases in plasma NFL after minocycline support a CNS action ..... 152
What kind of activated microglia is minocycline inhibiting? ..... 152
Is chronic microglial activation after TBI a friend or foe? ..... 153
6.3. Future research ..... 154
TSPO and microglial phenotype ..... 154
Minocycline treatment after TBI ..... 155
TBI as a chronic neurodegenerative disease ..... 156
7. References ..... 157
8. Appendix ..... 201
8.1. Evidence of permissions to reuse material ..... 201
Figure 1 ..... 201
Figure 2 ..... 202
Figure 3 ..... 203
Figure 4 ..... 204
Figure 5 ..... 205
Figure 6 & 7 ..... 206
Figure 8 ..... 207
Figure 9 ..... 208
Figure 10 ..... 209
Chapter 2 ..... 209
Chapter 3 ..... 210

# List of tables

Table 1. The Mayo TBI classification system (Malec *et al.*, 2007) ..... 23

Table 2. Neuroprotective actions of minocycline ..... 53

Table 3. Experimental studies of minocycline in TBI ..... 54

Table 4. Clinical studies of minocycline ..... 56

Table 5. Demographics and clinical data of TBI patients ..... 74

Table 6. Neuropsychological test results ..... 77

Table 7. Summary of statistical tests ..... 112

Table 8. Demographics and clinical characteristics of the TBI patients ..... 117

Table 9. Baseline group demographics ..... 119

Table 10. Baseline cognitive test results ..... 122

## List of figures

Figure 1. Long-term mortality after TBI ..... 28

Figure 2. Microglial processes after laser-induced injury ..... 33

Figure 3. Early time course of microglial activation after TBI ..... 36

Figure 4. Post-acute time course of microglial activation after TBI ..... 38

Figure 5. Chronic time-course of microglial activation after TBI ..... 40

Figure 6. Chronic microglial activation after TBI in humans ..... 41

Figure 7. TAI and microglial activation after TBI in humans ..... 42

Figure 8. Microglial activation and WM degeneration after TBI ..... 43

Figure 9. Imaging of chronic microglial activation after TBI ..... 44

Figure 10. Aβ pathology after TBI ..... 48

Figure 11. Overview of [$^{11}$C]PIB imaging analysis ..... 69

Figure 12. Lesion map in TBI patients ..... 75

Figure 13. [$^{11}$C]PIB binding following TBI ..... 78

Figure 14. Increased [$^{11}$C]PIB binding in TBI and AD ..... 79

Figure 15. [$^{11}$C]PIB binding ROI analysis ..... 80

Figure 16. Relationship between WM damage and regional [$^{11}$C]PIB BP in TBI patients ..... 82

Figure 17. Relationship between [$^{11}$C]PIB BP and time since injury in TBI patients ..... 84

Figure 18. Increased thalamic microglial activation and WM damage in TBI ..... 93

Figure 19. Correlation of thalamic microglial activation and WM damage in relation to distance from thalamus ..... 95

Figure 20. How chronic microglial activation and axonal injury may be linked after TBI ..... 96

Figure 21. Study design, TBI enrolment and control groups. ..... 105

Figure 22. Overview of image analysis ..... 109

Figure 23. Increased baseline [11C]PBR28 binding in TBI in WM and subcortical regions. ..... 120

Figure 24. Baseline WM volume loss and reduced WM tract integrity are greater in areas of high [$^{11}$C]PBR28 binding in TBI patients. ..... 125

Figure 25. Plasma NFL and associations with [$^{11}$C]PBR28 WM binding and time since injury. ..... 126

Figure 26. Minocycline in TBI patients reduces [$^{11}$C]PBR28 binding ..... 128

Figure 27. Longitudinal WM atrophy over six months in TBI patients is greater in areas of high baseline [$^{11}$C]PBR28 binding..... 131

Figure 28. Effect of minocycline treatment on plasma NFL, and the associations between NFL, [$^{11}$C]PBR28 WM binding and longitudinal atrophy..... 133

Figure 29. Effect of minocycline versus no drug on information processing speed performance in TBI patients. ..... 135

Figure 30. Association between change in white matter binding and change in information processing speed in patients. ..... 136

## List of abbreviations

| | |
|---|---|
| [$^{11}$C]PBR28 | (a 2$^{nd}$ generation TSPO ligand) |
| [$^{11}$C]PIB | Pittsburgh compound B |
| [$^{11}$C]PK11195 | (a 1$^{st}$ generation TSPO ligand) |
| Aβ | Amyloid beta |
| ACC | Anterior cingulate cortex |
| AD | Alzheimer's disease |
| ALS | Amyotrophic lateral sclerosis |
| ALSFRS-R | ALS functional rating scale (revised) |
| ANOVA | Analysis of variance |
| APP | Amyloid precursor protein |
| BBB | Blood-brain barrier |
| BDNF | Brain derived neurotrophic factor |
| BNF | British National Formulary |
| BP | Binding potential (non-displaceable) |
| CCI | Controlled cortical impact |
| CD | Cluster of differentiation |
| CNS | Central nervous system |
| CRT | Choice reaction task |
| CSF | Cerebrospinal fluid |
| CTE | Chronic traumatic encephalopathy |
| DF | Degrees of freedom |
| ERK | Extra-cellular signal related kinases |

| | |
|---|---|
| FA | Fractional anisotropy |
| FMRIB | Oxford Centre for Functional MRI of the Brain |
| FSL | FMRIB software library |
| FVC | Forced vital capacity |
| FOV | Field of view |
| FWHM | Full width at half maximum |
| GCS | Glasgow coma scale |
| GM | Grey matter |
| GTAC | Gene Therapy Advisory Committee |
| HAB | High affinity binder |
| HIV | Human immunovirus |
| IFN | Interferon |
| IFG | Inferior frontal gyrus |
| IL | Interleukin |
| IV | Intravenous |
| LAB | Low affinity binder |
| LOC | Loss of consciousness |
| LPS | Lipopolysaccharide |
| LSD | Least significant difference |
| MAB | Medium affinity binder |
| MAPER | Multi-atlas propagation with enhanced registration |
| MBP | Myelin basic protein |
| MCI | Mild cognitive impairment |
| MHC | Major histocompatibility complex |

| | |
|---|---|
| MMSE | Mini mental state examination |
| MNI | Montreal Neurological Institute |
| MRI | Magnetic resonance imaging |
| MS | Multiple sclerosis |
| MSA-P | Multiple system atrophy Parkinsonism type |
| NICE | National Institute for Health and Care Excellence |
| NFTs | Neurofibrillary tangles |
| NHS | National Health Service |
| PBR | Peripheral benzodiazepine receptor |
| PCC | Posterior cingulate cortex |
| PD | Parkinson's disease |
| PET | Positron emission tomography |
| PTA | Post-traumatic amnesia |
| RCT | Randomised controlled trial |
| REC | Research ethics committee |
| RMANOVA | Repeated measures analysis of variance |
| ROI | Region of interest |
| RT | Reaction time |
| SCI | Spinal cord injury |
| SD | Standard deviation |
| SFG | Superior frontal gyrus |
| TAI | Traumatic axonal injury (also called diffuse axonal injury) |
| TBI | Traumatic brain injury |
| TNF | Tumour necrosis factor |

| | |
|---|---|
| TSPO | Translocator protein |
| SD | Standard deviation |
| SEM | Standard error of the mean |
| UK | United Kingdom |
| US | United States |
| VBM | Voxel based morphometry |
| VT | Volume of distribution |
| WM | White matter |

Chapter 1

# 1. Introduction

In this chapter, I describe the aim, objectives and hypotheses of the thesis, and outline the remaining the chapters. I describe the socioeconomic, clinical, and pathological consequences of traumatic brain injury (TBI). I outline the pathophysiology of TBI. I discuss neuroinflammation and neurodegeneration after TBI, and how these can be studied in vivo. I introduce minocycline as a neuroprotective agent, and describe experimental TBI studies and clinical trials in other neurological disorders.

## 1.1. Aim and objectives

The aim of the thesis is to explore chronic microglial activation and neurodegeneration following TBI. A combination of TSPO and amyloid PET, structural and diffusion MRI, cognitive assessment, serum biomarker measurement, and drug intervention are used.

The objectives of the thesis are:

- To image Aβ plaque burden in long-term survivors of TBI, test whether TAI and Aβ are correlated, and compare the spatial distribution of Aβ to AD;
- To test whether chronic thalamic microglial activation after TBI is correlated with thalamo-cortical tract TAI;
- To assess chronic microglial activation after TBI, its relation to MRI measures of injury, and to test the effect of minocycline on microglial activation as well explore the effect of minocycline on measures of injury;

- To test whether plasma NFL and tau are elevated after TBI, and how levels relate to cognitive impairment, brain atrophy, chronic microglial activation and minocycline.

## 1.2. Hypotheses

The main hypotheses of the thesis are:

- Aβ plaque pathology is present in long-term non-demented survivors of TB, and Aβ pathology after TBI is related to the amount and distribution of TAI;
- Chronic thalamic microglial activation after TBI is correlated with thalamo-cortical TAI;
- Chronic microglial activation is present in patients after TBI, and higher in areas of WM damage that show progressive atrophy; minocycline reduces chronic microglial activation after TBI;
- Plasma NFL and tau levels are persistently elevated after TBI, and correlated with chronic microglial activation; longitudinal WM atrophy is predicted by NFL and tau levels at baseline.

## 1.3. Chapter summary

In Chapter 2, I investigate the relationship between Aβ plaque burden and TAI after TBI using a [$^{11}$C]PIB PET and diffusion MRI, and compare the spatial distribution of Aβ to AD.

In Chapter 3, I investigate the relationship between chronic thalamic microglial activation after TBI, measured using [$^{11}$C]PK11195 PET, and thalamo-cortical TAI, measured using diffusion MRI.

In Chapter 4, I investigate chronic microglial activation after TBI using [$^{11}$C]PBR PET, and its relation to MRI and other measures of brain injury including plasma NFL. I also investigate the effect of minocycline on chronic microglial activation. The findings are developed further in Chapter 5.

In Chapter 5, I develop the findings of the Chapter 4 by investigating the effect of minocycline on other measures of brain injury and recovery. To conclude, I discuss the findings from both chapters.

In Chapter 6, I summarise and interpret the main findings of the thesis, and discuss how they contribute to our understanding of TBI. To conclude, I discuss directions for possible research in the future.

## 1.4. Traumatic brain injury (TBI)

### Definition of TBI

Traumatic brain injury (TBI) has been defined as "an alteration in brain function or other evidence of brain pathology, caused by an external force" (Menon *et al.*, 2010). It is commonly caused by road traffic accidents, falls, and violence (Bruns Jr. and Hauser, 2003). In military personnel, TBI may occur following blast injury, which has become the signature injury from the recent conflicts in Iraq and Afghanistan (Okie, 2005).

### Public health and socioeconomic consequences of TBI

TBI constitutes a major public health and economic problem that afflicts all societies (Maas, Stocchetti and Bullock, 2008). Worldwide, TBI is a leading cause of mortality and disability in young adults (Fleminger and Ponsford, 2005). In the United States (US) alone, an estimated 1.7 million people sustain a TBI each year, with 1.4 million of these individuals treated in emergency departments, and 52,000 fatalities (Roozenbeek, Maas and Menon, 2013).

Whilst advances in acute care have improved early outcomes after TBI (Bigler, 2013), survivors are often left with cognitive, neuropsychiatric and behavioural disorders (Bazarian *et al.*, 2009; McMillan, Teasdale and Stewart, 2012). The disability caused by TBI poses significant socioeconomic challenges. In the US, approximately 5.3 million people are living with a long-term TBI related disability (Corrigan *et al.*, 2010), and the cost of TBI, including medical costs and lost productivity, has been estimated at $60 billion per year (Langlois, Rutland-

Brown and Wald, 2006). The cost of TBI to the United Kingdom (UK) economy in 2010 was estimated as €5.7 billion (Gustavsson *et al.*, 2011).

### The need for drug treatments in TBI

There is currently no drug treatment that would be considered a targeted therapy for the majority of TBI patients (Lowenstein, 2009). Although pre-clinical studies have suggested many promising treatments for the acute management of TBI, more than 30 phase III clinical trials have failed to show significance for their primary endpoint (Maas, Roozenbeek and Manley, 2010). A Cochrane review in 2011 concluded: "In the absence of clear evidence of benefit from [acute] neuroprotective drug use, there is an urgent need to explore other potential modulators of late outcome from TBI." (Forsyth *et al.*, 2011)

### The Mayo classification of TBI severity

TBI is a heterogeneous disease with a wide variety of clinical consequences. These range from death or coma, to momentary unconsciousness and amnesia, to long-term physical and mental disability. The classification of TBI according to severity is important clinically to help guide acute management and indicate long-term outcome (Malec *et al.*, 2007; Andriessen *et al.*, 2011). A reliable system of injury classification is also important for the selection of patients into clinical research studies (Saatman *et al.*, 2008).

Several TBI classification systems have been proposed, and typically use a combination of measures to grade severity, including the duration of any loss of consciousness (LOC), the duration of any post-traumatic amnesia (PTA), and the lowest recorded Glasgow coma scale (GCS). The Mayo TBI classification system uses these clinical estimates and incorporates neuroimaging measures of injury severity (Malec *et al.*, 2007). It provides a validated way of retrospectively assessing TBI severity without the need to rely heavily on medical records, which are often incomplete. The Mayo system (

Table 1) defines three levels of increasing injury severity: *symptomatic (possible)*, *mild (probable),* and *moderate-severe* TBI.

**Table 1. The Mayo TBI classification system** (Malec *et al.*, 2007)

**A.** Classify as *Moderate-Severe (Definite) TBI* if one or more of the following criteria apply:

Death due to this TBI
Loss of consciousness of 30 min or more
Post-traumatic anterograde amnesia of 24 h or more
Worst Glasgow Coma Scale full score in first 24 h <13 (unless invalidated upon review e.g., attributable to intoxication, sedation, systemic shock)
One or more of the following present:

- Intracerebral haematoma
- Subdural haematoma
- Epidural haematoma
- Cerebral contusion
- Haemorrhagic contusion
- Penetrating TBI (dura penetrated)
- Subarachnoid haemorrhage
- Brainstem injury

**B.** If none of Criteria A apply, classify as *Mild (Probable) TBI* if one or more of the following criteria apply:

Loss of consciousness momentarily to less than 30 min
Post-traumatic anterograde amnesia momentarily to less than 24 h
Depressed, basilar or linear skull fracture (dura intact)

**C.** If none of Criteria A or B apply, classify as *Symptomatic (Possible) TBI* if one or more of the following symptoms are present:

Blurred vision
Confusion (mental state changes)
Daze
Dizziness
Focal neurological symptoms
Headache
Nausea

As expected, research has demonstrated that the minority of head injury patients who suffer a moderate-severe TBI have the highest mortality and poorest likelihood of good recovery (Thornhill *et al.*, 2000; McMillan and Teasdale, 2007).

### Use of the Mayo classification in this thesis

The Mayo classification is used in this thesis for several reasons. Firstly, as described, it provides a way to classify injury severity without relying on a single measure (such as lowest GCS), which may be missing from the medical

records. Secondly, as a research group, we have used this measure in our previous work and have found it to be a useful and practicable system. Thirdly, we use this measure in our clinical work to classify patients' brain injuries, and this also helps to stratify patients for possible selection into research studies.

## 1.5. Long-term consequences of TBI

### Clinical consequences of TBI

In the UK, of the patients presenting to an emergency department with a head injury, only 0.2% will die as a result of this injury, and only 1-3% of the patients admitted to hospital will require neurosurgical intervention (NICE, 2007). Nevertheless, the long-term outcome for many TBI survivors is poor (Fleminger and Ponsford, 2005). Approximately half of all patients, regardless of injury severity, have some residual disability affecting their lifestyle at one year (Thornhill *et al.*, 2000). Long-term post-traumatic problems include cognitive impairment, depression, anxiety, behavioural disorders, headache, seizures, sleep disturbance, dizziness, fatigue and pituitary dysfunction (Masel and DeWitt, 2010; Sharp and Jenkins, 2015).

### Cognitive impairment after TBI

The presence of cognitive impairment is an important determinant of long-term disability after TBI. Patients often show a characteristic pattern of impairment, with prominent deficits in information processing speed, sustained attention, executive function and memory (Kinnunen *et al.*, 2011). This "subcortical" pattern of cognitive impairment (Cummings and Benson, 1984) appears consistently across injury severities (Draper and Ponsford, 2008). Impaired performance on cognitive tests after TBI is predictive of disability (Goldstein *et al.*, 2012) as well as the likelihood of long-term unemployment (Wood and Rutterford, 2006).

### Long-term clinical deterioration after TBI

Survivors of TBI face an uncertain future (Fleminger, 2006), because long-term clinical outcomes are highly variable (Whitnall *et al.*, 2006). Although historically

TBI was thought to involve a static insult from a single event, new clinical effects, seemingly linked to the original injury, can emerge many years later. For example, patients may improve or deteriorate long after the injury, or develop unforeseen complications such as post-traumatic epilepsy (Annegers *et al.*, 1998) and late cognitive decline (Guo *et al.*, 2000).

A large longitudinal observational study in Glasgow, Scotland has followed a cohort of TBI patients of varying injury severities for 14 years post injury (Whitnall *et al.*, 2006; McMillan, Teasdale and Stewart, 2012). Participants were periodically assessed using measures of global outcome, cognitive impairment, psychological wellbeing and health status. Of the survivors followed up at 5-7 years (n=320), the frequency of disability was 53%, similar to that found at one year (57%) (Whitnall *et al.*, 2006). Over the first seven years, 29% of patients had improved in terms of global outcome, but over the same time period, 25% had deteriorated. A similar pattern was seen in patients between 7-14 years, with 23% improving in terms of disability and 32% deteriorating (McMillan, Teasdale and Stewart, 2012). Another longitudinal TBI study (n=210), which extended to 30 years of follow up, also found that a proportion of TBI patients deteriorated long after the injury (Himanen *et al.*, 2006). Together, these clinical observations suggest that TBI can initiate long-term dynamic processes that, in some patients, may be harmful.

### The risk of dementia after TBI

Epidemiological evidence indicates that a moderate-severe TBI is associated with an increased risk of dementia (Smith, Johnson and Stewart, 2013). TBI has been implicated as a risk factor in a variety of chronic neurodegenerative diseases, including Alzheimer's disease (AD) (Johnson, Stewart and Smith, 2010; Smith, Johnson and Stewart, 2013), Parkinson's disease (PD) (Gardner *et al.*, 2015), and amyotrophic lateral sclerosis (ALS) (Chen *et al.*, 2007). Some data support not only a link between TBI and neurodegeneration, but additionally a "dose-response" relationship. For example, the risk of dementia has been shown to be higher in severe compared to moderate TBI survivors (Plassman *et al.*, 2000), and higher in those patients with LOC after injury

compared to those without (Guo *et al.*, 2000). Other studies suggest that TBI can accelerate the age of onset of dementia (Gedye *et al.*, 1989; Nemetz *et al.*, 1999). (PK *et al.*, 2016)

There has recently been increasing awareness that TBI can lead to chronic traumatic encephalopathy (CTE), a progressive neurodegenerative disorder most commonly linked to repetitive mild TBI (McKee *et al.*, 2013). This condition has been long recognized in professional boxers, and was termed “dementia pugilistica” (Millspaugh, 1937). However, more recent evidence suggests CTE can occur after other causes of repeated head injury, implying that any repeated blows to the head, such as those that may occur during contact sports, have the potential to cause dementia (Turner *et al.*, 2013). Given the popularity of sports such as American football and rugby, the possible link between even mild head injury and the development of dementia is a growing public health concern.

The evidence linking a head injury to the development of dementia is not unequivocal, however. For example, a recent study which pooled clinical and neuropathological data from three prospective cohort studies found that TBI with loss of consciousness is associated with increased risk for Lewy body accumulation and Parkinsonism, but not dementia or neurofibrillary tangle (NFT) pathology (PK *et al.*, 2016).

Whilst much of the epidemiological evidence suggests TBI predisposes to the development of AD, it is uncertain whether the dementia that may follow a history of single TBI is the same clinicopathological entity as AD or CTE (Smith, Johnson and Stewart, 2013). Whilst neuropathological criteria for CTE have been proposed (McKee *et al.*, 2013), little consensus exists on the specific features of post-TBI dementia syndromes that might allow their confident diagnosis. Furthermore, the pathological processes which link TBI to the development of dementia are poorly understood (Johnson, Stewart and Smith, 2010; Smith, Johnson and Stewart, 2013).

### Long-term brain atrophy after TBI

Animal models of TBI and human neuroimaging studies support clinical and epidemiological observations that suggest an association between TBI and long-term neurodegeneration. In experimental TBI studies, progressive brain atrophy has been shown to continue for up to a year after injury (Saatman *et al.*, 1997; Acosta *et al.*, 2013; Loane *et al.*, 2014). In humans, magnetic resonance imaging (MRI) is sensitive to the changes in brain structure that follow TBI, and atrophy has been consistently observed for months and years after injury (Ross, 2011). Furthermore, longitudinal imaging studies have shown progressive atrophy in white matter (WM) and grey matter (GM), using T1-weighted volumetric MRI (Bendlin *et al.*, 2008; Sidaros *et al.*, 2009), as well as progressive changes in the integrity of WM tracts, using diffusion tensor imaging (DTI) (Bendlin *et al.*, 2008; Sidaros *et al.*, 2008; Farbota *et al.*, 2012).

### Long-term mortality after TBI

In addition to the clinical, epidemiological and radiological evidence for long-term deterioration after TBI, emerging data suggests TBI survivors are at persistently greater risk of death for years after injury (Baguley *et al.*, 2000; McMillan and Teasdale, 2007; Baguley, Nott and Slewa-Younan, 2008; McMillan *et al.*, 2011). A large (n=757) study of TBI patients in Glasgow showed an increased all-cause mortality that continued to deviate from socio-economically matched uninjured controls at 13 years (40.3% vs. 19.0%) (McMillan *et al.*, 2011) (Figure 1).




**Figure 1. Long-term mortality after TBI**

Kaplan–Meier curves with confidence intervals for cumulative deaths over 13 years in TBI patients, non-head injured patient controls and non-injured community controls (n=757 per group). Reproduced from (McMillan *et al.*, 2011).

Whilst the risk of death post-TBI was predictably highest in the first year, death after 12 years was still 2.8 times more likely after a TBI than for uninjured controls. The increased long-term mortality was not only isolated to the patients with the most severe injuries. Mortality in TBI patients was also higher than in a second control group of patients with comparably severe physical injuries but without TBI (40.3% vs. 28.2%). The causes of death in the TBI group were similar to those found in the general population, and were mainly due to cardiovascular disease, respiratory disease and cancer.

TBI was classically considered a static insult. However, TBI survivors may deteriorate long the after injury, show progressive brain atrophy, and have an increased risk of dementia and neurodegenerative disease, even death. Together, these observations suggest a dynamic and persistent element to the pathophysiology of TBI (Masel and DeWitt, 2010; Bigler, 2013).

It should be noted that the timeframe of follow-up for many of the longitudinal studies cited above is far longer than for the new work undertaken in this thesis.

Within the timeframe of the project (three years), it would have been challenging to design and execute even a small longitudinal study with follow-up intervals of greater than six months or one year. A possible alternative would have been to bring back patients who were involved in our previous completed research studies for further assessment. However, loss of up-to-date contact details and the potential for exposure to multiple doses of radiation across studies may well have hindered this approach.

## 1.6. Pathophysiology of TBI

### Primary and second injury

TBI is a complex disease process causing structural damage and functional deficits due to both primary and secondary injury mechanisms (Werner and Engelhard, 2007).

Primary injury is the result of mechanical damage that occurs at the time of trauma, principally as a result of direct physical contact or acceleration–deceleration. Primary injury includes haemorrhage, axonal tearing and shearing, and necrotic cell death. These effects can be focal or diffuse. Focal injuries may result from an object directly striking the head, or the brain striking the inside of the skull, producing haematomas or contusions (Graham *et al.*, 2000). Subdural and extradural haematomas are frequently seen after TBI, as well as haematomas within the parenchyma, and subarachnoid haemorrhage. Focal injuries have a characteristic distribution in the orbitofrontal, anterior temporal and occipital regions (Gurdjian, 1975). However, the presence and spatial distribution of focal injuries often correlates poorly with clinical outcomes (Bigler, 2007).

Secondary injury, initiated by the primary event, is thought to evolve over minutes to months, and is the result of cascades of interacting neurochemical, metabolic and cellular processes, ultimately leading to cell damage and death (Kunz, Dirnagl and Mergenthaler, 2010). A variety of mechanisms responsible for secondary injury have been identified, which include widespread neuronal depolarization, glutamate excitotoxicity, disturbance of calcium homeostasis,

mitochondrial dysfunction, free radical formation, apoptosis and neuroinflammation. Treatment of secondary injury processes may prevent further tissue damage and improve clinical outcome (Werner and Engelhard, 2007; Kumar and Loane, 2012).

### Traumatic axonal injury (TAI)

Diffuse or multifocal injuries in TBI often occur after rapid acceleration–deceleration, which imparts shear, tensile and compressive forces. Axons in WM are highly susceptible to injury from such biomechanical forces, hence traumatic axonal injury (TAI, also called diffuse axonal injury) is one of the most common pathologies of TBI (Adams *et al.*, 1989; Geddes *et al.*, 1997; Johnson, Stewart and Smith, 2013). TAI is documented in all severities of injury (Adams *et al.*, 1989; Johnson, Stewart and Smith, 2013) and shows a characteristic distribution across the brain, involving midline and parasagittal WM tracts such as the corpus callosum, internal capsule and brainstem (Johnson, Stewart and Smith, 2013). Pathologically, TAI encompasses a spectrum of abnormalities from primary mechanical breaking of the axonal cytoskeleton, to axonal transport interruption, swelling and proteolysis, through secondary physiological changes (Johnson, Stewart and Smith, 2013).

### TAI and cognitive impairment

Unlike for focal injuries such as haematomas, the presence of TAI is closely related to clinical outcome, and an important factor in determining persistent cognitive impairments (Sidaros *et al.*, 2008; Kinnunen *et al.*, 2011; Bonnelle *et al.*, 2012). As a consequence, TBI is the archetypal example of a brain network disorder, in which traumatic damage to the large-scale WM connections important for cognitive functions, such as attention and memory, underlies cognitive impairment (Sharp, Scott and Leech, 2014).

### TAI and long-term WM degeneration

TAI is described as progressive pathology, from initial disruption in axonal transport, to axonal swelling and secondary disconnection, which finally results in Wallerian degeneration (Johnson, Stewart and Smith, 2013). This process

was previously thought to be limited to the acute and sub-acute phases post-injury. However, recent experimental and human autopsy evidence has demonstrated axonal degeneration continuing for months and years after injury (Pierce *et al.*, 1998; Chen *et al.*, 2004, 2009; Johnson *et al.*, 2013). These neuropathological findings are consistent with longitudinal neuroimaging studies in TBI patients which demonstrate chronic WM degeneration (Trivedi *et al.*, 2007; Sidaros *et al.*, 2008).

The pathophysiological mechanisms underlying the chronic progressive degeneration of WM remain unknown. Notably, recent evidence suggests damaged axons may serve an important role in the development of AD-like pathologies long after injury (Chen *et al.*, 2004, 2009; Johnson, Stewart and Smith, 2010; Tran *et al.*, 2011). Other evidence suggests chronic neuroinflammation, triggered by the injury, occurs alongside ongoing WM degeneration for many years (Johnson *et al.*, 2013).

## 1.7. Microglial activation after TBI

### Neuroinflammation after TBI

Neuroinflammation is one of the most important secondary events to evolve after TBI (Finnie, 2013). Primary brain injury induces a complex array of neuroinflammatory processes, characterised by glial cell activation, infiltration of peripheral leucocytes from the systemic circulation, and up-regulation of inflammatory mediators (Cederberg and Siesjo, 2010; Hellewell and Morganti-Kossmann, 2012; Finnie, 2013).

Neuroinflammation after TBI is known to bring short-term beneficial effects for injured tissue and neuronal survival, but also harmful effects that contribute to secondary injury and neuronal loss (Morganti-Kossmann *et al.*, 2007; Hellewell and Morganti-Kossmann, 2012). The mechanisms underlying the paradoxical amelioration and aggravation of brain injury after TBI are complex and not well understood, with no single factor, molecule or cell seen as purely harmful or beneficial (Morganti-Kossmann *et al.*, 2007).

### The role of microglia in response to brain injury

Microglia are integral to the neuroinflammatory response after brain injury (Kettenmann *et al.*, 2011). Microglia are of mononuclear phagocyte lineage and comprise about 10% of cells in the mature brain (Mittelbronn *et al.*, 2001). Microglia typically exist in a "resting" state, characterized by a ramified morphology, and constantly monitor their microenvironment (Nimmerjahn, Kirchhoff and Helmchen, 2005). In response to brain injury, however, microglia undergo dramatic changes in cell morphology, gene expression and behaviour, summarily defined as "activation" (Kettenmann *et al.*, 2011). Microglia undergo rapid transformation from their quiescent ramified state into an amoeboid morphology and present a variety of upregulated surface molecules, including major histocompatibility complex (MHC) molecules (Block, Zecca and Hong, 2007).

Activated microglia are the prime mediators of the neuroinflammatory response to injury, acting as antigen presenting cells and releasing pro-inflammatory cytokines and chemokines (Hernandez-Ontiveros *et al.*, 2013). In their activated state, microglia can serve a variety of neuroprotective functions, including clearing toxic debris by phagocytosis and releasing anti-inflammatory and trophic factors (Block, Zecca and Hong, 2007; Loane and Byrnes, 2010). Microglia react to signals released by damaged cells (Liu *et al.*, 2009) with a migratory response towards the site of injury (Figure 2), and act as a barrier between injured and healthy tissue (Davalos *et al.*, 2005). Microglia also facilitate repair through the guided migration of stem cells to the site of injury (Aarum *et al.*, 2003). In addition, microglia have an active role in synaptic pruning and rewiring of neuronal circuits following injury (Tremblay *et al.*, 2011; Wake *et al.*, 2013). However, microglia can induce detrimental effects by the excessive production of pro-inflammatory cytokines, such as interleukin (IL)-1β and tumour necrosis factor (TNF)-α, as well neurotoxic molecules like superoxide free radicals, which are essential for host defence but cause secondary injury to healthy tissue (Block, Zecca and Hong, 2007).

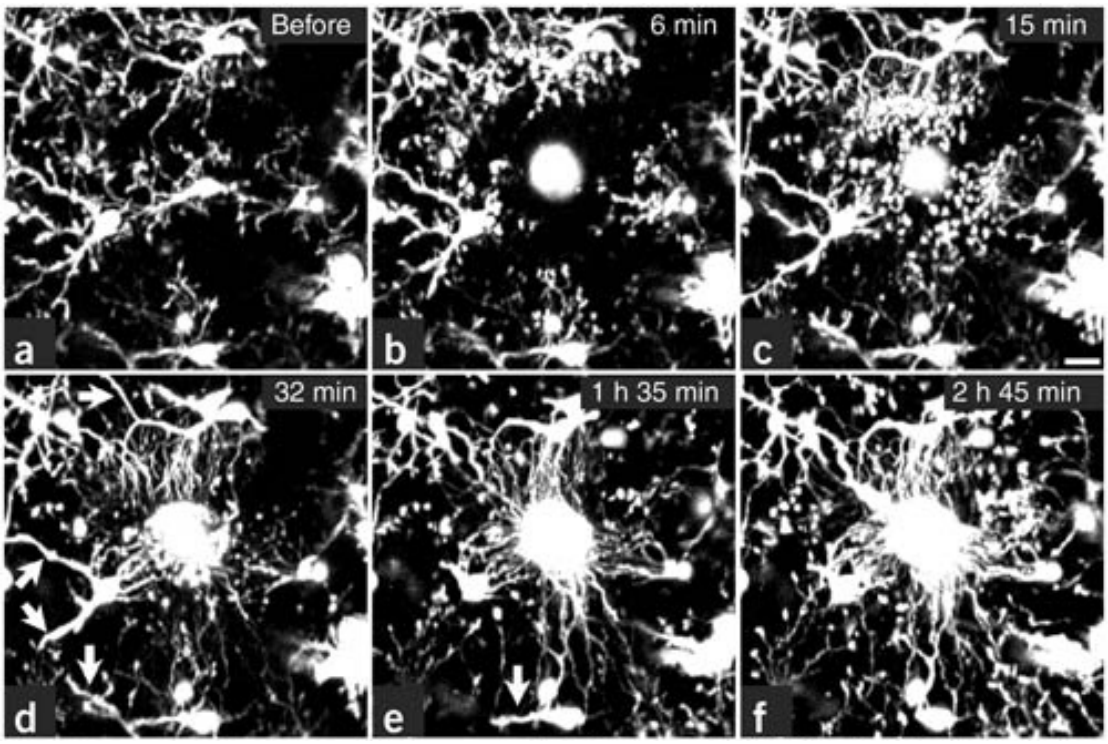



**Figure 2. Microglial processes after laser-induced injury**

*In vivo* two-photon microscopy of fluorescently labelled mouse microglia shows microglial processes move rapidly towards the site of injury induced by a two-photon laser localized ablation (15$\mu$m in diameter) (a) Pre-ablation (b-f) Nearby microglial processes respond with bulbous termini (b) and extend towards the ablation until they form a spherical containment around it (c–f). Simultaneously, the same cells retract processes lying in directions opposite to the site of injury (arrows in d and e). Scale bar = 10$\mu$m. Reproduced and cropped from (Davalos *et al.*, 2005).

## Microglial activation phenotypes

Microglia mediate both harmful and beneficial effects through their ability to adopt diverse activation states, or phenotypes (Kettenmann *et al.*, 2011; Boche, Perry and Nicoll, 2013). Microglia, like macrophages, under experimental conditions are capable of polarising into two major phenotypes (David and Kroner, 2011; Kettenmann *et al.*, 2011). Briefly, the “classically activated” (M1) phenotype is pro-inflammatory and destructive, marked by production of high levels of TNF-$\alpha$, interferon (IFN)-$\gamma$, IL-1$\beta$, IL-12, and low levels of IL-10, as well as expression of the cell surface markers CD68 and CD86. Conversely, the “alternatively activated” (M2) phenotype suppresses destructive processes and promotes tissue remodelling and angiogenesis. M2 microglia produce different molecules, such as IL-4, transforming growth factor (TGF)-$\beta$, and IL-10, and express different antigens, which include Arg1, Ym1, Fizz1 and CD206. In

experimental studies, lipopolysaccharide (LPS) and IFN-γ promote M1 microglial polarisation, whereas IL-4 or IL-13 promote M2 polarisation (David and Kroner, 2011).

It is increasingly recognised, however, that the M1/M2 dichotomy of microglial differentiation is an oversimplification, with M1 and M2 better seen as extremes of the spectrum of microglial phenotypes which occur *in vivo* (David and Kroner, 2011; Boche, Perry and Nicoll, 2013).

### Factors influencing microglial activation phenotype

Whether microglia differentiate into an M1-like phenotype that exacerbates brain injury, or into an M2-like phenotype that promotes brain repair depends on a variety of factors (Boche, Perry and Nicoll, 2013; Chhor *et al.*, 2013; Norden and Godbout, 2013). A major influence on microglial differentiation is the stimuli in the microglial microenvironment (Nimmerjahn, Kirchhoff and Helmchen, 2005). The microenvironment is affected by primary injury but also the signals released from other resident cells and infiltrating leucocytes (Hanisch and Kettenmann, 2007; David and Kroner, 2011; Luo and Chen, 2012). Neurotransmitter signalling may also modulate microglial phenotype after injury (Domercq, Vazquez-Villoldo and Matute, 2013). In addition, GM and WM may harbour phenotypically different microglial populations, with cellular expression of pro-inflammatory factors higher in WM than cortical GM (Olah *et al.*, 2011).

Some influences on microglial differentiation may originate from outside the CNS. Peripheral stress and systemic inflammation produce stimuli which "prime" microglia to produce an exaggerated pro-inflammatory phenotype (Perry, Cunningham and Holmes, 2007). The normal ageing process has been shown to induce microglial priming, leading to excessive and prolonged neuroinflammation after brain injury (Norden and Godbout, 2013).

The pro-inflammatory aggravation of microglial activation with increasing age is likely to be a factor in the poorer outcomes from TBI seen in elderly patients (Loane and Byrnes, 2010; Kumar *et al.*, 2013). A recent study in a mouse model

of TBI showed that aged animals had a chronically altered shift of microglial activation towards an M1-like phenotype and developed larger lesions (Kumar *et al.*, 2013).

### Early time course of and phenotype of microglial activation after TBI

After TBI, microglia become activated within minutes, resembling infiltrating macrophages (Koshinaga *et al.*, 2000; Tambuyzer, Ponsaerts and Nouwen, 2009). In humans, microglial activation can clearly be demonstrated by 72 hours post injury (Engel *et al.*, 2000), and by 3–5 days there is lymphocyte and monocyte infiltration, alongside microglial as well as astrocytic activation (Holmin *et al.*, 1998).

The spatial distribution of early microglial activation is concentrated in and around sites of focal injury such as contusions (Holmin *et al.*, 1998; Chen, Pickard and Harris, 2003). However the microglial response is not limited to the local environment of macroscopic lesions (Figure 3) (Chen, Pickard and Harris, 2003; Gentleman *et al.*, 2004). For example, microglial activation may be seen in adjacent WM or in subcortical nuclei anatomically connected to lesioned areas, such as the thalamus (Chen, Pickard and Harris, 2003; Maxwell *et al.*, 2006; Onyszchuk *et al.*, 2009).

Recently, experimental studies have examined the dynamics of microglial activation phenotype early after injury. Following controlled cortical impact (CCI) in mice (Kumar *et al.*, 2015), microglia and infiltrating macrophages initially express both M1- and M2-like phenotypic markers, but up-regulation of the anti-inflammatory M2-like phenotype is gradually replaced by an M1-predominant or “mixed transitional” phenotype, by seven days post-injury. The

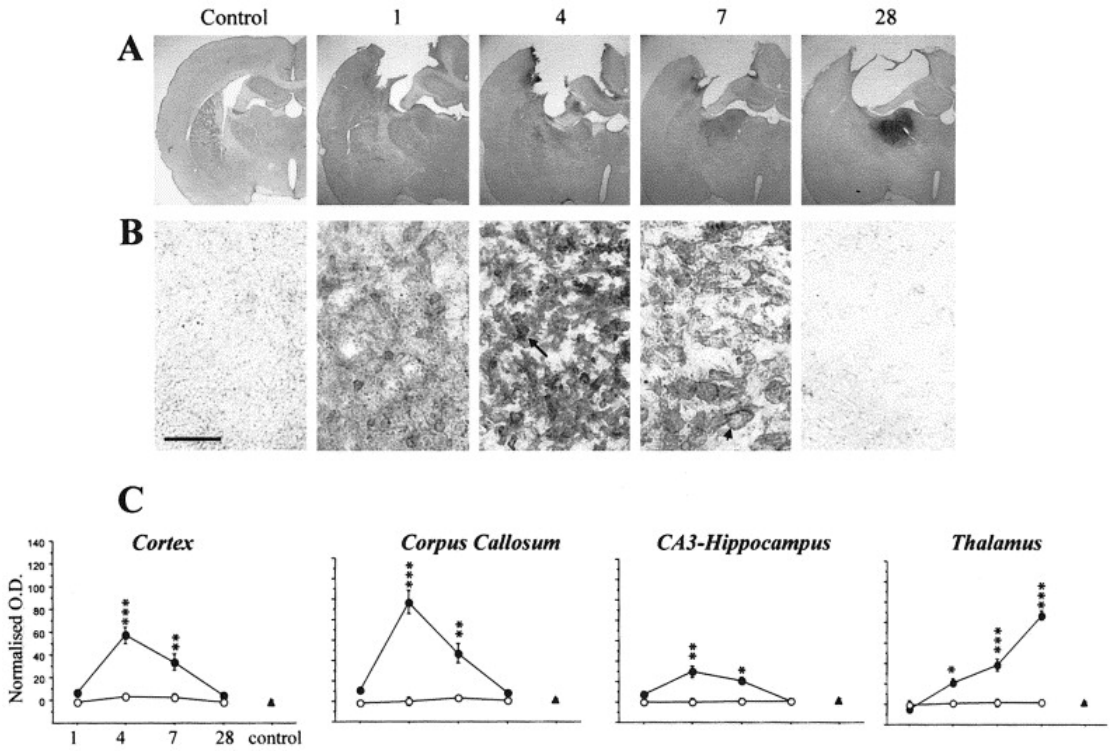



**Figure 3. Early time course of microglial activation after TBI**

OX42 immunoreactivity (a marker of microglial and macrophage activation) in a rat model of TBI (CCI). (A) Low magnification views of the ipsilateral hemisphere of a sham-control rat (Control) and rats at different time points after CCI show the accumulation of microglial/macrophages in peri-contusional cortex by 4 days. A more gradual accumulation is seen in the dorsolateral thalamus. (B) High magnification views of the peri-contusional cortex showing reactive microglia with stellate morphologies (arrow) and macrophage-like round cells (arrow head). (C) Time course of OX42 in different regions of interest, measured by optical density (O.D). and normalized to a remote unaffected region. Markers indicate sham-injured (○), injured (•), and control rats (▲). OX42 immunoreactivity peaked at 4 days after CCI in cortex, corpus callosum, and hippocampus but was persistently elevated in the thalamus. *** ($p < 0.001$), ** ($p < 0.01$), and * ($p < 0.05$) indicate a significant difference compared to the sham-control group. Scale bar is 50 µm. Reproduced from (Chen, Pickard and Harris, 2003).

M1- predominant phenotype is associated with high expression of NOX2, a super-oxide generating enzyme. In a follow up experiment, delayed administration of a selective NOX2 inhibitor, gp91ds-tat, altered the M1-/M2-like balance in favour of the M2-like phenotype, and this was associated with reduced oxidative damage in neurons at seven days (Kumar *et al.*, 2015). In another murine CCI study, the number of M1-like microglia/macrophages increased in cortex, striatum and corpus callosum during the first seven days and remained elevated until at least 14 days after injury (Wang *et al.*, 2013). In contrast, the numbers of M2-like microglia/macrophages peaked at five days

and then decreased rapidly. Notably, the degree of WM damage was strongly correlated with the number of M1-like cells.

Currently, the *in vivo* conditions that determine whether microglial activation is detrimental or beneficial to neuronal survival are poorly understood. A predominance of M1-like microglial may exacerbate damage after injury (Wang *et al.*, 2013). A greater understanding of the mechanisms that differentiate microglia towards a more neuroprotective and regenerative, M2-like, phenotype may yield opportunities for therapeutic intervention (Kumar and Loane, 2012; Kumar *et al.*, 2015).

### Post-acute and chronic microglial activation after experimental TBI

Recent animal and human studies suggest that microglial activation after TBI can persist well beyond the acute phase, for weeks, months and even years (Smith, 2013; Faden and Loane, 2015). Growing evidence implicates microglia as a key causative factor in the chronic neuroinflammation underlying a range of neurodegenerative diseases, including AD (Block, Zecca and Hong, 2007; Gentleman, 2013; Faden and Loane, 2015). Together, these observations suggest that chronic microglial activation, triggered by TBI, may play a role in the development of neurodegeneration long after injury.

Most animal studies in TBI have focused on short-term survival times, in the range of hours to days, and have rarely extended beyond one month after injury to what could be considered the chronic phase (Xiong, Mahmood and Chopp, 2013). Nevertheless, those experimental studies which have assessed prolonged survival periods show persistent microglial activation for up to a year post TBI, often at locations far removed from sites of focal lesions.

In a repetitive closed-skull mouse model of TBI, with animals euthanised at up to 49 days survival, increases in Iba1-positive microglia (a marker of activation) were first detectible at two days, with a peak of the microglial response seen at seven days in the cortex and 28 days in the thalamus, with microglial activation persisting as late as 49 days in the corpus callosum (Shitaka *et al.*, 2011) (Figure 4). Additionally, silver staining for WM damage revealed transient

abnormalities in the ipsilateral cortex, ipsilateral thalamus and contralateral hippocampus, with persistently increased staining in the corpus callosum through to 49 days.

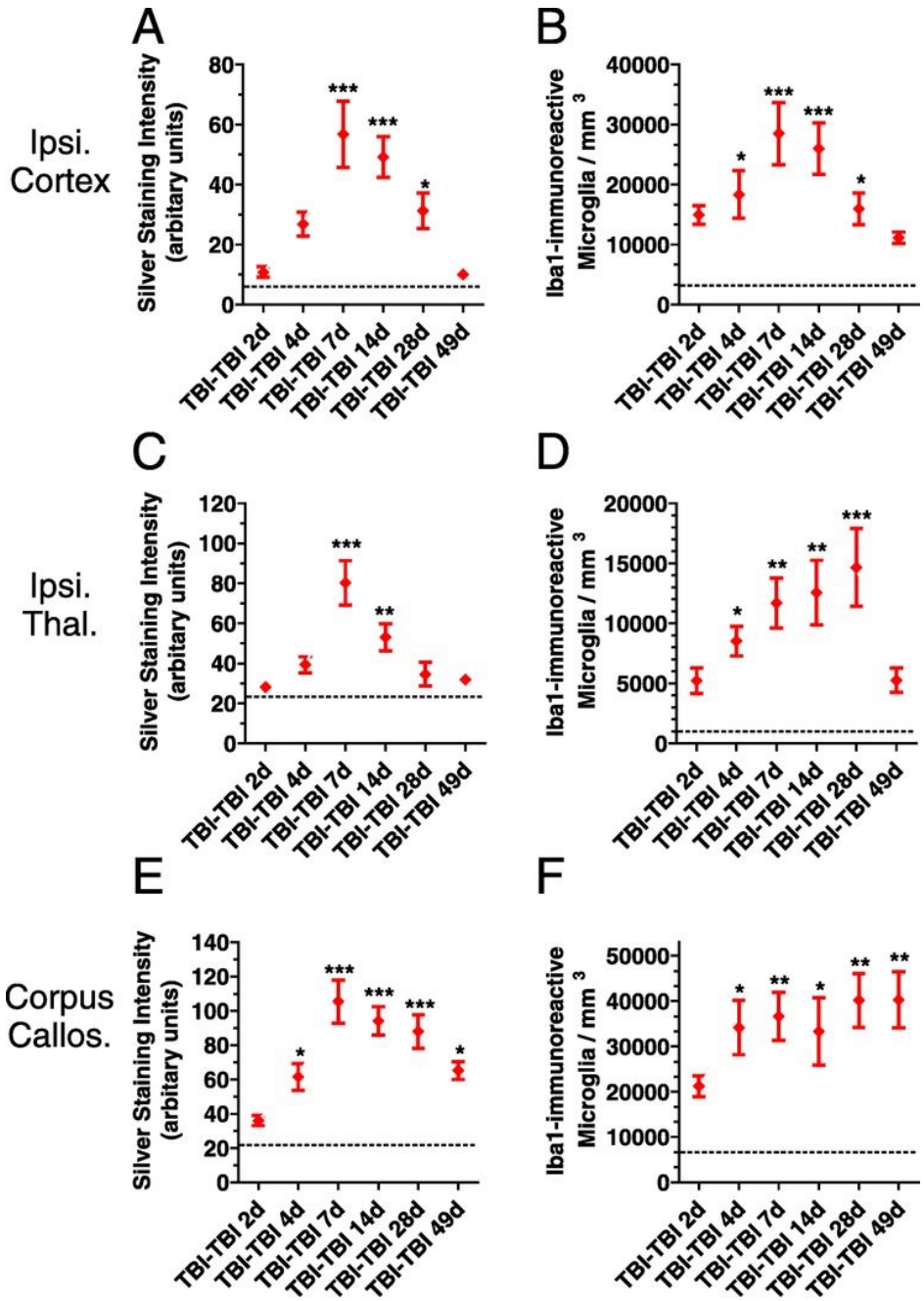



**Figure 4. Post-acute time course of microglial activation after TBI**

Plots of Iba1-immunoreactive activated microglial cell numbers (right column) and of silver staining intensity (a marker of WM damage, left column). Separate groups of mice (n=5-8) were killed at each time point following repetitive TBI (TBI-TBI). Dashed lines show levels in control (Sham-Sham) mice. (A, B) Ipsilateral cortex. (C, D) Ipsilateral thalamus. (E, F) Corpus callosum. * ($p < 0.05$), **($p < 0.005$), and *** ($p < 0.0005$) indicate a significant difference compared to Sham-Sham levels (Dunnett's post-hoc test). Reproduced and cropped from (Shitaka *et al.*, 2011).

In Sprague-Dawley rats sixty days after a CCI, antibodies against the activated microglial marker OX6 (MHC class II) showed significant increases in the striatum, thalamus, and cerebral peduncle (Acosta *et al.*, 2013). In addition, there was an increase of OX6-positive microglial cell volume in WM regions contralateral as well as ipsilateral to the injury. Notably, the highest up-regulation of activated microglia was seen in the thalamus, despite its distal subcortical location.

Another study in aged mice (21-24 months old) found Iba-1 staining was increased in the ipsilateral thalamus and internal capsule two months after CCI to the sensorimotor cortex (Onyszchuk *et al.*, 2009).

Sprague-Dawley rats subjected to a focal TBI were examined at a survival time of three months (Holmin and Mathiesen, 1999). ED1-positive (a marker for rat microglia/macrophage activation) microglia/macrophages were detected at this interval, and these cells were associated with IL-1 and TNF-$\alpha$ synthesis. Notably, while the highest number ED1-positive cells were detected around the focal lesion, they were also found in the ipsilateral corpus callosum, and large numbers of cells were scattered over the entire ipsilateral hemisphere.

A recent study using a CCI model in adult mice followed animals for up to one year after TBI (Loane *et al.*, 2014). Chronic microglial activation was observed in the lesioned cortex and peri-lesional cortex through to one year post-injury (Figure 5).

Studies in non-human primates have also shown microglia remain active both at the site of injury and at sites of WM abnormality for at least one year (Nagamoto-Combs *et al.*, 2007, 2010). After a combined lesion to the primary motor cortex and lateral premotor cortex, CD68 (a classical activation microglial/macrophage marker) immunoreactivity was increased in the lesion area and the contralateral corticospinal tract in the spinal cord at one, six and 12 months (Nagamoto-Combs *et al.*, 2007). Notably, activated microglia, including a subpopulation of CD68-immunoreactive cells, were observed to release brain derived neurotrophic factor (BDNF) around the lesion site and in the spinal cord at six months. In contrast, expression of TNF-α and IL-1-β was

less prominent at one, six, and 12 months, suggesting the immediate inflammatory response had subsided. In a further study, following a unilateral lesion to the motor cortex, activated microglia were observed up to 12 months later in the lateral corticospinal tract of the cervical spinal cord (Nagamoto-Combs *et al.*, 2010). In addition, microglia co-localised with extracellular signal-regulated kinases (ERK1/2) (kinases which mediate BDNF signalling and support cell survival) for up to 12 months after injury. These studies suggest that chronically activated remote microglial may have a long-term trophic role.

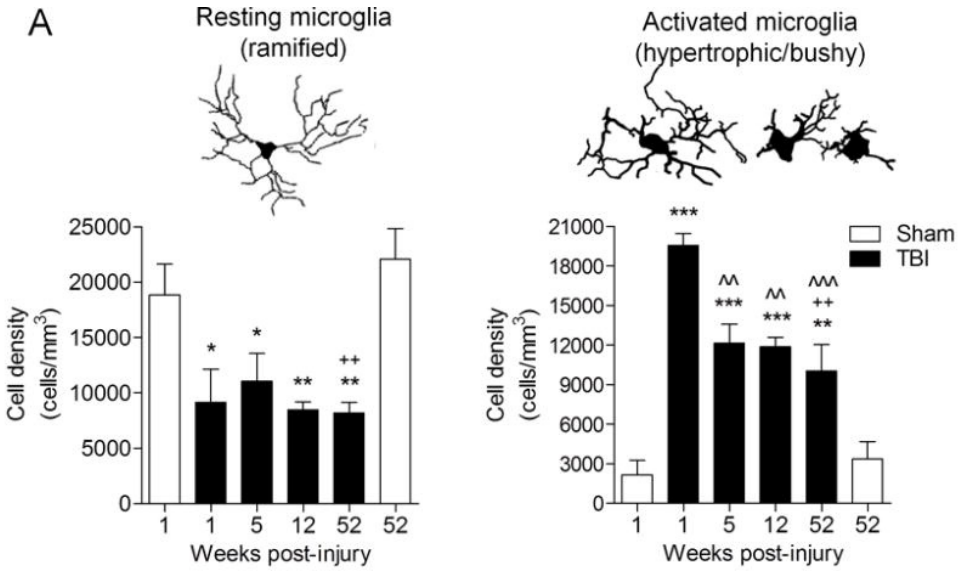



**Figure 5. Chronic time-course of microglial activation after TBI**

(A) Measurement of microglial activation phenotypes in the cortex at 1, 5, 12 and 52 weeks post-injury, compared to phenotypes in sham controls. (A) Computer reconstructions of ramified and activated (hypertrophic and bushy morphologies) microglia. TBI produced a significant reduction in the number of resting microglia (ramified) at 1-week (*$p < 0.05$), 5-week (*$p < 0.05$), 12-week (**$p < 0.01$) and 52-week (**$p < 0.01$) versus sham (1 week) group, and in the 52-week (++$p < 0.01$) TBI group versus sham (52 week) group. TBI also resulted in a significant increase the number of activated microglia (hypertrophic and bushy) at 1-week (***$p < 0.001$), 5-week (***$p < 0.001$), 12-week (***$p < 0.001$) and 52-week (**$p < 0.01$) versus the sham (1 week) group, and in the 52-week (++$p < 0.01$) TBI group versus the sham (52 week) group. There was a significant difference in activated microglia numbers in the 5-week (^^$p < 0.01$), 12-week (^^$p < 0.001$), and 52-week (^^^$p < 0.001$) TBI groups versus the 1 week TBI group. One-way analysis of variance (ANOVA), Student Newman-Keuls post-hoc test. Values plotted are mean ± SEM, n = 6/group. Reproduced and cropped from (Loane *et al.*, 2014).

## Chronic microglial activation after TBI in humans

A small number of human neuropathological studies in TBI provide evidence for chronic neuroinflammation, and also suggest a link between microglial activation and axonal pathology. In an early series of TBI patients with survival

times of up to 22 years, there was an increase in CD68 immunoreactivity compared to age-matched controls in parasagittal and hippocampal WM up to four years after injury (Gentleman *et al.*, 2004). CR3/43 (MHC-II) immunoreactivity (another marker of microglial activation) was observed in WM up to 16 years post-injury.

A more recent neuropathological study examined TBI cases (n=99) with survival up to 47 years (Smith *et al.*, 2012). The regions of interest (ROIs) were the hippocampus, the inferior temporal gyrus, the corpus callosum and cingulate gyrus. CD68 and CR3/43 levels rose to a maximum around three months after injury, but then gradually fell again to control levels within several years (Figure 6). These findings were not related to focal pathologies such as contusions. In cases with a pathological diagnosis of TAI, there was a higher immunoload in all regions (Figure 7), but particularly in the corpus callosum.

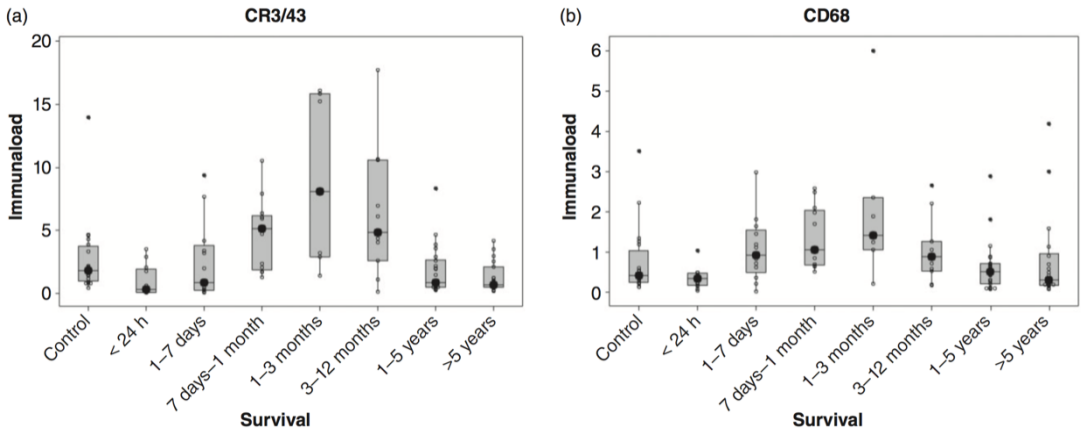



**Figure 6. Chronic microglial activation after TBI in humans**

Box and whisker plots are shown for overall CR3/43 (a) and CD68 (b) immunoload for patients examined at differing survival intervals. The large solid dot indicates median immunoload. Reproduced from (Smith *et al.*, 2012).

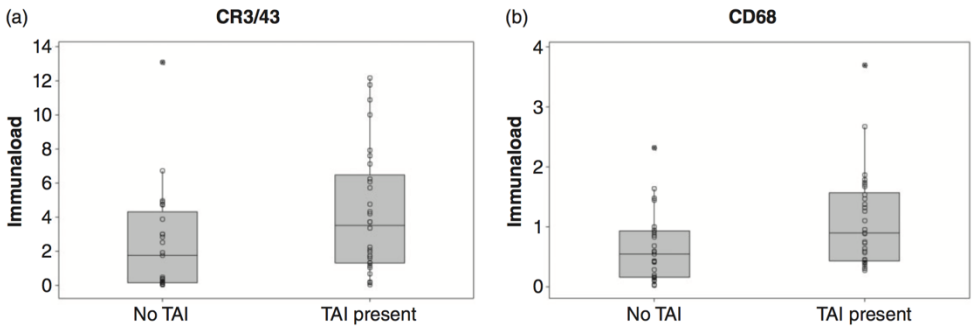



**Figure 7. TAI and microglial activation after TBI in humans**

Box and whisker plots are shown for overall CR3/43 (a) and CD68 (b) immunoload in those TBI cases who survived less than one year, divided into cases with and without evidence of TAI. Reproduced from (Smith *et al.*, 2012).

Another recent study also supports a link between chronic microglial activation and WM damage (Johnson *et al.*, 2013). Sections of the corpus callosum and adjacent cortex were examined in 52 cases of TBI with survivals ranging from 10 hours to 47 years. With survival of more than three months, TBI cases frequently displayed extensive reactive microglia (CD68 and/or CR3/43 positive), findings not seen in controls or acutely-injured cases. Notably, activated microglia were present in seven of the 25 cases (28%) with survival of more than one year, and up to 18 years post-TBI. Morphological analysis of microglia showed amoeboid cells were typically immunoreactive for both CD68 and CR3/43 and distributed throughout the corpus callosum. In cases displaying long-term inflammatory pathology, evidence of ongoing WM degradation was observed (for example, Figure 8).

Notably, confocal microscopy of adjacent sections double labelled for CR3/43 and myelin basic protein (MBP) showed MBP immunoreactive fragments within CR3/43 positive cells. These findings suggest chronically activated microglia are involved in phagocytosis of myelin fragments.

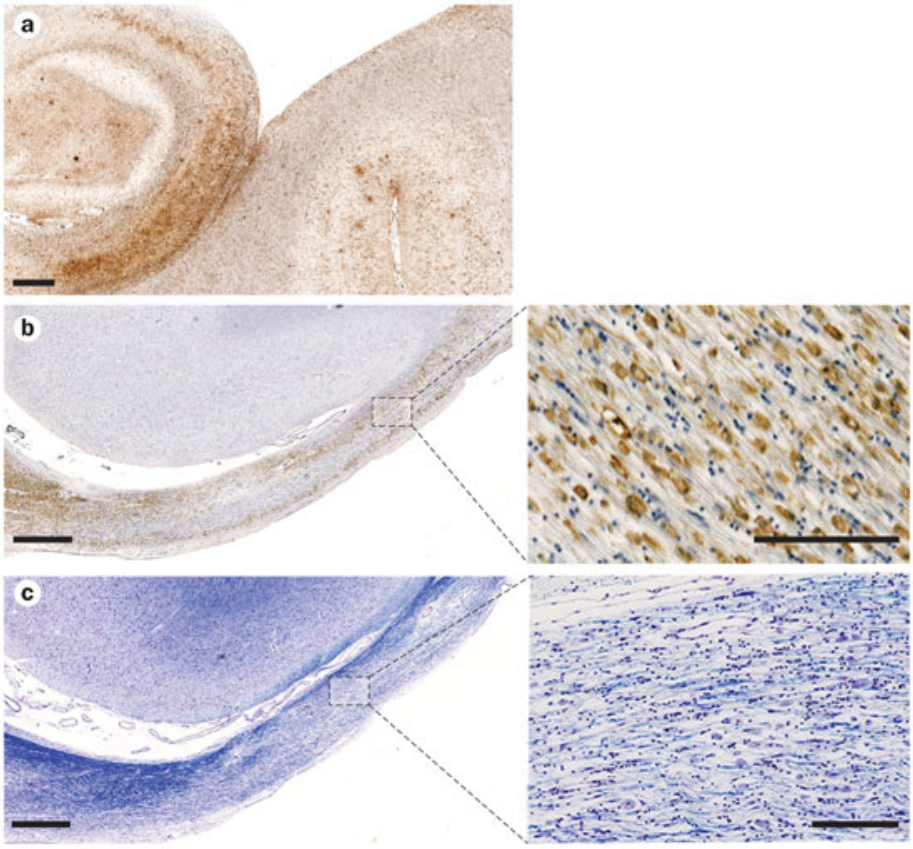



**Figure 8. Microglial activation and WM degeneration after TBI**

(a) Extensive microglial activation (immunostained with CR3/43 antibody) in the hippocampus and adjacent sulci of a 65-year-old man with CTE. Scale bar = 1 mm. (b) Extensive CR3/43-reactive cells with amoeboid morphology, suggesting activated microglia, in the atrophic corpus callosum of a 37-year-old male four years after a severe TBI. Scale bar = 1 mm for main image (left) and 100 µm for high-power image (right). (c) Adjacent section to b, stained with Luxol fast blue, indicating chronic WM damage and loss of myelin. Scale bars as for (b). Reproduced from (Smith, Johnson and Stewart, 2013).

## 1.8. *In vivo* imaging of chronic microglial activation

### TSPO positron emission tomography (PET)

Measurement of neuroinflammation *in vivo* has become possible using positron emission tomography (PET) because of the development of PET radioligands that bind the 18-kDa translocator protein (TSPO, previously called the peripheral benzodiazepine receptor, PBR). The TSPO is a mitochondrial outer membrane protein found within monocyte-derived cells, expressed at low levels on resting microglia as well as astrocytes (Rupprecht *et al.*, 2010). Increased levels of TSPO in the CNS was originally considered to be specific for activated microglia as well as infiltrating macrophages, representing a neuroinflammatory

biomarker, although it has since been established that TSPO expression is also increased in reactive astrocytes [22]. TSPO PET has been extensively used as a means of quantifying microglial activation *in vivo* in a variety of central nervous system (CNS) disorders (Owen and Matthews, 2011), including stroke (Thiel *et al.*, 2010), multiple sclerosis (MS) (Rissanen *et al.*, 2014), and AD (Edison *et al.*, 2008). As well as providing a means to monitor disease progression, TSPO imaging has the potential to be used to assess the action of therapies which target neuroinflammatory processes.

### TSPO imaging of chronic microglial activation after TBI

In our laboratory, a previous study used the TSPO radioligand [$^{11}$C]PK11195 to image chronic microglial activation in TBI patients (Ramlackhansingh *et al.*, 2011). Ten patients, 11 months to 17 years after moderate-severe TBI, underwent [$^{11}$C]PK11195 PET and structural MRI scans. Microglial activation, quantified by [$^{11}$C]PK11195 binding in a range of ROIs, was significantly increased in the thalami, putamen, occipital cortices and posterior limb of the internal capsule, compared to a group of seven aged-matched controls. Images in many individual patients also showed increased [$^{11}$C]PK11195 binding in WM (Figure 9). Furthermore, high [$^{11}$C]PK11195 binding in the thalamic region of interest (ROI) was associated with more severe cognitive impairment.

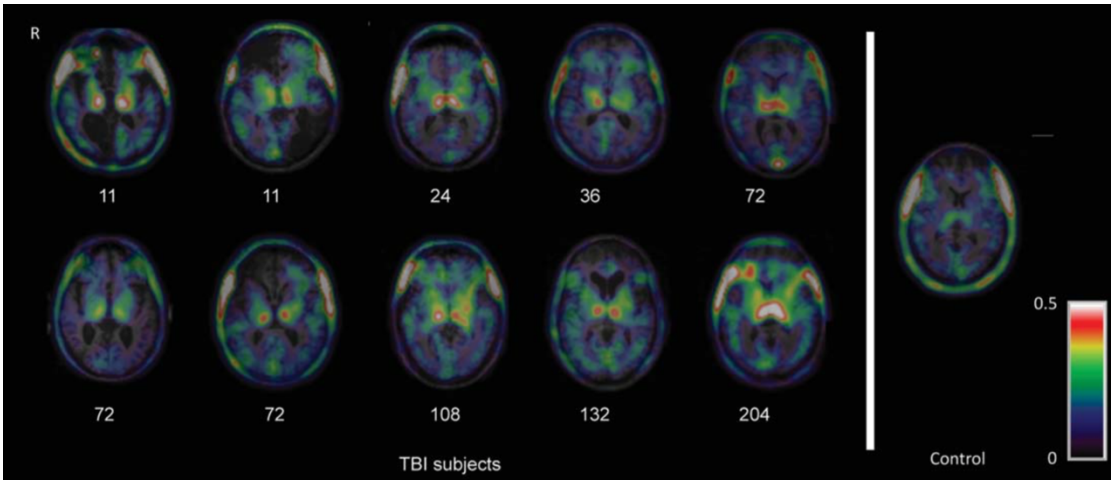



**Figure 9. Imaging of chronic microglial activation after TBI**

Images of [$^{11}$C]PK11195 PET images are shown superimposed on the T1 MRI scan at the level of the thalamus for 10 TBI patients, 11 months to 17 years after injury, and a representative control participant. Numbers indicate time since injury (months). R = right. Reproduced from (Ramlackhansingh *et al.*, 2011).

The finding of increased [$^{11}$C]PK11195 binding in several brain regions, far from focal damage, is consistent with remote chronic microglial activation. However, in the corpus callosum, where high [$^{11}$C]PK11195 binding might be expected based on the neuropathological evidence, the binding was the lowest of all regions assessed.

A subsequent [$^{11}$C]PK11195 PET study in eight TBI patients six months after injury also found increases in [$^{11}$C]PK11195 binding in several ROIs compared to age-matched controls, including the thalamus, putamen, pons, hippocampus, and frontal lobes (Folkersma *et al.*, 2011). The highest regional binding was found in the thalamus in six of the patients. Analysis of the corpus callosum was not reported.

These preliminary molecular imaging studies provide *in vivo* evidence for microglial activation persisting for months to years after TBI, including at locations far from sites of focal lesions. While these findings are broadly consistent with the neuropathological studies, the absence of increased [$^{11}$C]PK11195 binding in the corpus callosum (Ramlackhansingh *et al.*, 2011) is discrepant with the neuropathological evidence for persistent microglial activation in this region (Johnson *et al.*, 2013). Differences in the patient groups or the nature of injuries may explain this disparity. It is possible that TSPO imaging and CD68 and CR3/43 immunohistochemistry detect distinct populations of activated microglia. Alternatively, the sensitivity and resolution of PET may be insufficient to detect activated microglia specifically in the corpus callosum, an area which could be prone to partial volume effects, because of, for example, its proximity to the ventricular system.

Recently, second-generation TSPO radioligands have been developed which have a better signal-to-noise ratio than [$^{11}$C]PK11195, promising more accurate measurement of neuroinflammation. However, there is no evidence that TSPO PET radioligand binding can distinguish between activated microglial polarisation phenotypes (i.e. M1 or M2), which confounds interpretation of TSPO PET studies. Similarly, binding of TSPO radioligands to infiltrating blood-derived macrophages in the CNS may also complicate interpretation of

increased signal, particularly if these peripherally-originating cells have different effects to resident microglia (Schwartz *et al.*, 2013)

## 1.9. Neurodegenerative pathologies after TBI

The link between TBI and the development of dementia is supported by the detection of AD-like pathologies in the brains of TBI patients (Smith, Johnson and Stewart, 2013). AD is characterized by extracellular deposition of amyloid-beta (Aβ) protein as plaques, and intracellular aggregation of hyperphosphorylated tau, as NFTs (Swerdlow, 2007). Recently, Aβ plaque and NFT pathologies have been observed in the acute and chronic phases following a single moderate-severe TBI (Johnson, Stewart and Smith, 2012), and after repetitive mild TBI (McKee *et al.*, 2009; Smith, Johnson and Stewart, 2013).

### Aβ pathology after TBI

Aβ plaques have been found in the brains of up to 30% of patients who died in the acute phase after a single moderate-severe TBI and in surgically excised tissue (Roberts *et al.*, 1994; Ikonomovic *et al.*, 2004) (Figure 10). Aβ plaques were detected in all age groups, even children, and were widely distributed, with no correlation with the presence of contusions, haematomas, TAI or ischaemic damage. The Aβ plaques observed post-TBI largely appear in GM, but they have been identified in WM (Johnson, Stewart and Smith, 2010). For example, in a study of 12 patients who died within nine days of injury, in the eight patients with Aβ plaque formations observed in cortical GM, some Aβ plaque like profiles were also found in the white matter close to Aβ-immunoreactive axons (Douglas H. Smith *et al.*, 2003). These findings are supported by an experimental swine model of TBI, whereby plaques were found predominantly in WM as well as cortical GM, and appeared to relate to the degree of axonal injury (Smith *et al.*, 1999).

The plaques found in TBI patients can appear within hours of injury yet are strikingly similar to those observed in the early stages of AD. Furthermore, most of the Aβ peptide in the plaques formed after TBI, and in the soluble Aβ found in the brains of TBI patients, is Aβ42, the AD-associated form of Aβ that is prone

to aggregation and believed to be pathogenic (Johnson, Stewart and Smith, 2010).

A recent study has examined the time course of Aβ plaques in material from 39 long-term survivors of a single moderate-severe TBI, 1-47 years post-injury (mean 8.2 years) (Johnson, Stewart and Smith, 2012). Aβ plaques were present in up to one third of patients. Plaques were observed in greater density and wider distribution in TBI survivors than age-matched non-head injured controls. Whereas the plaques observed in the acute phase were typically diffuse, like those observed in early AD, those observed in long-term survivors of TBI were the denser, neuritic plaques characteristic of advanced AD. Typically, following TBI cases were more likely to have widespread plaques across the entire cortical region examined. This was particularly true extending from the cingulate gyrus through the superior frontal gyrus, which frequently displayed extensive pathology.

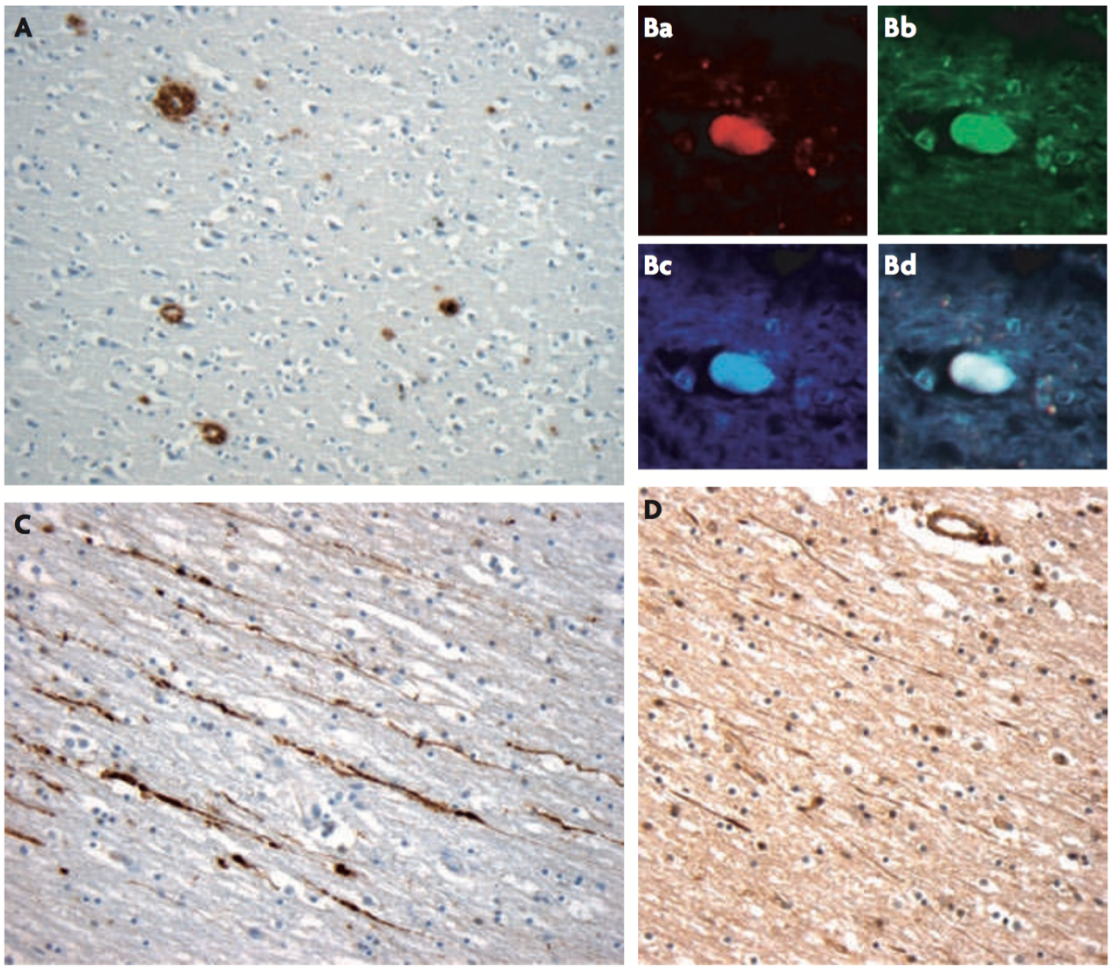



**Figure 10. Aβ pathology after TBI**

(A) Aβ plaques (brown ring-like areas) seen acutely following a single TBI, caused by a fall in an 18-year-old male. The survival time was 10 hours. Plaques were identified using an antibody specific for Aβ. (B) Immunohistochemistry showing APP (Ba), β-site-APP-cleaving enzyme (Bb) and presenilin-1 (Bc) co-accumulating (Bd) in the disconnected terminal of an axon (an axon bulb). (C) Example of axonal pathology identified using APP immunohistochemistry. APP (brown) accumulates within the tortuous varicosities along the length of damaged axons. (D) Increased neprilysin immunoreactivity (brown) is also observed in damaged axons after TBI. Reproduced from (Johnson, Stewart and Smith, 2010).

## Mechanisms of acute and chronic Aβ plaque genesis after TBI

Axonal pathology after TBI provides a potential means for the genesis of Aβ plaques. A key feature of TAI is the interruption of axonal transport due to cytoskeletal disruption. This causes an accumulation of proteins in the axon, including amyloid precursor protein (APP). Accumulations of APP occur in varicosities along the length of the axon or at the disconnected axon terminals (axon bulbs). (As a consequence, immunostaining for APP is a standard method for identifying TAI in tissue sections.) It has been postulated that

abundant APP in injured axons might be aberrantly cleaved to form Aβ (Johnson, Stewart and Smith, 2010). Interestingly, the enzymes necessary for Aβ cleavage from APP, including presenilin-1 and B-site APP cleaving enzyme have been observed accumulating in damaged axons along with Aβ itself in a pig model of TAI (Smith *et al.*, 1999) and subsequently in humans (Chen *et al.*, 2009). TBI appears to create "a unique situation whereby all the necessary substrates for Aβ formation are forced to coexist in the same place at the same time" (Johnson, Stewart and Smith, 2010). It has been proposed that eventual breakdown of damaged axons allows expulsion of Aβ into the parenchyma, where it aggregates and causes formation of plaques (Johnson et al., 2010).

Traditionally regarded as an event limited to the acute phase, recent studies suggest axonal degeneration may persist for years and even decades after TBI, in a proportion of patients (Johnson *et al.*, 2013). The continued presence of axonal damage therefore provides a potential mechanism by which Aβ is chronically generated. Intra-axonal Aβ plaque accumulation has been identified alongside long-term progressive axonal damage following human TBI, persisting for years after injury (Chen *et al.*, 2009).

Whilst there is good evidence that damaged axons are a potential source of post-traumatic Aβ, it is likely that this is only one of several mechanisms contributing to Aβ plaque genesis in the aftermath of TBI. Furthermore, many questions remain about the possible link between TAI and Aβ plaque pathology (Johnson et al., 2010). For example, it is not clear why plaque formation is more prevalent in the GM after TBI, if WM damage is a source of Aβ. In addition, the variability in Aβ plaque burden in humans and experimental models of TBI suggests differences in activity of Aβ degrading mechanisms. Neprilysin, a membrane zinc metalloendopeptidase, is a major Aβ degrading enzyme which has increasingly been implicated in the pathogenesis of AD. In TBI, extensive neprilysin immunoreactivity was found in the neuronal soma and axonal bulbs of long term survivors of TBI, cases comprising a group that had a visual absence of Aβ plaques (Chen *et al.*, 2009). These findings suggest some TBI

patients may have long-term upregulation of neprilysin that continuously clears Aβ, promoting plaque regression.

### Microglia and Aβ plaque pathology after TBI

Microglia may have a role in both Aβ accumulation and clearance after TBI (Mannix and Whalen, 2012). Microglia are a source of several proteins upregulated both in AD and after TBI, including APP and pro-inflammatory cytokines, including IL-1β and TNF-α (Smith, 2013). Aβ itself is a pro-inflammatory microglial activator, resulting in increased production of reactive oxygen species, which are neurotoxic. However, microglia containing Aβ have been found associated with plaques after TBI, suggesting they may play a role in phagocytic clearance of plaques (Mannix and Whalen, 2012).

### NFT pathology after TBI

The presence of NFTs, formed by hyperphosphorylation of tau protein, is one of the most consistent pathologies reported in patients with dementia associated with repetitive mild TBI, or CTE (McKee *et al.*, 2013). There are fewer reports of tau pathology following a single moderate-severe TBI. However, in the study of (Johnson, Stewart and Smith, 2012) (above), NFTs were seen at greater density and in wider distribution in up to 30% of TBI cases compared with age-matched controls. The tau pathology after TBI was described as involving predominantly superficial cortical layers, accumulating in the depths of sulci, and in a perivascular distribution. Clusters were also seen extending through the cingulate and superior frontal gyri. However, the distribution of NFT pathology was not similar to that of activated microglia, suggesting an indirect link, if any, between microglial activation and the presence of NFT pathology.

### *In vivo* imaging of Aβ and NFT pathology

Imaging of Aβ plaques and NFT pathology *in vivo* has become possible through development of PET ligands which target these pathologies. The amyloid tracer [$^{11}$C]-Pittsburgh compound-B ([$^{11}$C]PIB) shows robust retention in brains of AD patients in a pattern that corresponds with neuropathological studies of Aβ

plaque distribution (Klunk *et al.*, 2004). The more recently developed tau ligand [18F]-T807 has been shown to exhibit high cortical binding in patients with mild cognitive impairment (MCI) and AD, compared to health controls, particularly in the inferior temporal gyrus, where prominent NFT pathology would be expected (Johnson *et al.*, 2016). Such studies suggest that Aβ and tau PET imaging in the chronic phase after TBI may inform our understanding of neurodegeneration in long-term survivors of TBI.

### Fluid biomarkers of TBI and neurodegeneration

There is a great interest in developing clinically available fluid biomarkers of TBI, to support the diagnosis and prognostication of patients. A range of possible blood and CSF biomarkers of acute brain damage have been identified in TBI (DeKosky *et al.*, 2013; Zetterberg, Smith and Blennow, 2013). Neurofilament light chain (NFL) and tau protein levels are particularly promising markers (DeKosky *et al.*, 2013). Neurofilaments are major structural proteins of neurons (Liu *et al.*, 2004), and NFL is especially abundant in large-calibre myelinated axons in the CNS (Friede and Samorajski, 1970). Tau is a microtubule-associated protein predominantly expressed in neurons, and preferentially localized in axons (AVILA *et al.*, 2004). Elevated CSF levels of NFL and tau have been observed in acute severe TBI, with higher levels seen in more severe injuries (Zetterberg, Smith and Blennow, 2013). Increases in NFL and tau have also been reported in repetitive mild TBI (Zetterberg, Smith and Blennow, 2013). NFL levels in the peripheral blood have been shown to be highly correlated with levels in the CSF (Gaiottino *et al.*, 2013), and in severe TBI, elevated plasma levels are predictive of early outcome (Zetterberg, Smith and Blennow, 2013).

Persistent elevations in both NFL and tau have been reported in a variety of neurodegenerative diseases, including AD (Schraen-Maschke *et al.*, 2008; Gaiottino *et al.*, 2013). These observations suggest that NFL and tau may provide a biomarker for neurodegeneration and dementia risk in the chronic phase after TBI. However, it is currently unclear whether CSF or plasma

biomarkers of axonal injury remain elevated in the chronic phase after TBI, or whether levels relate to progressive long-term neurodegeneration.

## 1.10. Translational prospects of minocycline after TBI

### Chronic neuroinflammation as a therapeutic target after TBI

There is currently no drug treatment that would be considered targeted therapy for the majority of TBI patients (Lowenstein, 2009). A drug treatment that improves brain recovery and prevents the development of late complications after TBI would have a major effect on patients' quality of life and dramatically reduce the cost of their long-term care.

While a rapid microglial response soon after injury may be beneficial, prolonged microglial activation triggered by TBI may be deleterious, and so inhibiting chronic microglial activation after TBI may improve brain recovery and prevent the late complications from developing (Kumar and Loane, 2012; Finnie, 2013; Smith, 2013).

### Minocycline

Minocycline (7-dimethylamino-6-dimethyl-6-deoxytetracycline) is a second-generation semi-synthetic tetracycline which has been used as an antibiotic for forty years (Yong *et al.*, 2004). Minocycline shows a better pharmacokinetic profile than the first-generation tetracyclines, being almost completely absorbed, with a longer half-life, almost complete bioavailability and superior CNS penetration (Garrido-Mesa, Zarzuelo and Gálvez, 2013a).

Independent of their anti-bacterial activity, tetracyclines have increasingly been recognised as a family of drugs with pleiotropic effects, including anti-inflammatory, immunomodulatory and anti-apoptotic actions (Sapadin and Fleischmajer, 2006; Griffin *et al.*, 2010). Recognition of the anti-inflammatory activities of tetracyclines has prompted their use in the treatment of a range of diseases with an inflammatory basis, such as acne vulgaris, sarcoidosis and rheumatoid arthritis (Garrido-Mesa, Zarzuelo and Gálvez, 2013b).

Minocycline has been shown to be neuroprotective in animal models of a variety of CNS disorders including TBI. The neuroprotective effect of tetracyclines was first demonstrated in a study which showed that doxycycline, another second-generation tetracycline, improved recovery in a rabbit model of focal brain ischaemia (Clark *et al.*, 1994). A further study in a rat model of global ischaemia found that doxycycline and minocycline were neuroprotective (Yrjänheikki *et al.*, 1998). Then followed several hundred reports of the neuroprotective effects of tetracyclines in a range of in vitro studies and animal models of neurological disease, including stroke, MS, TBI, spinal cord injury (SCI), Huntington's disease, PD and ALS (Plane *et al.*, 2010; Kumar and Loane, 2012; Garrido-Mesa, Zarzuelo and Gálvez, 2013a). Minocycline has emerged as the most effective neuroprotective tetracycline (Garrido-Mesa, Zarzuelo and Gálvez, 2013a).

## Mechanisms of minocycline neuroprotection

A variety of mechanisms are thought to account for the neuroprotective effects of minocycline. These mechanisms can broadly be categorized into anti-inflammatory, anti-apoptotic, and anti-oxidant actions (Table 2) (Elewa *et al.*, 2006; Plane *et al.*, 2010; Garrido-Mesa, Zarzuelo and Gálvez, 2013b).

**Table 2. Neuroprotective actions of minocycline**

| Anti-inflammatory actions | Anti-apoptotic actions | Anti-oxidant / other actions |
|---|---|---|
| ↓microglial activation<br>↓release of cytokines (e.g. IL-1β, TNF-α) and chemokines (e.g. MIP-1α)<br>↓release and activity of MMPs | Caspase-dependent actions<br>↓release of cytochrome C (pro-apoptotic) from mitochondria<br>↓expression of caspase-1 and -3 (pro-apoptotic) | Suppression of free radical production<br>↓activity of COX2<br>↓activity of NOS |
| ↓ T-cell transmigration and activity | Caspase-independent actions<br>↑Bcl-2 (anti-apoptotic)<br>↓release of apoptosis-inducing factor (AIF) from mitochondria | ↓PARP-1<br>↓mitochondrial [11C]PBR/TSPO |
| ↓p38 mitogen-activated protein kinase (MAPK) signalling | | ↓glutamate excitotoxicity<br>Calcium sequestration |

Abbreviations: ↓ = decrease, inhibition or suppression. ↑ = increase. IL-1β = interleukins (IL) 1-beta; COX-2 = cyclooxygenase 2; NOS = nitric oxide synthase. PARP-1 = poly (ADP [adenosine diphosphate]–ribose) polymerase-1 (PARP-1) (involved in excitotoxicity, oxidative stress and inflammation); [$^{11}$C]PBR/TSPO = mitochondrial peripheral benzodiazepine receptor. TNF-α = tumour necrosis factor-alpha. Reproduced from (Garrido-Mesa, Zarzuelo and Gálvez, 2013b).

## Experimental studies of minocycline administered in acute TBI

In experimental TBI, minocycline has been shown to improve neurological recovery in a variety of animal models (Table 3). An important mechanism underlying the beneficial effect of minocycline appears to be the inhibition of microglial activation (Sanchez Mejia *et al.*, 2001; Bye *et al.*, 2007; Homsi *et al.*, 2010; Ng *et al.*, 2012). Levels of microglial activation are frequently assessed pathologically using immunohistochemical methods to detect cell surface markers expressed by activated microglia, such as CD11b (Homsi *et al.*, 2010). In one study, minocycline treatment was able to reduce the post-TBI increase of CD11b immunolabelled cells by 59%, and this was associated with significantly improved functional outcome (Homsi *et al.*, 2010).

**Table 3. Experimental studies of minocycline in TBI**

| Model and species | | Dose | Dose intervals | Outcomes with minocycline | Ref. |
|---|---|---|---|---|---|
| WD | Ms | 45 mg/kg IP | 30 minutes, 12 hourly for 2 weeks | Reduced microglial activation at 1 week; improved neurological recovery sustained over 6 weeks | (Ng *et al.*, 2012) |
| MB | Rat | 50 mg/kg IP | 4 hours, daily | Same performance in behavioural tasks versus sham at 45 days; normalized levels of majority of inflammatory, vascular, neuronal and glial markers | (Kovesdi *et al.*, 2012) |
| WD | Ms | 90 mg/kg IP; 45 mg/kg IP | 5 minutes; 3 hours, 9 hours | Attenuation of recognition memory impairment at 13 weeks; sAPPα decrease significantly attenuated, corpus callosum and striatal atrophy, ventriculomegaly, astrogliosis, and microglial activation significantly reduced at 3 months | (Siopi *et al.*, 2011, 2012) |
| CCI | Rat | 45 mg/kg IP ± NAC | 1 hour, 1 day, 2 days | Improved performance on 2 hour memory task at 1 week; impairment on 24 hour memory task; improved spatial learning (with NAC); reduced myelin loss at 2 weeks (with NAC) | (Abdel Baki *et al.*, 2010) |
| WD | Ms | 90 mg/kg IP; 45 mg/kg IP | 5 minutes; 3 hours, 9 hours | Attenuated microglial activation by 59%; reduced brain lesion volume by 58%; significantly decreased TBI-induced locomotor hyperactivity at 48 hours to 8 weeks | (Homsi *et al.*, 2010) |
| WD | Ms | 45 or 90 mg/kg (1st dose); | 5 min or 5 min + 3 hours or | Reduced increase of IL1β and MMP9 at 6 hours, reduced cerebral oedema at 6 hours (2x doses) and | (Homsi *et al.*, 2009) |

| Model and species | | Dose | Dose intervals | Outcomes with minocycline | Ref. |
|---|---|---|---|---|---|
| | | 45mg/kg (subsequent) | 5 min + 3 hours + 9 hours | 24 h ours (3x doses), improved neurological recovery (3x doses) | |
| WD | Ms | 45 mg/kg IP | 30 min, 12 hourly for 3 days | Decrease lesion volume and improved neurological recovery at 1 day not maintained at 4 days; microglial activation and IL1β expression reduced, neutrophil infiltration and expression of multiple cytokines not affected; density of apoptotic cells not affected | (Bye *et al.*, 2007) |
| CCI | Ms | 90mg/kg IP; 45mg/kg IP | 12 hours pre-; 30min post, 12 hourly | Improved functional outcome; decrease in lesion size; reduced caspase-1 activity | (Sanchez Mejia *et al.*, 2001) |

Studies are listed in descending order of publication date. Abbreviations: CCI = controlled cortical impact; MB = mild blast TBI; Ms = mouse; IL1β = interleukin 1 beta; IP = intraperitoneal MMP9 = matrix metalloproteinase 9; sAPPα = soluble form α of APP (thought to be neuroprotective after TBI); WD = weight drop

While all of the studies summarised have investigated short-term treatments of minocycline administered within minutes to hours after injury, five studies examined neurological recovery of animals to beyond one month post injury. In four of these studies, neurological improvement was sustained for up to three months survival in animals treated with minocycline (Homsi *et al.*, 2010; Kovesdi *et al.*, 2012; Ng *et al.*, 2012; Siopi *et al.*, 2012), although in one study there was only a transient improvement in recovery compared to vehicle-treated animals (Bye *et al.*, 2007).

No experimental studies in TBI have investigated the effect of minocycline first administered during what could be considered the chronic stage after injury. Experimental studies of minocycline administered in this delayed phase will be important in supporting any case for its use as a modulator of chronic neuroinflammation after TBI.

### Experimental studies of minocycline in neurodegenerative disease

Studies of minocycline in chronic neurodegenerative diseases, including AD, may be seen as increasingly relevant to TBI as the pathophysiological links

between TBI and subsequent long-term neurodegeneration become clearer (Johnson *et al.*, 2013; Smith, 2013; Smith, Johnson and Stewart, 2013).

Minocycline has been shown to inhibit microglial-mediated inflammation in a variety of neurodegenerative disease models (Kim and Suh, 2009). For example, *in vivo* and *in vitro* studies of minocycline in models of AD have showed reduced microglial activation, attenuated neuronal cell death and improved behavioural performance (Kim and Suh, 2009).

### Clinical trials of minocycline in CNS disorders

The promise shown by minocycline in experimental studies, its established use as an antibiotic, as well as its excellent CNS penetration, fuelled interest in the drug as a possible treatment of neurological disease (Blum *et al.*, 2004; Domercq and Matute, 2004; Chen *et al.*, 2011). This prompted human minocycline studies in a variety of CNS disorders (Table 4). There are no published clinical studies of minocycline treatment in TBI.

**Table 4. Clinical studies of minocycline**

| Dx | Des | N/tot | Age | Dose and duration | | Outcomes with minocycline | Ref. |
|---|---|---|---|---|---|---|---|
| HIV | RCT | 36/73 | 20-60 | 100mg BD | 24w | No improvement in HIV-associated cognitive impairment | (Nakasujja *et al.*, 2013) |
| HIV | RCT | 52/107 | 50±7 | 100mg PO BD | 6m | No improvement in HIV-associated cognitive impairment | (Sacktor *et al.*, 2011) |
| SCI | RCT | 27/52 | 41 | 800 mg IV → 400mg BD IV | 7d | Improvement in motor score in subgroup of patients with cervical injury | (Casha *et al.*, 2012) |
| MSA-P | RCT | 32/63 | 63±7 | 200mg PO OD | 12m | No difference in clinical motor function | (Dodel *et al.*, 2010) |
| Acute stroke | RCT | 47/95 | 68±11 | 100mg IV BD 12h | 5d | Minocycline safe but not efficacious | (Kohler *et al.*, 2013) |
| Acute stroke | NRDE | 60/89 | 65±13 | 3-10mg/kg BD IV | 3d | Minocycline well tolerated; reduced IL-6 | (Fagan, Cronic and Hess, 2011) |

| Dx | Des | N/tot | Age | Dose and duration | | Outcomes with minocycline | Ref. |
|---|---|---|---|---|---|---|---|
| Acute stroke | RCT | 23/50 | 53±15 | 200mg PO OD 12h | 5d | Improvement in NIHSS, mRS, BI scores significant at days 30 and 90 | (Padma Srivastava *et al.*, 2012) |
| Acute stroke | RCT | 74/152 | 67±11 | 200mg PO OD 6-24h | 5d | Improvement in NIHSS, mRS, BI at days 7, 30, and 90 | (Lampl *et al.*, 2007) |
| MS | RCT | 44 | | 100mg PO BD | 9m | Reduced MRI lesions and relapse risk | (Metz *et al.*, 2009) |
| MS | Pilot | 10 | 42±4 | 100mg PO BD | 6m – 3y | Minocycline safe and well tolerated. Reduced relapse rate during treatment, stable mean T2 lesion volume | (Zhang *et al.*, 2008) |
| ALS | RCT | 206/412 | 59±12 | 400mg PO/day (up to) | 9m | Decline in ALSFRS-R, tendencies towards faster decline in other measures and mortality | (Gordon *et al.*, 2007) |
| ALS | RCT | 10/19 | 54±12 | 200mg PO OD | 6m | Decline in ALSFRS-R | (Gordon *et al.*, 2004) |
| ALS | Pilot | 23/23 | 57±11 | 400mg PO OD (up to) | 8m | Trend toward more gastrointestinal AE, blood urea nitrogen and liver enzymes elevated | (Gordon *et al.*, 2004) |
| PD | RCT | 66/200 | 65±11 | 200mg PO OD | 12m | Futility study; minocycline did not adversely influence the response to symptomatic therapy nor increase AE | (NET-PD, 2006) |
| HD | RCT | 87/114 | | 200mg PO OD | | Futility study; no safety abnormalities. Further study of minocycline 200 mg/day not warranted. | (HSG, 2010) |
| HD | Pilot | 30/30 | 21-66 | 100mg PO BD | 6m | Minocycline well tolerated | (Thomas, Ashizawa and Jankovic, 2004) |
| HD | Pilot | 14/14 | 20-65 | 100mg PO BD | 24 m+ | Minocycline well tolerated. Amelioration of psychiatric symptoms. MMSE, TMS, TFCS, stabilized after 3 years of treatment. | (Bonelli *et al.*, 2004) |

| Dx | Des | N/tot | Age | Dose and duration | Outcomes with minocycline | Ref. |
|---|---|---|---|---|---|---|
| HD | RCT | 60/60 | 46±9 | 100mg PO BD or 100mg PO BD 8w | Minocycline safe and well tolerated. | (HSG, 2004) |

Age is stated in years. Abbreviations: AE = adverse events; AIMS = abnormal involuntary movement score; ALSFRS-R = ALS functional rating scale; BD = twice daily; BI = Barthel Index; Dx = disorder; GA = glatiramer acetate; HIV = human immunovirus; IL-6 = interleukin-6; IV = intravenous; MMSE = mini mental state examination; mRSS = modified Rankin Scale; MSA-P = multiple system atrophy Parkinson type; NIHSS = National Institutes of Health Stroke Scale; N/tot = N (minocycline)/total; NRDE = non-randomised dose escalation study; OD = once daily; PO = oral; RCT = randomised controlled trial or study (minocycline vs placebo/other control); TFCS = total functional capacity scale; TMS = total motor score; TPA = tissue plasminogen activator; UHDRS = unified Huntington's disease rating scale; Times: d = day; w = week; m = month; y = year

A number of clinical trials reported beneficial effects of minocycline treatment without increased incidence of severe adverse events, and the success of some studies generated optimism that minocycline may be translated into neurological practice (Plane *et al.*, 2010). However, other studies showed no benefit, and some have raised serious concerns. The most relevant studies are discussed in more detail.

In multiple system atrophy-Parkinson type (MSA-P), a RCT in 63 patients found no significant difference in clinical disease progression between minocycline (200mg/day) and placebo groups after one year of treatment (Dodel *et al.*, 2010). Notably, this study used TSPO PET to measure the effects of minocycline on microglial activation in a small subgroup of patients. Eight participants (minocycline n = 3, placebo n = 5) underwent PET scanning using [$^{11}$C]PK11195 at baseline and after 24 weeks. At baseline, increased [$^{11}$C]PK11195 binding was evident in regions including the putamen, thalamus and frontal cortex. At 24 weeks, the three patients in the minocycline group had an attenuated mean increase in microglial activation as compared to the placebo group (p=0.07), with two of them individually showing decreased [$^{11}$C]PK11195 binding.

In a study of patients with ALS, following successful animal work and two feasibility studies (Gordon *et al.*, 2004), a multi-centre randomised placebo-controlled phase III trial of minocycline versus placebo found minocycline to

have detrimental effects (Gordon *et al.*, 2007). 412 patients received minocycline at doses up to 400 mg/day or placebo for 9 months. Outcome measures included the revised ALS functional rating scale (ALSFRS-R), forced vital capacity (FVC), manual muscle testing scores, quality of life, survival, and drug safety. Patients treated with minocycline showed faster deterioration than the placebo group in ALSFRS-R scores and there was a trend towards faster decline in FVC and manual muscle testing. The mean rate of decline in ALSFRS-R was not affected by minocycline dose. Despite the unfavourable effects of minocycline treatment on disease progression and adverse events, there was no significant difference in quality of life scores compared to the placebo group.

In patients with acute SCI, a double-blind RCT investigated a dosing regime of minocycline administered for seven days at doses including those higher than previously reported in humans (Casha *et al.*, 2012). Adverse events did not vary significantly among the placebo, low-dose or high-dose minocycline groups. Overall, there was not a significant improvement in motor recovery at one year in minocycline treated patients versus placebo, but an improvement in motor score that approached significance was observed in patients with cervical injury ($p = 0.05$).

In acute stroke, an RCT of oral administration of 200 mg daily of minocycline versus placebo for five days, started six to 24 hours after acute stroke, found minocycline was associated with significantly improved functional outcome scores up to 90 days of follow-up (Lampl *et al.*, 2007). Similar positive outcomes were seen in a later RCT of a similar design (Padma Srivastava *et al.*, 2012). Recently, in another RCT in acute stroke (Kohler *et al.*, 2013), minocycline 100mg was administered intravenously within 24 hours of onset of stroke and continued 12 hourly for a total of five doses. Minocycline was found to be safe but not efficacious. An accompanying meta-analysis of the three human trials suggested minocycline may increase the odds of handicap-free survival by three-fold but found substantial heterogeneity among the trials.

## Pharmacology of minocycline

Tetracyclines were discovered in the 1940s as natural fermentation products of soil bacterium, *Streptomyces aureosaciens* (Nelson and Levy, 2011). Minocycline is a second-generation semi-synthetic tetracycline analogue, with the same basic ring structure as tetracycline but with a substitution of a dimethylamino group at C7 and lacking a functional group at C6, making it more lipophilic (Kim and Suh, 2009).

*Absorption*

Minocycline shows a more favourable pharmacokinetic profile than the first-generation tetracyclines (Garrido-Mesa, Zarzuelo and Gálvez, 2013a). Minocycline is rapidly and almost completely absorbed (95-100%) from the stomach and small bowel (Saivin and Houin, 1988). Unlike first-generation tetracyclines, absorption of minocycline is not affected by food, however absorption is reduced by iron and antacids containing magnesium and calcium (BNF, 2012).

The maximum serum concentration (Cmax) of minocycline is attained within about 2-3 hours after oral administration (Saivin and Houin, 1988). The Cmax increases with increasing dose, being 2.2mg/l after 150mg, 3-3.6mg/L after 200mg and about 4mg/l after a 300mg dose (Saivin and Houin, 1988; Agwuh and MacGowan, 2006). After intravenous (IV) administration, the Cmax concentrations are 3–8.75 mg/l after a 200 mg dose (Saivin and Houin, 1988). After long term administration of minocycline 100mg 12-hourly, the steady state concentration is between 2.3 and 3.5mg/l (Saivin and Houin, 1988).

*Distribution and CNS penetration*

Minocycline plasma protein binding is between 70-80% and the volume of distribution ranges from 80-115L, or 1.17 L/kg (Agwuh and MacGowan, 2006). Minocycline is a small (495 kDa), highly lipophilic molecule with excellent distribution in all the tissues (Saivin and Houin, 1988). It can easily pass through the BBB into the CSF (Yong *et al.*, 2004). In humans, minocycline penetrates the CSF better than doxycycline and other tetracyclines (Macdonald *et al.*,

1973; Cunha, 2000). The CSF concentration after extended dosing is approximately 0.5 mg/L (Saivin and Houin, 1988). The ratio of CSF:plasma concentrations reported is about 11-56% (Cunha, 2000; Elewa *et al.*, 2006).

*Metabolism and excretion*

Minocycline is subject to biotransformation in the liver (Saivin and Houin, 1988). Up to six metabolites have been found in urine and faeces (Agwuh and MacGowan, 2006). Elimination of unaltered minocycline in the urine represents 8-12% of the administered dose, faecal elimination of the compound is 20 to 35% of the dose, and the rest is eliminated as metabolites in urine or faeces (Saivin and Houin, 1988). Renal clearance is about 2.2–1.2 mL/min (Agwuh and MacGowan, 2006).The elimination half-life of minocycline is about 16 hours (Saivin and Houin, 1988).

### Safety and tolerability of minocycline

A good safety record for long-term clinical use of minocycline has been established (Garrido-Mesa, Zarzuelo and Gálvez, 2013a). Chronic treatment with dosages of up to 200 mg/day is generally well-tolerated (BNF, 2012). According to registry records in the UK, over six million individuals have been treated for acne with minocycline for an average of nine months (Yong *et al.*, 2004).

Safety and tolerance in long-term treatment with minocycline doses of 200 mg/day has been demonstrated by tolerability tests and clinical trials in a variety of CNS and other diseases (Garrido-Mesa, Zarzuelo and Gálvez, 2013a), although doses beyond this level may be less well tolerated. For example, in an early phase placebo-controlled trial of minocycline in ALS, there were no significant differences in adverse events at doses of 200 mg/day for six months (Gordon *et al.*, 2004). However, in a subsequent trial, 23 subjects received up to 400 mg/day for an eight month period. Nineteen patients tolerated the target dose of minocycline, and the mean tolerated dose was 387 mg/day. There was a trend towards more gastrointestinal side effects compared to placebo ($p=0.057$) and liver and renal function measures were elevated at the higher

doses (Gordon *et al.*, 2004). In the phase III trial in ALS (above), the number of serious adverse events during the nine month study period did not differ significantly between groups but patients in the minocycline group were more likely to have non-serious gastrointestinal or neurological adverse events than those in the placebo group (Gordon *et al.*, 2007). The most common non-serious gastrointestinal adverse events were nausea, diarrhoea, and constipation. The most frequent non-serious neurological events were dizziness and fatigue.

Rare side effects of minocycline include hearing loss, hyperaesthesia, acute renal failure, skin photosensitivity and hyperpigmentation, which may be irreversible (BNF, 2012). Serious cases of liver toxicity, serum sickness, and systemic lupus erythematosus have been reported but the frequency of these adverse events is of the order of one in a million individuals treated (Yong *et al.*, 2004).

Chapter 2

# 2. Amyloid pathology and axonal injury after brain trauma

In this chapter, I investigate the relationship between Aβ plaque burden and traumatic axonal injury after TBI using [$^{11}$C]PIB PET and diffusion MRI, and compare the spatial distribution of Aβ to AD.

## 2.1. Abstract


### Objective

To image Aβ plaque burden in long-term survivors of TBI, to test whether traumatic axonal injury and Aβ are correlated, and compare the spatial distribution of Aβ to AD.

### Methods

Patients 11 months to 17 years after moderate-severe TBI had [$^{11}$C]PIB PET, structural and diffusion MRI and neuropsychological examination. Healthy aged controls and AD patients had PET and structural MRI. Binding potential (BP) images of [$^{11}$C]PIB, which index Aβ plaque density, were computed using an automatic reference region extraction procedure. Voxelwise and regional differences in BP were assessed. In TBI, a measure of WM integrity, FA, was estimated and correlated with [$^{11}$C]PIB BP.

### Results

28 participants (9 TBI, 9 controls, 10 AD) were assessed. Increased [$^{11}$C]PIB BP was found in TBI versus controls in the PCC and cerebellum. Binding in the PCC increased with decreasing FA of associated WM tracts, and increased

with time since injury. Compared to AD, binding after TBI was lower in neocortical regions, but increased in the cerebellum.

**Conclusions**

Increased Aβ burden was observed in TBI. The distribution overlaps with, but is distinct from, that of AD. This suggests a mechanistic link between TBI and the development of neuropathological features of dementia, which may relate to axonal damage produced by the injury.

## 2.2. Introduction

TBI is a leading cause of disability in young adults (Fleminger and Ponsford, 2005). Survivors may deteriorate clinically many years after injury, and TBI is thought to be a major risk factor for dementia (Smith, Johnson and Stewart, 2013). However, the mechanisms relating acute injury to later neurodegeneration are unclear, and the prevalence of distinct types of post-TBI dementia such as AD and CTE is uncertain (Smith, Johnson and Stewart, 2013).

A mechanistic link between moderate-severe TBI and AD is suggested by the observation that Aβ aggregates are found in brains of up to a third of patients who die acutely after TBI (Smith, Johnson and Stewart, 2013), and in a similar proportion who survive for a year or more (Johnson, Stewart and Smith, 2012). TAI, a pathology consistently observed after TBI (Johnson, Stewart and Smith, 2013), offers a potential mechanism for Aβ genesis (Johnson, Stewart and Smith, 2010). It is postulated that APP, which accumulates in damaged axons, is aberrantly cleaved to form Aβ, which subsequently aggregates as Aβ plaques (Johnson, Stewart and Smith, 2010). Immunohistochemical evidence also shows that the enzymes necessary for Aβ cleavage accumulate at sites of TAI (Johnson, Stewart and Smith, 2010).

Localization of fibrillar Aβ pathology in vivo is possible using PET. The amyloid tracer [$^{11}$C]PIB shows robust retention in brains of AD patients (Quigley, Colloby and O'Brien, 2011) in a pattern that corresponds with neuropathological studies

of Aβ plaque distribution, with increases initially in the precuneus/ PCC, frontal cortex, and caudate nuclei, then lateral temporal and parietal cortex (Rowe *et al.*, 2007). Recently, a pilot [$^{11}$C]PIB PET study in moderate-severe TBI patients less than one year after injury found increased uptake in cortical GM and striatum (Hong *et al.*, 2014). These findings suggest Aβ imaging in the chronic phase after TBI may inform our understanding of neurodegeneration in long-term survivors of TBI.

DTI can be used to estimate in vivo the degree of axonal injury following TBI (Mac Donald *et al.*, 2007; Sharp *et al.*, 2011; Sharp, Scott and Leech, 2014; Magnoni *et al.*, 2015). Here, we combine [$^{11}$C]PIB PET and DTI to test the hypotheses: (1) Aβ pathology is present in long-term non-demented survivors of TBI; (2) Aβ pathology after moderate-severe TBI is related to the amount and distribution of TAI.

## 2.3. Methods

### Study design and participants

In this cross-sectional study, nine TBI patients with a history of a single moderate-severe TBI based on Mayo criteria (Malec *et al.*, 2007) were assessed with [$^{11}$C]PIB PET, structural T1 MRI, DTI and neuropsychological examination. Patients were recruited at least 11 months after their injury from specialist TBI clinics. Eligible patients had a history of a single moderate-severe TBI based on Mayo criteria, without pre-existing psychiatric or neurological illness, a history of other significant TBI, current or previous drug or alcohol abuse, pregnancy or breast feeding, or contraindications to MRI.

For comparison of [$^{11}$C]PIB binding, a group of patients with a diagnosis of clinically probable idiopathic AD based on NINDS-ADRDA criteria (McKhann *et al.*, 1984) had [$^{11}$C]PIB PET and structural MRI. AD patients were recruited from specialist dementia clinics at the Hammersmith Hospitals Trust and the National Hospital for Neurology and Neurosurgery, London, UK.

Data were collected between 2006 and 2010. Controls were recruited by local advertisement and from spouses of patients. We derived the study sample size on the basis of earlier PET studies that had explored PIB binding in AD patients and control subjects (e.g. (Klunk *et al.*, 2004)).

We used three healthy controls groups. (a) For comparison of [$^{11}$C]PIB binding, a group of healthy aged controls had [$^{11}$C]PIB PET and structural MRI. (b) For comparison of neuropsychological performance, a second group of healthy controls, age-matched to the TBI patients, underwent neuropsychological assessment. (c) For comparison of WM integrity, a third group of healthy aged-matched controls underwent structural MRI and DTI.

The project was approved by Hammersmith and Queen Charlotte's and Chelsea Research Ethics Committee. All participants gave written informed consent.

### Procedures

A neuropsychological test battery was performed on TBI patients and age-matched controls. The test battery was designed to assess domains of cognitive function often observed to be impaired following TBI. The Verbal Fluency/Letter Fluency (F + A + S) and Color-Word Interference subtests from the Delis-Kaplan Executive Function System (D-KEFS) (Delis, Kaplan and Kramer, 2001) were administered to assess word generation fluency, complex information processing speed, inhibition and cognitive flexibility. The Trail Making Test (TMT) (Reitan, 1958) was used to assess basic perceptual and complex processing speed, attentional capacity, set maintenance and set shifting. A computerised two-choice left/right (<<< or >>>) button-press CRT was used as a simple measure of processing speed (median reaction time on correct trials). The TMT Part A, as well as the two baseline conditions of the D-KEFS Color-Word Interference test, Color Naming and Word Reading also measured simple processing speed. The Digit Span subtest of the Wechsler Memory Scale – Third Edition (WMS-III) (Wechsler, 1997) assessed initial and working memory. The Logical Memory I and II subtests of the WMS-III were used as a measure of immediate and delayed verbal recall. The People Test

(PT) from the Doors and People Test battery (Baddeley, Emslie and Nimmo-Smith, 1994) was used as a measure of associative learning and recall (immediate recall). In addition, the Wechsler Test of Adult Reading (WTAR) (Wechsler, 2001) was used to provide an estimate of pre-morbid intellectual functioning. Current verbal and nonverbal reasoning ability were assessed via the Wechsler Abbreviated Scale of Intelligence (WASI) (Wechsler, 1999) Similarities and Matrix Reasoning subtests. 15 age-matched controls (12 males, mean age 37.3±11.3 years, range 19-60 years) underwent neuropsychological assessment. Following exploratory data analysis, control subjects identified as extreme outliers (≥ 3 x interquartile range) were excluded from subsequent analyses. Group differences in neuropsychological measures were examined using independent sample t-tests, using Levene's test for equality of variances. We repeated the analyses using Mann-Whitney U tests. All tests were performed using SPSS Version 21. The number of patient and control subjects used for each test as well as Cohen's d values (Cohen, 2013) are shown in

Table 6.

Patients with AD and healthy aged controls underwent the MMSE.

An overview of the imaging methods is shown in Figure 11. All patients and healthy aged controls had [$^{11}$C]PIB PET using a Siemens ECAT EXACT HR+ scanner (Siemens Medical Systems, Erlangen, Germany). [$^{11}$C]PIB was manufactured and supplied by Hammersmith Imanet (London, UK). All participants had an intravenous bolus injection of [$^{11}$C]PIB, mean dose 370 MBq, and dynamic PET emission scans were acquired over 90 minutes.

### Procedure for automatic reference region extraction

To generate non-displaceable binding potential (BP) images of [$^{11}$C]PIB, a supervised clustering procedure for automatic reference region extraction was used. [$^{11}$C]PIB binding in AD and healthy aging studies is usually quantified using the cerebellum as a reference region, where it is assumed that Aβ plaque density (and hence minimal specific binding) is minimal. Under this assumption, the ratio of cortical to cerebellar binding provides an accurate measure of cortical Aβ burden (Rowe and Villemagne, 2011). If there is significant Aβ plaque pathology in the cerebellum, however, then this assumption is invalid. For example, cerebellar binding is observed in certain types of familial AD (Knight *et al.*, 2011).

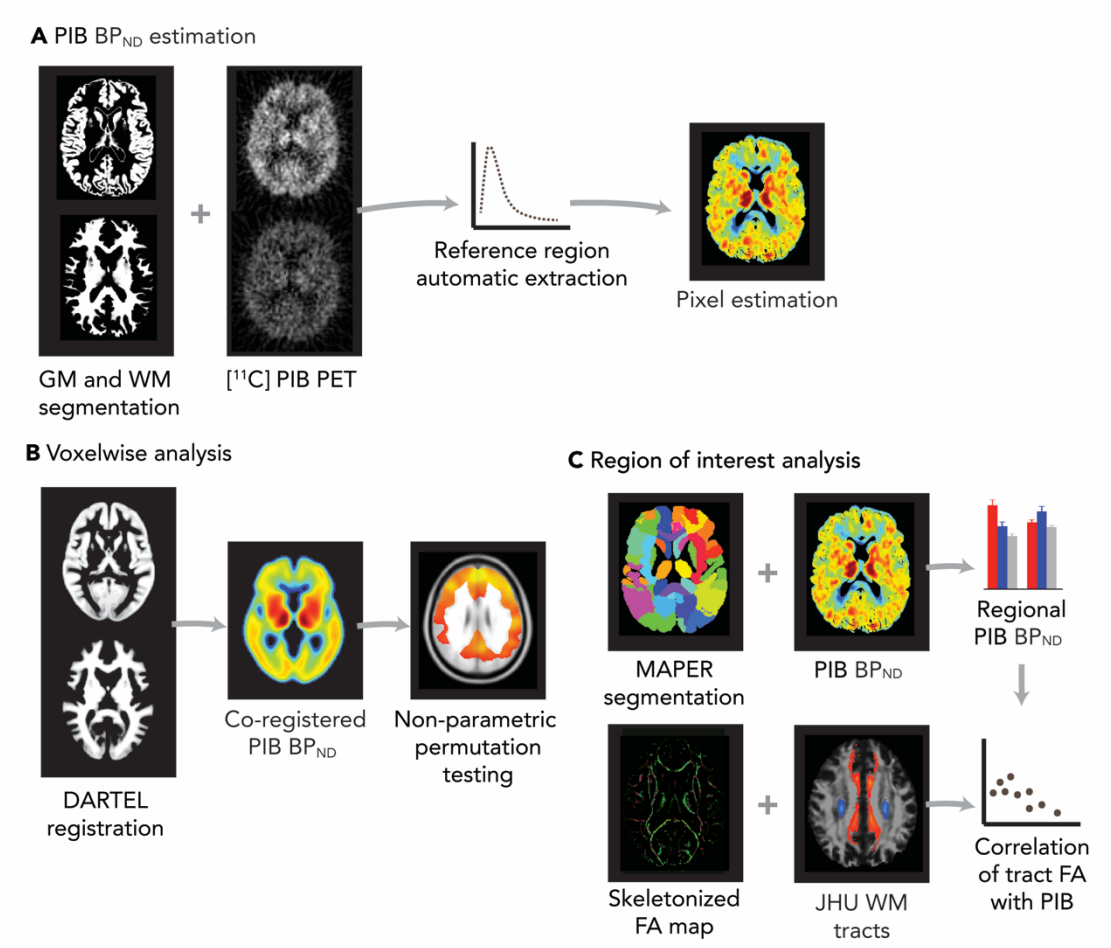



**Figure 11. Overview of [$^{11}$C]PIB imaging analysis**

(A) Binding potential (BP) images of [$^{11}$C]PIB, proportional to amyloid-β plaque density, were estimated from dynamic [$^{11}$C]PIB PET data with an automatic reference region extraction procedure, using GM and WM segmentations from T1 MRI to define tissue classes. (B) GM and WM segmentations were warped to a group template image using a diffeomorphic non-linear image registration procedure (DARTEL). The same normalisation was applied to [$^{11}$C]PIB BP images. Voxelwise differences in BP between groups were assessed using non-parametric permutation tests. (C) Native space anatomical regions of interest (ROIs) for sampling BP were generated using the MAPER (multi-atlas propagation with enhanced registration) procedure. In TBI patients, fractional anisotropy (FA), a measure of WM integrity, was sampled from the skeletonized WM tracts defined by the Johns Hopkins University WM tractography atlas, and related to regional [$^{11}$C]PIB binding.

It was unclear whether cerebellar Aβ plaque pathology is present in the chronic phase, and our initial analyses using the cerebellum as a reference region suggested increased cerebellar binding (i.e. values <1 for the cortical/cerebellar ratio). For these reasons, we used a supervised clustering method (Ikoma *et al.*, 2013). This analysis approach models each gray matter voxel as the linear combination of three predefined kinetic classes (normal grey matter, lesion grey matter, and blood pool), and extracts reference voxels in which the contribution

of the normal gray matter class is high. This approach has been validated in idiopathic AD and shown to be effective in familial AD, where increased cerebellar uptake has been demonstrated. The automated reference region extraction procedure and pixel estimation were carried out as described in (Ikoma *et al.*, 2013) to produce individual [$^{11}$C]PIB BP images in native space. A qualitative assessment of the automatically selected reference voxels found they were not located in the same areas as those showing statistically significant increases in binding in TBI patients.

### PET and T1 processing

PET and T1 MRI data were processed in SPM8. T1 images were automatically segmented into GM and WM (Ashburner and Friston, 2005). The tissue segmentations were warped to a group template image, representing the average of all participants (TBI, AD, healthy aged controls), with a diffeomorphic non-linear image registration procedure (DARTEL), and the group template image registered to Montreal Neurological Institute (MNI) space using affine registration. This procedure is a standard feature of the DARTEL implementation of SPM8, whereby the complete transformation from each individual's native T1 to MNI is achieved by applying the individual flow-fields to the T1 followed by the affine transformation from template to MNI space. Each individual's [$^{11}$C]PIB BP image was registered to the T1 image using affine registration. The DARTEL transformation to MNI space was then used to warp the T1 space BP image to MNI space.

For voxelwise statistical analysis, the normalized PET images obtained were masked so as to include only GM voxels of interest, and to prevent any overlap between voxels included in analyses with GM and those with WM. The GM mask was obtained by thresholding the GM customized template to >0.3. This approach has the benefit of reducing possible edge effects around the border between GM, WM and CSF (Chetelat *et al.*, 2008; Villain *et al.*, 2008; Oh *et al.*, 2013). The same binary mask was applied twice, before and after smoothing, to avoid contamination of misclassified voxels by smoothing in the first case, and large edge effects in the second case (Chetelat *et al.*, 2008). For

smoothing, we used a Gaussian kernel of 8mm full-width at half-maximum (FWHM).

### Region of interest analysis

[$^{11}$C]PIB binding potentials were also sampled from anatomically defined ROIs. The selection of ROIs was independent of the voxelwise results and similar to our previous work (Ramlackhansingh *et al.*, 2011). The MAPER (multi-atlas propagation with enhanced registration) procedure was used to generate ROIs in native space (Heckemann *et al.*, 2006, 2010). This approach minimises the potential sampling error associated with misregistration and brain atrophy. The procedure has previously been shown to yield accurate and robust segmentations in normal subjects and patients with dementia.

The following regions were chosen to provide a representative sampling of cortical and sub-cortical structures and to include a number of regions likely to be affected by TBI: the anterior and posterior cingulate cortices, inferior and superior frontal gyri, occipital lobes, hippocampi, cerebellum, caudate, putamen, and thalamus. Bilateral masks were combined into a single ROI.

To improve sampling accuracy, ROI masks were intersected with thresholded tissue probability maps determined from MRI. As in (Ikoma *et al.*, 2013), a 90% threshold (i.e. >0.9) was applied to the GM and WM probability maps to create tissue-specific masks. The cortical and cerebellar ROIs were then intersected with the GM tissue mask, and subcortical regions with the union of GM and WM masks.

To confirm that the hippocampal ROI results were not an effect of mislabeling due to atrophy, sampling was repeated on hippocampal masks that were manually segmented using a harmonized protocol (Frisoni and Jack, 2011).

### Manual segmentation and sampling of lesions

In TBI patients with focal injuries, lesions apparent on T1 imaging were manually segmented. Voxels corresponding to lesions were excluded from ROI and voxelwise analyses. In the ROI analysis, voxels which occurred within a lesion mask were excluded from calculation of the mean regional binding of

ROIs. In the voxelwise analyses, the statistical contrasts incorporated a tool which uses voxelwise regressors to exclude individual (inconsistently located) lesions from the analysis (http://fsl.fmrib.ox.ac.uk/fsl/fslwiki/Randomise/UserGuide#Lesion_Masking). A group lesion map was also created by summing the co-registered lesion masks.

We also investigated [$^{11}$C]PIB binding within lesions, the lesion penumbra, and normal-appearing gray matter in the same hemisphere. We defined spherical ROIs with a 4 mm radius around the most prominent lesion and in the gray matter of the superior temporal gyrus on the same side, as this region was not seen to be affected by lesions in any patients.

### Diffusion tensor image acquisition

TBI patients and a group of healthy aged-matched controls had DTI. For DTI in TBI patients, diffusion-weighted volumes with gradients applied in 16 non-collinear directions were collected in each of the four DTI runs, resulting in a total of 64 directions. The following parameters were used: 73 contiguous slices, slice thickness = 2 mm, field of view (FOV) 224 mm, matrix 128 × 128 (voxel size = 1.75 × 1.75 × 2 mm$^3$), b value = 1000, and four images with no diffusion weighting (b = 0 s/mm$^2$).

### Diffusion tensor imaging analysis

The images were registered to the B0 image by affine transformation. For brain extraction, BET (Smith, 2002) from the FSL was used (Smith *et al.*, 2004). FA maps were generated using the FSL Diffusion Toolbox (Behrens *et al.*, 2003). Voxelwise analysis of the FA was carried out using TBSS in FSL (Smith *et al.*, 2006). The FA maps were skeletonized, leaving the central section of tracts, reducing the impact of partial volume effects at the edge of tracts. Image analysis using TBSS involved the following steps: A) nonlinear alignment of each individual's FA image into common FMRIB58_FA template space; B) affine transformation of the aligned images into standard MNI152 space; C) averaging of the aligned FA images to create a 4D mean FA image; D) thinning

of the mean FA image to create a mean FA skeleton representing the centre of all WM tracts, and in this way reducing partial-volume confounds; and E) thresholding of the FA skeleton at FA≥0.2 to suppress areas of extremely low mean FA and exclude those with considerable inter-individual variability.

In each individual we then calculated the mean FA sampled from a number of WM tracts defined by the Johns Hopkins University WM tractography atlas (Mori *et al.*, 2000; Wakana *et al.*, 2004; Hua *et al.*, 2008). The probabilistic tracts were thresholded at 95%, and voxels within the FA skeleton were sampled from each tract. We used the left and right cingulum-cingulate tracts (which project from posterior to anterior cingulate cortex) and the left and right cingulum-hippocampus tracts (which project from the posterior cingulate to the hippocampi). These tracts were chosen because they were connected to GM regions which had shown an increased [$^{11}$C]PIB BP. As a control, we also sampled the left and right corticospinal tract, since this was not directly connected to these regions. We also calculated the mean FA of the entire WM skeleton.

### Statistical analysis

Group differences in neuropsychological measures were examined using independent sample t-tests and Mann-Whitney U tests in SPSS Version 21. Voxelwise differences in BP between groups were assessed using non-parametric permutation tests in FSL with 10,000 permutations. Results were cluster corrected using threshold-free cluster enhancement and a family-wise error rate of <0.05. For presentation, images were thresholded at $p<0.001$ uncorrected. For ROI analysis, regional BP was compared using repeated measures analysis of variance (ANOVA) with planned post-hoc comparisons performed between the three groups using independent sample t-tests, in SPSS.

Mean FA values of WM tracts were compared between TBI patients and controls using unpaired two-sample t-tests. Regional [$^{11}$C]PIB was correlated with mean FA values, age, time since injury and neuropsychological test scores. Mean FA values were correlated with age and time since injury. To

correct for multiple comparisons, a false discovery rate threshold was calculated using q=0.05.

## 2.4. Results

Nine TBI patients (mean age 44.1±4.9 years, range 38-54) were recruited 11 months to 17 years after injury (Table 5).

**Table 5. Demographics and clinical data of TBI patients**

| Age | Sex | Education level | Aetiology | Lowest GCS | PTA (hours) | Medication | Time since trauma (months) | Focal lesion/ s |
|---|---|---|---|---|---|---|---|---|
| **45** | M | PG | Unknown | 4 | 24 | Gabapentin Modafinil Amitriptyline | 76 | Yes |
| **55** | M | PG | Fall | 4 | UK | Nil | 28 | Yes |
| **42** | M | School to 18 years | RTA | 4 | 432 | Nil | 72 | No |
| **42** | M | School to 16 years | RTA | 4 | UK | Tropium chloride Folic acid | 198 | Yes |
| **40** | M | Graduate | RTA | 4 | 1008 | Nil | 125 | Yes |
| **42** | F | PG | RTA | 3 | 144 | Codeine Paracetamol | 76 | Yes |
| **45** | M | School to 16 | Assault | 4 | 5040 | Thiamine | 11 | No |
| **49** | M | School to 18 | Probable assault | 4 | 2 | Nil | 11 | No |
| **38** | M | Graduate | RTA | 6 | UK | Citalopram Modafanil Omeprazole | 106 | No |

UK = known; PG = postgraduate; RTA = road traffic accident

Ten AD patients (mean age 67.3±4.5, range 58-76) and nine healthy aged controls (62.3±4.3, 55-66) were also assessed. In addition, a group of 15 age-matched controls (37.3±11.3, 19-60) underwent neuropsychological assessment and a separate group of 11 age-matched controls (40.9±5.4, 35-51) underwent MRI and DTI. None of the patients had a clinical diagnosis of

post-traumatic stress disorder or anxiety disorder. One patient had a diagnosis of depression following the TBI.

Structural T1 scans were reviewed by a senior neuroradiologist. Four TBI patients had no abnormalities. The remaining five had focal lesions, with damage in the frontal (n=3) or temporal (n=3) lobes (Figure 12). One patient had undergone a parieto-temporal lobectomy following TBI.

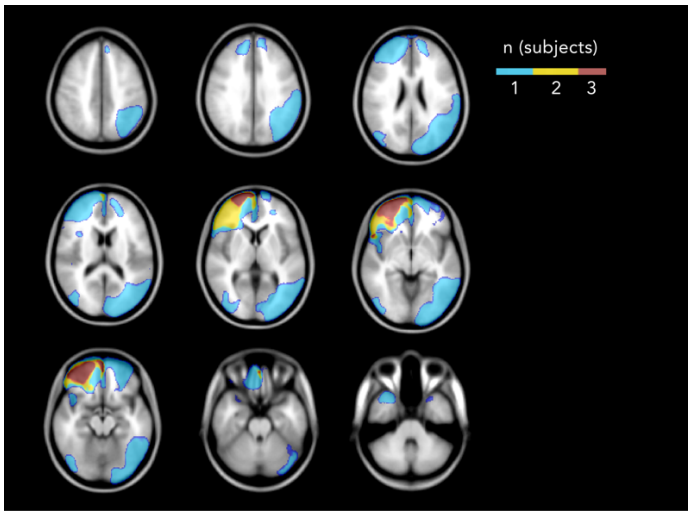



**Figure 12. Lesion map in TBI patients**

Lesion map in TBI patients. Colored regions indicate regions affected by lesions in one or more patients. Maps were formed by summation of the co-registered lesion masks of individual patients. Voxels corresponding to lesions were removed from subsequent analyses (see main text).

## Neuropsychological impairment after TBI

The TBI patients showed impairments in neuropsychological performance compared to age-matched healthy controls. Significantly poorer responses were seen across a range of tasks, including tests of attention, information processing speed, and cognitive flexibility (

Table 6). In other tests the patients were well matched with controls. As expected, the AD group had a lower MMSE (mean 21.1/30±4.1) than healthy aged controls (all 30/30,t=-6.54,df=9,p<0.001).

**Table 6. Neuropsychological test results**

| Cognitive Domain | Cognitive Variable | TBI Mean±SD | Control Mean±SD | TBI vs. Control | Cohen's d |
|---|---|---|---|---|---|
| Information processing speed | | | | | |
| Visual search | TMT Trail A (s) | 32.9±15.4 (N=9) | 19.7±4.5‡ (N=14) | t = 2.50 *† | 1.30 |
| Complex | TMT Trails B (s) | 60.4±28.5 (N=9) | 43.0±12.6‡ (N=14) | t = 1.73 ns | 0.86 |
| Naming | Stroop Colour Naming (s) | 38.6±12.6 (N=8) | 23.3±9.9 (N=14) | t = 3.18 **† | 1.41 |
| Reading | Stroop Word Reading (s) | 26.8±6.6 (N=8) | 28.9±6.3 (N=15) | t = –0.78 ns | -0.34 |
| Complex | Stroop Inhibition (s) | 73.1±30.9 (N=8) | 23.3±4.4‡ (N=15) | t = 4.53 **†† | 2.74 |
| Choice reaction time | CRT median RT (ms) | 459±66 (N=8) | 408±51 (N=15) | t = 2.05 ns | 0.91 |
| Executive function | | | | | |
| Inhibition | Inhibition – naming (s) | 34.5±22.3 (N=8) | 28.7±17.6 (N=15) | t = 0.69 ns | 0.30 |
| Cognitive flexibility | Inhibition/switching – naming + reading ÷ 2 (s) | 50.1±27.8 (N=8) | 32.2±10.5 (N=14) | t = 2.18 *† | 0.97 |
| Word generation fluency | Letter Fluency F+A+S total | 40.4±8.1 (N=8) | 46.0±12.0 (N=15) | t = -1.19 ns | -0.52 |
| Set-shifting | Alternating-switch cost TMT Trails B minus A (s) | 27.7±17.7 (N=9) | 23.3±9.8 (N=14) | t= 0.74 ns | 0.32 |
| Memory | | | | | |
| Immediate/Working | Digit Span forward | 10.4±1.6 (N=9) | 11.5±2.2 (N=15) | t = – 1.27 ns | -0.54 |
| | Digit Span backward | 6.8±1.1 (N=9) | 7.5±2.0‡ (N=15) | t = – 0.94 ns | -0.34 |
| Logical | WMS-III LM I first recall total | 28.6±4.0 (N=8) | 26.4±9.0‡ (N=15) | t = 0.82 ns | 0.29 |
| | WMS-III LM I total | 47.3±5.7 (N=8) | 42.7±13.7‡ (N=15) | t = 1.12 ns | 0.39 |
| | WMS-III LM II delayed | 31.6±5.4 (N=8) | 25.6±9.2 (N=15) | t = 1.69 ns | 0.74 |
| Associative | PT immediate recall total | 25.5±5.9 (N=9) | 26.9±7.1 (N=15) | t = –0.49 ns | -0.20 |
| Intellectual ability | | | | | |
| Reading | WTAR age-scaled score | 107±10.8 (N=8) | 112±9.8 (N=15) | t = – 1.11 ns | -0.49 |

| Cognitive Domain | Cognitive Variable | TBI Mean±SD | Control Mean±SD | TBI vs. Control | Cohen's d |
|---|---|---|---|---|---|
| Verbal | WASI Similarities | 39.3±3.9 (N=8) | 34.5±6.3‡ (N=15) | t = 2.25 * | 0.85 |
| Non-verbal | WASI Matrix Reasoning | 27.9±3.7 (N=9) | 26.8±5.0 (N=15) | t = 0.56 ns | 0.24 |

Neuropsychological results for TBI patient and age-matched control group. Differences in variances between patient and control group (Levene's test for equality of variances $P < 0.05$) shown by ‡. Significant group differences shown by * t-test $P \leq 0.05$ and **t-test $P \leq 0.01$; † Mann-Whitney U $P \leq 0.05$ and †† Mann-Whitney $P \leq 0.01$; ns indicates a non-significant result on t-test and Mann-Whitney U test. TMT = Trail Making Test; Colour Naming, Word Reading, Inhibition, Inhibition/switching, and Letter Fluency are subtests of the Delis-Kaplan Executive Function System; CRT = Choice-Reaction Task; WMS-III = Wechsler Memory Scale-Third Edition; PT = People Test; WTAR = Wechsler Test of Adult Reading; WASI = Wechsler Abbreviated Scale of Intelligence. One patient could not be assessed fully because of an upper limb disability and difficulty communicating verbally.

## Amyloid pathology after TBI detected by [$^{11}$C]PIB binding

[$^{11}$C]PIB BP images of the TBI group are shown for individual patients (Figure 13). Slices from a representative AD patient and healthy aged control are shown.

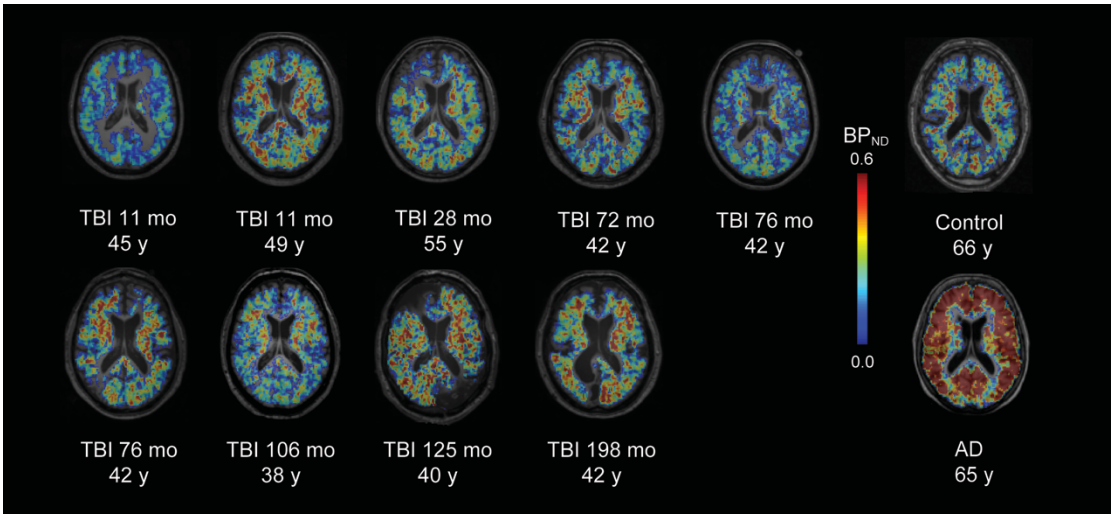



**Figure 13. [$^{11}$C]PIB binding following TBI**

Overlay images of axial T1 magnetic resonance imaging are superimposed with [$^{11}$C]PIB BP maps for all TBI patients and a representative healthy aged control and AD participant. For TBI patients, the interval in months (mo) from the time of TBI to PET scanning and the age in years (y) of each participant at scanning is also shown.

Direct comparison of TBI patients and healthy aged controls showed areas of increased [$^{11}$C]PIB BP following TBI (Figure 14A).

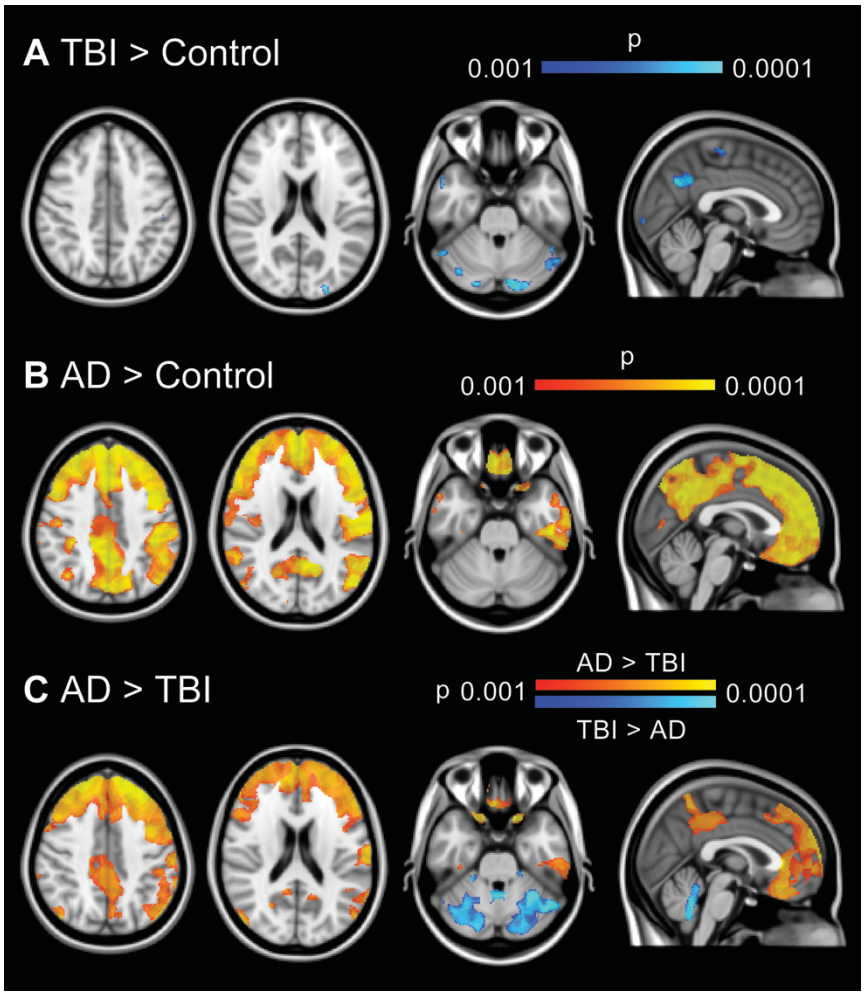



**Figure 14. Increased [$^{11}$C]PIB binding in TBI and AD**

(A) Blue-light blue areas showed significantly increased [$^{11}$C]PIB BP in TBI compared to healthy aged controls. (B) Red-yellow areas showed significantly increased binding in AD compared to controls. (C) Blue-light blue areas showed significantly increased [$^{11}$C]PIB BP in TBI compared to AD. Red-yellow areas showed significantly increased binding in AD compared to TBI. Images are shown thresholded at p <0.001 uncorrected.

Peaks of increased [$^{11}$C]PIB BP corrected for multiple comparisons were observed in the precuneus/PCC and cerebellum. There were no areas of decreased binding in TBI compared to controls.

We performed a confirmatory ROI analysis using anatomically defined regions (Figure 15). ANOVA of BP sampled from 10 ROIs in the TBI and healthy control groups showed a significant group-by-region interaction ($F(3.127,50.036)=2.984, p=0.038$, Greenhouse-Geisser correction applied). The Partial eta-squared effect size estimate was 0.157. The interaction was driven by increased binding in the putamen of TBI patients

(t=2.573,df=16,p=0.020) and a decrease in the superior frontal gyrus (t=-2.312,df=16,p=0.034), but non-significant differences elsewhere.

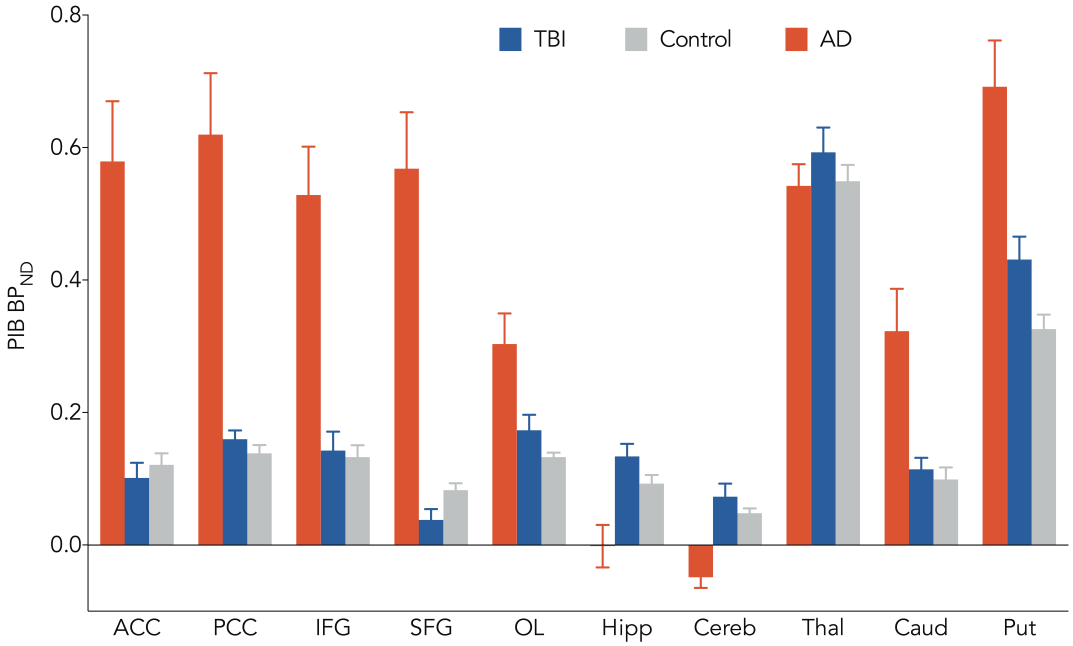



**Figure 15. [$^{11}$C]PIB binding ROI analysis**

Mean group [$^{11}$C]PIB BP ± standard error of the mean is shown for TBI patients (blue), patients with AD (red) and healthy aged controls (grey). AC = anterior cingulate cortex; PC = posterior cingulate cortex; IFG = inferior frontal gyrus; SFG = superior frontal gyrus; OL = occipital lobe; Hipp = hippocampus; Cere = cerebellum; Thal = thalamus; Caud = caudate; Put = putamen.

## [$^{11}$C]PIB binding is decreased around focal lesions

Visual inspection of individual TBI BP images showed no binding in the vicinity of focal cortical lesions evident on structural MR imaging. To confirm this, we sampled binding in ROIs placed in and around the most prominent lesion each brain. As expected, there was no specific binding in the focal lesion. In addition, binding in the penumbra was reduced compared to normal-appearing GM in the same hemisphere (t=-11.54,df=4,p<0.001).

## [$^{11}$C]PIB binding after TBI is correlated with WM damage and time since injury

We next examined whether Aβ plaque pathology in the PCC was associated with the degree of TAI in the TBI patients. We tested the hypothesis that regional GM [$^{11}$C]PIB binding increases with lower FA (indicative of axonal injury) in the cingulum bundles that were directly connected to the PCC (Figure 16A). Mean FA in all tracts examined was reduced as expected (Figure 16B).

PCC BP was negatively correlated with FA in both the left cingulum (R=-0.733,p=0.031) and right cingulum (R=-0.750,p=0.025, Figure 16C), a relationship that survived correction for the age of the patient (R=-0.758,p=0.029;R=-0.787,p=0.020). The mean FA of the WM skeleton also showed a correlation with PCC binding (R=-0.733,p=0.031), although this was only of borderline significance when correcting for age (R=-0.694,p=0.056). There was no significant correlation found with the corticospinal tract FA. [$^{11}$C]PIB binding in the PCC also increased with time since injury duration (R=0.767,p=0.021), although this was not significant after correcting for age (R=0.625,p=0.097). Of the four FA measures, the mean FA of the left cingulum also correlated with time since injury (R=-0.717,p=0.037). There was no independent relationship between [$^{11}$C]PIB binding and FA when after correction for time since injury. There was also no correlation between patient age and [$^{11}$C]PIB binding or FA.

### [$^{11}$C]PIB binding is not correlated with cognitive impairment in TBI

There were no significant correlations between PCC binding and behavioural performance in the TBI patients.

### Distinct distributions of [$^{11}$C]PIB binding in TBI and AD

The direct contrast of AD and controls showed increased [$^{11}$C]PIB binding in AD association cortex and cingulate (Figure 14B). Conjunction analysis showed [$^{11}$C]PIB binding was increased in a cluster within the precuneus/PCC in both AD and TBI compared to controls. In general, [$^{11}$C]PIB binding was higher in AD than TBI across regions but the TBI cases had relatively increased binding in the cerebellum (Figure 2C). Interrogating ROI data with ANOVA confirmed the voxel level findings. All ROI results were similar when the analyses were repeated for manually drawn hippocampal segmentations. There was no correlation between patient age and regional [$^{11}$C]PIB binding within any of the three participant groups.

Increased [$^{11}$C]PIB binding was seen in cortical association and cingulate regions in AD whereas increased cerebellar binding was seen in TBI.

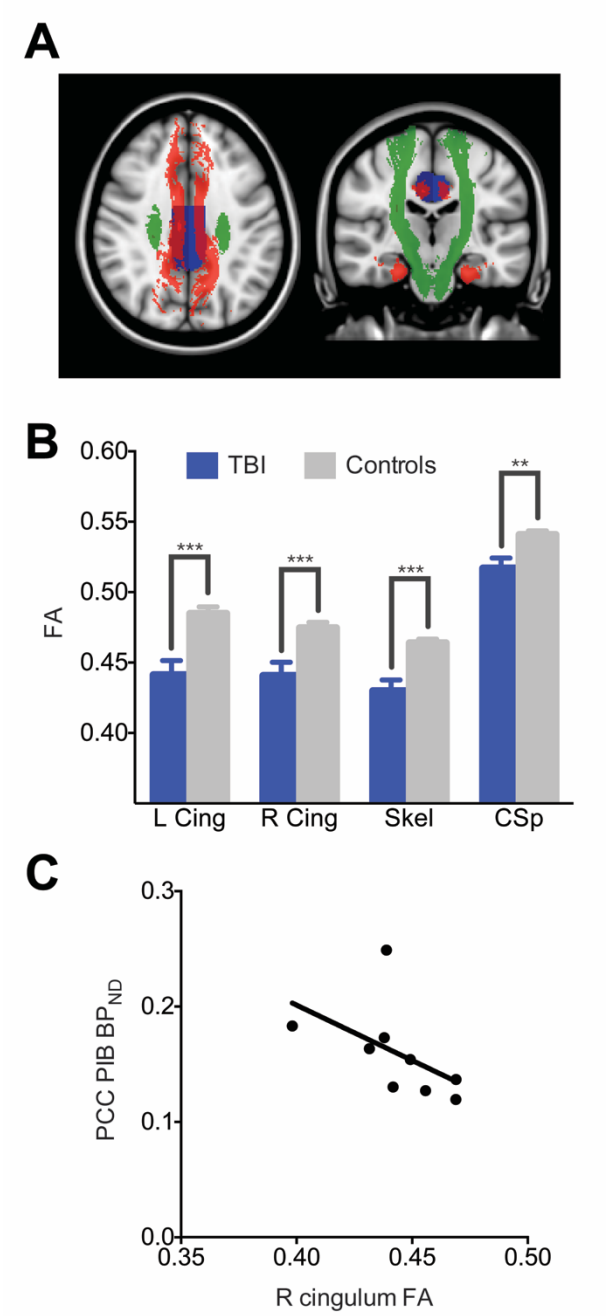



**Figure 16. Relationship between WM damage and regional [$^{11}$C]PIB BP in TBI patients**

(A) Selected WM tracts from the Johns Hopkins University tractography atlas and ROI from the MAPER (multi-atlas propagation with enhanced registration) segmentation are shown on an MNI152 standard image. The tracts in red are the left and right cingulum-cingulate bundle combined with left and right cingulum-hippocampus tract. The regional segmentation of the PCC is shown (blue), which receives connections from these tracts. The corticospinal tract (green) is not connected to the PCC. FA, a measure of white matter integrity, was sampled from the tracts in TBI patients using DTI and related to regional [$^{11}$C]PIB BP sampled in the PCC. (B) The mean FA of all tracts tested was reduced in TBI compared to controls (** = $p<0.01$, *** = $p<0.001$). (C) [$^{11}$C]PIB BP in the PCC increased with decreasing FA in the right cingulum.

ANOVA of BP sampled from 10 ROIs in the AD and TBI groups showed a significant group-by-region interaction ($F(2.227,37.851)=23.64$, $P<0.001$,

Greenhouse-Geisser correction applied). The partial eta-squared effect size estimate was 0.582.

### *Regional differences in AD versus TBI*

There was significantly increased binding in anterior cingulate cortex (ACC) ($t=4.841$, $df=17$, $p<0.001$), PCC ($t=4.653$, $df=17$, $p<0.001$), inferior frontal gyrus (IFG) ($t=4.712$, $df=17$, $p<0.001$), superior frontal gyrus (SFG) ($t=5.792$, $df=17$, $p<0.001$), occipital lobe ($t=2.437$, $df=17$, $p=0.026$), caudate ($t=2.989$, $df=17$, $p=0.008$) and putamen ($t=3.339$, $df=13.030$, $p=0.005$), no difference in the thalamus and decreased binding in hippocampus ($t=-3.532$, $df=17$, $p=0.003$) and cerebellum ($t=-4.786$, $df=17$, $p<0.001$).

### *Regional differences in AD versus controls*

ANOVA in the AD and Control groups also showed a group-by-region interaction ($F(1.996,33.934)=22.148$, $P<0.001$,Greenhouse-Geisser correction applied). The partial eta-squared effect size estimate was 0.566. There was significantly increased binding in ACC ($t=4.688$, $df=17$, $p<0.001$), PCC ($t=4.872$, $df=17$, $p<0.001$), IFG ($t=5.001$, $df=17$, $p<0.001$), SFG ($t=5.349$, $df=17$, $p<0.001$), occipital lobe ($t=3.479$, $df=17$, $p=0.003$), caudate ($t=3.202$, $df=17$, $p=0.005$) and putamen ($t=4.984$ $df=10.720$, $p<0.001$), no difference in the thalamus and decreased binding in hippocampus ($t=-2.611$, $df=17$, $p=0.018$) and cerebellum ($t=-5.433$, $df=12.640$, $p<0.001$).

## Exploring regional PIB binding and time since injury

The relationship between PIB binding and time since injury was explored for three regions, the cerebellum, PCC and putamen (which had all shown increases in either voxelwise or ROI analysis) (Figure 17). This appeared to show a distinct relationship with time for the cerebellum (which shows a decrease with time) compared to the other regions, which both showed increased binding over time.

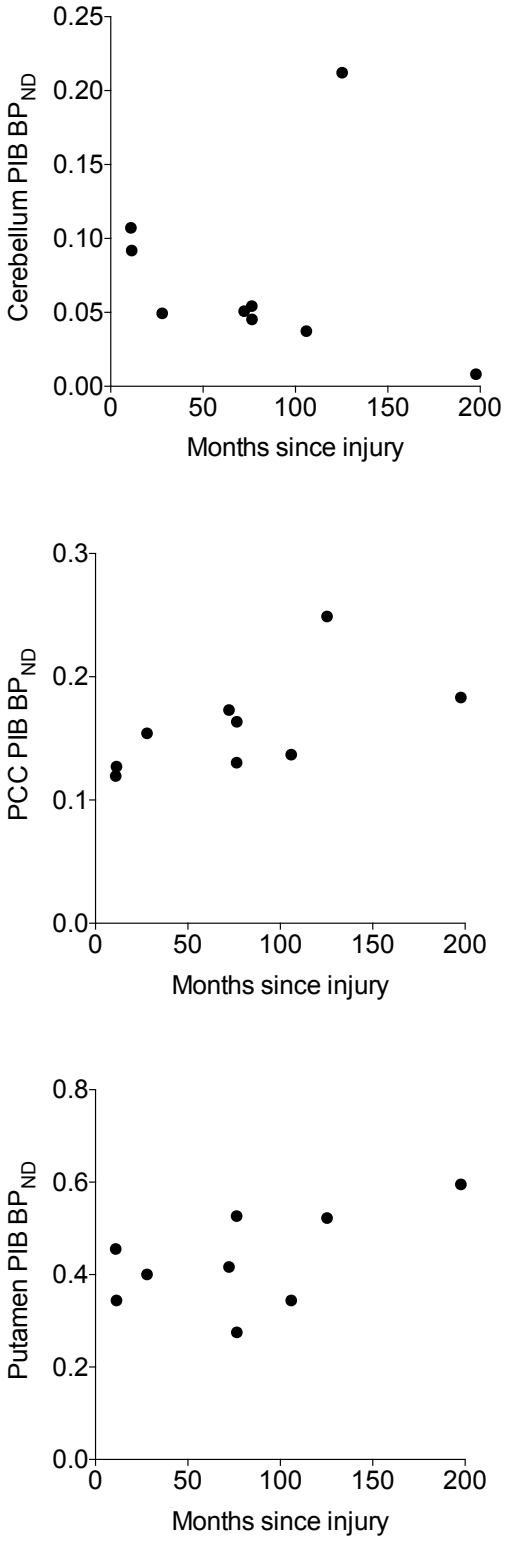



**Figure 17. Relationship between [$^{11}$C]PIB BP and time since injury in TBI patients**

[11C]PIB BP is plotted against time since injury for regions which had shown increases either in ROI analysis or voxelwise analysis: the cerebellum (top), posterior cingulate cortex (PCC) (middle) and putamen (bottom). Note the BP values are derived from ROI analysis in all cases.

## 2.5. Discussion

TBI can predispose patients to various types of dementia, but there is no consensus about how post-TBI dementia syndromes should be classified or diagnosed. Patients often clinically deteriorate years after TBI (Whitnall *et al.*, 2006), but it is difficult to determine whether this is related to the prior head injury. Improved methods of characterising neurodegenerative processes triggered by TBI are needed. We investigated amyloid pathology using [$^{11}$C]PIB PET. For the first time, we show in vivo that increases in [$^{11}$C]PIB binding are present in long-term survivors of TBI in a distribution overlapping with AD but also involving the cerebellum (Thal *et al.*, 2002). A mechanistic link between axonal injury and amyloid pathology is suggested by the relationship between cortical [$^{11}$C]PIB binding and white matter damage in connected tracts.

In AD, Aβ deposition usually begins in inferior frontal and cingulate association cortex, extending into other association cortical regions. Early deposition is seen in the PCC (Tosun *et al.*, 2011), and we observed increased [$^{11}$C]PIB uptake in both TBI and AD patients. While the ventromedial frontal cortex is affected early in AD, the hippocampus and cerebellum are not usually involved until much later in the disease (Thal *et al.*, 2002). In keeping with this pattern we observed strong [$^{11}$C]PIB binding in the prefrontal cortex in our AD patients, but relatively low levels in the hippocampus and cerebellum. However, a different pattern was observed in TBI patients, who had increased cerebellar [$^{11}$C]PIB binding relative to both AD and controls. The distinct distribution of [$^{11}$C]PIB binding in the two contexts suggests that amyloid pathology is triggered by a different mechanism after TBI, which is likely to relate to biomechanical forces underlying the distinctive pattern of Aβ plaque pathology seen in cases of CTE (Stein *et al.*, 2015). TBI might also accelerate an ageing process (Cole *et al.*, 2015) and our results may reflect this change in ageing trajectory, particularly considering that the increased [$^{11}$C]PIB binding after TBI was observed in comparison to a much older aged control group. However, in keeping with studies of AD (Rowe *et al.*, 2007), [$^{11}$C]PIB binding did not correlate with cognitive impairment.

Axonal damage produced at the time of injury may act as an initial trigger for Aβ production and accumulation of amyloid pathology (Johnson, Stewart and Smith, 2010). In keeping with this possibility we observed an association between the extent of white matter damage and [$^{11}$C]PIB binding in the PCC following TBI. The biomechanical effects of torsional and shear stress on white matter tracts produce TAI, and this is thought to be an important factor driving over-production of Aβ, leading to its aggregation in the acute phase (Smith, Johnson and Stewart, 2013). Axons and their surrounding myelin are damaged, and the pathological effects of injury remain visible for many years, particularly in long-distance white matter tracts (Johnson *et al.*, 2013). Animal models and human autopsy studies provide evidence that Aβ is produced at the site of axonal injury shortly after TBI (Johnson, Stewart and Smith, 2010).

The relationship between [$^{11}$C]PIB binding and white matter damage was seen in the cingulum bundles, which connect to the PCC. The relationship was not observed in the corticospinal tract, which is not directly connected to the PCC, suggesting a more specific link between the two observations. Misfolded proteins, including Aβ, have the capacity to move from neuron to neuron via prion-like trans-synaptic spread (Polymenidou and Cleveland, 2012), and computational simulations show that a simple diffusion mechanism can produce the complex patterns of brain atrophy observed in AD if large-scale white matter structure is factored into the model (Raj, Kuceyeski and Weiner, 2012).The implication for TBI is that the white matter may be both a source of Aβ and a conduit for Aβ diffusion. The correlation between measures of TAI and Aβ pathology in the PCC may reflect its role as a highly connected cortical hub (Crossley *et al.*, 2014), which integrates damage that spreads from damaged white matter tracts. The time elapsed since a patient's injury also correlated with [$^{11}$C]PIB binding, suggesting there is a progressive neurodegenerative process. Our results suggest that [$^{11}$C]PIB binding, white matter structure, age and time since injury are inter-related, and longitudinal studies with larger numbers will be need to clarify the causal relationships. Larger studies are also required to better understand the role of time in since injury on factors such as PIB binding and white matter damage, and in order

better account for such factors as covariates in analysis without substantially affecting the degrees of freedom. that Such studies should also examine [$^{11}$C]PIB binding in the context of host genotype, particularly apolipoprotein E (APOE) (Ponsford *et al.*, 2011), which was not addressed here.

Our findings are broadly consistent with a previous [$^{11}$C]PIB study in TBI patients scanned less than one year after injury (median 11 days) (Hong *et al.*, 2014). Hong and colleagues showed increased cortical and striatal [$^{11}$C]PIB binding early after TBI. Importantly, the validity of in vivo neuroimaging was supported by [3H]PIB autoradiography and Aβ immunohistochemistry (Hong *et al.*, 2014). In contrast to our study, this earlier work used the cerebellum as a reference region for quantification of [$^{11}$C]PIB binding, assuming that there was minimal Aβ plaque density in the cerebellum and that the ratio of cortical:cerebellar binding provided a measure of cortical Aβ burden (Rowe and Villemagne, 2011). Hong and colleagues provide evidence to support this assumption early after TBI. However, our results demonstrate that this is not the case in the chronic phase after TBI. Our initial analyses in TBI using the cerebellum as a reference region suggested decreased cortical [$^{11}$C]PIB binding. Therefore, we used a procedure for automatic reference region extraction which has been validated in familial AD and does not require a single anatomically-defined reference region (Ikoma *et al.*, 2013).

Our study has a number of potential limitations. First, given the small sample size, our findings should be regarded as preliminary. In particular, the relationship between PCC PIB binding and white matter damage was not significant once time since injury had been included as a covariate. Second, the [$^{11}$C]PIB healthy controls were age matched to the AD group, and so were older than the TBI group. Although two separate age-matched control groups would have been preferable, Aβ pathology increases with age (Rowe *et al.*, 2010) and so a comparison with older healthy controls is likely to have reduced our sensitivity to detect a relative increase in the younger TBI group. Therefore, the presences of abnormalities in a relatively young TBI group is even more striking. Third, it is possible that GM tissue differences such as atrophy,

associated with AD or aging, could have biased our group contrast results. A number of analysis steps were used to minimize this possibility: we used an advanced algorithm for optimised registration of brain images into standard space (DARTEL) (Klein *et al.*, 2009); [$^{11}$C]PIB binding was only assessed in regions where the GM probability was high; and ROI analyses, based on both automated segmentations, were used to provide confirmatory results. To control for the possible effects of focal injury after TBI, we also excluded lesioned areas from the analysis. It is possible that the extent of focal lesions was underestimated as we used T1 imaging to segment the lesions. However, since [$^{11}$C]PIB binding was reduced in visible lesions, this possibility would have biased the analysis against detecting increases in [$^{11}$C]PIB. The effect of missed lesions may explain why binding in the ACC and SFG ROIs appeared reduced in the TBI group compared to controls.

We provide [$^{11}$C]PIB PET evidence for the presence of amyloid pathology many years after injury in non-demented TBI patients. The distribution of [$^{11}$C]PIB binding partially overlapped with that seen in typical AD but also affected the cerebellum, unlike in AD. This suggests a different mechanism for amyloid plaque genesis. Our findings support the hypothesis that amyloid plaque pathology is related to the presence of axonal damage produced subsequent to the TBI.

Chapter 3

# 3. Thalamic inflammation after brain trauma is associated with thalamo-cortical white matter damage

In this chapter, I investigate the relationship between chronic thalamic microglial activation after TBI, measured using [$^{11}$C]PK11195 PET, and thalamo-cortical TAI, measured using diffusion MRI.

## 3.1. Abstract


**Background**

TBI can trigger chronic neuroinflammation, which may predispose to neurodegeneration. Animal models and human pathological studies demonstrate persistent inflammation in the thalamus associated with axonal injury, but this relationship has never been shown in vivo.

**Findings**

Using [$^{11}$C]PK11195 PET, which provides a marker of microglial activation, we previously demonstrated thalamic inflammation up to 17 years after TBI. Here, we use diffusion MRI to estimate axonal injury and show that thalamic inflammation is correlated with thalamo-cortical tract damage.

**Conclusions**

These findings support a link between axonal damage and persistent inflammation after brain injury.

## 3.2. Introduction

TBI is a risk factor for dementia (Smith, Johnson and Stewart, 2013) and survivors may deteriorate years after their injury (Whitnall *et al.*, 2006). However, the mechanisms relating TBI to neurodegeneration are unclear (Smith, Johnson and Stewart, 2013). An important factor is likely to be neuroinflammation in the form of glial activation triggered by the TBI and which can persist for many years (Ramlackhansingh *et al.*, 2011). Chronic activation of microglia is implicated in many neurodegenerative disorders (Frank-Cannon *et al.*, 2009). Previously, using [$^{11}$C]PK11195 PET, a marker of the TSPO expressed by activated microglia, we observed inflammation in the thalamus up to 17 years after TBI (Ramlackhansingh *et al.*, 2011). Why thalamic inflammation persists, remote from sites of focal injury, remains uncertain.

The spatial pattern of microglial activation following brain injury may relate to the white matter architecture of the CNS (Cagnin *et al.*, 2001; Banati, 2002). Experimental axotomy induces microglial activation remote from the primary lesion site (Banati, 2002). The thalamus is highly connected and shows chronic inflammation after central and peripheral nerve damage (Banati *et al.*, 2001; Banati, 2002). After stroke, microglial activation is seen at the primary lesion but later emerges in projection areas including the thalamus (Pappata *et al.*, 2000; Thiel *et al.*, 2010). Following TBI, axons in white matter are highly susceptible to damage, making TAI one of the most common pathologies of TBI (Johnson, Stewart and Smith, 2013). Together, these observations suggest thalamic inflammation following TBI may result from the high density of connectivity between the thalamus and damaged axons.

DTI can map the structure of thalamo-cortical white matter tracts using probabilistic tractography (Mac Donald *et al.*, 2007) but TBI patients with TAI pose challenges to these methods (Squarcina *et al.*, 2012). Recently, we developed a template-based approach for more robust estimation of thalamo-cortical tract integrity after TBI (Squarcina *et al.*, 2012).

Here, we combine this approach with [$^{11}$C]PK11195 PET to test the hypothesis that chronic thalamic inflammation after TBI can be explained by thalamo-cortical white matter damage.

## 3.3. Methods

Ten patients with a history of moderate-severe TBI (Mayo classification) (mean age±SD 43±5.3 years, range 36–54; mean time since injury±SD 6.2±5.3 years, range 0.9-17) had [$^{11}$C]PK11195 PET and structural MRI scans including DTI (see Chapter 2 for details). Two age-matched healthy control groups were used. Seven controls (mean age 46±4.0,range 42–50) had PET and structural MRI. Thirteen controls (41.8±6.6,35-56) of similar premorbid intellectual ability had MRI including DTI. The project was approved by Hammersmith and Queen Charlotte's and Chelsea Research Ethics Committee. All participants gave informed consent.

Standard MRI T1 and DTI protocols were used (see Chapter 2 for details). For DTI analysis, we used a method for assessing thalamo-cortical white matter connections that is robust to the presence of TAI (Squarcina *et al.*, 2012). We combined ten thalamo-cortical tracts, previously defined in healthy controls using probabilistic tractography, into a single ROI (see Figure 18C for example of one tract, and (Squarcina *et al.*, 2012)). A mask of cortico-cortical tracts through the body of the corpus callosum was used as a control (from (Hellyer *et al.*, 2013)), since these tracts were not connected to the thalamus. Voxel-wise maps of FA, a measure of directionality of water flow along white matter tracts and hence their integrity, were calculated, and FA maps were skeletonized (Smith *et al.*, 2006), leaving the central section of tracts, to minimise partial volume effects (see (Squarcina *et al.*, 2012)). We calculated the mean FA of voxels within the ROIs, and of all voxels in the skeleton. The B0 data for one patient contained an image artifact, so their DTI data were excluded.

To test whether thalamic [$^{11}$C]PK11195 binding is more strongly correlated to proximal than distal thalamo-cortical damage, FA was sampled from a series of

non-overlapping ring-shaped ROIs extending centripetally from the thalamus from 2-60mm diameter, and intersected with the thalamo-cortical tract mask. ROIs were created by repeatedly dilating a thalamic mask by two voxels (2mm). Ring-shaped ROIs were produced by subtracting the previous mask from each step.

[$^{11}$C]PK11195 PET acquisition and analysis are described in (Ramlackhansingh *et al.*, 2011). To produce maps of [$^{11}$C]PK11195 binding potential (BP), we used a supervised clustering procedure to identify reference clusters of voxels in grey matter having [$^{11}$C]PK11195 time activity curves mirroring those of controls (Ramlackhansingh *et al.*, 2011). [$^{11}$C]PK11195 BP was sampled in the bilateral thalamus as well as the cortical grey matter regions that were used to define the thalamo-cortical tracts (Squarcina *et al.*, 2012)).

Regional [$^{11}$C]PK11195 BP was compared between groups using independent sample t-tests. Mean FA values were similarly compared. Bonferroni multiple comparisons correction was used. In TBI, we tested for a relationship between regional [$^{11}$C]PK11195 BP and thalamo-cortical FA using linear partial correlations, controlling for age and time since injury as both factors potentially influence DTI (Grieve *et al.*, 2007) and [$^{11}$C]PK11195 binding (Kumar *et al.*, 2012).

## 3.4. Results

A voxel-wise contrast showed increases in thalamic [$^{11}$C]PK11195 BP in TBI patients versus controls (Figure 18A, reproduced from (Ramlackhansingh *et al.*, 2011)). [$^{11}$C]PK11195 binding in the thalamus ROI was significantly increased ($t=4.64$, $df=15$, $p<0.001$, Figure 18B). In contrast, there was no difference in cortical grey matter [$^{11}$C]PK11195 binding between the groups.

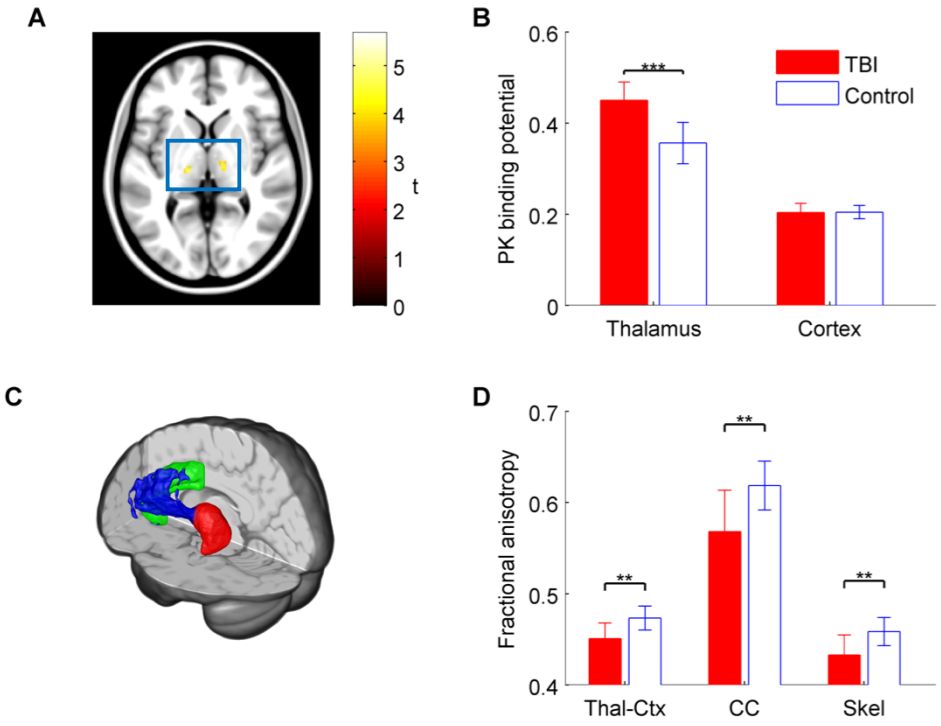



**Figure 18. Increased thalamic microglial activation and WM damage in TBI**

(A) Statistical parametric maps (reproduced from [3]) rendered onto a standard T1 MRI image showing areas of significant increased [$^{11}$C]PK11195 binding potentials (BP) in the TBI patients relative to controls. Bilateral increases in [$^{11}$C]PK11195 binding are seen in thalami (highlighted using a blue surrounding box). T-values are shown. Voxels shown as significant surpass the voxel-wise threshold ($p<0.001$) and the spatial extent threshold (10 voxels). Voxel-wise contrasts were performed on spatially normalised [$^{11}$C]PK11195 BP images, smoothed with a 12mm FWHM Gaussian kernel, using SPM5 (see [3] for details). (B) PK BP in thalamus and cortical grey matter, defined using anatomical regions of interest, in TBI patients (red) and controls. Group mean +/- standard error of the mean (SEM) are shown. ***=$p<0.001$. (C) Illustration of the tract mask (blue) connecting the left thalamus (red) to the left anterior cingulate cortex (ACC) (green), produced using probabilistic tractography in healthy controls (see [12]). Fractional anisotropy (FA) was sampled using bilateral thalamo-cortical tract masks. (D) FA in thalamo-cortical (Thal-Ctx), body of the corpus callosum (CC) and across the white matter skeleton (Skel), in TBI patients (red) and controls. **=$p<0.01$.

FA was decreased in TBI patients versus controls in thalamo-cortical projections ($df=20$, $t=-3.68$, $p=0.0015$), the corpus callosum ($df=20$, $t=-3.264$, $p=0.004$), and the white matter skeleton ($df=20$, $t=-3.450$, $p=0.003$) (Figure 1D).

In TBI, we found a significant negative correlation between thalamic [$^{11}$C]PK11195 BP and mean thalamo-cortical tract FA ($r=-0.770$, $p=0.042$). The strength of this correlation decreased with the distance at which FA was sampled from thalamo-cortical tracts (Figure 19A). Thalamic [$^{11}$C]PK11195 binding was most strongly correlated with FA of voxels within 10mm of the thalamus, maximally within 2mm distance (Figure 19B). There was no

correlation between thalamic [$^{11}$C]PK11195 binding and FA of the corpus callosal tracts, nor between cortical [$^{11}$C]PK11195 and thalamo-cortical FA, either when sampled as a whole or ROIs at different distances (Figure 19C). We also found no significant correlation between time since injury and either mean thalamo-cortical FA or thalamic [$^{11}$C]PK11195.

## 3.5. Discussion

Axonal injury underlies many long-term problems after TBI (Meythaler *et al.*, 2001). Glia become activated at sites of injury (Banati, 2002; Maxwell *et al.*, 2006) but also at distant sites (Johnson *et al.*, 2013), including subcortical nuclei like the thalamus (Maxwell *et al.*, 2006). Our TBI patients showed both TAI and persistent thalamic microglial activation. For the first time in vivo, we show that the degree of thalamic microglial activation and thalamo-cortical white matter tract damage are closely related.

Several mechanisms might underlie persistent thalamic inflammation after TBI (Figure 3). It may be a response to focal injury. However, there was no T1 MRI evidence of focal thalamic injury. (It is possible that thalamic injury may have been undetected on the T1-weighted imaging.) Furthermore, there was no increase in [$^{11}$C]PK11195 binding in focal lesions (Ramlackhansingh *et al.*, 2011), making a prolonged response to direct damage an unlikely explanation. Alternatively, thalamic inflammation may relate to a persistent effect of TAI. This is made more likely by the observation that activated microglia are seen at sites of TAI in acute and chronic phases (Johnson *et al.*, 2013). The co-localization of myelin basic protein immunoreactivity within microglia at sites of TAI suggests myelin fragments may provide a persistent trigger for inflammation (Johnson *et al.*, 2013). The strong correlation we observed between thalamic [$^{11}$C]PK11195 binding and white matter close to the thalamus suggests a causative role for the persistent effects of TAI years after injury.

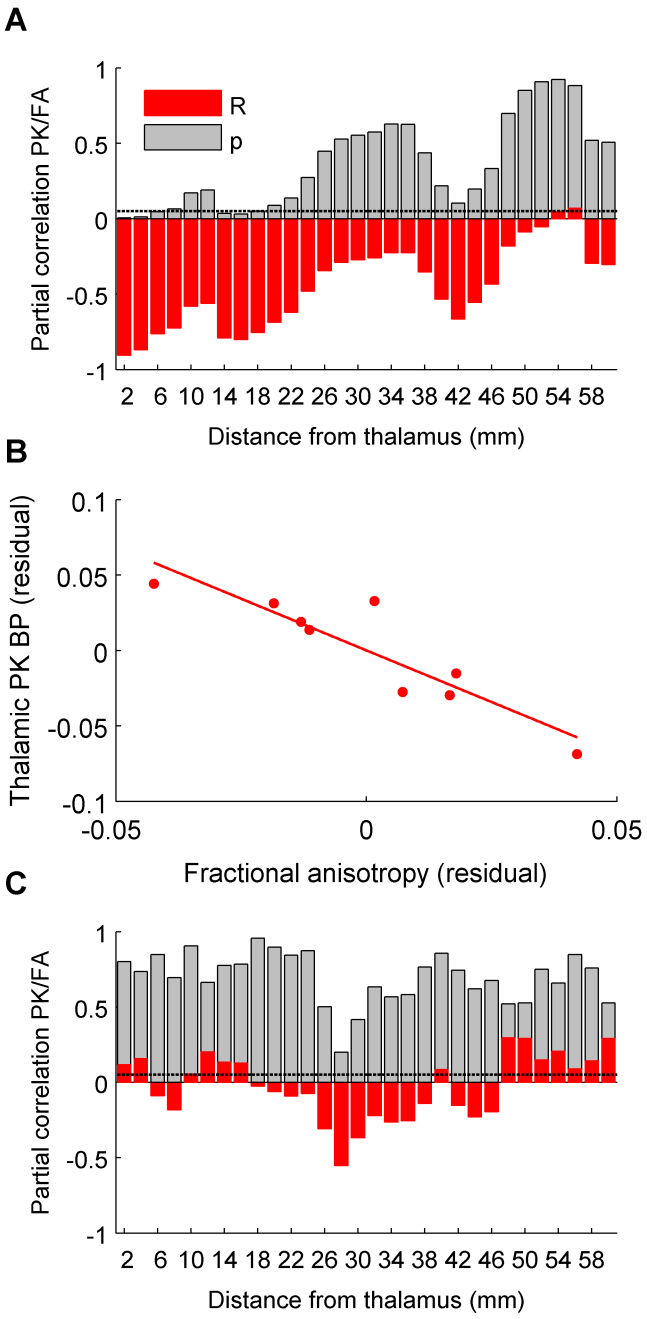



**Figure 19. Correlation of thalamic microglial activation and WM damage in relation to distance from thalamus**

(A) Partial correlation of thalamic [$^{11}$C]PK11195 (PK) BP and thalamo-cortical FA, sampled with increasing distance from the thalamus, in TBI patients. Distance of 0mm reflects sampling from tracts involving the thalamus proper. R (red) and p values are shown, with a threshold of p=0.05 (dotted line). (B) Plot of residuals after for thalamo-cortical FA (x-axis), sampled from a ring-shaped mask 2mm from the outer border of the thalamus (where the relationship was strongest), versus thalamic [$^{11}$C]PK11195 BP (y-axis). The residuals were produced by regressing out from the original values age and time since injury, as both factors potentially influence DTI (Grieve et al. 2007) and [11C]PK11195 binding (Kumar et al. 2012). (C) Partial correlation of [$^{11}$C]PK11195 BP in cortical grey matter and thalamo-cortical FA, sampled and plotted as in (A).

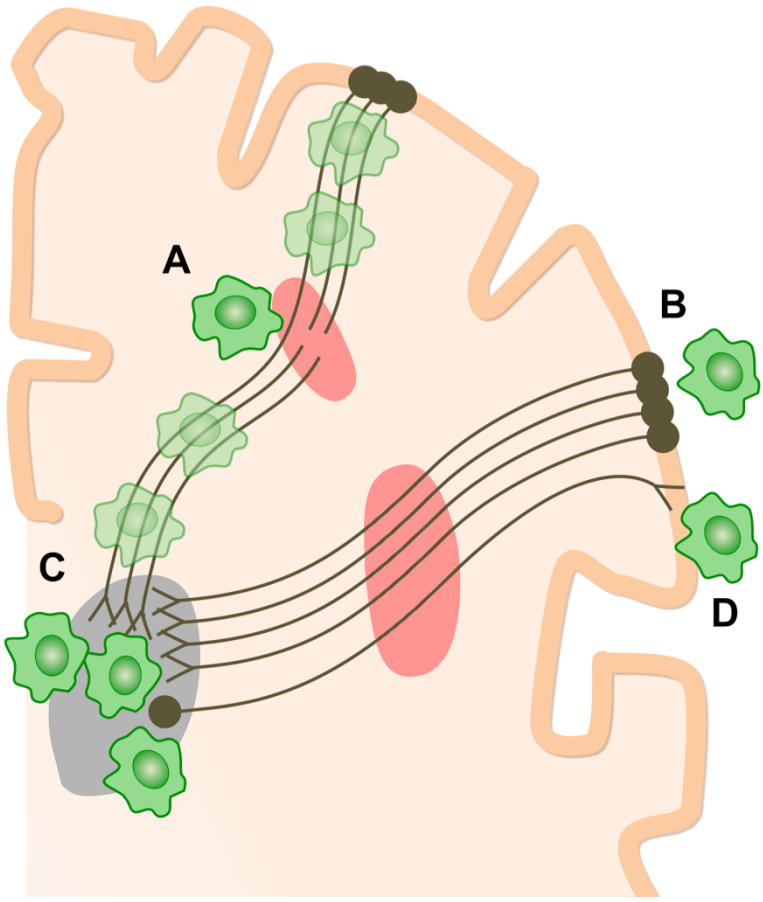



**Figure 20. How chronic microglial activation and axonal injury may be linked after TBI**

Microglial activation (green cells) and traumatic axonal injury in thalamo-cortical white matter tracts (red areas) have been demonstrated after TBI. Sites of chronic microglial activation can co-localise with axonal abnormality (A) as well as along the entire axonal tract affected by injury. Remote from sites of primary axonal injury, microglia may be observed both in retrograde projection areas, towards the cell bodies of damaged neurons (B), or in anterograde areas (C, i.e. the thalamus, and D). The thalamus is a highly connected structure. Thalamic microglial activation may be observed after TBI because of the high density of connections to damaged axons. The number of cortico-thalamic projections far exceeds thalamo-cortical projections. If microglial activation preferentially favours anterograde involvement, then relatively increased activation would be expected in the thalamus (C) compared to corresponding cortical areas (B).

Following experimental axotomy, microglial activation is seen in both anterograde and retrograde projection areas (Banati, 2002). Hence, an inflammatory response might be expected in cortical and subcortical projection areas following TAI. Several factors may explain the lack of [$^{11}$C]PK11195 binding in cortex versus thalamus. Firstly, corticothalamic projections are ~10-fold more numerous than thalamocortical projections (Jones, 2012). This asymmetry is especially relevant if there is also a difference in the magnitude of anterograde and retrograde microglial reactions to TAI, potentially a second factor. If both factors are important then high [$^{11}$C]PK11195 binding in the

thalamus rather than cortex would suggest an anterograde, rather than retrograde, reaction predominates (Figure 3). However, a third factor is the high density of thalamocortical (and corticothalamic) neurons in thalamus versus cortex. As Banati and colleagues observe, the high density of neurons converging in the thalamus might lead to a cumulative signal that represents a "regional amplification of … widespread but sub-threshold cortical pathology" (Cagnin, Gerhard and Banati, 2003).

An anterograde evolution of microglial activation is seen in other conditions. After stroke, microglial activation spreads in an anterograde fashion along damaged tracts (Pappata *et al.*, 2000; Thiel *et al.*, 2010) and the degree of anterograde activity in the brainstem has been shown to be correlated with pyramidal tract damage. Other diseases involving white matter damage, including multiple sclerosis and peripheral nerve injury (Banati, 2002), and another study of TBI (Folkersma *et al.*, 2011), also show thalamic inflammation, suggesting the thalamus is a common "sink" of secondary inflammation in response to axonal damage, perhaps related to its dense white matter connectivity.

Whether chronic thalamic inflammation is harmful or restorative is uncertain. This question is challenging partly because the relationship between activated microglial phenotype and TSPO expression is not clear (Liu *et al.*, 2014). It may be that microglia's role in synaptic plasticity may underlie much of what we have labelled "neuroinflammation" (Banati *et al.*, 2001; Graeber, 2014). How TSPO expression and microglial activation are related has recently been addressed by Banati and colleagues, who showed using TSPO knockout mice that TSPO expression and activation of microglia following injury are not mutually dependent (Banati *et al.*, 2014).

An important limitation of the study is that it involved a small sample of patients, and with a history of a single moderate-severe TBI. There is a need to replicate these preliminary findings in larger cohorts, which might benefit from investigating a wider range of diffusion metrics. Studies from animal models of repetitive mild TBI show persistent inflammation both at sites of axonal injury

and locations remote from the site of focal lesions, suggesting a similar microglial response in cases of lower injury severity (Shitaka *et al.*, 2011). Finally, whilst the TSPO PET binding and FA relationship was significant when the mean of the whole tract was used, it is possible that, since the relationship was strongest very close to the thalamus, that the data are driven by a "bystander injury" of the thalamus to the closest WM, rather than a true relationship between thalamic inflammation and thalamo-cortical WM injury.

Our previous study using [$^{11}$C]PK11195, a first-generation TSPO ligand, showed thalamic inflammation up to 17 years after injury, but no statistically significant increases in WM binding. This is somewhat at odds with the neuropathological studies in TBI (see Chapter 1), as well our own [$^{11}$C]PBR28 data (i.e. second-generation TSPO PET radioligand, see Chapters 4 and 5). That we found prominent WM [$^{11}$C]PBR28 binding compared with [$^{11}$C]PK11195 may reflect the greater sensitivity of this second-generation ligand. It would be interesting to explore the relationship with FA data described here using the [$^{11}$C]PBR28 data.

Evidence of persistent neuroinflammation suggests the window of opportunity for therapeutic intervention following TBI may be longer than is usually considered. Inflammatory PET imaging provides a biomarker to investigate this prolonged inflammatory reaction, and potentially the effects of interventions targeting glial activation. Our findings emphasise the need for large multi-modal longitudinal studies combining inflammatory PET with diffusion MRI to image axonal injury.

Chapter 4

# 4. Chronic microglial activation and the effect of minocycline after brain trauma

In this chapter, I investigate chronic microglial activation after TBI using [$^{11}$C]PBR PET, and its relation to MRI and other measures of brain injury including plasma NFL. I also investigate the effect of minocycline on chronic microglial activation. The findings are developed further in Chapter 5.

The Abstract and Methods presented here are for both chapters combined. The results of both chapters are discussed together in Chapter 5.

## 4.1. Abstract

TBI can trigger chronic microglial activation, but it is unclear whether this harms long-term recovery. The antibiotic minocycline inhibits microglial activation and is neuroprotective in animal models of acute TBI. The PET ligand [$^{11}$C]PBR28 binds the translocator protein up-regulated by activated microglia. We combined [$^{11}$C]PBR28 PET with MRI, cognitive assessment, and plasma NFL and tau sampling (putative markers of axonal damage), to measure microglial activation and neurodegeneration after TBI and the effects of minocycline. Fifteen patients at least six months after a single moderate-to-severe TBI received either minocycline 100mg orally twice daily or no drug, for 12-weeks. As presented in this chapter, at baseline, [$^{11}$C]PBR28 binding in patients was increased compared to controls in cerebral WM and thalamus. MRI measures of WM damage were highest in areas of greater [$^{11}$C]PBR28 binding. Plasma levels of NFL, but not tau, were elevated in patients. Minocycline reduced

[$^{11}$C]PBR28 binding (mean ΔWM binding=-23.30%, CI -40.9 to -5.64%, p=0.018). However, as presented in Chapter 5, minocycline was associated with an increase in NFL levels, reduced corpus callosal WM integrity and borderline slowing of information processing speed. Together, these findings suggest minocycline inhibits chronic microglial activation but may impede recovery after brain trauma.

## 4.2. Introduction

TBI is a leading cause of disability and mortality in young adults (Fleminger and Ponsford, 2005). Historically, TBI was considered a static insult. However, survivors can deteriorate years after injury (Whitnall *et al.*, 2006), developing unforeseen consequences such as post-traumatic epilepsy (Annegers *et al.*, 1998), brain atrophy (Faden and Loane, 2015), AD (Smith, Johnson and Stewart, 2013) and CTE (McKee *et al.*, 2013). These observations suggest TBI can trigger chronic pathological processes.

Microglia are the primary mediators of CNS inflammation (Kettenmann *et al.*, 2011). With a rapid response to injury (Engel *et al.*, 2000; Koshinaga *et al.*, 2000), activated microglia mediate both pro-inflammatory (Block, Zecca and Hong, 2007) and neuroprotective effects through their ability to adopt diverse activation phenotypes (Kettenmann *et al.*, 2011). Animal models (Holmin and Mathiesen, 1999; Acosta *et al.*, 2013; Loane *et al.*, 2014), autopsy series (Gentleman *et al.*, 2004; Smith *et al.*, 2012; Johnson *et al.*, 2013), and PET studies (Folkersma *et al.*, 2011; Ramlackhansingh *et al.*, 2011) show that microglial activation can persist for months and years after TBI. Chronic microglial activation is frequently observed in WM (Smith *et al.*, 2012; Johnson *et al.*, 2013) and locations far from sites of focal injury (Ramlackhansingh *et al.*, 2011; Acosta *et al.*, 2013; Loane *et al.*, 2014). However, the significance of this prolonged extensive microglial activation is unclear (Faden and Loane, 2015).

Chronic microglial activation has been implicated in a variety of neurodegenerative diseases, including AD and ALS (Turner *et al.*, 2004; Frank-Cannon *et al.*, 2009; Gentleman, 2013). In rodent TBI models with survival of

up to one year, these cells have a predominantly pro-inflammatory phenotype, associated with expression of NADPH oxidase, IL-1 and TNF-$\alpha$ (Holmin and Mathiesen, 1999; Loane *et al.*, 2014). However, studies in non-human primates show microglial activation months after injury is associated with expression of brain derived neurotrophic factor (BDNF) and extracellular signal-regulated kinases (ERK1/2), factors which support cell survival, suggesting a trophic role for chronically activated microglia (Nagamoto-Combs *et al.*, 2007, 2010). The effects of chronic microglial activation after TBI in humans therefore remains uncertain.

There is growing evidence that TBI triggers chronic neurodegeneration (Faden and Loane, 2015). Longitudinal volumetric and diffusion magnetic resonance imaging (MRI) studies show WM damage continuing for months and years post injury (Tomaiuolo *et al.*, 1999; Isoniemi *et al.*, 2006; Trivedi *et al.*, 2007; Bendlin *et al.*, 2008; Sidaros *et al.*, 2008). Neuropathological evidence of ongoing axonal damage is associated with chronic microglial activation more than a year after injury (Gentleman *et al.*, 2004; Johnson *et al.*, 2013). These findings suggest a relationship between progressive neurodegeneration and chronic microglial activation following TBI, but this has never been investigated *in vivo*.

PET can be used to measure microglial activation after TBI in humans (Ramlackhansingh *et al.*, 2011). Expression of the TSPO is thought to increase with microglial activation, and although TSPO is not exclusively expressed in microglia, TSPO PET is widely used as a marker for microglial activation (Owen and Matthews, 2011). Previously, using [$^{11}$C]PK11195, which binds to the TSPO, we observed inflammation in the thalamus up to 17 years after TBI (Ramlackhansingh *et al.*, 2011). The second-generation TSPO ligand [$^{11}$C]PBR28 has a higher signal-to-noise ratio than [$^{11}$C]PK11195, promising more accurate quantification (Owen and Matthews, 2011). Recently, increased [$^{11}$C]PBR28 binding has been demonstrated in a number of neurodegenerative disorders associated with microglial activation, including AD (Lyoo *et al.*, 2015) and ALS (Zürcher *et al.*, 2015).

An accessible biomarker of disease progression in TBI may allow patients at risk of poor long-term outcomes to be identified and facilitate the study of treatments targeting neurodegenerative processes (Zetterberg, Smith and Blennow, 2013). A range of putative blood and CSF biomarkers of brain damage have been identified (DeKosky *et al.*, 2013; Zetterberg, Smith and Blennow, 2013). NFL and tau are promising markers of TAI (DeKosky *et al.*, 2013). Neurofilaments are major structural proteins of neurons (Liu *et al.*, 2004), and NFL is especially abundant in large-calibre myelinated axons in the CNS (Friede and Samorajski, 1970). Tau is a microtubule-associated protein predominantly expressed in neurons, and preferentially localized in axons (AVILA *et al.*, 2004). Elevated CSF levels of NFL and tau have been observed in acute severe TBI, with higher levels seen after more severe injuries (Zetterberg, Smith and Blennow, 2013). NFL levels in the peripheral blood have been shown to be highly correlated with levels in the CSF (Gaiottino *et al.*, 2013), while levels of tau protein in the CSF and plasma do not appear to be correlated (Sjögren *et al.*, 2001). A recent study did find an increase in plasma tau in concussed ice hockey players that correlated with clinical outcome (Shahim *et al.*, 2014). However, it is unknown whether NFL or tau remain elevated in the chronic phase after TBI, or whether levels relate to progressive neurodegeneration. Persistent elevations in NFL and tau have been reported in a variety of neurodegenerative diseases (Eikelenboom *et al.*, 2003; Liu *et al.*, 2004; Gaiottino *et al.*, 2013; Lu *et al.*, 2015), suggesting that these biomarkers may prove useful in monitoring neurodegenerative processes following TBI.

The protracted time-course of neuroinflammation and neurodegeneration after TBI suggests a window of opportunity for disease-modifying therapy well beyond the acute setting, where many trials have failed (Maas, Roozenbeek and Manley, 2010). A successful strategy could be to target chronic microglial activation. For example, eliminating microglia in an AD model prevented neuronal loss, raising the possibility that reducing microglial activation may limit the neurodegenerative consequences of TBI (Spangenberg *et al.*, 2016). Minocycline is a tetracycline antibiotic which has been used clinically for over forty years (Garrido-Mesa, Zarzuelo and Gálvez, 2013b). It has anti-

inflammatory and immunomodulatory properties independent of its anti-bacterial action (Garrido-Mesa, Zarzuelo and Gálvez, 2013a), and is neuroprotective in animal models of acute TBI (Bye *et al.*, 2007; Homsi *et al.*, 2009, 2010; Abdel Baki *et al.*, 2010; Siopi *et al.*, 2011; Haber *et al.*, 2013) and a variety of CNS disorders (Plane *et al.*, 2010). One proposed mechanism is the reduction of microglial activation (Bye *et al.*, 2007; Homsi *et al.*, 2010), through actions including inhibition of nuclear factor kappa light-chain enhancer of activated B cells (NF-κB) and interference with mitogen-activated protein kinase (MAPK) pathways (Garrido-Mesa, Zarzuelo and Gálvez, 2013b). Animal studies show minocycline reduces the post-TBI rise of microglial activation by up to 59% (Homsi *et al.*, 2010) and improves early functional outcomes (Bye *et al.*, 2007; Homsi *et al.*, 2009, 2010; Abdel Baki *et al.*, 2010; Siopi *et al.*, 2011; Haber *et al.*, 2013). Clinical trials in acute brain and spinal cord injury are promising (Lampl *et al.*, 2007; Casha *et al.*, 2012). For example, 30-day functional outcome was improved following acute treatment with minocycline after ischaemic stroke (Lampl *et al.*, 2007). However, human studies of minocycline in neurodegenerative diseases have had mixed outcomes (Plane *et al.*, 2010).

We combined [$^{11}$C]PBR28 PET with MRI, cognitive assessment, and plasma NFL sampling to measure chronic microglial activation and neurodegeneration after TBI and the effects of minocycline treatment. We show that chronic microglial activation is present, positively correlated with NFL levels, and higher in areas of WM that show greater neurodegeneration. We also show that minocycline reduces chronic microglial activation but is associated with an increase in NFL levels, reduced WM integrity and slowing of information processing speed.

## 4.3. Methods

The following methods relate to the results presented in Chapters 4 and 5.

The study was approved by the West London and Gene Therapy Advisory Committee (GTAC) NHS Research Ethics Committee (13/LO/1813). All participants provided written, informed consent.

### Study design

A cross-sectional study of TBI patients compared to age-matched controls was performed, followed by a randomized open-label study of minocycline versus no drug in patients (Figure 21).

At baseline, patients had [$^{11}$C]PBR28 PET, structural and diffusion MRI, and neuropsychological testing. One group of controls had [$^{11}$C]PBR28 PET and structural MRI. A second control group had structural and diffusion MRI, and neuropsychological testing.

Patients were then randomized to one of two parallel groups in a 2:1 ratio, balanced for age, gender, TSPO genotype and time since injury. One group (n=10) received minocycline 100mg orally twice daily for 12 weeks; the other (n=5) had no drug. Patients were followed up after 12 weeks and again at six months after the baseline visit. The untreated group was used to assess the normal variation in [$^{11}$C]PBR28 binding over 12 weeks. At 12 weeks, patients had [$^{11}$C]PBR28 PET, MRI and neuropsychological testing. Patients in the minocycline group continued the medication up to the evening of the visit. At six months, patients had MRI and neuropsychological testing only. A third control group had longitudinal structural MRI.

### Recruitment, eligibility criteria and screening

Patients were recruited from specialist TBI clinics in London, UK. Inclusion criteria were: (1) age between 20-65 years; (2) history of a single moderate-severe TBI (Mayo classification (Malec *et al.*, 2007)) at least 6 months prior; (3) no significant neurological or psychiatric illness prior to the TBI. Exclusion criteria were: (1) use of any medication or substance or alcohol abuse (e.g. recreational drugs) that would interfere with the study or compromise safety;

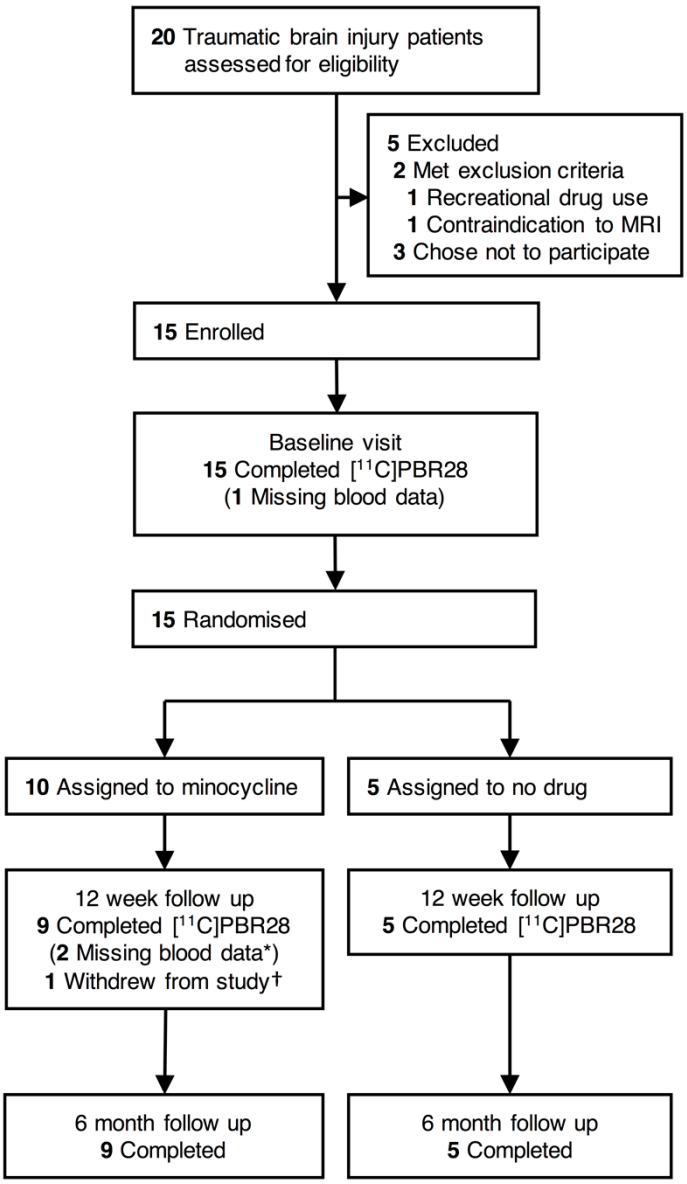



**Figure 21. Study design, TBI enrolment and control groups.**

Baseline data in TBI patients were compared to two control groups, and longitudinal MRI data in patients were compared to a third control group. Patients were recruited at least six months after injury. *Arterial blood sampling in two patients in the minocycline group failed (one baseline visit, one 12-week visit), so PET data for these participants were excluded, including follow-up comparisons. †A third patient in the minocycline group had an anxiety episode at the start of the 12-week scan and immediately withdrew from the study, so all follow-up data from this participant were excluded.

(2) contraindication to MRI scanning (e.g. claustrophobia); (3) contraindication to PET (e.g. pregnancy) or arterial line insertion (e.g. coagulopathy).

Three separate groups of healthy volunteer control participants, age and gender matched to the TBI group, were used for PET and MRI analyses. They were in good general health with no history of significant neurological or psychiatric illness including TBI, and ineligible if they met any of the exclusion criteria above.

A screening visit involved medical history and physical examination, as well as genotyping for the rs6971 (Ala147Thr) polymorphism in the TSPO gene using a Taqman SNP Genotyping Assay. This produces three classes of binding affinity for second-generation TSPO ligands: high-affinity binders (HABs), mixed-affinity binders (MABs) and low-affinity binders (LABs)(Owen *et al.*, 2012). Individuals with LAB genotype were excluded as they show negligible specific binding of the tracer. PET controls were matched to the patients for TSPO genotype.

### Study procedures

Study procedures were carried out at the Hammersmith Hospital campus, Imperial College London (London, UK) and Imanova Centre for Imaging Sciences (London, UK).

[$^{11}$C]PBR28 radiopharmaceutical preparation and quality control were performed as in (Owen *et al.*, 2014). [$^{11}$C]PBR28 was injected as an intravenous bolus (mean ± SD 340.04 ± 18.07 MBq) over ~20 seconds at the start of a 90 minute dynamic PET acquisition. Arterial blood samples were collected from a radial artery for generation of an arterial plasma input function. Acquisition and reconstruction of PET imaging data, arterial blood sampling, analysis of plasma metabolism, and measurement of blood and plasma radioactivity concentrations were performed as previously described(Owen *et al.*, 2014).

All participants underwent high resolution T1-weighted structural 3T MRI. Baseline structural MRI scans were reviewed by a senior neuroradiologist. Diffusion-weighted images were acquired along 64 non-colinear directions with

b=1000s/mm$^2$ and four averages with b=0s/mm$^2$, with TE/TR 103/9,500ms, 64 contiguous slices, FoV 256 mm, and voxel size 2 × 2 × 2 mm$^3$.

A neuropsychological battery assessed cognitive domains often previously observed to be impaired after TBI (Ramlackhansingh *et al.*, 2011). A computer tablet-based left/right choice-reaction task (CRT) assessed simple processing speed (median reaction time (RT) on correct trials); Colour-Word Interference (Stroop) subtests from the Delis-Kaplan Executive Function System assessed complex processing speed and executive function (inhibition and cognitive flexibility); the Trail Making Test (TMT) assessed complex processing speed and executive function (set maintenance and set shifting); the Logical Memory I and II subtests of the Wechsler Memory Scale (Third Edition, WMS-III) and People Test (PT) from the Doors and People Test assessed episodic memory; the Wechsler Abbreviated Scale of Intelligence (WASI) Matrix Reasoning subtest assessed current non-verbal reasoning; the Wechsler Test of Adult Reading (WTAR) estimated pre-morbid intelligence. Please see (Ramlackhansingh *et al.*, 2011) for references.

A venous blood sample was taken on the morning of the 12-week visit for a trough drug level. Plasma concentrations of minocycline were determined using liquid chromatography–mass spectrometry (Antimicrobial Reference Laboratory, Southmead Hospital, Bristol).

A venous blood sample was taken for measurement of NFL and tau. We were able to build on recent advances in plasma biomarker assessment that have dramatically improved the sensitivity of plasma NFL assessment. The single molecule array platform (Simoa) was used to assess plasma NFL and tau, which provides a 100-1000-fold increase in analytical sensitivity compared to regular ELISA (Wilson *et al.*, 2015). Plasma NFL measured on Simoa has been shown to correlate with CSF NFL measured with ELISA (Gisslén *et al.*, 2016), demonstrating its validity. The analytical sensitivity of the assay is 0.6 pg/mL. Plasma tau levels were measured on Simoa using the Human Total Tau 2.0 kit (Quanterix Corp, Boston, MA, USA) following the instructions by the manufacturer. All analyses were performed on one round of experiments using

one batch of reagents by board-certified laboratory technicians who were blinded to clinical data. Intra-assay coefficients of variation were 8.9-11% for NFL and 4.1-8.9% for tau.

### [$^{11}$C]PBR28 PET image analysis

An overview of the main image analysis is shown in Figure 22. Motion correction of dynamic PET images, co-registration of PET with structural MRI, and generation of metabolite-corrected plasma input function were performed using previously published methods (Owen *et al.*, 2014). The Logan graphical method (Logan *et al.*, 1990), using a metabolite-corrected plasma input function, 5% fixed blood volume and a linear start time (T*) at 35 minutes, was used to generate parametric maps of volume of distribution ($V_T$).

Previous pharmacological [$^{11}$C]PBR28 studies have shown drug effects on $V_T$ (Jucaite *et al.*, 2015; Sandiego *et al.*, 2015). Therefore, $V_T$ was the primary outcome measure for assessing within-subject drug effects. $V_T$ allows absolute quantification. This is important since drugs can have a global action, which would impact on quantification approaches that use a reference region. In contrast, the distribution volume ratio (DVR) was used as the primary outcome measure for the analysis of between-subjects group effects. TSPO PET studies show high between-subject variability in tracer uptake, even after accounting for TSPO genotype (Guo *et al.*, 2012). To reduce variability, previous cross-sectional studies have generally used measures which are normalized either by levels in the whole brain (Loggia *et al.*, 2015) or a pseudo-reference region(Lyoo *et al.*, 2015). Therefore, the DVR, the ratio of regional $V_T$ to whole brain $V_T$, was the primary outcome measure for cross-sectional analysis. The analysis was repeated using cerebellar or cortical GM as alternative pseudo-reference regions, to determine if the choice of reference region influenced the findings.

T1 MRI images were segmented into GM and WM using SPM12, and warped to an average group template using a diffeomorphic nonlinear registration (DARTEL) (Ashburner, 2007) (Figure 22A). Separate templates were created for cross-sectional and longitudinal analyses. Templates were registered to

Montreal Neurological Institute (MNI) 152 space. Each individual [$^{11}$C]PBR28 parametric map (DVR or $V_T$) was registered to its corresponding subject-space T1, then the individual flow-fields and template transformation from DARTEL were applied to produce MNI space images, without modulation. Normalized maps were spatially smoothed (8mm full width at half maximum (FWHM) Gaussian kernel).

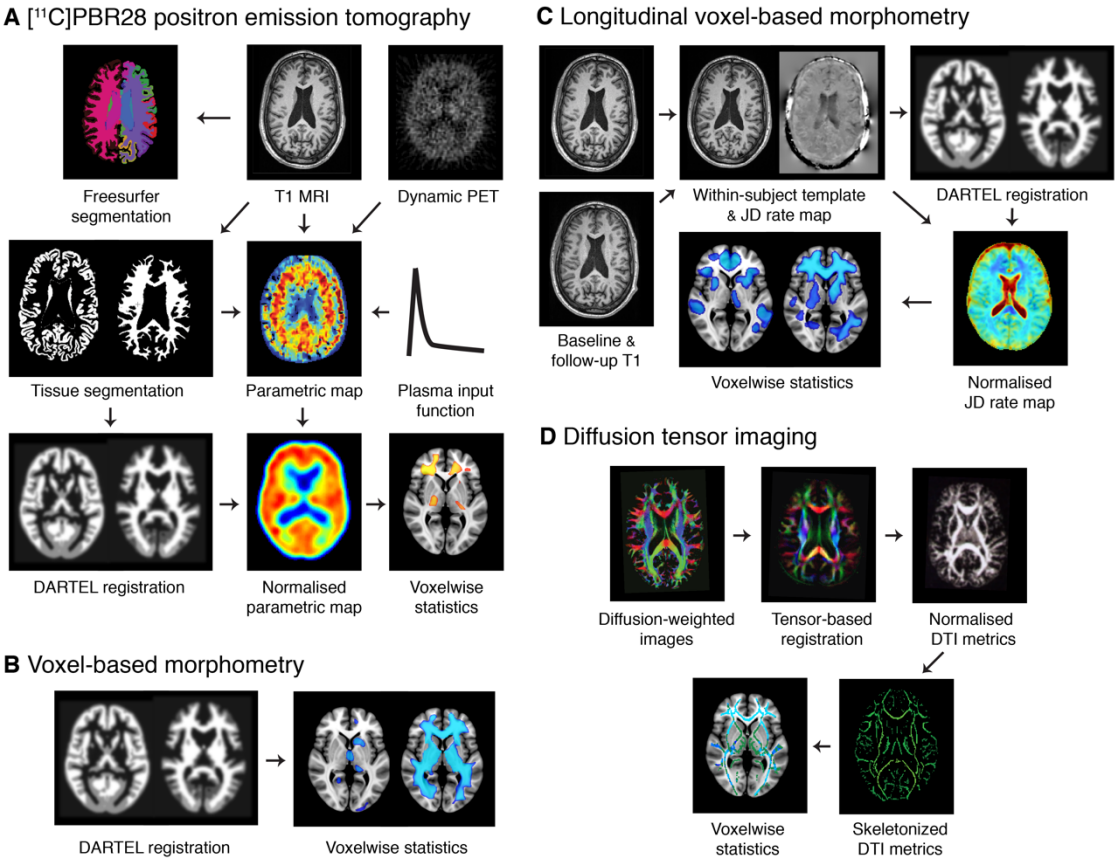



**Figure 22. Overview of image analysis**

(A) [$^{11}$C]PBR28 PET parametric maps were generated in MIAKAT (http://www.miakat.org). A Freesurfer T1 MRI segmentation was used for ROI analysis. Grey matter (GM) and white matter (WM) segmentations from T1 were used to improve ROI sampling. GM and WM segmentations were normalized to MNI space using DARTEL in SPM and the same normalization was applied to co-registered parametric maps. (B) Voxel-based morphometry was performed using normalized and modulated GM and WM segmentations. (C) Longitudinal voxel-based morphometry was performed using an unbiased within-subject longitudinal registration in SPM to generate annualized Jacobian determinant (JD) images, which were normalized with DARTEL (D) Diffusion tensor imaging (DTI) data were processed in FSL and DTI-TK. DTI metrics were skeletonised in FSL, leaving the central section of tracts, to minimize partial volume effects.

Volumetric segmentation of T1 scans was performed using Freesurfer (Desikan-Killiany atlas) (Fischl, 2012), for ROI analysis of cerebral WM,

thalamus and cortical GM. To improve sampling accuracy, ROI masks were intersected with thresholded tissue probability maps ($p>0.5$). Co-registered [$^{11}$C]PBR28 parametric maps were sampled from the ROIs and mean values calculated.

In patients, images of change in $V_T$ ($\Delta V_T$) were calculated as: $\Delta V_T = V_T(12\ weeks) - V_T(baseline)$. These 'delta' images were calculated in subject space after within-subject registration of the 12-week parametric map to the baseline map. Delta images were then normalized to MNI space (as above). Similar results were obtained when delta images were computed in MNI space instead. To calculate $\Delta V_T$ in ROIs, the same formula was used.

### Lesion segmentation

In patients, lesions apparent on T1 MRI were manually segmented and excluded from all imaging analyses.

### VBM and longitudinal registration

For cross-sectional VBM (Figure 22B), T1 images were segmented into GM and WM, and warped to MNI space (as above) but including modulation by the Jacobian determinants (JDs) derived from DARTEL. The normalized segmentations were then smoothed (8mm FWHM) and masked (group mean $p>0.2$). Total GM and WM tissue volumes, and intracranial volume (ICV), were calculated using SPM12.

To investigate longitudinal volume changes between baseline and 6-months, first the annualized change in GM and WM volumes were calculated as: $\%\Delta/year = ([volume(6\text{-}month)/volume(baseline)] - 1) \times 100) / follow\text{-}up\ interval\ (years)$. Secondly, an unbiased within-subject pairwise longitudinal registration approach provided a voxelwise measure of change (Ashburner and Ridgway, 2013) (Figure 22C). In SPM12, deformation fields mapping baseline and 6-month T1s to a within-subject average template T1 were computed, from which annualized JD images were created, representing the per-year contraction or expansion of each voxel. Within-subject templates were segmented into GM and WM. The segmentations and individual JD images were normalized to MNI

space using DARTEL (as above), without modulation, and smoothed (8mm FWHM). Each JD image was then multiplied by GM and WM tissue segmentation images to yield tissue-specific JD images for voxelwise analysis. These tissue-specific images were masked as per cross-sectional VBM. TBI patients and the longitudinal MRI control group were analysed separately.

### DTI

Diffusion-weighted images (Figure 22D) were preprocessed using standard methods (Kinnunen *et al.*, 2011) and tensor-based registration performed using DTI-TK (Zhang *et al.*, 2007). For cross-sectional analysis, normalization of tensor images was performed by bootstrapping subject volumes to the IXI Aging Template then refining the group template using affine followed by nonlinear diffeomorphic registration (Zhang *et al.*, 2007). A final study template was registered to MNI space (IIT Human Brain Atlas) using an affine registration step. All subject images were then transformed to MNI space by combining the subject-to-group and group-to-MNI transformations. For longitudinal analysis, an unbiased longitudinal DTI-TK processing pipeline was used by including an initial within-subject registration stage (Keihaninejad *et al.*, 2013).

Maps of FA were generated from normalised tensor images and analysed using tract-based spatial statistics (TBSS) in FSL (as described in (Kinnunen *et al.*, 2011)). The “skeletonisation” of FA maps, leaving the central section of tracts, reduces the impact of partial volume effects at the edge of tracts. This procedure does have the disadvantage of reducing sensitivity.

In patients, to investigate longitudinal changes, voxelwise delta images (e.g. ΔFA) were calculated using the same formula as for $\Delta V_T$, from baseline to 12-weeks and baseline to 6-months.

For ROI analysis of the body and splenium of the corpus callosum, masks of these regions from the ICBM-DTI-81 atlas (Mori *et al.*, 2008) were combined, and the resulting mask was intersected with the TBSS skeleton. In each participant the mean FA sampled from this mask was calculated.

**Table 7. Summary of statistical tests**

| Analysis | Test | Data |
|---|---|---|
| **Group characteristics** | Independent sample t-test | Age |
| | Fisher's exact test | Gender, TSPO genotype |
| | Mann-Whitney U test | Time since injury, PTA duration, visit intervals |
| **Cognitive tests** | Shapiro-Wilk test (test of normality) | Cognitive scores |
| | Independent sample t-test or Mann-Whitney U test | |
| **Voxelwise cross-sectional** | nonparametric permutation tests | [11C]PBR28 DVR<br>Tissue volumes (GM, WM) |
| **ROI cross-sectional** | ANCOVA | Regional [11C]PBR28 DVR |
| **Within-patient correlation (cross-sectional)** | Partial correlation | [11C]PBR28 DVR, time since injury, cognitive scores, blood measures |
| **Within-patient modality comparison (cross-sectional)** | Paired-sample t-test | [11C]PBR28 DVR, tissue volumes, FA |
| **Voxelwise longitudinal** | Nonparametric permutation tests | [11C]PBR28 VT, JD images, delta FA images |
| **ROI longitudinal** | RMANOVA | Regional [11C]PBR28 VT, regional FA |
| | One-sample t-test | Regional [11C]PBR28 VT, tissue volumes |
| **NFL longitudinal** | RMANOVA | Blood measures |
| **Cognitive tests (longitudinal)** | RMANOVA | Cognitive measures |
| **Within-patient correlation (longitudinal)** | Partial correlation | Regional [11C]PBR28 VT, blood measures |

## Statistical analyses

A number of statistical tests were performed, which are summarised in Table 7 and described in detail here.

Group characteristics were compared using independent sample t-tests (for age), Fisher's exact test (gender, TSPO genotype) and Mann–Whitney U tests (time since injury, PTA duration, visit intervals). Differences in cognitive tests were assessed using either independent sample t-tests or Mann–Whitney tests (where data were not normally distributed according to the Shapiro-Wilk test).

Voxelwise cross-sectional comparison of [$^{11}$C]PBR28 DVR, tissue volumes (i.e. VBM) and FA were performed using nonparametric permutation tests (Nichols and Holmes, 2002) in FSL (10,000 permutations). For all analyses, age was added as a nuisance covariate. For comparisons of [$^{11}$C]PBR28, TSPO genotype was included as a covariate and, for VBM analysis, ICV. All results were cluster corrected using threshold-free cluster enhancement (Smith and Nichols, 2009) with family-wise error rate of $p<0.05$. For [$^{11}$C]PBR28 ROI analysis, mean DVR for each ROI was compared between groups using ANCOVA, with DVR as the dependent variable and genotype and age as covariates, and Fisher LSD post-hoc tests.

To create a composite information processing speed measure for patients, the separate test scores in this domain (Table 10) were converted to Z-scores. Z-scores were calculated for each patient, using controls as a reference (control Z-score mean=0 and SD=1), incorporating a sign flip if necessary such that a positive score corresponded to better performance (e.g. faster reaction time). The composite score was calculated as the arithmetic mean of the component Z-scores.

In patients, partial correlation was used to assess whether DVR in ROIs with increased binding was associated with time since injury or cognitive impairment, with genotype and age as nuisance covariates. Bonferroni correction was used.

To enable direct comparison of modalities, maps of [$^{11}$C]PBR28 DVR, tissue volumes and DTI metrics were converted to Z-score maps (Z-maps). Z-maps were calculated for each patient and modality, using controls as a reference (control Z-map mean=0 and SD=1). To create Z-maps of [$^{11}$C]PBR28 DVR adjusted for age and genotype, first a voxelwise regression was performed in FSL on baseline patient and control DVR maps, with age and genotype as covariates. Second, Z-maps for each patient were computed using the voxelwise formula: *Z=(patient's residual – mean of residuals in controls)/SD of residuals in controls.* A similar procedure was used to create Z-maps of (modulated) tissue volumes (adjusted for age and ICV) and FA (adjusted for

age). All maps were generated from smoothed MNI space images. Then, to directly compare [$^{11}$C]PBR28 DVR with other modalities within a patient, firstly masks of voxels with "high" DVR (thresholded at *Z>+2*) and "normal" DVR (*-1<Z<+1)* were defined. Then, the two masks were used to sample the Z-maps of the other modalities. The mean Z-scores sampled using high and normal masks were then compared in patients using a paired-sample t-test.

Serum levels of NFL and tau were described by their median and interquartile range (IQR), and were log-transformed to achieve a normal distribution for subsequent analysis. In patients, partial correlation was used to assess whether the cerebral WM ROI DVR was associated plasma NFL or tau, with genotype and age as nuisance covariates.

Voxelwise differences in baseline [$^{11}$C]PBR28 binding between treatment groups were assessed using nonparametric permutation tests (as above). Changes in $V_T$ between baseline and 12-weeks in the two groups were first analysed separately using one-sample t-test equivalent nonparametric permutation tests on $\Delta V_T$ images, with TSPO genotype as a nuisance covariate. The two groups were then directly compared using permutation tests, with genotype as a covariate.

For ROI analysis, the effect of minocycline versus no drug on $V_T$ for each ROI was first assessed using repeated-measures ANOVA (RMANOVA), with time as the within-subjects factor (baseline and 12-week) and treatment group (minocycline or no drug) and genotype as between-subjects factors. Post hoc tests using Fisher LSD were planned after significant group by time interactions. $\%\Delta V_T$ and 95% confidence intervals (CI) for each ROI were calculated in each group and tested for significance using a one-sample t-test. A partial correlation assessed whether drug levels were associated with regional $\Delta V_T$, with genotype as a nuisance covariate.

Longitudinal changes in tissue volumes (JD) were first assessed in patients without modeling treatment group. Voxelwise analyses on JD images were performed using one-sample t-test ($\Delta>0, \Delta<0$) equivalents of nonparametric permutation tests. This approach was used in TBI patients combined and

separately in the longitudinal MRI control group. To assess longitudinal changes in total tissue volumes, a one-sample t-test was used on *%Δ/year* measures (above), for GM and WM separately. For voxelwise analysis of ΔFA a similar approach was used as for JD.

To assess longitudinal changes in JD between the two treatment groups, the two groups were directly compared using permutation tests, with time since injury as an additional covariate. The same approach was taken for ΔFA images.

To assess the effect of minocycline versus no drug on NFL, a RMANOVA was used, with time as the within-subjects factor and treatment group as a between-subjects factor, and time since injury as a covariate. Post hoc tests using Fisher LSD were planned after significant group by time interactions. The analyses were performed separately for baseline to 12-week visits, and then for all three visits.

A partial correlation assessed whether percentage change in WM $V_T$ in was correlated with percentage change in NFL (both changes between baseline and 12 weeks), with genotype as a nuisance covariate. Baseline NFL levels were also correlated with the mean WM JD.

To assess the effect of treatment group on mean FA in the corpus callosum ROI, a RMANOVA was used, with time as the within-subjects factor and treatment group as a between-subjects factor, and time since injury as a covariate. Post hoc tests using Fisher LSD were planned after significant group by time interactions. The same approach was used to assess the effect of treatment group on composite information processing speed.

## 4.4. Results

Fifteen patients at least six months after a moderate-to-severe TBI, according to the Mayo classification (Malec *et al.*, 2007), were enrolled. A cross-sectional study of TBI patients compared to age-matched healthy volunteer controls was

performed, followed by a randomized open-label study in patients of minocycline versus no drug (Figure 21).

A screening visit included genotyping for the rs6971 (Ala147Thr) polymorphism in the TSPO gene which produces three classes of binding affinity for second-generation TSPO ligands: high-affinity binders (HABs), mixed-affinity binders (MABs) and low-affinity binders (LABs) (Owen *et al.*, 2012). Individuals with LAB genotype were excluded since they show negligible specific binding of the ligand.

Baseline demographics and clinical characteristics of the TBI patients (13 male (87%), 9 (60%) HABs, age mean age ± SD 42.3 ± 13.7 years, range 23-61; time since injury median 14.7 months, IQR 30.4, range 6-142 months) are provided in Table 8. No patients had undergone neurosurgery after TBI. All patients had one or more focal lesions. The majority of lesions appeared in frontal or temporal lobes.

**Table 8. Demographics and clinical characteristics of the TBI patients**

| Group | Sex | Age (years) | TSPO | Time since injury (mo.) | Cause of injury | LOC | PTA (days) | MRI | Medications | Compliance (%) |
|---|---|---|---|---|---|---|---|---|---|---|
| Mino | Female | 23 | HAB | 11 | Fall | Yes | 2 | Frontal and temporal pole gliosis | COCP OD | 75% |
| Mino | Male | 24 | HAB | 13 | RTA | UK | UK | Left subfrontal contusion | Nil | 23%* |
| Mino | Male | 26 | MAB | 17 | RTA | Yes | 3 | Bifrontal and right temporal contusions | Nil | 85% |
| Mino | Male | 30 | HAB | 67 | Assault | Yes | 90 | Left temporal contusion, gliosis superior vermis | Nil | 97% |
| Mino | Male | 37 | HAB | 41 | Assault | UK | 7 | Left frontal and temporal contusions; left temporal volume loss | Nil | 99% |
| Mino | Male | 51 | HAB | 142 | Unknown | Yes | 90 | Bifrontal, left temporal, right parietal, occipital and temporal lobe contusions | Gabapentin 300mg TDS Amitriptyline 50 mg ON, modafinil PRN | 95% |
| Mino | Male | 53 | HAB | 19 | Fall | Yes | 7 | Left temporal contusion | Vitamin D supp. OD | 95% |
| Mino | Male | 54 | MAB | 22 | RTA | Yes | 7 | Bifrontal contusions | Thyroxine 150mg OD, citalopram 30mg OD | 73% |
| Mino | Male | 57 | MAB | 6 | RTA | Yes | 7 | Bifrontal and right temporal pole contusions | Nil | 99% |
| Mino | Male | 61 | MAB | 10 | RTA | Yes | 2 | Subfrontal and left frontal pole contusions | Nil | 98% |
| No drug | Female | 29 | MAB | 7 | RTA | Yes | 10 | Bifrontal and bitemporal pole contusions | COCP OD | NA |
| No drug | Male | 37 | HAB | 14 | Fall | UK | 0 | Bifrontal contusions | Nil | NA |

| Group | Sex | Age (years) | TSPO | Time since injury (mo.) | Cause of injury | LOC | PTA (days) | MRI | Medications | Compliance (%) |
|---|---|---|---|---|---|---|---|---|---|---|
| No drug | Male | 39 | MAB | 65 | Assault | UK | 21 | Left temporal, bifrontal contusions; left temporal volume loss | Nil | NA |
| No drug | Male | 53 | HAB | 13 | Fall | UK | UK | Bifrontal and bitemporal pole contusions | Lamotrigine 50mg BD | NA |
| No drug | Male | 59 | HAB | 15 | RTA | Yes | 7 | Left and right frontal contusions, left temporal contusions | Simvastatin 40mg OD, omeprazole 20mg OD | NA |

Compliance was calculated as a percentage of expected number of tablets taken (=number of tablets provided-number of tablets returned). BD = twice daily; COCP = combined oral contraceptive pill; LOC = loss of consciousness; HAB = high affinity binder; MAB = medium affinity binder; Mino = minocycline; NA = not applicable; OD = once daily; ON = once nightly; PRN = as required; PTA = post-traumatic amnesia; RTA = road traffic accident; TDS = three times daily. TSPO = translocator protein genotype; UK = unknown; *Patient withdrew from study at start of 12-week visit.

At baseline, patients had [$^{11}$C]PBR28 PET, structural and diffusion MRI, blood sampling for NFL, and cognitive assessment. A group of 28 age- and gender-matched controls had [$^{11}$C]PBR28 PET and structural MRI, and a second group of healthy controls (n=21) had structural and diffusion MRI, blood sampling for NFL (in a subset of 12 participants), and cognitive assessment (Table 9).

**Table 9. Baseline group demographics**

| Group | n | Age (years) mean +/- SD (min-max) | p | Gender N male (%) | p | N HABs (%) | p |
|---|---|---|---|---|---|---|---|
| TBI | 15 | 42.3 ± 13.7 (23-61) | - | 13 (87%) | - | 9 (60%) | - |
| Control 1 ([11C]PBR28 PET) | 28 | 40.8 ± 14.8 (21-63) | 0.756 | 23 (82%) | 0.532 | 16 (57.1%) | 0.559 |
| Control 2 (MRI, NFL, cognitive assessment) | 21 | 41.6 ± 11.8 (21-61) | 0.881 | 17 (81%) | 0.507 | - | - |
| Control 3 (Longitudinal MRI) | 15 | 36.2 ± 8.9 (27-65) | 0.168 | 12 (80%) | 0.500 | - | - |

p-values denote comparisons with the TBI group; SD = standard deviation

## [$^{11}$C]PBR28 binding in TBI patients is increased in WM and subcortical regions

At baseline, areas of high [$^{11}$C]PBR28 distribution volume ratio (DVR), a local measure of binding normalized to whole brain levels, were present in individual TBI patients, particularly within WM (Figure 23A). Voxelwise comparison of patients versus controls showed clusters of significantly increased [$^{11}$C]PBR28 DVR in frontal and temporal WM, striatum, thalamus and brain stem (Figure 23B). There was no increased binding in controls compared to patients.

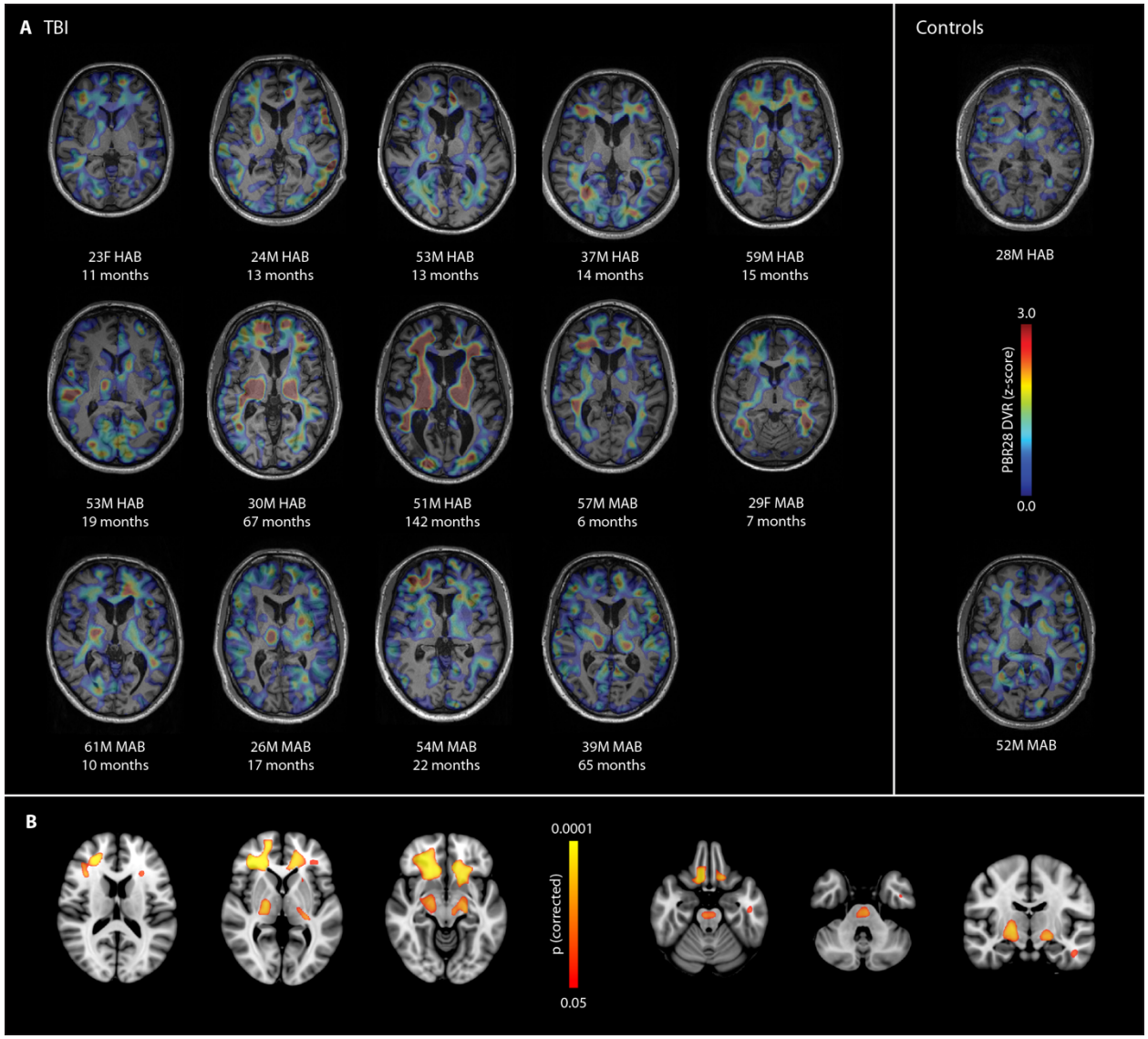



**Figure 23. Increased baseline [11C]PBR28 binding in TBI in WM and subcortical regions.**

(A) Individual standardized (z-score) images of baseline [11C]PBR28 DVR are superimposed on axial T1 MRIs. Voxels with increased DVR (z>0) compared to the control mean, when controlling for age and TSPO genotype, are shown. Baseline images for 14 TBI patients and two representative controls are shown (one patient had missing blood data). The age (years), gender and TSPO genotype of participants is shown. In patients, the time since injury to baseline scanning is also shown. M = male; F = female; HAB = high affinity binder; MAB = medium affinity binder. (B) Red-yellow areas show significantly increased [11C]PBR28 DVR in patients compared to controls. Results are thresholded using threshold free cluster enhancement (family-wise error correction $p<0.05$).

Previous studies suggest chronic microglial activation is prominent in the thalamus and WM (Ramlackhansingh *et al.*, 2011; Smith *et al.*, 2012; Johnson *et al.*, 2013). A confirmatory region of interest (ROI) analysis of [$^{11}$C]PBR28 DVR in thalamus ($F(1,38)=5.11$, $p=0.03$, partial eta squared=0.12) and cerebral WM ($F(1,38)=7.42$, $p=0.01$, partial eta squared=0.16) showed significant increases in TBI patients compared to controls. As a control, we found no significant difference in binding in a cortical gray matter ROI.

In patients, thalamic DVR was positively correlated with time since injury ($r=0.847$, $p=0.001$). Binding in WM did not not correlate with time since injury.

### Cognitive impairment in TBI patients is associated with increased thalamic [$^{11}$C]PBR28 binding

Patients at baseline showed impaired performance in a range of cognitive domains, including tests of information processing speed and executive function (Table 10). In contrast, patients were well matched with controls on the Wechsler Test of Adult Reading, a test of premorbid intellectual ability.

We previously reported an association between thalamic microglial activation and information processing speed (Ramlackhansingh *et al.*, 2011). We investigated whether increased [$^{11}$C]PBR28 binding in the thalamus as well as WM was related to information processing speed. A composite measure of a patient's information processing speed was calculated as the mean of the standardized (z-score) individual test scores in this domain (Table 10), using controls as a reference. The composite z-score in patients was $z=-0.98 \pm 0.8$ (mean ± standard deviation, SD), 95% confidence intervals (CI) -1.44 to -0.52. Thalamic [$^{11}$C]PBR28 DVR was strongly correlated with poorer composite processing speed score ($r=-0.592$, $p=0.026$), supporting our previous findings (Ramlackhansingh *et al.*, 2011), but WM binding was not significantly correlated ($r=-0.336$, $p=0.240$).

**Table 10. Baseline cognitive test results**

| | TBI | Controls | p | TBI Minocycline | TBI No drug | p |
|---|---|---|---|---|---|---|
| N | 15 | 21 | - | 10 | 5 | - |
| Information processing speed | | | | | | |
| CRT median RT (s) | 0.51 ± 0.07 | 0.45 ± 0.08 | 0.024* | 0.51 ± 0.07 | 0.51 ± 0.08 | 0.959 |
| Stroop Colour Naming (s) | 33.0 ± 5.2 | 28.2 ± 5.4 | 0.013* | 34.0 ± 6.3 | 31.6 ± 1.3 | 0.219 |
| Stroop Word Reading (s) | 24.0 ± 5.0 | 20.8 ± 4.3 | 0.058 | 25.7 ± 4.8 | 20.8 ± 4.1 | 0.074 |
| Trail Making Test A (s) | 28.8 ± 11.1 | 20.5 ± 7.1 | 0.019*† | 26.6 ± 11.0 | 33.12 ± 11.2 | 0.304 |
| Trail Making Test B (s) | 63.1 ± 22.9 | 42.4 ± 15.1 | 0.004**† | 64.8 ± 26.7 | 59.6 ± 14.5 | 0.693 |
| Executive function | | | | | | |
| Stroop Inhibition (s) | 59.5 ± 21.4 | 50.7 ± 12.3 | 0.128 | 62.6 ± 25.7 | 54.0 ± 10.4 | 0.49 |
| Stroop Inhibition-Switching (s) | 64.1 ± 12.3 | 55.3 ± 10.6 | 0.032* | 63.8 ± 14.1 | 65.0 ± 9.5 | 0.845 |
| Trail Making Test B-A (s) | 34.3 ± 19.0 | 22.5 ± 12.1 | 0.031* | 38.2 ± 21.2 | 26.5 ± 11.5 | 0.274 |
| Memory | | | | | | |
| WMS-III LM1 immediate recall | 43.1 ± 12.1 | 48.9 ± 8.5 | 0.107 | 44.3 ± 14.0 | 41.0 ± 8.6 | 0.64 |
| WMS-III LM2 delayed recall | 28.2 ± 10.2 | 32.3 ± 7.2 | 0.177 | 30.1 ± 10.6 | 25.0 ± 9.8 | 0.392 |
| PT immediate total | 28.7 ± 5.2 | 29.6 ± 4.5 | 0.584 | 28.1 ± 6.0 | 29.8 ± 3.4 | 0.579 |
| PT delayed total | 9.6 ± 3.0 | 11.3 ± 1.1 | 0.192† | 9.6 ± 3.2 | 9.4 ± 3.0 | 0.882 |
| Intellectual ability | | | | | | |
| WTAR scaled | 107.6 ± 10.6 | 112.9 ± 8.7 | 0.112 | 105.3 ± 12.3 | 111.6 ± 5.5 | 0.306 |
| WASI Matrix reasoning | 24.7 ± 4.6 | 28.3 ± 3.2 | 0.009*† | 25.6 ± 4.6 | 23.4 ± 4.8 | 0.424 |

CRT = choice-reaction task (CRT); PT = People Test; RT = reaction time; s = seconds; WASI = Wechsler Abbreviated Scale of Intelligence; WMS-III = Wechsler Memory Scale; WTAR = Wechsler Test of Adult Reading. See Materials and Methods for details. Numerical values are mean ± standard deviation. *p<0.05, **p<0.01. †Mann-Whitney test.

### WM damage in TBI patients is greater in areas of high [$^{11}$C]PBR28 binding

At baseline, most of the WM in TBI patients showed reduced tissue volume compared to controls, measured using volumetric MRI (Figure 24A). In addition, significant clusters of gray matter (GM) reduction were also observed in frontal and temporal cortex, hippocampus and subcortical structures (Figure 24B). There were no areas of volume increase in patients versus controls. Diffusion MRI showed widespread decreases in fractional anisotropy (FA) (Figure 24C), indicating reduced WM tract integrity. The areas of volume loss and reduced WM integrity extended far beyond sites of focal lesions (Figure 24D).

These cross-sectional findings support previous neuroimaging studies in chronic TBI showing widespread tissue volume loss (Tomaiuolo *et al.*, 1999; Isoniemi *et al.*, 2006; Trivedi *et al.*, 2007; Bendlin *et al.*, 2008; Sidaros *et al.*, 2008) and WM disruption (Kinnunen *et al.*, 2011). Neuropathological studies suggest chronic microglial activation co-localizes with markers of ongoing WM damage (Smith *et al.*, 2012; Johnson *et al.*, 2013), but this association has never been established *in vivo.* Brain areas showing increased baseline [$^{11}$C]PBR28 DVR in TBI patients (Figure 23. Increased baseline [11C]PBR28 binding in TBI in WM and subcortical regions.

(A) Individual standardized (z-score) images of baseline [11C]PBR28 DVR are superimposed on axial T1 MRIs. Voxels with increased DVR (z>0) compared to the control mean, when controlling for age and TSPO genotype, are shown. Baseline images for 14 TBI patients and two representative controls are shown (one patient had missing blood data). The age (years), gender and TSPO genotype of participants is shown. In patients, the time since injury to baseline scanning is also shown. M = male; F = female; HAB = high affinity binder; MAB = medium affinity binder. (B) Red-yellow areas show significantly increased [11C]PBR28 DVR in patients compared to controls. Results are thresholded using threshold free cluster enhancement (family-wise error correction $p<0.05$).

B) overlapped with areas of WM volume loss (Figure 24A) and reduced FA (Figure 24C). Co-registered and standardized [$^{11}$C]PBR28 and MRI images were used to assess the relationship between microglial activation and WM damage. In individual patients, WM voxels with high [$^{11}$C]PBR28 binding (DVR)

showed a greater reduction in tissue volume than those voxels with normal binding (Figure 24E) (p=0.004). Similarly, WM voxels with high binding also had lower FA than voxels with normal binding (Figure 24F) (p=0.003).

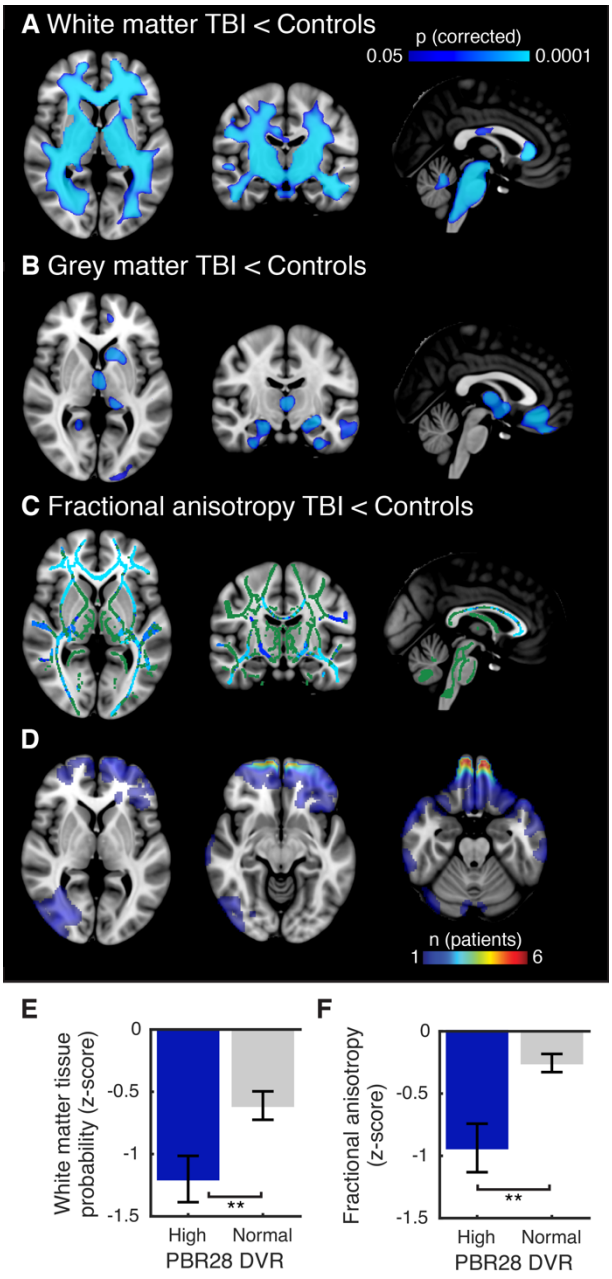



**Figure 24. Baseline WM volume loss and reduced WM tract integrity are greater in areas of high [$^{11}$C]PBR28 binding in TBI patients.**

(A) Blue-light blue areas show significantly decreased WM volume loss in patients compared to controls. Results are thresholded using threshold free cluster enhancement (family-wise error correction $p<0.05$). (B) Significantly decreased GM volume in patients compared to controls. Thresholding and colour bar are as for A. (C) Blue-light blue areas show significantly decreased FA in patients compared to controls. The contrast is overlaid on the mean FA skeleton (green). Thresholding and colour bar are as for A. (D) Overlap map in patients of lesions visible on T1 structural imaging. The colour of the map indicates the number of patients with a lesion in that area. Maps were computed by summation of the normalized binary lesion masks of individual patients. (E) In patients, WM tissue probability, a measure of tissue volume expressed as a z-score with controls as a reference, is shown for areas of individually-defined high levels of WM [$^{11}$C]PBR28 DVR (blue bar) and normal levels of DVR (grey bar). (F) As for E, but showing fractional anisotropy, expressed as a z-score with controls as a reference. Bars for E and F are mean ± standard error of the mean (SEM) $^{**}p<0.01$.

## Increased plasma NFL levels in TBI patients are associated with time since injury and [$^{11}$C]PBR28 WM binding

Elevated peripheral levels of NFL have been observed hours and days after TBI (Zetterberg, Smith and Blennow, 2013), but it is unclear whether NFL remains elevated in the chronic phase, or how levels relate to other measures of injury. In TBI patients, all more than six months after injury, plasma NFL levels at baseline were significantly higher (mean 17.86 pg/ml, median 12.08 pg/ml, SD 18.06, IQR 10.20, range 5.75-72.11) than controls (n=12, 7.58 pg/ml, median 7.00 pg/ml, SD 1.29, IQR 1.66, range 5.84-9.99) (t=3.09, df=16.15, p=0.007) (Figure 25A). Plasma NFL levels in TBI patients were negatively correlated with time since injury (r=-0.546, p=0.035), but most patients had elevated NFL compared to control levels (Figure 25B). There was no correlation between plasma NFL and the duration of post-traumatic amnesia (PTA) (r=-0.268, p=0.377), a marker of initial injury severity. There was no correlation between NFL and composite information processing speed score.

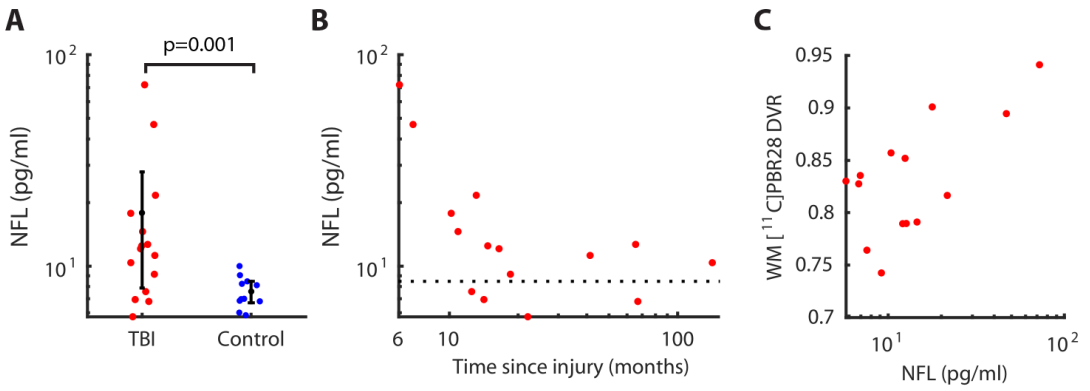



**Figure 25. Plasma NFL and associations with [$^{11}$C]PBR28 WM binding and time since injury.**

(A) Plasma NFL levels are shown for TBI patients (red dots) and controls (blue dots). Black bars show mean and 95% confidence intervals. Note y-axis is logarithmic. (B) Plasma NFL in TBI patients (y-axis) is plotted against time since injury in months (x-axis). Dotted horizontal line indicates upper limit of 95% confidence interval in controls. Note both axes are logarithmic. (C) [$^{11}$C]PBR28 DVR of the cerebral WM region of interest in TBI patients (y-axis) plotted against plasma neurofilament light chain (NFL) level (x-axis, logarithmic).

In contrast, plasma tau levels were not significantly different between TBI patients (mean 2.160 pg/ml, median 1.557 pg/ml, SD1.797, IQR 1.210, range 0.802-9.690) and controls (mean 1.660 pg/ml, median 1.392, SD 0.570, IQR 0.980, range 0.738-2.492) (t=0.895, df=35, p=0.377). Plasma tau did not

correlate with time since injury, duration of PTA or speed of information processing. For these reasons, tau levels were not used in subsequent analyses.

NFL has been proposed as a marker of active axonal degeneration in a variety of CNS disorders (Eikelenboom *et al.*, 2003; Liu *et al.*, 2004; Gaiottino *et al.*, 2013; Lu *et al.*, 2015; Gisslén *et al.*, 2016). Plasma NFL levels in chronic TBI may therefore be associated with processes related to WM damage. In patients, baseline plasma NFL levels were strongly positively correlated with [$^{11}$C]PBR28 DVR in cerebral WM (Figure 25C) (r=0.519, p=0.042).

### Minocycline in TBI patients reduces [$^{11}$C]PBR28 binding

The effect of minocycline on [$^{11}$C]PBR28 binding in the TBI patients was investigated. Patients were randomized to one of two parallel groups in a 2:1 ratio, balanced for age, gender, TSPO genotype and time since injury. One group (n=10) received minocycline 100mg orally twice daily for 12-weeks; the other (n=5) had no drug. Patients were followed up after 12-weeks with [$^{11}$C]PBR28 PET, MRI, plasma NFL and cognitive assessment, and again at six months after the baseline visit, but without PET. Demographics and clinical characteristics of the patients were similar between minocycline (n=10) and untreated (n=5) groups (Table 8). There were no significant baseline treatment arm differences in cognitive performance (Table 10), age (41.7 ± 15.0 years versus 43.4 ± 12.3, p=0.831), gender (9/10 (90%) male versus 4/5 (80%), p=0.571), genotype (6/10 (60%) HABs versus 3/5 (60%), p=0.713), time since injury (median 17.5, months IQR 37.0 versus 14.1, IQR 30.2, p=0.573) or duration of PTA (median 4 days, IQR 46 versus 8.5, IQR 17, p=0.511).

[$^{11}$C]PBR28 volume of distribution ($V_T$) allows absolute quantification (Jucaite *et al.*, 2015; Sandiego *et al.*, 2015) and so was used as the outcome measure for assessing within-subject drug effects. Voxelwise changes in $V_T$ between baseline and 12-weeks ($\Delta V_T$) were first analysed in the minocycline and untreated groups separately (Figure 26A and Figure 26B). In the minocycline group, [$^{11}$C]PBR28 $V_T$ was significantly reduced ($\Delta V_T<0$) at 12-weeks compared to baseline across most of the brain (Figure 26B), including large

clusters of white and GM. In the untreated group, there was no significant reduction in binding (Figure 26B). There were no areas of significant increase in either group. In the direct contrast of the two arms, $\Delta V_T$ in the minocycline group was significantly reduced compared to the untreated group in large clusters of white and GM (Figure 26C), with no areas of significantly increased $\Delta V_T$. There were no baseline voxelwise differences in $V_T$ between the two arms.

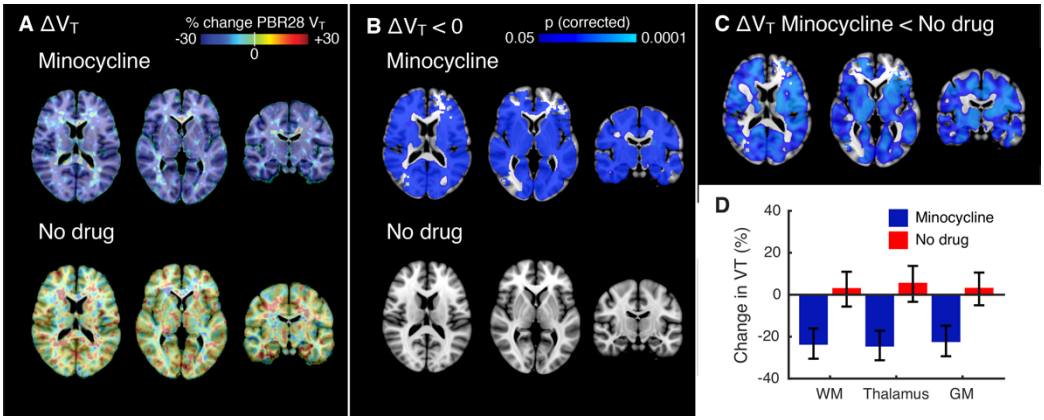



**Figure 26. Minocycline in TBI patients reduces [$^{11}$C]PBR28 binding**

(A) Mean change in [$^{11}$C]PBR28 volume of distribution (ΔVT) between baseline and 12-week visits, expressed as a percentage of baseline VT, in patients who received minocycline treatment (n=7) (top row) and no drug (n=5) (bottom row). (See Fig 1 for description of excluded data.) Green colours represent little or no change over time, yellow-red colours reflect VT increases over time, while blue-light blue colours reflect VT decreases. Images are superimposed on the MNI T1 template. (B) Blue-light blue areas show significantly decreased VT between baseline and 12-week visits (ΔVT < 0), in patients who received minocycline treatment (top row) and no drug (bottom row). Results are thresholded using threshold free cluster enhancement (family-wise error correction <0.05). Neither group showed areas of significantly increased VT (ΔVT > 0). (C) Blue-light blue areas show significantly reduced ΔVT in patients who received minocycline treatment compared to patients who received no drug. There were no areas of significantly increased ΔVT in patients versus controls. Thresholding and colour bar are as for B. (D) Mean ± SEM group change in VT, expressed as a percentage of baseline VT, in patients who received minocycline treatment (blue bars) and no drug (red bars), in WM, thalamus and cortical GM regions of interest.

An ROI analysis showed a significant treatment group × time interaction ($F(1,9)=7.178$, $p=0.025$, partial eta squared=0.444) in cerebral WM, with non-significant effects of group, time, genotype and genotype × time. Post-hoc Fisher LSD tests showed a significant $V_T$ reduction between baseline and 12-weeks in the minocycline group (mean difference ± standard error -0.741 ± 0.190, $p=0.004$, 95% CI -1.171 to -0.311) but no change in the no drug group (-0.048 ± 0.225, $p=0.835$, 95% CI -0.557 to 0.461). Analysis of the thalamus ROI showed a similar significant group × time interaction ($F(1,9)=7.569$,

p=0.022, partial eta squared=0.457, mean difference ± standard error in the minocycline group -1.097 ± 0.310, p=0.006, 95% CI -1.798 to -0.395) as well as cortical GM (F(1,9)=6.255, p=0.034, partial eta squared=0.410, mean difference ± standard error -0.855 ± 0.245, p=0.007, 95% CI -1.408 to -0.301).

Expressed as percentage change from baseline (Figure 26D), minocycline significantly reduced $V_T$ in WM (mean ± SD -23.30 ± 19.09%, 95% CI -40.9 to -5.64%, range -42.7 to +4.5%, p=0.018), thalamus (-24.18 ± 18.71%, CI -41.48 to -6.90%, range -43.59% to +0.90%, p=0.014) and cortical GM (-22.05 ± 19.33%, CI -39.93% to -4.17%, range -40.05-7.47%, p=0.023). There were no significant changes in the untreated group. In the minocycline group, the mean reduction in HABs was greater than MABs in each ROI (for example, mean reduction in WM $V_T$ was -31.07% versus -12.9%).

In the minocycline group, compliance (defined as the proportion of expected number of tablets taken) was 91±10% (mean ± SD), range 73-99%. Plasma trough minocycline levels at 12-weeks were 2.08 ± 0.55mg/L (mean ± SD), range 1.29-2.80mg/L. There was no significant correlation between drug levels and $\Delta V_T$ in any of the three ROIs.

Further related results appear in Chapter 5, followed by a discussion.

Chapter 5

# 5. Neurodegeneration and the effect of minocycline after brain trauma

In this chapter, I develop the findings of the Chapter 4 by investigating the effect of minocycline on other measures of brain injury and recovery. To conclude, I discuss the findings from both chapters.

## 5.1. Results

### Longitudinal WM atrophy in TBI patients is greater in areas of high baseline [$^{11}$C]PBR28 binding

As presented in the previous chapter, at baseline, [$^{11}$C]PBR28 binding in patients was increased compared to controls in cerebral WM and thalamus. We had also found tissue volume loss at baseline was present after TBI, particularly in WM, and related to microglial activation. To assess WM atrophy over time, i.e. longitudinally, and the effect of minocycline, TBI patients as well as a group of controls had repeated MRI scans.

Patients from minocycline and untreated arms were initially analysed as a single group, to provide an indication of longitudinal change in all patients, before comparing the two treatment arms directly. In patients, between baseline and 6-month scans the total WM volume significantly decreased (annualized mean ± SD -1.6 ± 2.8% per year, p=0.039, scan interval mean ± SD 0.50 ± 0.07 years). No significant change was seen in total GM volume. In comparison, in the longitudinal control group (scan interval 1.11 ± 0.18 years), there were no significant changes in total WM (0.06 ± 0.77% per year, p=0.758) or GM. In the combined patients, the group mean of annualized JD images, which provide a

voxelwise measure of longitudinal tissue volume change, showed contraction in WM and areas of GM, with corresponding expansion of the CSF-containing spaces (Figure 27A). Voxelwise analysis of JD images showed significant clusters of longitudinal atrophy (JD<0) in frontal and subcortical WM (Figure 27B). There was also significant atrophy in frontal, temporal and subcortical GM (Figure 27C). There were no areas of white or GM expansion (JD>0).

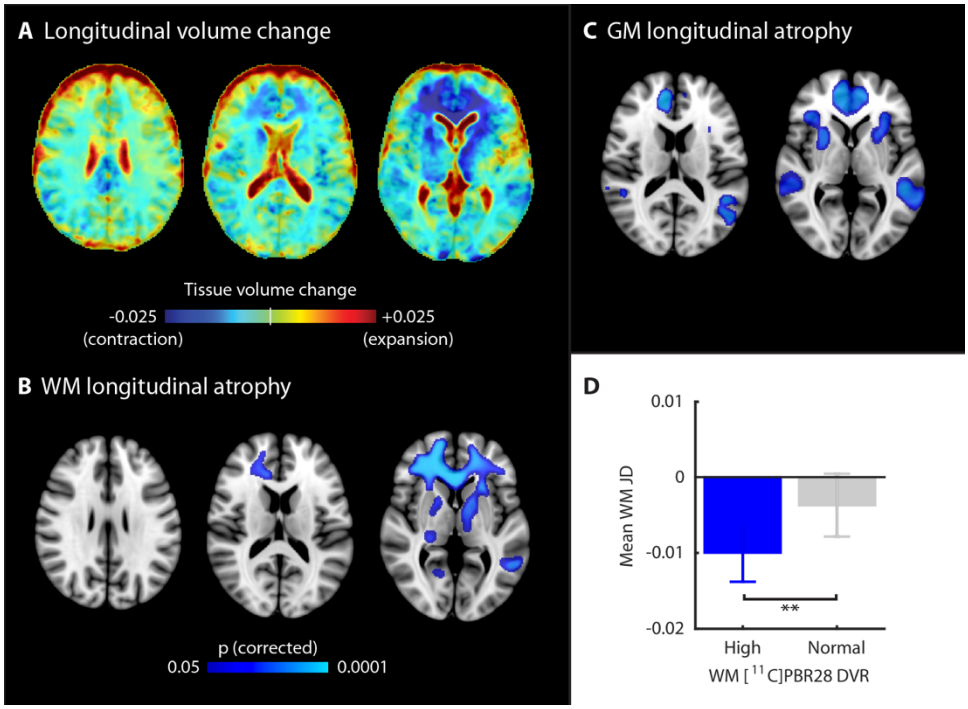



**Figure 27. Longitudinal WM atrophy over six months in TBI patients is greater in areas of high baseline [$^{11}$C]PBR28 binding**

(A) Mean annualized Jacobian determinant (JD) images, indexing longitudinal change over six months in patients. Green colours represent little or no change over time, yellow-red colors reflect volumetric increases (expansion, positive JD), while blue-light blue colors reflect volumetric decreases (contraction, negative JD). Mean JD images are superimposed on the MNI T1 template. (B) Blue-light blue areas show significantly decreased JD, indicating longitudinal atrophy in WM over six months (WM tissue-specific JD<0), in patients. Results are thresholded using threshold free cluster enhancement (family-wise error correction <0.05). (C) Significantly decreased JD in GM over six months in patients, indicating longitudinal atrophy in GM (GM tissue-specific JD<0). Thresholding and colour bar are as for B. (D) In patients, mean JD in WM is shown for areas of individually-defined high levels of WM [$^{11}$C]PBR28 binding (distribution volume ratio, DVR) (blue bar) and normal levels of DVR (grey bar). Bars are mean ± SEM **p<0.01.

In contrast, there were no areas of significant change detected in the control group, despite the longer scan interval.

These longitudinal findings are consistent with previous neuroimaging studies in TBI showing progressive longitudinal atrophy (Sidaros *et al.*, 2008, 2009;

Ross, 2011). To assess the relationship between longitudinal WM atrophy and microglial activation, co-registered images of longitudinal change (JD) and standardized baseline [$^{11}$C]PBR28 DVR were sampled. Within individual TBI patients, the mean longitudinal change (JD) in WM voxels with high [$^{11}$C]PBR28 binding at baseline was more negative (i.e. suggesting greater contraction) than those voxels with normal baseline binding (Figure 27D) (p=0.004).

### Minocycline in TBI patients has no effect on longitudinal WM atrophy

The effect of minocycline on longitudinal WM atrophy measures was explored. In the voxelwise comparison of JD images in the two treatment arms, there were no areas of significant difference in WM or GM. There were also no significant differences in mean JD values, nor in annualized change in total white WM volume.

### Minocycline in TBI patients increases plasma NFL levels, associated with reduction in [$^{11}$C]PBR28 binding

Minocycline has previously been shown to reduce elevated serum NFL levels in a small group of patients with acute human spinal cord injury (Kuhle *et al.*, 2015). NFL levels over time in the minocycline-treated TBI patients and untreated patients were compared. The minocycline group showed a distinct time course of NFL compared to the untreated group, with an increase at the 12-week visit, post minocycline (Figure 28A). A RMANOVA using baseline and 12-week visits showed a significant treatment group × time interaction ($F(1,11)=8.308$, $p=0.015$, partial eta squared=0.430) in NFL, with non-significant effects of time since injury. Post-hoc Fisher LSD tests showed a significant NFL increase between baseline and 12-weeks in the minocycline group (mean difference ± standard error +0.386 ± 0.093, p=0.002, 95% CI 0.182 to 0.591) but no change in the untreated group (-0.0687± 0.125, p=0.602, 95% CI -0.343 to 0.209). An analysis using all three visits showed a significant treatment group × time interaction ($F(2,22)=6.155$, $p=0.008$, partial eta squared=0.359).

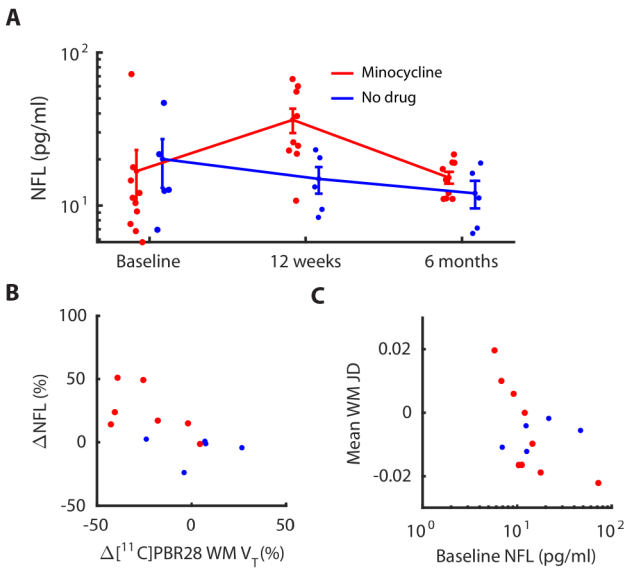



**Figure 28. Effect of minocycline treatment on plasma NFL, and the associations between NFL, [$^{11}$C]PBR28 WM binding and longitudinal atrophy.**

(A) Plasma NFL levels are shown for TBI patients treated with minocycline (red dots) and untreated patients (no drug, blue dots) for the three visits. Bars show visit mean (connected over time) and standard error. Note y-axis is logarithmic. (B) Percentage change in NFL between baseline and 12-weeks (y-axis) is plotted against percentage change in WM [$^{11}$C]PBR28 VT (x-axis) measured over the same period. Colors are defined as in A. (C) Mean WM JD (y-axis) (measured between baseline and six months) is plotted against baseline NFL in patients. Colours are defined as in A.

Since we had found a positive association at baseline between NFL and [$^{11}$C]PBR28 WM binding, the relationship between change in NFL and [$^{11}$C]PBR28 binding over the 12 week treatment period was investigated. In patients from both treatment arms combined, the percentage change in NFL between baseline and 12-week visits was strongly negatively correlated with the percentage change in WM [$^{11}$C]PBR28 $V_T$ measured over the same period (r=-0.558, p=0.048) (Figure 28B).

### Plasma NFL levels predict longitudinal WM atrophy in TBI patients

Since NFL has been proposed as potential prognostic indicator of degeneration (Lu *et al.*, 2015; Gisslén *et al.*, 2016) in other disorders, the relationship between baseline NFL and longitudinal atrophy was explored. In all TBI patients combined, baseline plasma NFL levels were negatively correlated with longitudinal WM volume change (mean JD) over the subsequent 6 months (r=-0.562, p=0.005). However, when the two treatment arms were analysed separately, we found a strong correlation in the minocycline group (r=-0.850, p=0.004) but no correlation in the untreated group (r=0.300, p=0.624) (Figure 28C). The association in the minocycline group also remained significant when the average of the baseline and 12-week NFL values was used (r=-0.667, p=0.05).

### Minocycline in TBI patients has a negative effect on WM tract integrity

In all TBI patients combined, a voxelwise longitudinal analysis of FA between baseline and 12-week visits as well between baseline and 6-month visits showed no areas of significant change. When voxelwise longitudinal change between the two treatment groups was compared, there were also no differences.

The corpus callosum is frequently a site of traumatic axonal injury (Johnson, Stewart and Smith, 2013), and shows neurodegenerative changes long after TBI (Johnson *et al.*, 2013). The corpus callosum also shows relatively high test-retest reliability in diffusion MRI measurements compared to other regions (Wang *et al.*, 2012). We have previous observed reduced FA in the body and splenium of the corpus callosum in the chronic stage of TBI (Kinnunen *et al.*, 2011). For these reasons, a ROI analysis using a mask of these areas was performed. The ROI analysis showed a significant treatment group × time interaction ($F(1,11)=5.085$, $p=0.045$, partial eta squared=0.316). Post-hoc Fisher LSD tests showed non-significant reductions in FA between baseline and 12-weeks in the minocycline group (mean difference ± standard error -0.007 ± 0.004, p=0.161, 95% CI -0.016 to -0.003) and increases in the untreated group (0.010 ± 0.006, p=0.114, 95% CI -0.003 to 0.023). Expressed

as percentage change from baseline, minocycline was associated with reduced mean FA (mean ± SD -0.74% ± 1.78%) over 12 weeks, compared to an increase (1.18 ± 1.98%) in the untreated group.

### Minocycline in TBI patients is associated with a borderline worsening of information processing speed

We investigated the effect of treatment arm on change in the composite information processing speed measure that had been analysed at baseline. There was a borderline significant treatment group × time interaction ($F(1,11)=4.147$, $p=0.067$, partial eta squared=0.274), with reduction in processing speed performance (more negative z-score) in the minocycline group from baseline to 12-weeks, compared to the untreated group (Figure 29). The change in performance in the two visits in the minocycline group was not significant on post-hoc testing (mean difference ± standard error -0.188 ± 0.143, $p=0.214$, 95% CI -0.502 to 0.126, Fisher LSD). There were no significant treatment group × time interactions when assessing baseline and 6-month visits.

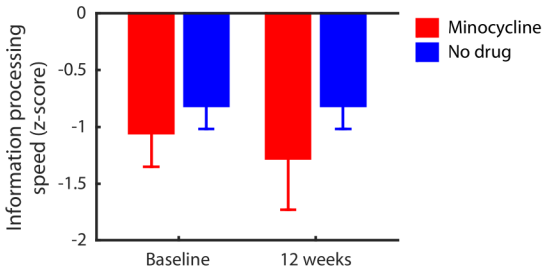



**Figure 29. Effect of minocycline versus no drug on information processing speed performance in TBI patients.**

The mean ± SEM of the composite information processing speed (expressed as as a mean of individual standardized test scores, with control performance as a reference) is shown for patients who received minocycline treatment (red bars) and no drug (blue bars), at baseline and 12-week visits.

We next investigated the relationship between the change in WM [$^{11}$C]PBR28 $V_T$ from baseline to 12-weeks and the corresponding change in information processing speed (Z-score, where a positive score indicates better than average performance). This showed a positive correlation between increasing

[$^{11}$C]PBR28 binding between the two visits and improved performance (Spearman's r=0.636, p=0.022).

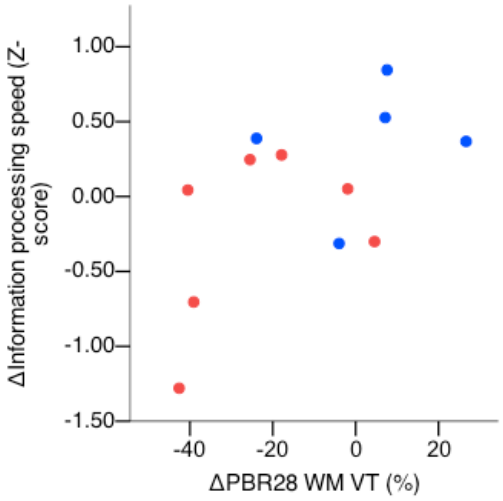



**Figure 30. Association between change in white matter binding and change in information processing speed in patients.**

Change in information processing speed (as a Z-score, i.e. in standard deviations) between baseline and 12-weeks (y-axis) is plotted against the percentage change in WM [$^{11}$C]PBR28 $V_T$ (x-axis) measured over the same period. Values are shown both for patients who received minocycline treatment (red) and no drug (blue). A positive value for Δ information process speed indicates an improved performance.

### Minocycline was generally well tolerated in TBI patients

Minocycline treatment was generally well tolerated in TBI patients. One patient had nausea and vomiting which was treated initially with anti-emetics and then by reducing the dose to 100mg once daily. One patient had mild subjective unilateral hearing impairment, which began within days of starting minocycline. This was treated initially with decongestants and resolved spontaneously despite continuation of the minocycline.

## 5.2. Discussion

The following discussion relates to the results presented in Chapters 4 and 5.

Brain trauma can trigger long-term neurodegenerative processes, including persistent neuroinflammation (Faden and Loane, 2015). Using [$^{11}$C]PBR28 PET, we provide evidence that chronic microglial activation is associated with WM damage months and years after moderate-severe TBI. Areas associated

with high [$^{11}$C]PBR28 binding show greater damage and atrophy. These findings, albeit in a small and variable sample of patients, suggest a mechanistic link between TBI-induced chronic neuroinflammation and neurodegeneration. We also show that plasma NFL can remain elevated months to years after TBI, and that levels are associated with WM inflammation. We also show that minocycline in TBI patients is associated with a widespread reduction in [$^{11}$C]PBR28 binding, providing *in vivo* evidence of an effect of minocycline on microglial activation. In analysis which should be considered exploratory in light of the small sample size, minocycline was associated with an increase in NFL, as well as reduced WM integrity in the corpus callosum and borderline slowing of information processing speed. These findings suggest minocycline inhibits chronic microglial activation but may also impede recovery after brain trauma.

We found evidence for chronic microglial activation in areas of damaged WM, as demonstrated by reduced baseline tissue volume and FA, and progressive atrophy over a six-month period. Increasing evidence links chronic microglial activation to post-traumatic neurodegeneration (Faden and Loane, 2015). Our findings are consistent with neuropathological studies showing persistently activated microglia at sites of ongoing WM degeneration many years after injury (Johnson *et al.*, 2013). Chronically activated microglia co-locate with myelin breakdown products but their role in this situation is unclear (Johnson *et al.*, 2013). Some evidence suggests microglia exhibit a predominantly pro-inflammatory activation phenotype (Loane *et al.*, 2014; Kumar *et al.*, 2015). Such observations motivate a strategy targeting inhibition of activated microglia in the chronic phase after TBI as a means to reduce post-traumatic neurodegeneration. However, studies in non-human primates show microglial activation months after injury may have a trophic role (Nagamoto-Combs *et al.*, 2007, 2010).

We show for the first time, albeit in a small group of patients that plasma NFL can remain chronically elevated after TBI, although it falls slowly with time since injury. Plasma and CSF NFL have been shown to be highly correlated (Gisslén

*et al.*, 2016), and elevated CSF levels of NFL have been observed in acute stages of severe TBI and in repetitive mild TBI (Zetterberg, Smith and Blennow, 2013). In acute severe TBI, plasma neurofilament levels have been shown to be elevated and predictive of early outcomes (Siman *et al.*, 2009). However, the long-term time course and clinical relevance of plasma NFL has been unclear.

What is the source of the plasma elevation in NFL after TBI? Acute increases in plasma biomarkers of brain injury have been thought to partly reflect breakdown in BBB permeability seen shortly after TBI. This is assumed to be a transient change and so this may not explain how NFL accesses the blood from the brain. Recent work has highlighted the importance of the glymphatic system as a conduit from brain to blood via the cervical lymphatic system (Plog *et al.*, 2015). It has been proposed that plasma NFL levels reflect the release of neurofilaments from myelinated axons damaged following TBI. The relationships we observed between plasma NFL levels, neuroinflammation and brain atrophy are in keeping with this hypothesis and our results begin to validate its use as a biomarker of post-acute axonal injury. Elevations in plasma NFL have been observed in a variety of neurodegenerative diseases, including AD (Schraen-Maschke *et al.*, 2008; Gaiottino *et al.*, 2013), ALS and human immunovirus (HIV)-related cognitive impairment. In these contexts NFL has been proposed to be a biomarker of active neurodegeneration (Gaiottino *et al.*, 2013; Lu *et al.*, 2015; Gisslén *et al.*, 2016), which is in keeping with our results in TBI. It is possible that persistence of BBB leakage in the chronic phase contributed to the increased plasma levels of NFL. In this study, unfortunately no index of BBB permeability was available. Studies combining CSF and plasma NFL in TBI patients in the chronic phase would be beneficial in this regard, as would more studies examining the BBB permeability in the chronic phase.

Our results provide evidence that minocycline has a CNS effect and reduces microglial activation. In animal studies, minocycline can produce more than a 50% reduction in microglial activation following experimental TBI (Homsi *et al.*,

2010). Here we show a ~25% reduction in [$^{11}$C]PBR28 binding long after TBI. It had been unclear whether standard clinical doses of 100-200mg/day would provide an adequate CNS concentration to inhibit microglial activation (Plane *et al.*, 2010). Animal studies have typically used much higher doses (human-equivalent ~3-7g/day) (Plane *et al.*, 2010), which are likely to be toxic in humans (Plane *et al.*, 2010). Our findings, whilst in small numbers, provide evidence that a 100mg twice daily dose is sufficient to produce a demonstrable effect on CNS microglial activation in humans.

An important question is what the effects of reducing chronic microglial activation with minocycline will be. Several factors make this challenging. Firstly, microglia can adopt both pro-inflammatory and restorative activation phenotypes (Kettenmann *et al.*, 2011), hence inhibition of these disparate phenotypes may have different effects. Some experimental TBI work suggests the predominant phenotype early after injury may be restorative, but this shifts over time towards a pro-inflammatory state associated with neurodegeneration (Kumar *et al.*, 2015). In addition, a pro-inflammatory phenotype is more common in WM than GM (Olah *et al.*, 2011). On the basis of such observations, the increased WM [$^{11}$C]PBR28 binding may be more attributable to pro-inflammatory microglia. Secondly, minocycline may have a differential action on minocycline according to phenotype. For example, recent animal studies suggests minocycline shifts microglia towards a more restorative (M2-like) phenotype (Kobayashi *et al.*, 2013; Burke *et al.*, 2014). If a pro-inflammatory phenotype predominates in the chronic phase post-TBI, then the effect of minocycline might therefore be beneficial. However, if minocycline additionally acts to reduce the activity of all phenotypes then this benefit may be cancelled out. Thirdly, evidence is lacking that [$^{11}$C]PBR28 binding can discriminate microglial activation phenotypes. The TSPO PET imaging alone therefore limits the interpretation of the reduction in signal seen after minocycline. Fourthly, whether the neuroprotective action of minocycline can be solely attributed to the inhibition of microglia has been drawn into question (Möller *et al.*, 2016). Minocycline has a variety of actions and it may be that the reduction of [$^{11}$C]PBR28 binding is produced via one or more indirect mechanisms rather

than the direct inhibition of microglia. Evidently further basic and translational work is required to answer these questions with confidence.

We found preliminary evidence for negative effects of minocycline on measures of neurodegeneration and cognitive outcome after TBI. Minocycline increased plasma NFL levels after 12 weeks of treatment, and the increase in NFL was in proportion to the reduction in [$^{11}$C]PBR28 binding seen over the same period. Furthermore, whilst longitudinal atrophy measures did not differ between treated and untreated arms, in the minocycline group, baseline NFL was predictive of WM atrophy over the subsequent six months. These findings are contrary to a study of minocycline in acute spinal cord injury, where treatment was associated with a reduction in NFL levels in a subgroup of patients (Kuhle *et al.*, 2015). We also found minocycline had a very small but negative effect on WM tract integrity and a borderline negative effect on information processing speed after 12 weeks of treatment. One interpretation of these exploratory findings is that the effect on microglia of minocycline exacerbates chronic neurodegeneration after TBI, a process charted by plasma NFL levels. An alternative interpretation is that minocycline has secondary, harmful, effects which dominate over any beneficial effects of microglial inhibition. Our findings resonate with the outcome of the largest neurological study of minocycline (n=412) to date, a randomized placebo-controlled study in ALS (Gordon *et al.*, 2007), a condition in which elevated NFL is a prognostic indicator (Lu *et al.*, 2015). In that study, minocycline was found to have detrimental effects on functional rating scores in a dose-independent manner (Gordon *et al.*, 2007).

There are several limitations to our study. As highlighted already in the discussion, the small sample size means our findings should be regarded as preliminary. For example, we could have missed important relationships with voxelwise imaging measures, or between plasma NFL and cognitive performance, because of power issues. Larger studies would be necessary to properly evaluate whether plasma NFL levels correlate with clinical outcome. However, it is worth noting that in the broader neurodegenerative field, plasma and neuroimaging biomarkers frequently fail to correlate well with clinical

measures, despite reflecting well-validated measures of disease progression. In addition, host factors, including age (Perry, Cunningham and Holmes, 2007; Kumar *et al.*, 2013; Rawji *et al.*, 2016) and genetics (for example apolipoprotein E (*APOE*) genotype) (Hartman *et al.*, 2002; Cudaback *et al.*, 2011) are already known to influence the neuroinflammatory and neurodegenerative sequelae of injury, but these were not factored in.

Several of our results are clinically important. Firstly, we have demonstrated chronic microglial activation accompanying markers of progressive damage following brain trauma. These findings should highlight to clinicians that TBI is not a static insult, but rather a chronic disease with potentially persistent neuroinflammatory and neurodegenerative sequelae. Secondly, our results suggest that plasma NFL, in combination with neuroimaging measures of progressive WM atrophy, is a promising approach to evaluating long-term axonal injury. Many TBI survivors make a poor recovery or deteriorate long after the injury, but it is not currently possible to identify patients who are likely to do so. A biomarker of disease progression would allow patients at risk of poor outcomes to be identified, and would facilitate clinical studies of long-term sequelae of TBI. This could have great clinical utility, for example, in quantifying the accumulated brain injury sustained as a result of multiple repetitive mild TBIs, such as during a professional sporting career (Oliver *et al.*, 2015), and estimating the risk of developing post-traumatic dementia, including CTE (McKee *et al.*, 2013). Thirdly, our findings serve as a caution for future research in minocycline treatment for TBI patients in the chronic phase.

## Further discussion on TSPO PET

The TSPO PET work in Chapters 4 and 5, combined with that in Chapter 3, highlight many challenges of TSPO imaging, which are discussed further here.

Despite being the TSPO PET radioligand of choice for two decades, [$^{11}$C]PK11195 has posed a number of significant challenges for quantification (for review, see (Hinz and Boellaard, 2015; Turkheimer *et al.*, 2015)). Firstly, PK11195 is highly lipophilic and shows a high level of non-specific binding (e.g. to brain fat) (Petit-Taboue *et al.*, 1991). By increasing the background non-specific signal, this reduces the signal to noise ratio. Because of the low level of TSPO in the normal brain, the high non-specific binding of [$^{11}$C]PK11195, as well as specific binding to TSPO in brain blood vessels, becomes predominant (Turkheimer *et al.*, 2007). Secondly, [$^{11}$C]PK11195 shows highly variable kinetic behaviour in plasma (Banati *et al.*, 2000), precluding calculation of an arterial input function for kinetic modelling. [$^{11}$C]PK11195 also binds strongly to plasma alpha1-acid glycoprotein (AGP), and changes in AGP concentration, which have been shown in neuroinflammatory diseases such as multiple sclerosis, could significantly alter the free fraction (Lockhart *et al.*, 2003). The latter is particularly important because PK11195 also adheres to glass and plastic, and therefore accurate measurement of plasma levels is very difficult to achieve. Thirdly, [$^{11}$C]PK11195 is typically analyzed using reference tissue models but, because of the ubiquitous low-level expression of TSPO in the brain, a true reference region, devoid of specific binding, is lacking (Turkheimer *et al.*, 2015). Furthermore, the choice of an anatomically-defined pseudo-reference region (i.e. which contains low levels of TSPO, similar between patient and control groups) may be challenging without prior pathological validation. In the case of disorders with widespread or heterogeneous patterns of microglial activation, such as in TBI, an anatomically-defined reference may not be feasible. Hence, a variety of data-driven methods have been adopted to circumvent this problem, and so the “SuperPK” approach (see http://tinyurl.com/gqe979a) was used to generate the parametric maps of [$^{11}$C]PK11195 binding potential which were used in this thesis (see Chapter 3) (Turkheimer *et al.*, 2007).

The limitations of [$^{11}$C]PK11195 motivated the development of second-generation TSPO radioligands with the promise of improved signal-to-noise ratio compared to [$^{11}$C]PK11195. More than 50 candidate TSPO ligands have been introduced preclinically, including [$^{18}$F]FEPPA, [$^{18}$F]PBR-111, [$^{11}$C]PBR28, and [$^{11}$C]DPA-713 (see for review (Chauveau *et al.*, 2008; Owen and Matthews, 2011)). Human studies using these second-generation ligands have demonstrated increased TSPO expression in a variety of CNS disorders, including Alzheimer's disease (Suridjan *et al.*, 2015), amyotrophic lateral sclerosis (Zürcher *et al.*, 2015), and multiple sclerosis (Colasanti *et al.*, 2014). However, the application of second-generation TSPO radioligands has been complicated by the fact that their binding affinities to TSPO are influenced by a common polymorphism (rs6971) in the *TSPO* gene which causes a single amino acid substitution (A147T) in the protein (Owen *et al.*, 2012). Because 147T TSPO binds ligands with lower affinity than 147A, this produces three classes of binding affinity across a population: high-affinity (HABs) and low-affinity binders (LABs) express only the 147A or 147T variants respectively, whereas mixed-affinity binders (MABs) are heterozygotes and express both in equal proportion (Owen *et al.*, 2010). Therefore, for a given level of TSPO expression, the specific PET signal will have the rank order HABs > MABs > LABs. The magnitude of the difference in PET signal between the 3 binding affinity classes is radioligand specific. For example, [$^{11}$C]PBR28 has a ~50 fold difference in binding affinity between the 147A and 147T variants. Therefore, LABs have negligible specific signal, and the specific signal in HABs is virtually twice that of MABs. In Caucasians, 49% of subjects are HABs, 42% MABs, and 9% are LABs, but this distribution varies across ethnic groups (Guo *et al.*, 2012). Studies must control for this confound, so subjects are genotyped *a priori.* For ligands with a large 147A/T binding affinity ratio like [$^{11}$C]PBR28, LAB subjects are typically excluded. If both HAB and MAB subjects are included, then subjects are matched for TSPO genotype, or genotype is modelled as a covariate. Recently, because [$^{11}$C]PBR28 volume of distribution ($V_T$) in HABs is about 40% higher than in MABs, to account for the effect of genotype,

Gershen et al. multiplied the $V_T$ of the MAB group by 1.4 (Gershen *et al.*, 2015). However, this approach is yet to be validated.

Even after accounting for TSPO genotype, many second-generation radioligands show high between-subject variability in uptake when using analysis methods which rely on measuring the radioligand in the blood (Guo *et al.*, 2012). As for [$^{11}$C]PK11195, high and variable plasma protein binding may be a factor (Bloomfield *et al.*, 2016). To account for this, $V_T$ can be corrected by dividing by the measured free fraction of the ligand in plasma ($f_p$) (i.e. $V_T/f_p$) (e.g. (Gershen *et al.*, 2015)). However, accurate measurement of the free fraction ($f_p$) is difficult, and errors in $f_p$ may increase the variability in corrected $V_T$ ($V_T/f_p$) (Park *et al.*, 2015). Another more complex issue is whether the free concentration of the radioligand in the arterial plasma, routinely used for the input function in PET studies, is appropriate for TSPO radioligands. Unlike most CNS PET targets, TSPO is very highly expressed in the blood. It may therefore be that the free concentration of TSPO ligand in the arterial plasma is not an accurate reflection of the true input function. To reduce variability associated with blood based analysis methods, cross-sectional studies have typically used a pseudo-reference region approach, as used in this thesis, for example whereby regional $V_T$ is normalized by the $V_T$ of a pseudo-reference region, yielding a distribution volume ratio (i.e. DVR).

As for [$^{11}$C]PK11195, the in cases like TBI, where there is potentially widespread or heterogeneous microglial activation, definition of a (pseudo-) reference region is challenging. In this thesis, a whole brain normalisation was used (see Chapter 4, Methods). The results were similar when using cortical grey matter and cerebellum as reference tissues.

Use of the whole brain as a reference region does suggest the theoretical possibility that, in cases of widespread WM microglial activation which produce enough binding, the value for the reference (whole-brain) mean would become significantly greater in patient versus control groups. Furthermore, an increase in whole brain mean would produce a relative reduction in regional DVRs in the patient group (as the denominator gets larger), limiting the sensitivity to detect

increases. It would be interesting in future work to model (using simulations) the likelihood of such scenarios (i.e. where effects in a whole brain reference region have important effects for regional measures), and their effect cross-sectional comparisons.

Another contribution to the high variability in signal is thought to be the large and ubiquitous TSPO component of [$^{11}$C]PBR28 binding at the BBB, which masks the signal from the parenchymal brain tissues (i.e., GM, WM and “inflamed” tissue), thus impeding the identification of a suitable reference region, be it manually or automatically derived (i.e., there is no “SuperPBR” equivalent of SuperPK) (Turkheimer *et al.*, 2015).

Chapter 6

# 6. Discussion

In this chapter, I summarise and interpret the main findings of the thesis, and discuss how they contribute to our understanding of TBI. To conclude, I discuss directions for possible research in the future.

## 6.1. Summary of findings

The aim of the thesis was to explore chronic microglial activation and neurodegeneration following TBI. I used a combination of TSPO and amyloid PET, structural and diffusion MRI, cognitive assessment, serum biomarker measurement, and a drug intervention with minocycline.

The objectives of the thesis were:

- To image Aβ plaque burden in long-term survivors of TBI, test whether TAI and Aβ are correlated, and compare the spatial distribution of Aβ to AD;
- To test whether chronic thalamic microglial activation after TBI is correlated with thalamo-cortical tract TAI;
- To assess chronic microglial activation after TBI, its relation to MRI measures of injury, and to test the effect of minocycline on microglial activation as well explore the effect of minocycline on measures of injury;
- To test whether plasma NFL and tau are elevated after TBI, and how levels relate to cognitive impairment, brain atrophy, chronic microglial activation and minocycline.

### Chapter 2

In Chapter 2, I investigated the relationship between Aβ plaque burden and TAI after TBI using [$^{11}$C]PIB PET and diffusion MRI. I also compared the distribution of Aβ after TBI to that seen in a group of patients with AD. I found increased [$^{11}$C]PIB binding in TBI patients versus controls in the PCC and cerebellum. [$^{11}$C]PIB binding in the neocortex was lower in TBI than AD, but was higher in the cerebellum. Binding in the PCC increased with decreasing FA in connected WM tracts, and increased with time since injury. These findings support the hypothesis that progressive Aβ plaque pathology is related to the presence of axonal damage produced subsequent to TBI. Previous neuropathological series and imaging studies have separately provided evidence for Aβ pathology (Johnson, Stewart and Smith, 2010; Hong *et al.*, 2014) and chronic axonal injury (Kinnunen *et al.*, 2011; Johnson, Stewart and Smith, 2013). Pathological studies have also suggested a link between these two pathologies in the aftermath of TBI (Smith *et al.*, 1999; Chen *et al.*, 2009). However, through the use of multi-modal imaging, this is the first time that such a relationship has been demonstrated *in vivo.*

### Chapter 3

In Chapter 3, I investigated the relationship between chronic thalamic microglial activation post TBI, which had been demonstrated using the first-generation TSPO ligand [$^{11}$C]PK11195 (Ramlackhansingh *et al.*, 2011), and thalamo-cortical TAI, measured using diffusion MRI. The thalamus is highly connected and a site of microglial activation following central and peripheral axonal damage (Banati, 2002). After stroke, for example, microglial activation is seen at the primary lesion but later develops in projection areas including the thalamus (Pappata *et al.*, 2000; Thiel *et al.*, 2010). Other diseases involving WM damage, including MS, also show thalamic inflammation (Banati, 2002). In this first study in TBI to relate inflammation and WM damage *in vivo*, I found that the degree of thalamic chronic microglial activation was highly correlated with the amount of thalamo-cortical WM tract damage. The thalamus appears to be a common “sink” of secondary inflammation in response to axonal

damage, perhaps related to its dense connections to traumatically-injured WM tracts.

### Chapter 4

In Chapter 4, I investigated chronic microglial activation after TBI using [$^{11}$C]PBR28, a second-generation TSPO ligand, and its relation to MRI and other measures of brain injury, including plasma NFL and tau. I found [$^{11}$C]PBR28 binding in patients was increased compared to controls in WM and thalamus. Previously using [$^{11}$C]PK11195, we observed microglial activation in the posterior limb of the internal capsule as well as the thalamus (Ramlackhansingh *et al.*, 2011), but the WM involvement of [$^{11}$C]PBR28 binding was far more extensive. This may reflect the greater signal-to-noise ratio of the second-generation ligand. I also found that MRI measures of WM damage, in the form of tissue volume loss and reduced FA, were highest in areas of greater [$^{11}$C]PBR28 binding. This is the first *in vivo* support of previous neuropathological reports in long-term TBI survivors showing chronic microglial activation alongside evidence of ongoing WM damage (Smith *et al.*, 2012; Johnson *et al.*, 2013). Thalamic [$^{11}$C]PBR28 binding was also strongly correlated with poorer composite processing speed score ($r=-0.592$, $p=0.026$), supporting our previous findings (Ramlackhansingh *et al.*, 2011).

I found levels of plasma NFL, but not tau, were elevated in patients, who were all at least six months after injury. Elevated CSF levels of NFL have been observed in acute TBI, with higher levels seen after more severe injuries (Zetterberg, Smith and Blennow, 2013). NFL levels in the peripheral blood have been shown to be highly correlated with levels in the CSF (Gaiottino *et al.*, 2013). However, it was unknown whether NFL remains elevated in the chronic phase after TBI. Although there was a negative correlation with time since injury, most patients still had levels above the control range. Baseline plasma NFL levels were positively correlated with [$^{11}$C]PBR28 WM binding.

I found 12 weeks of oral minocycline 100mg twice daily, a standard clinical dose, was associated with widespread reduction in [$^{11}$C]PBR28 binding,

including in WM. This finding provides *in vivo* evidence in humans for a CNS action of minocycline on microglia.

### Chapter 5

In Chapter 5, I went on to investigate the effect of minocycline on other measures of brain injury and recovery. First, I assessed atrophy longitudinally in the TBI patients from both treatment arms combined. Patients showed longitudinal atrophy in WM as well as some GM regions over the six month period between baseline and the final visit, a change which was undetectable in a group of controls scanned over one year. In keeping with the relationship seen at baseline between [$^{11}$C]PBR28 and tissue volumes, I found that WM atrophy longitudinally was greater in voxels with higher baseline [$^{11}$C]PBR28 binding.

I found plasma NFL was unexpectedly increased following minocycline. In addition, this increase was proportional to the decrease in WM [$^{11}$C]PBR28 binding over the same period. In patients in the minocycline group, but not the treatment group, there was also a strong correlation between baseline NFL and longitudinal WM atrophy. However, when the two treatment arms were compared, there was no difference in longitudinal atrophy per se.

I also found that there was a negative effect of minocycline on WM tract integrity in the corpus callosum and a borderline significant deterioration in information processing speed. I discuss these results in more detail below. Together, they suggest that minocycline, either through its action on microglia, or via other pathways, may harm long-term recovery after TBI in spite of the [$^{11}$C]PBR28 PET changes suggesting a reduction in microglial activation.

## 6.2. Interpretation

### A multi-modal investigation of chronic disease processes after TBI

The findings of this thesis shed light on the chronic pathophysiological consequences of TBI. Historically, TBI was thought to involve a static insult from a single event. However, previous clinical and epidemiological

observations – for example the evidence that patients can deteriorate many years post-TBI and are at risk of dementia – suggest this is not the case. In support of these observations, the thesis provides a variety of evidence that TBI triggers processes which persist for months and years after injury. These processes include the presence of Aβ plaque pathology, chronic microglial activation, tissue volume loss, progressive atrophy and elevated plasma NFL. Such processes have hitherto been largely researched in isolation, and using experimental models or in human autopsy series. Here, by combining molecular imaging, structural and diffusion MRI, and other measures of injury, I have been able to explore the interaction of these processes *in vivo*.

### Importance of WM damage in the chronic pathophysiology of TBI

The presence of WM damage is a hallmark of TBI (Johnson, Stewart and Smith, 2013), and the thesis links WM damage to other processes which have been implicated in chronic neurodegenerative disease. WM damage in the chronic phase post-TBI is known to be an important determinant of brain function (Kinnunen *et al.*, 2011; Sharp *et al.*, 2011; Sharp, Scott and Leech, 2014; Hellyer *et al.*, 2015). I found evidence for WM injury in TBI patients, as measured by structural and diffusion MRI, in keeping with our previous work (Kinnunen *et al.*, 2011; Sharp *et al.*, 2011; Cole *et al.*, 2015). I also found that after TBI, the burden of Aβ plaques in the PCC – a frequent site of Aβ pathology in AD – was proportional to the amount of WM damage in connected tracts. This supports the hypothesis that WM damage plays a role in the genesis of Aβ pathology after TBI (Johnson, Stewart and Smith, 2010). In addition, WM damage was found to be greater in areas of increased chronic microglial activation. Together, these findings suggest WM damage has an important role in the long-term pathophysiology of TBI. Further work is required to establish whether this WM damage is a cause or effect of processes like Aβ plaque deposition and chronic microglial activation.

### Biomarkers of chronic neurodegeneration after TBI

The findings of persistently elevated plasma NFL in association with WM inflammation and neurodegeneration are clinically important because of the

need to develop validated biomarkers for WM damage. It is well-known that the presence of TAI plays a fundamental role in determining long-term outcome. However, the pathophysiology of TAI in humans is poorly understood and at present we have no validated methods for assessing TAI clinically. A key goal for TBI research is to develop and validate sensitive and specific measures of TAI that demonstrate the extent of injury and its progression. This should improve the ability to predict clinical outcome and also provide biomarkers to assess novel neuroprotective drugs that become available.

The results of the thesis suggest that combining plasma NFL and neuroimaging measures of progressive WM atrophy is a promising approach to evaluating axonal injury after TBI. This could have great clinical utility across a wide range of settings, for example, in quantifying the accumulated brain injury sustained as a result of multiple repetitive mild TBIs, such as during a professional sporting career (Oliver *et al.*, 2015), or in estimating the risk of developing post-traumatic dementia, including CTE (McKee *et al.*, 2013). NFL could also be used to enrich clinical trials of chronic TBI, by selecting patients at increased risk of late complications.

### Does a reduction in [$^{11}$C]PBR28 binding after minocycline imply a direct action on microglia?

The thesis moved beyond an observational approach through the intervention of minocycline to target chronic microglial activation. Minocycline was associated with a widespread reduction in [$^{11}$C]PBR28 binding. This finding provides *in vivo* evidence that minocycline at standard clinical doses reaches sufficient concentration in the CNS to have an immunomodulatory action. There are many possible explanations for this finding, beyond a direct inhibition of microglial activation. One alternative is that minocycline caused a change in measured [$^{11}$C]PBR28 binding through a peripheral (non-CNS) action, for example by altering the metabolism of the ligand or a via interrupting ligand transport across the BBB. Another explanation for the change in [$^{11}$C]PBR28 binding is that minocycline caused about a reduction in microglial activation through a pathway other than the direct inhibition of microglia. Minocycline is

known to be a pluripotent compound with a variety of actions potentially underlying its immunomodulatory effects (see Chapter 1) (Garrido-Mesa, Zarzuelo and Gálvez, 2013b). Effects on one pathway are likely to impact on another, and may lead to an effect on microglia, for example by changing the chemical stimuli in the microglial microenvironment. It is therefore possible that one or more of these other effects led to a secondary reduction in microglial activation (Möller *et al.*, 2016).

### Increases in plasma NFL after minocycline support a CNS action

The finding that minocycline was associated with an increase in plasma NFL, whilst an unexpected direction of change, nevertheless provides additional support for a CNS action of the drug. The elevation post-minocycline at 12 weeks and subsequent fall at six months, long after minocycline cessation, suggest an effect of the drug on the nervous system for the duration of treatment. Again, it is possible that minocycline indirectly brought about an increase in NFL through a peripheral mechanism, for example by increasing the availability of NFL in plasma, rather than an effect on axons. However, a previous study of minocycline in acute spinal cord injury found treatment was associated with a reduction in NFL levels in a subgroup of patients (Kuhle *et al.*, 2015), suggesting minocycline does not increase NFL as a non-specific side effect.

### What kind of activated microglia is minocycline inhibiting?

The minocycline interventional study was motivated by two important assumptions, which were informed by previous evidence.

Firstly, that minocycline exerts an inhibitory effect on microglial activation. There is good evidence that minocycline reduces microglial activation in a variety of animal models of CNS disorders including acute TBI (Chapter 1). However, the effect of minocycline is likely to vary according to the underlying disease, the underlying microglial phenotype, and also the phase of the disease. This variability might explain the discrepant results in clinical trials of minocycline. For example, the largest study of minocycline in ALS, a

neurodegenerative condition associated with elevated NFL levels, found minocycline to be harmful (Gordon *et al.*, 2007). However, other studies, for example in clinically isolated syndrome and acute stroke, have shown a beneficial effect (Lampl *et al.*, 2007; Metz *et al.*, 2015). The beneficial or detrimental effects exerted by minocycline may also be independent of any direct action on microglia (Garrido-Mesa, Zarzuelo and Gálvez, 2013b; Möller *et al.*, 2016).

### Is chronic microglial activation after TBI a friend or foe?

The second assumption was that chronically activated microglia are harmful to recovery, i.e. of a phenotype whose activity ultimately leads to tissue loss or interferes with normal neuronal function. The existing evidence was more equivocal here. In TBI, there are only a small number of experimental studies of the chronic phase, with contrasting findings (Chapter 1). Those studies which have focused on phenotype from early in the disease suggest an evolving pro-inflammatory predominance of microglia over time (Chapter 1).

In the broader neurodegeneration literature, chronic microglial activation is frequently implicated in the pathogenesis of neurodegenerative disease (Dheen, Kaur and Ling, 2007; Frank-Cannon *et al.*, 2009; Lull and Block, 2010; Gentleman, 2013). However, as Gentleman observes in a review on the role of microglia in relation to AD, PD and ALS, "…what remains unclear is the precise nature of that activation and whether it is similar in different diseases." (Gentleman, 2013). The review reaffirms that microglia have a role in the pathogenesis of these conditions, but that their precise role seems to vary between these diseases: "In AD there is evidence for a role in the initiation and progression of the disease. Alternatively, senescence and impaired function of the microglia may lead to loss of a neuroprotective function. In PD the microglial response does not seem to be quite so prolific and is perhaps more reactive and closely linked to astrocytic changes whereas in ALS the microglia expressing mutant protein seem to be directly toxic to motoneurons." (Gentleman, 2013). This summary highlights some of the challenges of understanding the role of microglia across different diseases, and in relation to

other cell types. Despite decades of research, there clearly remains a great deal of uncertainty about the role of microglia in neurodegenerative disease, and similar research into chronic TBI is, by comparison, only in its infancy (Faden and Loane, 2015).

Several findings from the thesis challenge the second assumption that chronic microglial activation after TBI is harmful. Minocycline led to reduced [$^{11}$C]PBR28 binding but increased plasma NFL levels. Furthermore, in patients who took minocycline, there was a positive correlation between baseline NFL (i.e. before patients had started the 12 week course of minocycline) and the degree of subsequent atrophy from baseline to six months. Whilst there were no differences in longitudinal atrophy detected over this period between the two treatment arms, and this was a small study, one interpretation of these findings is as follows: (1) chronically activated microglia after TBI (indexed by [$^{11}$C]PBR28 binding) are beneficial for suppressing long-term damage caused by other processes, whose effects are indexed by plasma NFL levels; (2) inhibition of microglia by minocycline increases the activity of these other processes, whose baseline activity was indexed by NFL, resulting in a greater degree of tissue damage. This interpretation would explain the rise in NFL, as well as the correlation observed between baseline NFL and atrophy which appeared in the minocycline group. This model is also supported by the finding that, in the corpus callosum, where TAI is common and diffusion MRI is sensitive to change, minocycline therapy was associated with a decrease in WM tract integrity.

## 6.3. Future research

### TSPO and microglial phenotype

TSPO PET imaging provides a biomarker to investigate microglial activation and the effect of immunomodulatory drugs. However, given the complexity of microglia and uncertainty regarding their role in CNS disease, this modality has some limitations. TSPO PET binding is a one dimensional measure, i.e. a single value for the strength of binding is ascribed to each ROI or voxel. Conversely,

microglial activation cannot *in vivo* be described along a single dimension, from "off" to "on". As we have seen, there is at least one other dimension, that of microglial activation phenotype. The phenotype can be projected onto a single axis, a spectrum, from "M1-like" (pro-inflammatory) to "M2-like" (restorative) microglia, but these are caricatures which do not reflect the range and complexity of microglial phenotypes occurring *in vivo* (David and Kroner, 2011; Boche, Perry and Nicoll, 2013). Crucially, on the basis of current evidence, TSPO PET cannot discriminate activation phenotype. This is an important limitation to the modality.

Future research should establish how TSPO expression, and TSPO PET ligand binding, varies with activation phenotype. Without this information, or supporting evidence from relevant experimental work or neuropathological data, it is difficult to interpret the TSPO PET signal in disease states, or any change in binding in response to a drug. A detailed characterization is needed of how TSPO expression varies with the diversity of microglial phenotypes seen in vivo. For TBI research, a detailed description of the timecourse of microglial phenotype in humans after TBI, and its relation to TSPO expression, would greatly advance the utility of *in vivo* TSPO imaging in this condition.

I have found that the multi-modal approach used in this thesis has yielded many insights into the chronic sequelae of TBI and contributed to our understanding of long-term processes after TBI. This approach has also, to some extent, helped to overcome the limitations of TSPO PET, by providing complimentary markers of brain injury for direct comparison with TSPO measures. This has helped to understand the cross-sectional differences seen in TSPO binding as well as the effects of minocycline.

### Minocycline treatment after TBI

On the basis of the findings in this thesis, there is little support for further investigation of minocycline as a treatment in chronic TBI. It is possible that some of the negative effects of minocycline, for example on MRI measures or cognitive performance, may have arisen by chance in this small study. However, the increase in NFL in particular appears a robust, adverse, result. In

light of these findings, further experimental work should be conducted before any further clinical study of minocycline in chronic TBI. An important animal study would be to administer minocycline at a delayed time point post TBI. No previous experimental studies have done so. This is important because the effect of minocycline may differ if first administered in the post-acute versus acute phase. It is also conceivable that the outcomes in a human study would be different if minocycline were administered acutely. In a similar vein to the TSPO and microglial phenotype research suggested, a more detailed characterization of the actions of minocycline is needed, focusing on microglial phenotype and the effects on brain injury.

### TBI as a chronic neurodegenerative disease

The use of longitudinal imaging and NFL has proven to be valuable in the thesis. The results suggest significant degrees of neurodegeneration continue in the chronic phase after TBI. Further longitudinal studies, ideally at higher frequency of visits and for longer follow-up, would help chart the prolonged and dynamic timecourse of change that occurs in the brain after TBI. This approach, focusing on quantifying the arc of neurodegeneration and accumulation of pathology, alongside clinical markers, has been been fruitful in the characterization of dementia (Buckner *et al.*, 2005; Schott *et al.*, 2005; Jack *et al.*, 2010).

Evidence for long-term processes after TBI suggests the window of opportunity for therapeutic intervention may be much longer than is usually considered. This is encouraging particularly in light of the failure of so many drug trials targeting the acute stage (Maas, Roozenbeek and Manley, 2010). Future research into late-stage disease modifying interventions in TBI is still warranted, supported by neuroimaging, peripheral biomarker assessment, and appropriate preclinical experimentation.

# 7. References


Aarum, J., Sandberg, K., Haeberlein, S. L. and Persson, M. A. (2003) 'Migration and differentiation of neural precursor cells can be directed by microglia', *Proc Natl Acad Sci U S A*. 2003/12/12, 100(26), pp. 15983–15988. doi: 10.1073/pnas.2237050100.

Abdel Baki, S. G., Schwab, B., Haber, M., Fenton, A. A. and Bergold, P. J. (2010) 'Minocycline Synergizes with N-Acetylcysteine and Improves Cognition and Memory Following Traumatic Brain Injury in Rats', *PLoS One*, 5(8). doi: 10.1371/journal.pone.0012490.

Acosta, S. A., Tajiri, N., Shinozuka, K., Ishikawa, H., Grimmig, B., Diamond, D., Sanberg, P. R., Bickford, P. C., Kaneko, Y. and Borlongan, C. V (2013) 'Long-Term Upregulation of Inflammation and Suppression of Cell Proliferation in the Brain of Adult Rats Exposed to Traumatic Brain Injury Using the Controlled Cortical Impact Model', *PLoS One*. Public Library of Science, 8(1), p. e53376. doi: 10.1371/journal.pone.0053376.

Adams, J. H., Doyle, D., Ford, I., Gennarelli, T. A., Graham, D. I. and McLellan, D. R. (1989) 'Diffuse axonal injury in head injury: definition, diagnosis and grading', *Histopathology*, 15(1), pp. 49–59. Available at: http://www.ncbi.nlm.nih.gov/entrez/query.fcgi?cmd=Retrieve&db=PubMed&dopt=Citation&list_uids=2767623.

Agwuh, K. N. and MacGowan, A. (2006) 'Pharmacokinetics and pharmacodynamics of the tetracyclines including glycylcyclines', *J Antimicrob Chemother*. 2006/07/04, 58(2), pp. 256–265. doi: 10.1093/jac/dkl224.

Andriessen, T. M., Horn, J., Franschman, G., van der Naalt, J., Haitsma, I., Jacobs, B., Steyerberg, E. W. and Vos, P. E. (2011) 'Epidemiology, severity classification, and outcome of moderate and severe traumatic brain injury: a prospective multicenter study', *J Neurotrauma*. 2011/07/27, 28(10), pp. 2019–

2031. doi: 10.1089/neu.2011.2034.

Annegers, J. F., Hauser, W. A., Coan, S. P. and Rocca, W. A. (1998) 'A population-based study of seizures after traumatic brain injuries', *N Engl J Med*. 1998/01/01, 338(1), pp. 20–24. doi: 10.1056/NEJM199801013380104.

Ashburner, J. (2007) 'A fast diffeomorphic image registration algorithm', *NeuroImage*, 38(1), pp. 95–113. doi: http://dx.doi.org/10.1016/j.neuroimage.2007.07.007.

Ashburner, J. and Friston, K. J. (2005) 'Unified segmentation', *NeuroImage*, 26(3), pp. 839–851. doi: http://dx.doi.org/10.1016/j.neuroimage.2005.02.018.

Ashburner, J. and Ridgway, G. R. (2013) 'Symmetric diffeomorphic modelling of longitudinal structural MRI ', *Frontiers in Neuroscience* . Available at: http://www.frontiersin.org/Journal/Abstract.aspx?s=1304&name=brain_imaging_methods&ART_DOI=10.3389/fnins.2012.00197.

AVILA, J., LUCAS, J. J., PÉREZ, M. A. R. and HERNÁNDEZ, F. (2004) 'Role of Tau Protein in Both Physiological and Pathological Conditions', *Physiological Reviews*, 84(2), pp. 361–384. Available at: http://physrev.physiology.org/content/84/2/361.abstract.

Baddeley, A. D., Emslie, H. and Nimmo-Smith, I. (1994) *Doors and People Test: A Test of Visual and Verbal Recall and Recognition*. Bury-St-Edmunds: Thames Valley Test Company.

Baguley, I. J., Nott, M. T. and Slewa-Younan, S. (2008) 'Long-term mortality trends in functionally-dependent adults following severe traumatic-brain injury.', *Brain injury*. England, 22(12), pp. 919–925. doi: 10.1080/02699050802448578.

Baguley, I., Slewa-Younan, S., Lazarus, R. and Green, A. (2000) 'Long-term mortality trends in patients with traumatic brain injury.', *Brain injury*. ENGLAND, 14(6), pp. 505–512.

Banati, R. B. (2002) 'Visualising microglial activation in vivo', *Glia*, 40(2), pp. 206–217. Available at: http://onlinelibrary.wiley.com/store/10.1002/glia.10144/asset/10144_ftp.pdf?v=

1&t=i9oe3tcp&s=36443734b5c22e5603ab6085a3d3b351551f3892.

Banati, R. B., Cagnin, A., Brooks, D. J., Gunn, R. N., Myers, R., Jones, T., Birch, R. and Anand, P. (2001) 'Long-term trans-synaptic glial responses in the human thalamus after peripheral nerve injury', *Neuroreport*, 12(16), pp. 3439–3442. Available at: http://graphics.tx.ovid.com/ovftpdfs/FPDDNCGCPHBGKP00/fs004/ovft/live/gv006/00001756/00001756-200111160-00012.pdf.

Banati, R. B., Middleton, R. J., Chan, R., Hatty, C. R., Kam, W. W.-Y., Quin, C., Graeber, M. B., Parmar, A., Zahra, D. and Callaghan, P. (2014) 'Positron emission tomography and functional characterization of a complete PBR/TSPO knockout', *Nature communications*, 5.

Banati, R. B., Newcombe, J., Gunn, R. N., Cagnin, A., Turkheimer, F., Heppner, F., Price, G., Wegner, F., Giovannoni, G., Miller, D. H., Perkin, G. D., Smith, T., Hewson, A. K., Bydder, G., Kreutzberg, G. W., Jones, T., Cuzner, M. L. and Myers, R. (2000) 'The peripheral benzodiazepine binding site in the brain in multiple sclerosis Quantitative in vivo imaging of microglia as a measure of disease activity', *Brain*, 123(11), pp. 2321–2337. doi: 10.1093/brain/123.11.2321.

Bazarian, J. J., Cernak, I., Noble-Haeusslein, L., Potolicchio, S. and Temkin, N. (2009) 'Long-term neurologic outcomes after traumatic brain injury', *J Head Trauma Rehabil*. 2009/11/27, 24(6), pp. 439–451. doi: 10.1097/HTR.0b013e3181c15600.

Behrens, T. E., Johansen-Berg, H., Woolrich, M. W., Smith, S. M., Wheeler-Kingshott, C. A., Boulby, P. A., Barker, G. J., Sillery, E. L., Sheehan, K., Ciccarelli, O., Thompson, A. J., Brady, J. M. and Matthews, P. M. (2003) 'Non-invasive mapping of connections between human thalamus and cortex using diffusion imaging', *Nat Neurosci*. 2003/06/17, 6(7), pp. 750–757. doi: 10.1038/nn1075nn1075 [pii].

Bendlin, B. B., Ries, M. L., Lazar, M., Alexander, A. L., Dempsey, R. J., Rowley, H. A., Sherman, J. E. and Johnson, S. C. (2008) 'Longitudinal changes in

patients with traumatic brain injury assessed with diffusion-tensor and volumetric imaging.', *NeuroImage*. United States, 42(2), pp. 503–514. doi: 10.1016/j.neuroimage.2008.04.254.

Bigler, E. D. (2007) 'Anterior and middle cranial fossa in traumatic brain injury: relevant neuroanatomy and neuropathology in the study of neuropsychological outcome', *Neuropsychology*, 21(5), pp. 515–531. Available at: http://www.ncbi.nlm.nih.gov/entrez/query.fcgi?cmd=Retrieve&db=PubMed&dopt=Citation&list_uids=17784800.

Bigler, E. D. (2013) 'Neuroinflammation and the dynamic lesion in traumatic brain injury', *Brain*, 136(1), pp. 9–11. doi: 10.1093/brain/aws342.

Block, M. L., Zecca, L. and Hong, J.-S. (2007) 'Microglia-mediated neurotoxicity: uncovering the molecular mechanisms', *Nat Rev Neurosci*, 8(1), pp. 57–69. Available at: http://dx.doi.org/10.1038/nrn2038.

Bloomfield, P. S., Selvaraj, S., Veronese, M., Rizzo, G., Bertoldo, A., Owen, D. R., Bloomfield, M. A. P., Bonoldi, I., Kalk, N., Turkheimer, F., McGuire, P., de Paola, V. and Howes, O. D. (2016) 'Microglial Activity in People at Ultra High Risk of Psychosis and in Schizophrenia: An [(11)C]PBR28 PET Brain Imaging Study.', *The American journal of psychiatry*. United States, 173(1), pp. 44–52. doi: 10.1176/appi.ajp.2015.14101358.

Blum, D., Chtarto, A., Tenenbaum, L., Brotchi, J. and Levivier, M. (2004) 'Clinical potential of minocycline for neurodegenerative disorders', *Neurobiology of Disease*, 17(3), pp. 359–366. doi: 10.1016/j.nbd.2004.07.012.

BNF, J. F. C. (2012) *British National Formulary. [65] ed.* . BMJ Group and Pharmaceutical Press.

Boche, D., Perry, V. H. and Nicoll, J. A. R. (2013) 'Review: Activation patterns of microglia and their identification in the human brain', *Neuropathology and Applied Neurobiology*, 39(1), pp. 3–18. doi: 10.1111/nan.12011.

Bonelli, R. M., H√∂dl, A. K., Hofmann, P. and Kapfhammer, H.-P. (2004) 'Neuroprotection in Huntington's disease: a 2-year study on minocycline',

*International Clinical Psychopharmacology*, 19(6), pp. 337–342. Available at: http://www.ncbi.nlm.nih.gov/pubmed/15486519.

Bonnelle, V., Ham, T. E., Leech, R., Kinnunen, K. M., Mehta, M. A., Greenwood, R. J., Sharp, D. J., Metha, M. A., Greenwood, R. J. and Sharp, D. J. (2012) 'Salience network integrity predicts default mode network function after traumatic brain injury.', *Proc Natl Acad Sci U S A*. 2012/03/07, 109(12), pp. 4690–4695. doi: 10.1073/pnas.1113455109.

Bruns Jr., J. and Hauser, W. A. (2003) 'The epidemiology of traumatic brain injury: a review', *Epilepsia*, 44 Suppl 1, pp. 2–10. Available at: http://www.ncbi.nlm.nih.gov/entrez/query.fcgi?cmd=Retrieve&db=PubMed&dopt=Citation&list_uids=14511388.

Buckner, R. L., Snyder, A. Z., Shannon, B. J., LaRossa, G., Sachs, R., Fotenos, A. F., Sheline, Y. I., Klunk, W. E., Mathis, C. A., Morris, J. C. and Mintun, M. A. (2005) 'Molecular, structural, and functional characterization of Alzheimer's disease: evidence for a relationship between default activity, amyloid, and memory', *J Neurosci*. 2005/08/27, 25(34), pp. 7709–7717. doi: 10.1523/JNEUROSCI.2177-05.2005.

Burke, N. N., Kerr, D. M., Moriarty, O., Finn, D. P. and Roche, M. (2014) 'Minocycline modulates neuropathic pain behaviour and cortical M1-M2 microglial gene expression in a rat model of depression.', *Brain, behavior, and immunity*. United States, 42, pp. 147–156. doi: 10.1016/j.bbi.2014.06.015.

Bye, N., Habgood, M. D., Callaway, J. K., Malakooti, N., Potter, A., Kossmann, T. and Morganti-Kossmann, M. C. (2007) 'Transient neuroprotection by minocycline following traumatic brain injury is associated with attenuated microglial activation but no changes in cell apoptosis or neutrophil infiltration', *Exp Neurol*. 2006/12/26, 204(1), pp. 220–233. doi: 10.1016/j.expneurol.2006.10.013.

Cagnin, A., Gerhard, A. and Banati, R. (2003) 'In Vivo Imaging of Neuroinflammation in Neurodegenerative Diseases', in Wood, P. (ed.) *Neuroinflammation: Mechanisms and Management*. New Jersey: Humana

Press Inc., pp. 379–385.

Cagnin, A., Myers, R., Gunn, R. N., Lawrence, A. D., Stevens, T., Kreutzberg, G. W., Jones, T. and Banati, R. B. (2001) 'In vivo visualization of activated glia by [11C](R)-PK11195-PET following herpes encephalitis reveals projected neuronal damage beyond the primary focal lesion', *Brain*, 124(10), pp. 2014–2027.

Casha, S., Zygun, D., McGowan, M. D., Bains, I., Yong, V. W. and Hurlbert, R. J. (2012) 'Results of a phase II placebo-controlled randomized trial of minocycline in acute spinal cord injury', *Brain*, 135(4), pp. 1224–1236. doi: 10.1093/brain/aws072.

Cederberg, D. and Siesjo, P. (2010) 'What has inflammation to do with traumatic brain injury?', *Childs Nerv Syst*. 2009/11/27, 26(2), pp. 221–226. doi: 10.1007/s00381-009-1029-x.

Chauveau, F., Boutin, H., Van Camp, N., Dollé, F. and Tavitian, B. (2008) 'Nuclear imaging of neuroinflammation: a comprehensive review of [11C] PK11195 challengers', *European journal of nuclear medicine and molecular imaging*. Springer, 35(12), pp. 2304–2319.

Chen, H., Richard, M., Sandler, D. P., Umbach, D. M. and Kamel, F. (2007) 'Head Injury and Amyotrophic Lateral Sclerosis', *American journal of epidemiology*, pp. 810–816. doi: 10.1093/aje/kwm153.

Chen, S. F., Richards, H. K., Smielewski, P., Johnstrom, P., Salvador, R., Pickard, J. D. and Harris, N. G. (2004) 'Relationship between flow-metabolism uncoupling and evolving axonal injury after experimental traumatic brain injury', *J Cereb Blood Flow Metab*. 2004/09/10, 24(9), pp. 1025–1036. doi: 00004647-200409000-00008 [pii].

Chen, S., Pickard, J. D. and Harris, N. G. (2003) 'Time course of cellular pathology after controlled cortical impact injury', *Experimental Neurology*, 182(1), pp. 87–102. doi: http://dx.doi.org/10.1016/S0014-4886(03)00002-5.

Chen, X. H., Johnson, V. E., Uryu, K., Trojanowski, J. Q. and Smith, D. H.

(2009) ‘A lack of amyloid beta plaques despite persistent accumulation of amyloid beta in axons of long-term survivors of traumatic brain injury’, *Brain Pathol*, 19(2), pp. 214–223. doi: 10.1111/j.1750-3639.2008.00176.x.

Chen, X., Ma, X., Jiang, Y., Pi, R., Liu, Y. and Ma, L. (2011) ‘The prospects of minocycline in multiple sclerosis’, *Journal of Neuroimmunology*. 2011/05/14, 235(1–2), pp. 1–8. doi: 10.1016/j.jneuroim.2011.04.006.

Chetelat, G., Desgranges, B., Landeau, B., Mezenge, F., Poline, J. B., de la Sayette, V., Viader, F., Eustache, F. and Baron, J. C. (2008) ‘Direct voxel-based comparison between grey matter hypometabolism and atrophy in Alzheimer’s disease’, *Brain*. 2007/12/08, 131(Pt 1), pp. 60–71. doi: 10.1093/brain/awm288.

Chhor, V., Le Charpentier, T., Lebon, S., Ore, M. V, Celador, I. L., Josserand, J., Degos, V., Jacotot, E., Hagberg, H., Savman, K., Mallard, C., Gressens, P. and Fleiss, B. (2013) ‘Characterization of phenotype markers and neuronotoxic potential of polarised primary microglia in vitro’, *Brain Behav Immun*. 2013/03/05. doi: 10.1016/j.bbi.2013.02.005.

Clark, W. M., Calcagno, F. A., Gabler, W. L., Smith, J. R. and Coull, B. M. (1994) ‘Reduction of central nervous system reperfusion injury in rabbits using doxycycline treatment’, *Stroke*, 25(7), pp. 1411–1415. doi: 10.1161/01.str.25.7.1411.

Cohen, J. (2013) *Statistical power analysis for the behavioral sciences*. Academic press.

Colasanti, A., Guo, Q., Muhlert, N., Giannetti, P., Onega, M., Newbould, R. D., Ciccarelli, O., Rison, S., Thomas, C., Nicholas, R., Muraro, P. A., Malik, O., Owen, D. R., Piccini, P., Gunn, R. N., Rabiner, E. A. and Matthews, P. M. (2014) ‘In Vivo Assessment of Brain White Matter Inflammation in Multiple Sclerosis with (18)F-PBR111 PET.’, *Journal of nuclear medicine : official publication, Society of Nuclear Medicine*. United States, 55(7), pp. 1112–1118. doi: 10.2967/jnumed.113.135129.

Cole, J. H., Leech, R., Sharp, D. J. and for the Alzheimer’s Disease Neuroimaging, I. (2015) ‘Prediction of brain age suggests accelerated atrophy

after traumatic brain injury', *Annals of neurology*, 77(4), pp. 571–581. doi: 10.1002/ana.24367.

Corrigan, J. D., Selassie, A. W., Orman, J. A. and Rehabil, J. H. T. (2010) 'The epidemiology of traumatic brain injury', (1550–509X (Electronic)).

Crossley, N. A., Mechelli, A., Scott, J., Carletti, F., Fox, P. T., McGuire, P. and Bullmore, E. T. (2014) 'The hubs of the human connectome are generally implicated in the anatomy of brain disorders', *Brain*. 2014/07/25, 137(Pt 8), pp. 2382–2395. doi: 10.1093/brain/awu132.

Cudaback, E., Li, X., Montine, K. S., Montine, T. J. and Keene, C. D. (2011) 'Apolipoprotein E isoform-dependent microglia migration', *The FASEB Journal*, 25(6), pp. 2082–2091. doi: 10.1096/fj.10-176891.

Cummings, J. L. and Benson, D. F. (1984) 'Subcortical dementia. Review of an emerging concept.', *Archives of neurology*. UNITED STATES, 41(8), pp. 874–879.

Cunha, B. A. (2000) 'Minocycline versus Doxycycline in the Treatment of Lyme Neuroborreliosis', *Clinical Infectious Diseases*, 30(1), pp. 237–238. doi: 10.1086/313604.

Davalos, D., Grutzendler, J., Yang, G., Kim, J. V, Zuo, Y., Jung, S., Littman, D. R., Dustin, M. L. and Gan, W.-B. (2005) 'ATP mediates rapid microglial response to local brain injury in vivo', *Nat Neurosci*. Nature Publishing Group, 8(6), pp. 752–758. doi: http://www.nature.com/neuro/journal/v8/n6/suppinfo/nn1472_S1.html.

David, S. and Kroner, A. (2011) 'Repertoire of microglial and macrophage responses after spinal cord injury', *Nat Rev Neurosci*. Nature Publishing Group, a division of Macmillan Publishers Limited. All Rights Reserved., 12(7), pp. 388–399. Available at: http://dx.doi.org/10.1038/nrn3053.

DeKosky, S. T., Blennow, K., Ikonomovic, M. D. and Gandy, S. (2013) 'Acute and chronic traumatic encephalopathies: pathogenesis and biomarkers', *Nat Rev Neurol*. Nature Publishing Group, a division of Macmillan Publishers

Limited. All Rights Reserved., 9(4), pp. 192–200. doi: 10.1038/nrneurol.2013.36.

Delis, D. C., Kaplan, E. and Kramer, J. H. (2001) *Delis-Kaplan Executive Function System*. San Antonio: San Antonio, TX: Psychological Corporation.

Dheen, S. T., Kaur, C. and Ling, E.-A. (2007) 'Microglial activation and its implications in the brain diseases.', *Current medicinal chemistry*. Netherlands, 14(11), pp. 1189–1197.

Dodel, R., Spottke, A., Gerhard, A., Reuss, A., Reinecker, S., Schimke, N., Trenkwalder, C., Sixel-D√∂ring, F., Herting, B., Kamm, C., Gasser, T., Sawires, M., Geser, F., K√∂llensperger, M., Seppi, K., Kloss, M., Krause, M., Daniels, C., Deuschl, G., B√∂ttger, S., Naumann, M., Lipp, A., Gruber, D., Kupsch, A., Du, Y., Turkheimer, F., Brooks, D. J., Klockgether, T., Poewe, W., Wenning, G., Schade-Brittinger, C., Oertel, W. H., Eggert, K., Sixel-Doring, F., Herting, B., Kamm, C., Gasser, T., Sawires, M., Geser, F., Kollensperger, M., Seppi, K., Kloss, M., Krause, M., Daniels, C., Deuschl, G., Bottger, S., Naumann, M., Lipp, A., Gruber, D., Kupsch, A., Du, Y., Turkheimer, F., Brooks, D. J., Klockgether, T., Poewe, W., Wenning, G., Schade-Brittinger, C., Oertel, W. H. and Eggert, K. (2010) 'Minocycline 1-year therapy in multiple-system-atrophy: effect on clinical symptoms and [(11)C] (R)-PK11195 PET (MEMSA-trial)', *Movement Disorders: Official Journal of the Movement Disorder Society*. 2009/12/17, 25(1), pp. 97–107. doi: 10.1002/mds.22732.

Domercq, M. and Matute, C. (2004) 'Neuroprotection by tetracyclines', *Trends in Pharmacological Sciences*. 2004/11/09, 25(12), pp. 609–612. doi: 10.1016/j.tips.2004.10.001.

Domercq, M., Vazquez-Villoldo, N. and Matute, C. (2013) 'Neurotransmitter signaling in the pathophysiology of microglia', *Front Cell Neurosci*. 2013/04/30, 7, p. 49. doi: 10.3389/fncel.2013.00049.

Mac Donald, C. L., Dikranian, K., Bayly, P., Holtzman, D. and Brody, D. (2007) 'Diffusion tensor imaging reliably detects experimental traumatic axonal injury and indicates approximate time of injury', *The Journal of Neuroscience: The*

*Official Journal of the Society for Neuroscience*, 27(44), pp. 11869–11876. doi: 10.1523/jneurosci.3647-07.2007.

Douglas H. Smith, Xiao-han Chen, Akira Iwata and David I. Graham (2003) 'Amyloid β accumulation in axons after traumatic brain injury in humans', *Journal of Neurosurgery*, 98(5), pp. 1072–1077. doi: 10.3171/jns.2003.98.5.1072.

Draper, K. and Ponsford, J. (2008) 'Cognitive functioning ten years following traumatic brain injury and rehabilitation', *Neuropsychology*, 22(5), pp. 618–625. doi: 10.1037/0894-4105.22.5.618.

Edison, P., Archer, H. A., Gerhard, A., Hinz, R., Pavese, N., Turkheimer, F. E., Hammers, A., Tai, Y. F., Fox, N., Kennedy, A., Rossor, M. and Brooks, D. J. (2008) 'Microglia, amyloid, and cognition in Alzheimer's disease: An [11C](R)PK11195-PET and [11C]PIB-PET study', *Neurobiol Dis*. 2008/09/13, 32(3), pp. 412–419. doi: S0969-9961(08)00188-5 [pii]10.1016/j.nbd.2008.08.001.

Eikelenboom, M. J., Petzold, A., Lazeron, R. H. C., Silber, E., Sharief, M., Thompson, E. J., Barkhof, F., Giovannoni, G., Polman, C. H. and Uitdehaag, B. M. J. (2003) 'Multiple sclerosis: Neurofilament light chain antibodies are correlated to cerebral atrophy.', *Neurology*. United States, 60(2), pp. 219–223.

Elewa, H. F., Hilali, H., Hess, D. C., Machado, L. S. and Fagan, S. C. (2006) 'Minocycline for Short-Term Neuroprotection', *Pharmacotherapy: The Journal of Human Pharmacology and Drug Therapy*, 26(4), pp. 515–521. doi: 10.1592/phco.26.4.515.

Engel, S., Schluesener, H., Mittelbronn, M., Seid, K., Adjodah, D., Wehner, H. D. and Meyermann, R. (2000) 'Dynamics of microglial activation after human traumatic brain injury are revealed by delayed expression of macrophage-related proteins MRP8 and MRP14.', *Acta neuropathologica*. GERMANY, 100(3), pp. 313–322.

Faden, A. I. and Loane, D. J. (2015) 'Chronic neurodegeneration after traumatic brain injury: Alzheimer disease, chronic traumatic encephalopathy, or

persistent neuroinflammation?', *Neurotherapeutics : the journal of the American Society for Experimental NeuroTherapeutics*. United States, 12(1), pp. 143–150. doi: 10.1007/s13311-014-0319-5.

Fagan, S. C., Cronic, L. E. and Hess, D. C. (2011) 'Minocycline Development for Acute Ischemic Stroke', *Transl Stroke Res*. 2011/09/13, 2(2), pp. 202–208. doi: 10.1007/s12975-011-0072-6.

Farbota, K. D. M., Sodhi, A., Bendlin, B. B., McLaren, D. G., Xu, G., Rowley, H. A. and Johnson, S. C. (2012) 'Longitudinal Volumetric Changes following Traumatic Brain Injury: A Tensor-Based Morphometry Study', *Journal of the International Neuropsychological Society*, 18(6), pp. 1006–1018.

Finnie, J. W. (2013) 'Neuroinflammation: beneficial and detrimental effects after traumatic brain injury', *Inflammopharmacology*.

Fischl, B. (2012) 'FreeSurfer', *Neuroimage*. Elsevier, 62(2), pp. 774–781.

Fleminger, S. (2006) 'Patients after a head injury face an uncertain long-term future', *J Neurol Neurosurg Psychiatry*. 2006/07/19, 77(10), p. 1105. doi: 10.1136/jnnp.2006.099697.

Fleminger, S. and Ponsford, J. (2005) 'Long term outcome after traumatic brain injury', *BMJ: British Medical Journal*, 331(7530), pp. 1419–1420. Available at: http://www.ncbi.nlm.nih.gov/entrez/query.fcgi?cmd=Retrieve&db=PubMed&dopt=Citation&list_uids=16356951.

Folkersma, H., Boellaard, R., Yaqub, M., Kloet, R. W., Windhorst, A. D., Lammertsma, A. A., Vandertop, W. P. and van Berckel, B. N. M. (2011) 'Widespread and prolonged increase in (R)-(11)C-PK11195 binding after traumatic brain injury', *Journal of Nuclear Medicine: Official Publication, Society of Nuclear Medicine*, 52(8), pp. 1235–1239. doi: 10.2967/jnumed.110.084061.

Forsyth, R. J., Jayamoni, B., Paine, T. C. and Macarenhas, S. (2011) 'Monoaminergic agonists for acute traumatic brain injury (Review)', *Cochrane Database Syst Rev*.

Frank-Cannon, T., Alto, L., McAlpine, F. and Tansey, M. (2009) 'Does

neuroinflammation fan the flame in neurodegenerative diseases?', *Molecular Neurodegeneration*. BioMed Central, 4(1), pp. 1–13. doi: 10.1186/1750-1326-4-47.

Friede, R. L. and Samorajski, T. (1970) 'Axon caliber related to neurofilaments and microtubules in sciatic nerve fibers of rats and mice.', *The Anatomical record*. UNITED STATES, 167(4), pp. 379–387. doi: 10.1002/ar.1091670402.

Frisoni, G. B. and Jack, C. R. (2011) 'Harmonization of magnetic resonance-based manual hippocampal segmentation: a mandatory step for wide clinical use', *Alzheimers Dement*. 2011/03/19, 7(2), pp. 171–174. doi: 10.1016/j.jalz.2010.06.007.

Gaiottino, J., Norgren, N., Dobson, R., Topping, J., Nissim, A., Malaspina, A., Bestwick, J. P., Monsch, A. U., Regeniter, A., Lindberg, R. L., Kappos, L., Leppert, D., Petzold, A., Giovannoni, G. and Kuhle, J. (2013) 'Increased Neurofilament Light Chain Blood Levels in Neurodegenerative Neurological Diseases', *PLoS ONE*. Edited by M. Reindl. San Francisco, USA. doi: 10.1371/journal.pone.0075091.

Gardner, R. C., Burke, J. F., Nettiksimmons, J., Goldman, S., Tanner, C. M. and Yaffe, K. (2015) 'Traumatic brain injury in later life increases risk for Parkinson disease', *Annals of neurology*. Wiley Online Library, 77(6), pp. 987–995.

Garrido-Mesa, N., Zarzuelo, A. and Gálvez, J. (2013a) 'Minocycline: far beyond an antibiotic', *British Journal of Pharmacology*, 169(2), pp. 337–352. doi: 10.1111/bph.12139.

Garrido-Mesa, N., Zarzuelo, A. and Gálvez, J. (2013b) 'What is behind the non-antibiotic properties of minocycline?', *Pharmacological Research*, 67(1), pp. 18–30. doi: 10.1016/j.phrs.2012.10.006.

Geddes, J. F., Vowles, G. H., Beer, T. W. and Ellison, D. W. (1997) 'The diagnosis of diffuse axonal injury: implications for forensic practice', *Neuropathol Appl Neurobiol*. 1997/08/01, 23(4), pp. 339–347. Available at: http://www.ncbi.nlm.nih.gov/entrez/query.fcgi?cmd=Retrieve&db=PubMed&do

pt=Citation&list_uids=9292874.

Gedye, A., Beattie, B. L., Tuokko, H., Horton, A. and Korsarek, E. (1989) 'Severe head injury hastens age of onset of Alzheimer's disease.', *Journal of the American Geriatrics Society*. UNITED STATES, 37(10), pp. 970–973.

Gentleman, S. M. (2013) 'Review: microglia in protein aggregation disorders: friend or foe?', *Neuropathol Appl Neurobiol*, 39(1), pp. 45–50. doi: 10.1111/nan.12017.

Gentleman, S. M., Leclercq, P. D., Moyes, L., Graham, D. I., Smith, C., Griffin, W. S. T. and Nicoll, J. A. R. (2004) 'Long-term intracerebral inflammatory response after traumatic brain injury', *Forensic Sci Int*. 2004/11/16, 146(2–3), pp. 97–104. doi: S0379-0738(04)00398-6 [pii]10.1016/j.forsciint.2004.06.027.

Gershen, L. P., Zanotti-Fregonara, P., Dustin, I. H., Liow, J. S., Hirvonen, J., Kreisl, W. C., Jenko, K. J., Inati, S. K., Fujita, M., Morse, C. L., Brouwer, C., Hong, J. S., Pike, V. W., Zoghbi, S. S., Innis, R. B. and Theodore, W. H. (2015) 'Neuroinflammation in Temporal Lobe Epilepsy Measured Using Positron Emission Tomographic Imaging of Translocator Protein', *JAMA Neurol*, 72(8), pp. 882–888. doi: 10.1001/jamaneurol.2015.0941.

Gisslén, M., Price, R. W., Andreasson, U., Norgren, N., Nilsson, S., Hagberg, L., Fuchs, D., Spudich, S., Blennow, K. and Zetterberg, H. (2016) 'Plasma Concentration of the Neurofilament Light Protein (NFL) is a Biomarker of CNS Injury in HIV Infection: A Cross-Sectional Study', *EBioMedicine*, 3, pp. 135–140. doi: http://dx.doi.org/10.1016/j.ebiom.2015.11.036.

Goldstein, L. E., Fisher, A. M., Tagge, C. A., Zhang, X. L., Velisek, L., Sullivan, J. A., Upreti, C., Kracht, J. M., Ericsson, M., Wojnarowicz, M. W., Goletiani, C. J., Maglakelidze, G. M., Casey, N., Moncaster, J. A., Minaeva, O., Moir, R. D., Nowinski, C. J., Stern, R. A., Cantu, R. C., Geiling, J., Blusztajn, J. K., Wolozin, B. L., Ikezu, T., Stein, T. D., Budson, A. E., Kowall, N. W., Chargin, D., Sharon, A., Saman, S., Hall, G. F., Moss, W. C., Cleveland, R. O., Tanzi, R. E., Stanton, P. K. and McKee, A. C. (2012) 'Chronic traumatic encephalopathy in blast-exposed military veterans and a blast neurotrauma mouse model', *Science*

*translational medicine*. 2012/05/18, 4(134), p. 134ra60. doi: 10.1126/scitranslmed.3003716.

Gordon, P. H., Moore, D. H., Gelinas, D. F., Qualls, C., Meister, M. E., Werner, J., Mendoza, M., Mass, J., Kushner, G. and Miller, R. G. (2004) 'Placebo-controlled phase I/II studies of minocycline in amyotrophic lateral sclerosis', *Neurology*, 62(10), pp. 1845–1847. Available at: http://www.ncbi.nlm.nih.gov/pubmed/15159491.

Gordon, P. H., Moore, D. H., Miller, R. G., Florence, J. M., Verheijde, J. L., Doorish, C., Hilton, J. F., Spitalny, G. M., MacArthur, R. B., Mitsumoto, H., Neville, H. E., Boylan, K., Mozaffar, T., Belsh, J. M., Ravits, J., Bedlack, R. S., Graves, M. C., McCluskey, L. F., Barohn, R. J. and Tandan, R. (2007) 'Efficacy of minocycline in patients with amyotrophic lateral sclerosis: a phase III randomised trial', *The Lancet Neurology*, 6(12), pp. 1045–1053. doi: http://dx.doi.org/10.1016/S1474-4422(07)70270-3.

Graeber, M. B. (2014) 'Neuroinflammation: no rose by any other name', *Brain Pathol*. 2014/10/28, 24(6), pp. 620–622. doi: 10.1111/bpa.12192.

Graham, D. I., McIntosh, T. K., Maxwell, W. L. and Nicoll, J. A. (2000) 'Recent advances in neurotrauma', *J Neuropathol Exp Neurol*. 2000/08/22, 59(8), pp. 641–651. Available at: http://www.ncbi.nlm.nih.gov/entrez/query.fcgi?cmd=Retrieve&db=PubMed&dopt=Citation&list_uids=10952055.

Grieve, S. M., Williams, L. M., Paul, R. H., Clark, C. R. and Gordon, E. (2007) 'Cognitive aging, executive function, and fractional anisotropy: a diffusion tensor MR imaging study', *AJNR Am J Neuroradiol*, 28(2), pp. 226–235. doi: 28/2/226 [pii].

Griffin, M. O., Fricovsky, E., Ceballos, G. and Villarreal, F. (2010) 'Tetracyclines: a pleitropic family of compounds with promising therapeutic properties. Review of the literature', *American Journal of Physiology - Cell Physiology*, 299(3), pp. C539–C548. doi: 10.1152/ajpcell.00047.2010.

Guo, Q., Owen, D. R., Rabiner, E. A., Turkheimer, F. E. and Gunn, R. N. (2012)

‘Identifying improved TSPO PET imaging probes through biomathematics: The impact of multiple TSPO binding sites in vivo’, *NeuroImage*, 60(2), pp. 902–910. doi: http://dx.doi.org/10.1016/j.neuroimage.2011.12.078.

Guo, Z., Cupples, L. A., Kurz, A., Auerbach, S. H., Volicer, L., Chui, H., Green, R. C., Sadovnick, A. D., Duara, R., DeCarli, C., Johnson, K., Go, R. C., Growdon, J. H., Haines, J. L., Kukull, W. A. and Farrer, L. A. (2000) ‘Head injury and the risk of AD in the MIRAGE study’, *Neurology*. 2000/04/04, 54(6), pp. 1316–1323. Available at: http://www.ncbi.nlm.nih.gov/entrez/query.fcgi?cmd=Retrieve&db=PubMed&dopt=Citation&list_uids=10746604.

Gurdjian, E. S. (1975) ‘Re-evaluation of the biomechanics of blunt impact injury of the head’, *Surg Gynecol Obstet*. 1975/06/01, 140(6), pp. 845–850.

Gustavsson, A., Svensson, M., Jacobi, F., Allgulander, C., Alonso, J., Beghi, E., Dodel, R., Ekman, M., Faravelli, C., Fratiglioni, L., Gannon, B., Jones, D. H., Jennum, P., Jordanova, A., Jonsson, L., Karampampa, K., Knapp, M., Kobelt, G., Kurth, T., Lieb, R., Linde, M., Ljungcrantz, C., Maercker, A., Melin, B., Moscarelli, M., Musayev, A., Norwood, F., Preisig, M., Pugliatti, M., Rehm, J., Salvador-Carulla, L., Schlehofer, B., Simon, R., Steinhausen, H. C., Stovner, L. J., Vallat, J. M., Van den Bergh, P., van Os, J., Vos, P., Xu, W., Wittchen, H. U., Jonsson, B. and Olesen, J. (2011) ‘Cost of disorders of the brain in Europe 2010’, *European neuropsychopharmacology : the journal of the European College of Neuropsychopharmacology*. 2011/09/20, 21(10), pp. 718–779. doi: 10.1016/j.euroneuro.2011.08.008.

Haber, M., Abdel Baki, S. G., Grin’kina, N. M., Irizarry, R., Ershova, A., Orsi, S., Grill, R. J., Dash, P. and Bergold, P. J. (2013) ‘Minocycline plus N-acetylcysteine synergize to modulate inflammation and prevent cognitive and memory deficits in a rat model of mild traumatic brain injury.’, *Experimental neurology*. United States, 249, pp. 169–177. doi: 10.1016/j.expneurol.2013.09.002.

Hanisch, U. K. and Kettenmann, H. (2007) ‘Microglia: active sensor and

versatile effector cells in the normal and pathologic brain', *Nat Neurosci*. 2007/10/30, 10(11), pp. 1387–1394. doi: 10.1038/nn1997.

Hartman, R. E., Laurer, H., Longhi, L., Bales, K. R., Paul, S. M., McIntosh, T. K. and Holtzman, D. M. (2002) 'Apolipoprotein E4 influences amyloid deposition but not cell loss after traumatic brain injury in a mouse model of Alzheimer's disease', *J Neurosci*. 2002/11/27, 22(23), pp. 10083–10087. doi: 22/23/10083 [pii].

Heckemann, R. A., Hajnal, J. V, Aljabar, P., Rueckert, D. and Hammers, A. (2006) 'Automatic anatomical brain MRI segmentation combining label propagation and decision fusion', *NeuroImage*. 2006/07/25, 33(1), pp. 115–126. doi: S1053-8119(06)00645-8 [pii]10.1016/j.neuroimage.2006.05.061.

Heckemann, R. A., Keihaninejad, S., Aljabar, P., Rueckert, D., Hajnal, J. V and Hammers, A. (2010) 'Improving intersubject image registration using tissue-class information benefits robustness and accuracy of multi-atlas based anatomical segmentation', *NeuroImage*. 2010/02/02, 51(1), pp. 221–227. doi: S1053-8119(10)00094-7 [pii]10.1016/j.neuroimage.2010.01.072.

Hellewell, S. C. and Morganti-Kossmann, M. C. (2012) 'Guilty molecules, guilty minds? The conflicting roles of the innate immune response to traumatic brain injury', *Mediators Inflamm*, 2012, p. 356494. doi: 10.1155/2012/356494.

Hellyer, P. J., Leech, R., Ham, T. E., Bonnelle, V. and Sharp, D. J. (2013) 'Individual prediction of white matter injury following traumatic brain injury', *Annals of neurology*, 73(4), pp. 489–499. Available at: http://onlinelibrary.wiley.com/store/10.1002/ana.23824/asset/ana23824.pdf?v=1&t=i9ogiv9j&s=9dedf575395f0ef66add1311f9f2e7ed140d20be.

Hellyer, P. J., Scott, G., Shanahan, M., Sharp, D. J. and Leech, R. (2015) 'Cognitive Flexibility through Metastable Neural Dynamics Is Disrupted by Damage to the Structural Connectome.', *The Journal of neuroscience : the official journal of the Society for Neuroscience*. United States, 35(24), pp. 9050–9063. doi: 10.1523/JNEUROSCI.4648-14.2015.

Hernandez-Ontiveros, D. G., Tajiri, N., Acosta, S., Giunta, B., Tan, J. and

Borlongan, C. V (2013) ‘Microglia activation as a biomarker for traumatic brain injury’, *Front Neurol*, 4, p. 30. doi: 10.3389/fneur.2013.00030.

Himanen, L., Portin, R., Isoniemi, H., Helenius, H., Kurki, T. and Tenovuo, O. (2006) ‘Longitudinal cognitive changes in traumatic brain injury: A 30-year follow-up study’, *Neurology*, 66(2), pp. 187–192. doi: 10.1212/01.wnl.0000194264.60150.d3.

Hinz, R. and Boellaard, R. (2015) ‘Challenges of quantification of TSPO in the human brain’, *Clinical and Translational Imaging*, 3(6), pp. 403–416. doi: 10.1007/s40336-015-0138-7.

Holmin, S. and Mathiesen, T. (1999) ‘Long-term intracerebral inflammatory response after experimental focal brain injury in rat’, *Neuroreport*. 1999/09/29, 10(9), pp. 1889–1891.

Holmin, S., Soderlund, J., Biberfeld, P. and Mathiesen, T. (1998) ‘Intracerebral inflammation after human brain contusion.’, *Neurosurgery*. UNITED STATES, 42(2), pp. 291–299.

Homsi, S., Federico, F., Croci, N., Palmier, B., Plotkine, M., Marchand-Leroux, C. and Jafarian-Tehrani, M. (2009) ‘Minocycline effects on cerebral edema: relations with inflammatory and oxidative stress markers following traumatic brain injury in mice’, *Brain Res Cogn Brain Res*. 2009/07/28, 1291, pp. 122–132. doi: 10.1016/j.brainres.2009.07.031.

Homsi, S., Piaggio, T., Croci, N., Noble, F., Plotkine, M., Marchand-Leroux, C. and Jafarian-Tehrani, M. (2010) ‘Blockade of acute microglial activation by minocycline promotes neuroprotection and reduces locomotor hyperactivity after closed head injury in mice: a twelve-week follow-up study’, *J Neurotrauma*. 2010/02/20, 27(5), pp. 911–921. doi: 10.1089/neu.2009.1223.

Hong, Y. T., Veenith, T., Dewar, D., Outtrim, J. G., Mani, V., Williams, C., Pimlott, S., Hutchinson, P. J., Tavares, A., Canales, R., Mathis, C. A., Klunk, W. E., Aigbirhio, F. I., Coles, J. P., Baron, J. C., Pickard, J. D., Fryer, T. D., Stewart, W. and Menon, D. K. (2014) ‘Amyloid imaging with Carbon 11-labeled Pittsburgh compound B for traumatic brain injury’, *JAMA Neurol*. 2013/11/13,

71(1), pp. 23–31. doi: 10.1001/jamaneurol.2013.4847.

HSG (2004) ‘Minocycline safety and tolerability in Huntington disease’, *Neurology*. 2004/08/12, 63(3), pp. 547–549.

HSG (2010) ‘A futility study of minocycline in Huntington’s disease’, *Mov Disord*. 2010/08/20, 25(13), pp. 2219–2224. doi: 10.1002/mds.23236.

Hua, K., Zhang, J., Wakana, S., Jiang, H., Li, X., Reich, D. S., Calabresi, P. A., Pekar, J. J., van Zijl, P. C. and Mori, S. (2008) ‘Tract probability maps in stereotaxic spaces: analyses of white matter anatomy and tract-specific quantification’, *NeuroImage*. 2007/10/13, 39(1), pp. 336–347. doi: S1053-8119(07)00688-X [pii]10.1016/j.neuroimage.2007.07.053.

Ikoma, Y., Edison, P., Ramlackhansingh, A., Brooks, D. J. and Turkheimer, F. E. (2013) ‘Reference region automatic extraction in dynamic [11C]-PIB’, *J Cereb Blood Flow Metab*. 2013/08/08. International Society for Cerebral Blood Flow & Metabolism, Inc., 33(11), pp. 1725–1731. doi: 10.1038/jcbfm.2013.133.

Ikonomovic, M. D., Uryu, K., Abrahamson, E. E., Ciallella, J. R., Trojanowski, J. Q., Lee, V. M., Clark, R. S., Marion, D. W., Wisniewski, S. R. and DeKosky, S. T. (2004) ‘Alzheimer’s pathology in human temporal cortex surgically excised after severe brain injury’, *Exp Neurol*. 2004/10/12, 190(1), pp. 192–203. doi: S0014488604002420 [pii]10.1016/j.expneurol.2004.06.011.

Isoniemi, H., Kurki, T., Tenovuo, O., Kairisto, V. and Portin, R. (2006) ‘Hippocampal volume, brain atrophy, and APOE genotype after traumatic brain injury’, *Neurology*. 2006/09/13, 67(5), pp. 756–760. doi: 67/5/756 [pii]10.1212/01.wnl.0000234140.64954.12.

Jack, C. R., Knopman, D. S., Jagust, W. J., Shaw, L. M., Aisen, P. S., Weiner, M. W., Petersen, R. C. and Trojanowski, J. Q. (2010) ‘Hypothetical model of dynamic biomarkers of the Alzheimer’s pathological cascade’, *The Lancet Neurology*. Elsevier, 9(1), pp. 119–128.

Johnson, K. A., Schultz, A., Betensky, R. A., Becker, J. A., Sepulcre, J., Rentz, D., Mormino, E., Chhatwal, J., Amariglio, R., Papp, K., Marshall, G., Albers, M.,

Mauro, S., Pepin, L., Alverio, J., Judge, K., Philiossaint, M., Shoup, T., Yokell, D., Dickerson, B., Gomez-Isla, T., Hyman, B., Vasdev, N. and Sperling, R. (2016) 'Tau positron emission tomographic imaging in aging and early Alzheimer disease', *Annals of Neurology*, 79(1), pp. 110–119. doi: 10.1002/ana.24546.

Johnson, V. E., Stewart, J. E., Begbie, F. D., Trojanowski, J. Q., Smith, D. H. and Stewart, W. (2013) 'Inflammation and white matter degeneration persist for years after a single traumatic brain injury', *Brain : a journal of neurology*. 2013/02/01, 136(Pt 1), pp. 28–42. doi: 10.1093/brain/aws322.

Johnson, V. E., Stewart, W. and Smith, D. H. (2010) 'Traumatic brain injury and amyloid-beta pathology: a link to Alzheimer's disease?', *Nat Rev Neurosci*. 2010/03/11, 11(5), pp. 361–370. doi: 10.1038/nrn2808.

Johnson, V. E., Stewart, W. and Smith, D. H. (2012) 'Widespread tau and amyloid-beta pathology many years after a single traumatic brain injury in humans', *Brain Pathol*. 2011/07/01, 22(2), pp. 142–149. doi: 10.1111/j.1750-3639.2011.00513.x.

Johnson, V. E., Stewart, W. and Smith, D. H. (2013) 'Axonal pathology in traumatic brain injury', *Experimental Neurology*, 246, pp. 35–43. doi: 10.1016/j.expneurol.2012.01.013.

Jones, E. G. (2012) *The thalamus*. Springer Science & Business Media.

Jucaite, A., Svenningsson, P., Rinne, J. O., Cselenyi, Z., Varnas, K., Johnstrom, P., Amini, N., Kirjavainen, A., Helin, S., Minkwitz, M., Kugler, A. R., Posener, J. A., Budd, S., Halldin, C., Varrone, A. and Farde, L. (2015) 'Effect of the myeloperoxidase inhibitor AZD3241 on microglia: a PET study in Parkinson's disease.', *Brain : a journal of neurology*. England, 138(Pt 9), pp. 2687–2700. doi: 10.1093/brain/awv184.

Keihaninejad, S., Zhang, H., Ryan, N. S., Malone, I. B., Modat, M., Cardoso, M. J., Cash, D. M., Fox, N. C. and Ourselin, S. (2013) 'An unbiased longitudinal analysis framework for tracking white matter changes using diffusion tensor imaging with application to Alzheimer's disease', *NeuroImage*, 72, pp. 153–

163. doi: http://dx.doi.org/10.1016/j.neuroimage.2013.01.044.

Kettenmann, H., Hanisch, U. K., Noda, M. and Verkhratsky, A. (2011) 'Physiology of microglia', *Physiol Rev*. 2011/04/30, 91(2), pp. 461–553. doi: 10.1152/physrev.00011.2010.

Kim, H. S. and Suh, Y. H. (2009) 'Minocycline and neurodegenerative diseases', *Behavioural Brain Research*. 2008/11/04, 196(2), pp. 168–179. doi: 10.1016/j.bbr.2008.09.040.

Kinnunen, K. M., Greenwood, R., Powell, J. H., Leech, R., Hawkins, P. C., Bonnelle, V., Patel, M. C., Counsell, S. J. and Sharp, D. J. (2011) 'White matter damage and cognitive impairment after traumatic brain injury', *Brain*. 2011/01/05, 134(Pt 2), pp. 449–463. doi: 10.1093/brain/awq347.

Klein, A., Andersson, J., Ardekani, B. A., Ashburner, J., Avants, B., Chiang, M.-C. C., Christensen, G. E., Collins, D. L., Gee, J., Hellier, P., Song, J. H., Jenkinson, M., Lepage, C., Rueckert, D., Thompson, P., Vercauteren, T., Woods, R. P., Mann, J. J. and Parsey, R. V (2009) 'Evaluation of 14 nonlinear deformation algorithms applied to human brain MRI registration', *NeuroImage*. 2009/02/07, 46(3), pp. 786–802. doi: S1053-8119(08)01297-4 [pii]10.1016/j.neuroimage.2008.12.037.

Klunk, W. E., Engler, H., Nordberg, A., Wang, Y., Blomqvist, G., Holt, D. P., Bergstrom, M., Savitcheva, I., Huang, G. F., Estrada, S., Ausen, B., Debnath, M. L., Barletta, J., Price, J. C., Sandell, J., Lopresti, B. J., Wall, A., Koivisto, P., Antoni, G., Mathis, C. A. and Langstrom, B. (2004) 'Imaging brain amyloid in Alzheimer's disease with Pittsburgh Compound-B', *Ann Neurol*, 55(3), pp. 306–319. Available at: http://www.ncbi.nlm.nih.gov/entrez/query.fcgi?cmd=Retrieve&db=PubMed&dopt=Citation&list_uids=14991808.

Knight, W. D., Okello, A. A., Ryan, N. S., Turkheimer, F. E., Rodriguez Martinez de Llano, S., Edison, P., Douglas, J., Fox, N. C., Brooks, D. J. and Rossor, M. N. (2011) 'Carbon-11-Pittsburgh compound B positron emission tomography imaging of amyloid deposition in presenilin 1 mutation carriers', *Brain*.

2010/11/19, 134(Pt 1), pp. 293–300. doi: 10.1093/brain/awq310.

Kobayashi, K., Imagama, S., Ohgomori, T., Hirano, K., Uchimura, K., Sakamoto, K., Hirakawa, A., Takeuchi, H., Suzumura, A., Ishiguro, N. and Kadomatsu, K. (2013) 'Minocycline selectively inhibits M1 polarization of microglia', *Cell Death Dis*. 2013/03/09, 4, p. e525. doi: 10.1038/cddis.2013.54.

Kohler, E., Prentice, D. A., Bates, T. R., Hankey, G. J., Claxton, A., van Heerden, J. and Blacker, D. (2013) 'Intravenous Minocycline in Acute Stroke: A Randomized, Controlled Pilot Study and Meta-Analysis', *Stroke*. 2013/07/23. doi: 10.1161/strokeaha.113.000780.

Koshinaga, M., Katayama, Y., Fukushima, M., Oshima, H., Suma, T. and Takahata, T. (2000) 'Rapid and widespread microglial activation induced by traumatic brain injury in rat brain slices', *J Neurotrauma*. 2000/04/11, 17(3), pp. 185–192. Available at: http://www.ncbi.nlm.nih.gov/entrez/query.fcgi?cmd=Retrieve&db=PubMed&dopt=Citation&list_uids=10757324.

Kovesdi, E., Kamnaksh, A., Wingo, D., Ahmed, F., Grunberg, N. E., Long, J. B., Kasper, C. E. and Agoston, D. V (2012) 'Acute minocycline treatment prevents neurobehavioral impairment in a rat model of mild blast traumatic brain injury', *Frontiers in Neurology*, 3. doi: 10.3389/fneur.2012.00111.

Kuhle, J., Gaiottino, J., Leppert, D., Petzold, A., Bestwick, J. P., Malaspina, A., Lu, C.-H., Dobson, R., Disanto, G., Norgren, N., Nissim, A., Kappos, L., Hurlbert, J., Yong, V. W., Giovannoni, G. and Casha, S. (2015) 'Serum neurofilament light chain is a biomarker of human spinal cord injury severity and outcome.', *Journal of neurology, neurosurgery, and psychiatry*. England, 86(3), pp. 273–279. doi: 10.1136/jnnp-2013-307454.

Kuhlmann, A. C. and Guilarte, T. R. (2000) 'Cellular and subcellular localization of peripheral benzodiazepine receptors after trimethyltin neurotoxicity.', *Journal of neurochemistry*. UNITED STATES, 74(4), pp. 1694–1704.

Kumar, A., Alvarez-Croda, D.-M., Stoica, B. A., Faden, A. I. and Loane, D. J. (2015) 'Microglial/Macrophage Polarization Dynamics following Traumatic

Brain Injury.', *Journal of neurotrauma*. doi: 10.1089/neu.2015.4268.

Kumar, A. and Loane, D. J. (2012) 'Neuroinflammation after traumatic brain injury: opportunities for therapeutic intervention', *Brain Behav Immun*. 2012/06/26, 26(8), pp. 1191–1201. doi: 10.1016/j.bbi.2012.06.008.

Kumar, A., Muzik, O., Shandal, V., Chugani, D., Chakraborty, P. and Chugani, H. T. (2012) 'Evaluation of age-related changes in translocator protein (TSPO) in human brain using (11)C-[R]-PK11195 PET', *J Neuroinflammation*. 2012/10/06, 9, p. 232. doi: 10.1186/1742-2094-9-232.

Kumar, A., Stoica, B. A., Sabirzhanov, B., Burns, M. P., Faden, A. I. and Loane, D. J. (2013) 'Traumatic brain injury in aged animals increases lesion size and chronically alters microglial/macrophage classical and alternative activation states', *Neurobiology of Aging*, 34(5), pp. 1397–1411. doi: http://dx.doi.org/10.1016/j.neurobiolaging.2012.11.013.

Kunz, A., Dirnagl, U. and Mergenthaler, P. (2010) 'Acute pathophysiological processes after ischaemic and traumatic brain injury', *Best Practice & Research Clinical Anaesthesiology*, 24(4), pp. 495–509. doi: http://dx.doi.org/10.1016/j.bpa.2010.10.001.

Lampl, Y., Boaz, M., Gilad, R., Lorberboym, M., Dabby, R., Rapoport, A., Anca-Hershkowitz, M. and Sadeh, M. (2007) 'Minocycline treatment in acute stroke An open-label, evaluator-blinded study', *Neurology*, 69(14), pp. 1404–1410. doi: 10.1212/01.wnl.0000277487.04281.db.

Langlois, J. A., Rutland-Brown, W. and Wald, M. M. (2006) 'The epidemiology and impact of traumatic brain injury: a brief overview', *The Journal of head trauma rehabilitation*, 21(5), pp. 375–378.

Liu, G. J., Middleton, R. J., Hatty, C. R., Kam, W. W., Chan, R., Pham, T., Harrison-Brown, M., Dodson, E., Veale, K. and Banati, R. B. (2014) 'The 18 kDa translocator protein, microglia and neuroinflammation', *Brain Pathol*. 2014/10/28, 24(6), pp. 631–653. doi: 10.1111/bpa.12196.

Liu, G. J., Nagarajah, R., Banati, R. B. and Bennett, M. R. (2009) 'Glutamate

induces directed chemotaxis of microglia', *Eur J Neurosci*. 2009/03/24, 29(6), pp. 1108–1118. doi: 10.1111/j.1460-9568.2009.06659.x.

Liu, Q., Xie, F., Siedlak, S. L., Nunomura, A., Honda, K., Moreira, P. I., Zhua, X., Smith, M. A. and Perry, G. (2004) 'Neurofilament proteins in neurodegenerative diseases.', *Cellular and molecular life sciences : CMLS*. Switzerland, 61(24), pp. 3057–3075. doi: 10.1007/s00018-004-4268-8.

Loane, D. J. and Byrnes, K. R. (2010) 'Role of microglia in neurotrauma', *Neurotherapeutics*. 2010/10/01, 7(4), pp. 366–377. doi: 10.1016/j.nurt.2010.07.002.

Loane, D. J., Kumar, A., Stoica, B. A., Cabatbat, R. and Faden, A. I. (2014) 'Progressive Neurodegeneration after Experimental Brain Trauma: Association with Chronic Microglial Activation', *Journal of neuropathology and experimental neurology*, pp. 14–29. doi: 10.1097/NEN.0000000000000021.

Lockhart, A., Davis, B., Matthews, J. C., Rahmoune, H., Hong, G., Gee, A., Earnshaw, D. and Brown, J. (2003) 'The peripheral benzodiazepine receptor ligand PK11195 binds with high affinity to the acute phase reactant alpha1-acid glycoprotein: implications for the use of the ligand as a CNS inflammatory marker.', *Nuclear medicine and biology*. England, 30(2), pp. 199–206.

Logan, J., Fowler, J. S., Volkow, N. D., Wolf, A. P., Dewey, S. L., Schlyer, D. J., MacGregor, R. R., Hitzemann, R., Bendriem, B. and Gatley, S. J. (1990) 'Graphical analysis of reversible radioligand binding from time-activity measurements applied to [N-11C-methyl]-(-)-cocaine PET studies in human subjects.', *Journal of cerebral blood flow and metabolism : official journal of the International Society of Cerebral Blood Flow and Metabolism*. UNITED STATES, 10(5), pp. 740–747. doi: 10.1038/jcbfm.1990.127.

Loggia, M. L., Chonde, D. B., Akeju, O., Arabasz, G., Catana, C., Edwards, R. R., Hill, E., Hsu, S., Izquierdo-Garcia, D., Ji, R.-R., Riley, M., Wasan, A. D., Zurcher, N. R., Albrecht, D. S., Vangel, M. G., Rosen, B. R., Napadow, V. and Hooker, J. M. (2015) 'Evidence for brain glial activation in chronic pain patients.', *Brain : a journal of neurology*. England, 138(Pt 3), pp. 604–615. doi:

10.1093/brain/awu377.

Lowenstein, D. H. (2009) ‘Traumatic brain injury: a glimpse of order among the chaos?’, *Ann Neurol*. 2009/10/23, 66(4), pp. A7-8. doi: 10.1002/ana.21876.

Lu, C.-H., Macdonald-Wallis, C., Gray, E., Pearce, N., Petzold, A., Norgren, N., Giovannoni, G., Fratta, P., Sidle, K., Fish, M., Orrell, R., Howard, R., Talbot, K., Greensmith, L., Kuhle, J., Turner, M. R. and Malaspina, A. (2015) ‘Neurofilament light chain: A prognostic biomarker in amyotrophic lateral sclerosis.’, *Neurology*. United States, 84(22), pp. 2247–2257. doi: 10.1212/WNL.0000000000001642.

Lull, M. and Block, M. (2010) ‘Microglial activation and chronic neurodegeneration’, *Neurotherapeutics*. Springer-Verlag, 7(4), pp. 354–365. doi: 10.1016/j.nurt.2010.05.014.

Luo, X.-G. and Chen, S.-D. (2012) ‘The changing phenotype of microglia from homeostasis to disease’, *Translational Neurodegeneration*, 1(1), p. 9. Available at: http://www.translationalneurodegeneration.com/content/1/1/9.

Lyoo, C. H., Ikawa, M., Liow, J.-S., Zoghbi, S. S., Morse, C. L., Pike, V. W., Fujita, M., Innis, R. B. and Kreisl, W. C. (2015) ‘Cerebellum Can Serve As a Pseudo-Reference Region in Alzheimer Disease to Detect Neuroinflammation Measured with PET Radioligand Binding to Translocator Protein.’, *Journal of nuclear medicine : official publication, Society of Nuclear Medicine*. United States, 56(5), pp. 701–706. doi: 10.2967/jnumed.114.146027.

Maas, A. I., Roozenbeek, B. and Manley, G. T. (2010) ‘Clinical trials in traumatic brain injury: past experience and current developments’, *Neurotherapeutics*, 7(1), pp. 115–126. doi: 10.1016/j.nurt.2009.10.022.

Maas, A. I., Stocchetti, N. and Bullock, R. (2008) ‘Moderate and severe traumatic brain injury in adults’, *Lancet Neurol*. 2008/07/19, 7(8), pp. 728–741. doi: S1474-4422(08)70164-9 [pii]10.1016/S1474-4422(08)70164-9.

Macdonald, H., Kelly, R. G., Allen, E. S., Noble, J. F. and Kanegis, L. A. (1973) ‘Pharmacokinetic studies on minocycline in man’, *Clin Pharmacol Ther*.

1973/09/01, 14(5), pp. 852–861.

Maeda, J., Higuchi, M., Inaji, M., Ji, B., Haneda, E., Okauchi, T., Zhang, M. R., Suzuki, K. and Suhara, T. (2007) 'Phase-dependent roles of reactive microglia and astrocytes in nervous system injury as delineated by imaging of peripheral benzodiazepine receptor', *Brain Res*. 2007/06/02, 1157, pp. 100–111. doi: 10.1016/j.brainres.2007.04.054.

Magnoni, S., Mac Donald, C. L., Esparza, T. J., Conte, V., Sorrell, J., Macrì, M., Bertani, G., Biffi, R., Costa, A., Sammons, B., Snyder, A. Z., Shimony, J. S., Triulzi, F., Stocchetti, N. and Brody, D. L. (2015) 'Quantitative assessments of traumatic axonal injury in human brain: concordance of microdialysis and advanced MRI', *Brain*. Available at: http://brain.oxfordjournals.org/content/early/2015/06/16/brain.awv152.abstract
.

Malec, J. F., Brown, A. W., Leibson, C. L., Flaada, J. T., Mandrekar, J. N., Diehl, N. N. and Perkins, P. K. (2007) 'The mayo classification system for traumatic brain injury severity', *J Neurotrauma*. 2007/09/26, 24(9), pp. 1417–1424. doi: 10.1089/neu.2006.0245.

Mannix, R. C. and Whalen, M. J. (2012) 'Traumatic Brain Injury, Microglia, and Beta Amyloid', *International Journal of Alzheimer's Disease*, 2012, pp. 1–5. doi: 10.1155/2012/608732.

Masel, B. E. and DeWitt, D. S. (2010) 'Traumatic brain injury: a disease process, not an event', *J Neurotrauma*, 27(8), pp. 1529–1540. doi: 10.1089/neu.2010.1358.

Maxwell, W. L., MacKinnon, M. A., Smith, D. H., McIntosh, T. K. and Graham, D. I. (2006) 'Thalamic nuclei after human blunt head injury', *J Neuropathol Exp Neurol*. 2006/06/15, 65(5), pp. 478–488. doi: 10.1097/01.jnen.

McKee, A. C., Cantu, R. C., Nowinski, C. J., Hedley-Whyte, E. T., Gavett, B. E., Budson, A. E., Santini, V. E., Lee, H. S., Kubilus, C. A. and Stern, R. A. (2009) 'Chronic traumatic encephalopathy in athletes: progressive tauopathy after repetitive head injury', *J Neuropathol Exp Neurol*. 2009/06/19, 68(7), pp.

709–735. doi: 10.1097/NEN.0b013e3181a9d503.

McKee, A. C., Stern, R. A., Nowinski, C. J., Stein, T. D., Alvarez, V. E., Daneshvar, D. H., Lee, H. S., Wojtowicz, S. M., Hall, G., Baugh, C. M., Riley, D. O., Kubilus, C. A., Cormier, K. A., Jacobs, M. A., Martin, B. R., Abraham, C. R., Ikezu, T., Reichard, R. R., Wolozin, B. L., Budson, A. E., Goldstein, L. E., Kowall, N. W. and Cantu, R. C. (2013) 'The spectrum of disease in chronic traumatic encephalopathy', *Brain*. 2012/12/05, 136(Pt 1), pp. 43–64. doi: 10.1093/brain/aws307.

McKhann, G., Drachman, D., Folstein, M., Katzman, R., Price, D. and Stadlan, E. M. (1984) 'Clinical diagnosis of Alzheimer's disease: report of the NINCDS-ADRDA Work Group under the auspices of Department of Health and Human Services Task Force on Alzheimer's Disease', *Neurology*, 34(7), pp. 939–944. Available at: http://www.ncbi.nlm.nih.gov/entrez/query.fcgi?cmd=Retrieve&db=PubMed&dopt=Citation&list_uids=6610841.

McMillan, T. M. and Teasdale, G. M. (2007) 'Death rate is increased for at least 7 years after head injury: a prospective study', *Brain*, 130(Pt 10), pp. 2520–2527. Available at: http://www.ncbi.nlm.nih.gov/entrez/query.fcgi?cmd=Retrieve&db=PubMed&dopt=Citation&list_uids=17686808.

McMillan, T. M., Teasdale, G. M. and Stewart, E. (2012) 'Disability in young people and adults after head injury: 12-14 year follow-up of a prospective cohort', *J Neurol Neurosurg Psychiatry*, 83(11), pp. 1086–1091. doi: 10.1136/jnnp-2012-302746.

McMillan, T. M., Teasdale, G. M., Weir, C. J. and Stewart, E. (2011) 'Death after head injury: the 13 year outcome of a case control study', *J Neurol Neurosurg Psychiatry*. 2011/02/02, 82(8), pp. 931–935. doi: 10.1136/jnnp.2010.222232.

Menon, D. K., Schwab, K., Wright, D. W. and Maas, A. I. (2010) 'Position statement: definition of traumatic brain injury.', *Archives of physical medicine*

*and rehabilitation*. United States, 91(11), pp. 1637–1640. doi: 10.1016/j.apmr.2010.05.017.

Metz, L. M., Li, D., Traboulsee, A., Duquette, P., Yong, V. W., Eliasziw, M., Cerchiaro, G., Greenfield, J., Riddehough, A. and Yeung, M. (2015) 'Minocycline reduces the relative risk of multiple sclerosis in people experiencing their first clinical demyelinating event by 44.6%: results of a phase III double-blind placebo controlled Canadian multicentre clinical trial', in *MULTIPLE SCLEROSIS JOURNAL*. SAGE PUBLICATIONS LTD 1 OLIVERS YARD, 55 CITY ROAD, LONDON EC1Y 1SP, ENGLAND, pp. 780–781.

Metz, L. M., Li, D., Traboulsee, A., Myles, M. L., Duquette, P., Godin, J., Constantin, M. and Yong, V. W. (2009) 'Glatiramer acetate in combination with minocycline in patients with relapsing--remitting multiple sclerosis: results of a Canadian, multicenter, double-blind, placebo-controlled trial', *Multiple Sclerosis (Houndmills, Basingstoke, England)*, 15(10), pp. 1183–1194. doi: 10.1177/1352458509106779.

Meythaler, J. M., Peduzzi, J. D., Eleftheriou, E. and Novack, T. A. (2001) 'Current concepts: diffuse axonal injury-associated traumatic brain injury', *Arch Phys Med Rehabil*. 2001/10/06, 82(10), pp. 1461–1471. doi: S0003999301969485 [pii].

Millspaugh, J. A. (1937) 'Dementia pugilistica', *US Naval Med Bull*, 35, pp. 297–303.

Mittelbronn, M., Dietz, K., Schluesener, H. J. and Meyermann, R. (2001) 'Local distribution of microglia in the normal adult human central nervous system differs by up to one order of magnitude', *Acta Neuropathol*. 2001/04/20, 101(3), pp. 249–255.

Möller, T., Bard, F., Bhattacharya, A., Biber, K., Campbell, B., Dale, E., Eder, C., Gan, L., Garden, G. A., Hughes, Z. A., Pearse, D. D., Staal, R. G. W., Sayed, F. A., Wes, P. D. and Boddeke, H. W. G. M. (2016) 'Critical data-based re-evaluation of minocycline as a putative specific microglia inhibitor', *Glia*, p. n/a--n/a. doi: 10.1002/glia.23007.

Morganti-Kossmann, M. C., Satgunaseelan, L., Bye, N. and Kossmann, T. (2007) 'Modulation of immune response by head injury', *Injury*. 2007/12/01, 38(12), pp. 1392–1400. doi: S0020-1383(07)00420-2 [pii]10.1016/j.injury.2007.10.005.

Mori, S., Kaufmann, W. E., Pearlson, G. D., Crain, B. J., Stieltjes, B., Solaiyappan, M. and van Zijl, P. C. (2000) 'In vivo visualization of human neural pathways by magnetic resonance imaging', *Ann Neurol*. 2000/03/15, 47(3), pp. 412–414. Available at: http://www.ncbi.nlm.nih.gov/pubmed/10716271.

Mori, S., Oishi, K., Jiang, H., Jiang, L., Li, X., Akhter, K., Hua, K., Faria, A. V, Mahmood, A., Woods, R., Toga, A. W., Pike, G. B., Neto, P. R., Evans, A., Zhang, J., Huang, H., Miller, M. I., van Zijl, P. and Mazziotta, J. (2008) 'Stereotaxic white matter atlas based on diffusion tensor imaging in an ICBM template', *NeuroImage*. 2008/02/08, 40(2), pp. 570–582. doi: 10.1016/j.neuroimage.2007.12.035.

Nagamoto-Combs, K., McNeal, D. W., Morecraft, R. J. and Combs, C. K. (2007) 'Prolonged microgliosis in the rhesus monkey central nervous system after traumatic brain injury', *J Neurotrauma*. 2007/11/16, 24(11), pp. 1719–1742. doi: 10.1089/neu.2007.0377.

Nagamoto-Combs, K., Morecraft, R. J., Darling, W. G. and Combs, C. K. (2010) 'Long-term gliosis and molecular changes in the cervical spinal cord of the rhesus monkey after traumatic brain injury', *J Neurotrauma*. 2009/12/25, 27(3), pp. 565–585. doi: 10.1089/neu.2009.0966.

Nakasujja, N., Miyahara, S., Evans, S., Lee, A., Musisi, S., Katabira, E., Robertson, K., Ronald, A., Clifford, D. B. and Sacktor, N. (2013) 'Randomized trial of minocycline in the treatment of HIV-associated cognitive impairment', *Neurology*. 2012/12/28, 80(2), pp. 196–202. doi: 10.1212/WNL.0b013e31827b9121.

Nelson, M. L. and Levy, S. B. (2011) 'The history of the tetracyclines', *Annals of the New York Academy of Sciences*. Blackwell Publishing Inc, 1241(1), pp. 17–32. doi: 10.1111/j.1749-6632.2011.06354.x.

Nemetz, P. N., Leibson, C., Naessens, J. M., Beard, M., Kokmen, E., Annegers, J. F. and Kurland, L. T. (1999) 'Traumatic brain injury and time to onset of Alzheimer's disease: a population-based study', *Am J Epidemiol*. 1999/01/12, 149(1), pp. 32–40.

NET-PD, N. (2006) 'A randomized, double-blind, futility clinical trial of creatine and minocycline in early Parkinson disease', *Neurology*. 2006/02/17, 66(5), pp. 664–671. doi: 10.1212/01.wnl.0000201252.57661.e1.

Ng, S. Y., Semple, B. D., Morganti-Kossmann, M. C. and Bye, N. (2012) 'Attenuation of microglial activation with minocycline is not associated with changes in neurogenesis after focal traumatic brain injury in adult mice', *J Neurotrauma*. 2012/01/21, 29(7), pp. 1410–1425. doi: 10.1089/neu.2011.2188.

NICE (2007) *Head injury: Triage, assessment, investigation and early management of head injury in infants, children and adults.* Report.

Nichols, T. E. and Holmes, A. P. (2002) 'Nonparametric permutation tests for functional neuroimaging: a primer with examples', *Human brain mapping*. Wiley Online Library, 15(1), pp. 1–25.

Nimmerjahn, A., Kirchhoff, F. and Helmchen, F. (2005) 'Resting microglial cells are highly dynamic surveillants of brain parenchyma in vivo', *Science*. 2005/04/16, 308(5726), pp. 1314–1318. doi: 10.1126/science.1110647.

Norden, D. M. and Godbout, J. P. (2013) 'Review: microglia of the aged brain: primed to be activated and resistant to regulation', *Neuropathol Appl Neurobiol*. 2012/10/09, 39(1), pp. 19–34. doi: 10.1111/j.1365-2990.2012.01306.x.

Oh, H., Madison, C., Villeneuve, S., Markley, C. and Jagust, W. J. (2013) 'Association of gray matter atrophy with age, $β$-amyloid, and cognition in aging', *Cerebral cortex*. Oxford Univ Press, p. bht017.

Okie, S. (2005) 'Traumatic Brain Injury in the War Zone', *New England Journal of Medicine*, 352(20), pp. 2043–2047. doi: doi:10.1056/NEJMp058102.

Olah, M., Biber, K., Vinet, J. and Boddeke, H. W. (2011) 'Microglia phenotype diversity', *CNS Neurol Disord Drug Targets*. 2010/12/15, 10(1), pp. 108–118.

Oliver, J., Jones, M., Kirk, M., Gable, D., Repshas, J., Johnson, T., Andreasson, U., Norgren, N., Blennow, K. and Zetterberg, H. (2015) 'Serum Neurofilament Light in American Football Athletes Over the Course of a Season.', *Journal of neurotrauma*.

Onyszchuk, G., Levine, S. M., Brooks, W. M. and Berman, N. E. J. (2009) 'Post-acute pathological changes in the thalamus and internal capsule in aged mice following controlled cortical impact injury: A magnetic resonance imaging, iron histochemical, and glial immunohistochemical study', *Neurosci Lett*. 2009/04/23, 452(2), pp. 204–208. doi: S0304-3940(09)00096-2 [pii]10.1016/j.neulet.2009.01.049.

Owen, D. R., Guo, Q., Kalk, N. J., Colasanti, A., Kalogiannopoulou, D., Dimber, R., Lewis, Y. L., Libri, V., Barletta, J., Ramada-Magalhaes, J., Kamalakaran, A., Nutt, D. J., Passchier, J., Matthews, P. M., Gunn, R. N. and Rabiner, E. A. (2014) 'Determination of [(11)C]PBR28 binding potential in vivo: a first human TSPO blocking study.', *Journal of cerebral blood flow and metabolism : official journal of the International Society of Cerebral Blood Flow and Metabolism*. United States, 34(6), pp. 989–994. doi: 10.1038/jcbfm.2014.46.

Owen, D. R., Howell, O. W., Tang, S.-P., Wells, L. A., Bennacef, I., Bergstrom, M., Gunn, R. N., Rabiner, E. A., Wilkins, M. R., Reynolds, R., Matthews, P. M. and Parker, C. A. (2010) 'Two binding sites for [3H]PBR28 in human brain: implications for TSPO PET imaging of neuroinflammation', *Journal of Cerebral Blood Flow & Metabolism*, 30(9), pp. 1608–1618. doi: 10.1038/jcbfm.2010.63.

Owen, D. R. and Matthews, P. M. (2011) 'Imaging brain microglial activation using positron emission tomography and translocator protein-specific radioligands', *Int Rev Neurobiol*. 2011/11/05, 101, pp. 19–39. doi: 10.1016/b978-0-12-387718-5.00002-x.

Owen, D. R., Yeo, A. J., Gunn, R. N., Song, K., Wadsworth, G., Lewis, A., Rhodes, C., Pulford, D. J., Bennacef, I., Parker, C. A., StJean, P. L., Cardon, L. R., Mooser, V. E., Matthews, P. M., Rabiner, E. A. and Rubio, J. P. (2012) 'An 18-kDa translocator protein (TSPO) polymorphism explains differences in

binding affinity of the PET radioligand PBR28', *J Cereb Blood Flow Metab*, 32(1), pp. 1–5. doi: 10.1038/jcbfm.2011.147.

Padma Srivastava, M. V, Bhasin, A., Bhatia, R., Garg, A., Gaikwad, S., Prasad, K., Singh, M. B. and Tripathi, M. (2012) 'Efficacy of minocycline in acute ischemic stroke: a single-blinded, placebo-controlled trial', *Neurol India*. 2012/03/13, 60(1), pp. 23–28.

Pappata, S., Levasseur, M., Gunn, R. N., Myers, R., Crouzel, C., Syrota, A., Jones, T., Kreutzberg, G. W. and Banati, R. B. (2000) 'Thalamic microglial activation in ischemic stroke detected in vivo by PET and [11C] PK11195', *Neurology*, 55(7), pp. 1052–1054. Available at: http://www.neurology.org/content/55/7/1052.full.pdf.

Park, E., Gallezot, J.-D., Delgadillo, A., Liu, S., Planeta, B., Lin, S.-F., O'Connor, K. C., Lim, K., Lee, J.-Y., Chastre, A., Chen, M.-K., Seneca, N., Leppert, D., Huang, Y., Carson, R. E. and Pelletier, D. (2015) '11C-PBR28 imaging in multiple sclerosis patients and healthy controls: test-retest reproducibility and focal visualization of active white matter areas', *European Journal of Nuclear Medicine and Molecular Imaging*, 42(7), pp. 1081–1092. doi: 10.1007/s00259-015-3043-4.

Perry, V. H., Cunningham, C. and Holmes, C. (2007) 'Systemic infections and inflammation affect chronic neurodegeneration', *Nat Rev Immunol*. 2007/01/16, 7(2), pp. 161–167. doi: nri2015 [pii]10.1038/nri2015.

Petit-Taboue, M. C., Baron, J. C., Barre, L., Travere, J. M., Speckel, D., Camsonne, R. and MacKenzie, E. T. (1991) 'Brain kinetics and specific binding of [11C]PK 11195 to omega 3 sites in baboons: positron emission tomography study.', *European journal of pharmacology*. NETHERLANDS, 200(2–3), pp. 347–351.

Pierce, J. E., Smith, D. H., Trojanowski, J. Q. and McIntosh, T. K. (1998) 'Enduring cognitive, neurobehavioral and histopathological changes persist for up to one year following severe experimental brain injury in rats', *Neuroscience*. 1998/09/18, 87(2), pp. 359–369. doi: S0306452298001420 [pii].

PK, C., LE, G., Dams-O'Connor, K. and Al, E. (2016) 'Association of traumatic brain injury with late-life neurodegenerative conditions and neuropathologic findings', *JAMA Neurology*, 73(9), pp. 1062–1069. Available at: http://dx.doi.org/10.1001/jamaneurol.2016.1948.

Plane, J. M., Shen, Y., Pleasure, D. E. and Deng, W. (2010) 'Prospects for minocycline neuroprotection', *Arch Neurol*. 2010/08/11, 67(12), pp. 1442–1448. doi: 10.1001/archneurol.2010.191.

Plassman, B. L., Havlik, R. J., Steffens, D. C., Helms, M. J., Newman, T. N., Drosdick, D., Phillips, C., Gau, B. A., Welsh-Bohmer, K. A., Burke, J. R., Guralnik, J. M. and Breitner, J. C. (2000) 'Documented head injury in early adulthood and risk of Alzheimer's disease and other dementias', *Neurology*. 2000/11/09, 55(8), pp. 1158–1166. Available at: http://www.ncbi.nlm.nih.gov/entrez/query.fcgi?cmd=Retrieve&db=PubMed&dopt=Citation&list_uids=11071494.

Plog, B. A., Dashnaw, M. L., Hitomi, E., Peng, W., Liao, Y., Lou, N., Deane, R. and Nedergaard, M. (2015) 'Biomarkers of traumatic injury are transported from brain to blood via the glymphatic system', *The Journal of Neuroscience*. Soc Neuroscience, 35(2), pp. 518–526.

Polymenidou, M. and Cleveland, D. W. (2012) 'Prion-like spread of protein aggregates in neurodegeneration', *The Journal of experimental medicine*. 2012/05/09, 209(5), pp. 889–893. doi: 10.1084/jem.20120741.

Ponsford, J., McLaren, A., Schonberger, M., Burke, R., Rudzki, D., Olver, J. and Ponsford, M. (2011) 'The association between apolipoprotein E and traumatic brain injury severity and functional outcome in a rehabilitation sample', *J Neurotrauma*, 28(9), pp. 1683–1692. doi: 10.1089/neu.2010.1623.

Quigley, H., Colloby, S. J. and O'Brien, J. T. (2011) 'PET imaging of brain amyloid in dementia: a review', *Int J Geriatr Psychiatry*, 26(10), pp. 991–999. doi: 10.1002/gps.2640.

Raj, A., Kuceyeski, A. and Weiner, M. (2012) 'A network diffusion model of disease progression in dementia', *Neuron*. 2012/03/27, 73(6), pp. 1204–1215.

doi: 10.1016/j.neuron.2011.12.040.

Ramlackhansingh, A. F., Brooks, D. J., Greenwood, R. J., Bose, S. K., Turkheimer, F. E., Kinnunen, K. M., Gentleman, S., Heckemann, R. A., Gunanayagam, K., Gelosa, G. and Sharp, D. J. (2011) 'Inflammation after trauma: Microglial activation and traumatic brain injury', *Annals of neurology*, 70(3), pp. 374–383. doi: 10.1002/ana.22455.

Rawji, K. S., Mishra, M. K., Michaels, N. J., Rivest, S., Stys, P. K. and Yong, V. W. (2016) 'Immunosenescence of microglia and macrophages: impact on the ageing central nervous system', *Brain*. Oxford Univ Press, p. awv395.

Reitan, R. (1958) 'The validity of the Trail Making test as an indicator of organic brain damage', *Perceptual and Motor Skills*, 8, pp. 271–276.

Rissanen, E., Tuisku, J., Rokka, J., Paavilainen, T., Parkkola, R., Rinne, J. O. and Airas, L. (2014) 'In vivo detection of diffuse inflammation in secondary progressive multiple sclerosis using PET imaging and the radioligand 11C-PK11195', *Journal of Nuclear Medicine*, 55(6), pp. 939–944. Available at: http://jnm.snmjournals.org/content/55/6/939.full.pdf.

Roberts, G. W., Gentleman, S. M., Lynch, A., Murray, L., Landon, M. and Graham, D. I. (1994) 'Beta amyloid protein deposition in the brain after severe head injury: implications for the pathogenesis of Alzheimer's disease', *J Neurol Neurosurg Psychiatry*. 1994/04/01, 57(4), pp. 419–425.

Roozenbeek, B., Maas, A. I. R. and Menon, D. K. (2013) 'Changing patterns in the epidemiology of traumatic brain injury', *Nat Rev Neurol*. Nature Publishing Group, a division of Macmillan Publishers Limited. All Rights Reserved., 9(4), pp. 231–236. Available at: http://dx.doi.org/10.1038/nrneurol.2013.22.

Ross, D. E. (2011) 'Review of longitudinal studies of MRI brain volumetry in patients with traumatic brain injury', *Brain Injury*. Taylor & Francis, 25(13–14), pp. 1271–1278.

Rowe, C. C., Ellis, K. A., Rimajova, M., Bourgeat, P., Pike, K. E., Jones, G., Fripp, J., Tochon-Danguy, H., Morandeau, L., O'Keefe, G., Price, R., Raniga,

P., Robins, P., Acosta, O., Lenzo, N., Szoeke, C., Salvado, O., Head, R., Martins, R., Masters, C. L., Ames, D. and Villemagne, V. L. (2010) 'Amyloid imaging results from the Australian Imaging, Biomarkers and Lifestyle (AIBL) study of aging', *Neurobiol Aging*. 2010/05/18, 31(8), pp. 1275–1283. doi: 10.1016/j.neurobiolaging.2010.04.007.

Rowe, C. C., Ng, S., Ackermann, U., Gong, S. J., Pike, K., Savage, G., Cowie, T. F., Dickinson, K. L., Maruff, P., Darby, D., Smith, C., Woodward, M., Merory, J., Tochon-Danguy, H., O'Keefe, G., Klunk, W. E., Mathis, C. A., Price, J. C., Masters, C. L. and Villemagne, V. L. (2007) 'Imaging beta-amyloid burden in aging and dementia', *Neurology*. 2007/05/16, 68(20), pp. 1718–1725. doi: 10.1212/01.wnl.0000261919.22630.ea.

Rowe, C. C. and Villemagne, V. L. (2011) 'Brain Amyloid Imaging', *Journal of Nuclear Medicine*, 52(11), pp. 1733–1740. doi: 10.2967/jnumed.110.076315.

Rupprecht, R., Papadopoulos, V., Rammes, G., Baghai, T. C., Fan, J., Akula, N., Groyer, G., Adams, D. and Schumacher, M. (2010) 'Translocator protein (18 kDa) (TSPO) as a therapeutic target for neurological and psychiatric disorders', *Nat Rev Drug Discov*. Nature Publishing Group, a division of Macmillan Publishers Limited. All Rights Reserved., 9(12), pp. 971–988. doi: http://www.nature.com/nrd/journal/v9/n12/suppinfo/nrd3295_S1.html.

Saatman, K. E., Contreras, P. C., Smith, D. H., Raghupathi, R., McDermott, K. L., Fernandez, S. C., Sanderson, K. L., Voddi, M. and McIntosh, T. K. (1997) 'Insulin-like growth factor-1 (IGF-1) improves both neurological motor and cognitive outcome following experimental brain injury', *Exp Neurol*, 147(2), pp. 418–427. Available at: http://www.ncbi.nlm.nih.gov/entrez/query.fcgi?cmd=Retrieve&db=PubMed&dopt=Citation&list_uids=9344566.

Saatman, K. E., Duhaime, A.-C., Bullock, R., Maas, A. I. R., Valadka, A. and Manley, G. T. (2008) 'Classification of traumatic brain injury for targeted therapies', *Journal of neurotrauma*. Mary Ann Liebert, Inc. 140 Huguenot Street, 3rd Floor New Rochelle, NY 10801 USA, 25(7), pp. 719–738.

Sacktor, N., Miyahara, S., Deng, L., Evans, S., Schifitto, G., Cohen, B. A., Paul, R., Robertson, K., Jarocki, B., Scarsi, K., Coombs, R. W., Zink, M. C., Nath, A., Smith, E., Ellis, R. J., Singer, E., Weihe, J., McCarthy, S., Hosey, L. and Clifford, D. B. (2011) 'Minocycline treatment for HIV-associated cognitive impairment: results from a randomized trial', *Neurology*. 2011/09/09, 77(12), pp. 1135–1142. doi: 10.1212/WNL.0b013e31822f0412.

Saivin, S. and Houin, G. (1988) 'Clinical Pharmacokinetics of Doxycycline and Minocycline', *Clinical Pharmacokinetics*. Springer International Publishing, 15(6), pp. 355–366. doi: 10.2165/00003088-198815060-00001.

Sanchez Mejia, R. O., Ona, V. O., Li, M. and Friedlander, R. M. (2001) 'Minocycline reduces traumatic brain injury-mediated caspase-1 activation, tissue damage, and neurological dysfunction', *Neurosurgery*. 2001/06/01, 48(6), pp. 1393–1401. Available at: http://www.ncbi.nlm.nih.gov/entrez/query.fcgi?cmd=Retrieve&db=PubMed&dopt=Citation&list_uids=11383749.

Sandiego, C. M., Gallezot, J.-D., Pittman, B., Nabulsi, N., Lim, K., Lin, S.-F., Matuskey, D., Lee, J.-Y., O'Connor, K. C., Huang, Y., Carson, R. E., Hannestad, J. and Cosgrove, K. P. (2015) 'Imaging robust microglial activation after lipopolysaccharide administration in humans with PET', *Proceedings of the National Academy of Sciences* , 112(40), pp. 12468–12473. doi: 10.1073/pnas.1511003112.

Sapadin, A. N. and Fleischmajer, R. (2006) 'Tetracyclines: nonantibiotic properties and their clinical implications', *J Am Acad Dermatol*. 2006/01/31, 54(2), pp. 258–265. doi: 10.1016/j.jaad.2005.10.004.

Schott, J. M., Price, S. L., Frost, C., Whitwell, J. L., Rossor, M. N. and Fox, N. C. (2005) 'Measuring atrophy in Alzheimer disease: a serial MRI study over 6 and 12 months.', *Neurology*. United States, 65(1), pp. 119–124. doi: 10.1212/01.wnl.0000167542.89697.0f.

Schraen-Maschke, S., Sergeant, N., Dhaenens, C.-M., Bombois, S., Deramecourt, V., Caillet-Boudin, M.-L., Pasquier, F., Maurage, C.-A.,

Sablonniere, B. and Vanmechelen, E. (2008) 'Tau as a biomarker of neurodegenerative diseases'. Future Medicine.

Schwartz, M., Kipnis, J., Rivest, S. and Prat, A. (2013) 'How Do Immune Cells Support and Shape the Brain in Health, Disease, and Aging?', *The Journal of Neuroscience*. Society for Neuroscience, 33(45), pp. 17587–17596. doi: 10.1523/JNEUROSCI.3241-13.2013.

Shahim, P., Tegner, Y., DH, W. and al, et (2014) 'BLood biomarkers for brain injury in concussed professional ice hockey players', *JAMA Neurology*, 71(6), pp. 684–692. Available at: http://dx.doi.org/10.1001/jamaneurol.2014.367.

Sharp, D. J., Beckmann, C. F., Greenwood, R., Kinnunen, K. M., Bonnelle, V., De Boissezon, X., Powell, J. H., Counsell, S. J., Patel, M. C. and Leech, R. (2011) 'Default mode network functional and structural connectivity after traumatic brain injury', *Brain*. 2011/08/16, 134(Pt 8), pp. 2233–2247. doi: 10.1093/brain/awr175.

Sharp, D. J. and Jenkins, P. O. (2015) 'Concussion is confusing us all', *Practical neurology*. BMJ Publishing Group Ltd, 15(3), pp. 172–186.

Sharp, D. J., Scott, G. and Leech, R. (2014) 'Network dysfunction after traumatic brain injury', *Nature Reviews Neurology*, 10(3), pp. 156–166.

Shitaka, Y., Tran, H. T., Bennett, R. E., Sanchez, L., Levy, M. A., Dikranian, K. and Brody, D. L. (2011) 'Repetitive closed-skull traumatic brain injury in mice causes persistent multifocal axonal injury and microglial reactivity', *Journal of Neuropathology and Experimental Neurology*. 2011/06/15, 70(7), pp. 551–567. doi: 10.1097/NEN.0b013e31821f891f.

Sidaros, A., Engberg, A. W., Sidaros, K., Liptrot, M. G., Herning, M., Petersen, P., Paulson, O. B., Jernigan, T. L. and Rostrup, E. (2008) 'Diffusion tensor imaging during recovery from severe traumatic brain injury and relation to clinical outcome: a longitudinal study', *Brain*, 131(Pt 2), pp. 559–572. Available at: http://www.ncbi.nlm.nih.gov/entrez/query.fcgi?cmd=Retrieve&db=PubMed&dopt=Citation&list_uids=18083753.

Sidaros, A., Skimminge, A., Liptrot, M. G., Sidaros, K., Engberg, A. W., Herning, M., Paulson, O. B., Jernigan, T. L. and Rostrup, E. (2009) 'Long-term global and regional brain volume changes following severe traumatic brain injury: a longitudinal study with clinical correlates', *Neuroimage*. Elsevier, 44(1), pp. 1–8.

Siman, R., Toraskar, N., Dang, A., McNeil, E., McGarvey, M., Plaum, J., Maloney, E. and Grady, M. S. (2009) 'A Panel of Neuron-Enriched Proteins as Markers for Traumatic Brain Injury in Humans', *Journal of Neurotrauma*. 140 Huguenot Street, 3rd FloorNew Rochelle, NY 10801USA: Mary Ann Liebert, Inc., 26(11), pp. 1867–1877. doi: 10.1089/neu.2009.0882.

Siopi, E., Cho, A. H., Homsi, S., Croci, N., Plotkine, M., Marchand-Leroux, C. and Jafarian-Tehrani, M. (2011) 'Minocycline restores sAPPalpha levels and reduces the late histopathological consequences of traumatic brain injury in mice', *J Neurotrauma*. 2011/07/21, 28(10), pp. 2135–2143. doi: 10.1089/neu.2010.1738.

Siopi, E., Llufriu-Daben, G., Fanucchi, F., Plotkine, M., Marchand-Leroux, C. and Jafarian-Tehrani, M. (2012) 'Evaluation of late cognitive impairment and anxiety states following traumatic brain injury in mice: the effect of minocycline', *Neurosci Lett*. 2012/02/09, 511(2), pp. 110–115. doi: 10.1016/j.neulet.2012.01.051.

Sjögren, M., Vanderstichele, H., Ågren, H., Zachrisson, O., Edsbagge, M., Wikkelsø, C., Skoog, I., Wallin, A., Wahlund, L.-O., Marcusson, J., Nägga, K., Andreasen, N., Davidsson, P., Vanmechelen, E. and Blennow, K. (2001) 'Tau and Aβ42 in Cerebrospinal Fluid from Healthy Adults 21–93 Years of Age: Establishment of Reference Values', *Clinical Chemistry* , 47(10), pp. 1776–1781. Available at: http://www.clinchem.org/content/47/10/1776.abstract.

Smith, C. (2013) 'Review: The long-term consequences of microglial activation following acute traumatic brain injury', *Neuropathology and Applied Neurobiology*, 39(1), pp. 35–44. doi: 10.1111/nan.12006.

Smith, C., Gentleman, S. M., Leclercq, P. D., Murray, L. S., Griffin, W. S. T.,

Graham, D. I. and Nicoll, J. A. R. (2012) 'The neuroinflammatory response in humans after traumatic brain injury', *Neuropathol Appl Neurobiol*. 2012/12/13. England, 39(6), pp. 654–666. doi: 10.1111/nan.12008.

Smith, D. H., Chen, X. H., Nonaka, M., Trojanowski, J. Q., Lee, V. M., Saatman, K. E., Leoni, M. J., Xu, B. N., Wolf, J. A. and Meaney, D. F. (1999) 'Accumulation of amyloid beta and tau and the formation of neurofilament inclusions following diffuse brain injury in the pig', *J Neuropathol Exp Neurol*. 1999/09/28, 58(9), pp. 982–992.

Smith, D. H., Johnson, V. E. and Stewart, W. (2013) 'Chronic neuropathologies of single and repetitive TBI: substrates of dementia?', *Nat Rev Neurol*. Nature Publishing Group, a division of Macmillan Publishers Limited. All Rights Reserved., 9(4), pp. 211–221. doi: 10.1038/nrneurol.2013.29.

Smith, S. M. (2002) 'Fast robust automated brain extraction', *Hum Brain Mapp*. 2002/10/23, 17(3), pp. 143–155. doi: 10.1002/hbm.10062.

Smith, S. M., Jenkinson, M., Johansen-Berg, H., Rueckert, D., Nichols, T. E., Mackay, C. E., Watkins, K. E., Ciccarelli, O., Cader, M. Z., Matthews, P. M. and Behrens, T. E. (2006) 'Tract-based spatial statistics: voxelwise analysis of multi-subject diffusion data', *NeuroImage*. 2006/04/21, 31(4), pp. 1487–1505. doi: S1053-8119(06)00138-8.

Smith, S. M., Jenkinson, M., Woolrich, M. W., Beckmann, C. F., Behrens, T. E., Johansen-Berg, H., Bannister, P. R., De Luca, M., Drobnjak, I., Flitney, D. E., Niazy, R. K., Saunders, J., Vickers, J., Zhang, Y., De Stefano, N., Brady, J. M. and Matthews, P. M. (2004) 'Advances in functional and structural MR image analysis and implementation as FSL', *NeuroImage*. 2004/10/27, 23 Suppl 1, pp. S208-19. doi: 10.1016/j.neuroimage.2004.07.051.

Smith, S. M. and Nichols, T. E. (2009) 'Threshold-free cluster enhancement: addressing problems of smoothing, threshold dependence and localisation in cluster inference', *Neuroimage*. Elsevier, 44(1), pp. 83–98.

Spangenberg, E. E., Lee, R. J., Najafi, A. R., Rice, R. A., Elmore, M. R. P., Blurton-Jones, M., West, B. L. and Green, K. N. (2016) 'Eliminating microglia

in Alzheimer's mice prevents neuronal loss without modulating amyloid-beta pathology.', *Brain : a journal of neurology*. England, 139(Pt 4), pp. 1265–1281. doi: 10.1093/brain/aww016.

Squarcina, L., Bertoldo, A., Ham, T. E., Heckemann, R. and Sharp, D. J. (2012) 'A robust method for investigating thalamic white matter tracts after traumatic brain injury', *NeuroImage*. 2012/07/21, 63(2), pp. 779–788. doi: 10.1016/j.neuroimage.2012.07.016.

Stein, T. D., Montenigro, P. H., Alvarez, V. E., Xia, W., Crary, J. F., Tripodis, Y., Daneshvar, D. H., Mez, J., Solomon, T., Meng, G., Kubilus, C. A., Cormier, K. A., Meng, S., Babcock, K., Kiernan, P., Murphy, L., Nowinski, C. J., Martin, B., Dixon, D., Stern, R. A., Cantu, R. C., Kowall, N. W. and McKee, A. C. (2015) 'Beta-amyloid deposition in chronic traumatic encephalopathy.', *Acta neuropathologica*. Germany, 130(1), pp. 21–34. doi: 10.1007/s00401-015-1435-y.

Suridjan, I., Pollock, B. G., Verhoeff, N. P. L. G., Voineskos, A. N., Chow, T., Rusjan, P. M., Lobaugh, N. J., Houle, S., Mulsant, B. H. and Mizrahi, R. (2015) 'In-vivo imaging of grey and white matter neuroinflammation in Alzheimer's disease: a positron emission tomography study with a novel radioligand, [18F]-FEPPA.', *Molecular psychiatry*. England, 20(12), pp. 1579–1587. doi: 10.1038/mp.2015.1.

Swerdlow, R. H. (2007) 'Pathogenesis of Alzheimer's disease', *Clin Interv Aging*. 2007/11/30, 2(3), pp. 347–359.

Tambuyzer, B. R., Ponsaerts, P. and Nouwen, E. J. (2009) 'Microglia: gatekeepers of central nervous system immunology', *Journal of Leukocyte Biology*, 85(3), pp. 352–370. doi: 10.1189/jlb.0608385.

Thal, D. R., Rub, U., Orantes, M. and Braak, H. (2002) 'Phases of A beta-deposition in the human brain and its relevance for the development of AD', *Neurology*. 2002/06/27, 58(12), pp. 1791–1800.

Thiel, A., Radlinska, B. A., Paquette, C., Sidel, M., Soucy, J. P., Schirrmacher, R. and Minuk, J. (2010) 'The temporal dynamics of poststroke

neuroinflammation: a longitudinal diffusion tensor imaging-guided PET study with 11C-PK11195 in acute subcortical stroke', *J Nucl Med*. 2010/08/20, 51(9), pp. 1404–1412. doi: jnumed.110.076612.

Thomas, M., Ashizawa, T. and Jankovic, J. (2004) 'Minocycline in Huntington's disease: a pilot study', *Movement Disorders: Official Journal of the Movement Disorder Society*, 19(6), pp. 692–695. doi: 10.1002/mds.20018.

Thornhill, S., Teasdale, G. M., Murray, G. D., McEwen, J., Roy, C. W. and Penny, K. I. (2000) 'Disability in young people and adults one year after head injury: prospective cohort study', *BMJ*, 320(7250), pp. 1631–1635. Available at: http://www.ncbi.nlm.nih.gov/entrez/query.fcgi?cmd=Retrieve&db=PubMed&dopt=Citation&list_uids=10856063.

Tomaiuolo, F., MacDonald, J. D., Caramanos, Z., Posner, G., Chiavaras, M., Evans, A. C. and Petrides, M. (1999) 'Morphology, morphometry and probability mapping of the pars opercularis of the inferior frontal gyrus: an in vivo MRI analysis', *Eur J Neurosci*, 11(9), p. 3033–46. Available at: http://www.ncbi.nlm.nih.gov/htbin-post/Entrez/query?db=m&form=6&dopt=r&uid=10510168.

Tosun, D., Schuff, N., Mathis, C. A., Jagust, W. and Weiner, M. W. (2011) 'Spatial patterns of brain amyloid-beta burden and atrophy rate associations in mild cognitive impairment', *Brain*. 2011/03/25, 134(Pt 4), pp. 1077–1088. doi: 10.1093/brain/awr044.

Tran, H. T., LaFerla, F. M., Holtzman, D. M. and Brody, D. L. (2011) 'Controlled cortical impact traumatic brain injury in 3xTg-AD mice causes acute intra-axonal amyloid-beta accumulation and independently accelerates the development of tau abnormalities', *J Neurosci*. 2011/07/01, 31(26), pp. 9513–9525. doi: 10.1523/jneurosci.0858-11.2011.

Tremblay, M. E., Stevens, B., Sierra, A., Wake, H., Bessis, A., Nimmerjahn, A., Tremblay Me Fau - Stevens, B., Stevens B Fau - Sierra, A., Sierra A Fau - Wake, H., Wake H Fau - Bessis, A., Bessis A Fau - Nimmerjahn, A., Nimmerjahn, A. and Neurosci, J. (2011) 'The role of microglia in the healthy

brain', *J Neurosci*. 2011/11/11, 31(45), pp. 16064–16069. doi: 10.1523/jneurosci.4158-11.2011.

Trivedi, M. A., Ward, M. A., Hess, T. M., Gale, S. D., Dempsey, R. J., Rowley, H. A. and Johnson, S. C. (2007) 'Longitudinal changes in global brain volume between 79 and 409 days after traumatic brain injury: relationship with duration of coma', *Journal of neurotrauma*. Mary Ann Liebert, Inc. 2 Madison Avenue Larchmont, NY 10538 USA, 24(5), pp. 766–771.

Turkheimer, F. E., Edison, P., Pavese, N., Roncaroli, F., Anderson, A. N., Hammers, A., Gerhard, A., Hinz, R., Tai, Y. F. and Brooks, D. J. (2007) 'Reference and target region modeling of [11C]-(R)-PK11195 brain studies', *J Nucl Med*. 2007/01/06, 48(1), pp. 158–167. doi: 48/1/158 [pii].

Turkheimer, F. E., Rizzo, G., Bloomfield, P. S., Howes, O., Zanotti-Fregonara, P., Bertoldo, A. and Veronese, M. (2015) 'The methodology of TSPO imaging with positron emission tomography', *Biochemical Society Transactions*. Portland Press Limited, 43(4), pp. 586–592.

Turner, M. R., Cagnin, A., Turkheimer, F. E., Miller, C. C., Shaw, C. E., Brooks, D. J., Leigh, P. N. and Banati, R. B. (2004) 'Evidence of widespread cerebral microglial activation in amyotrophic lateral sclerosis: an [11C](R)-PK11195 positron emission tomography study', *Neurobiol Dis*. 2004/04/02, 15(3), pp. 601–609. doi: 10.1016/j.nbd.2003.12.012S0969996103002845 [pii].

Turner, R. C., Lucke-Wold, B., Robson, M. J., Omalu, B., Petraglia, A. L. and Bailes, J. E. (2013) 'Repetitive Traumatic Brain Injury and Development of Chronic Traumatic Encephalopathy: A Potential Role for Biomarkers in Diagnosis, Prognosis, and Treatment?', *Frontiers in Neurology*, 3. doi: 10.3389/fneur.2012.00186.

Villain, N., Desgranges, B., Viader, F., De La Sayette, V., Mézenge, F., Landeau, B., Baron, J.-C., Eustache, F. and Chételat, G. (2008) 'Relationships between hippocampal atrophy, white matter disruption, and gray matter hypometabolism in Alzheimer's disease', *The Journal of Neuroscience*. Society for Neuroscience, 28(24), pp. 6174–6181. doi: 10.1523/JNEUROSCI.1392-

08.2008.

Wakana, S., Jiang, H., Nagae-Poetscher, L. M., van Zijl, P. C. and Mori, S. (2004) 'Fiber tract-based atlas of human white matter anatomy', *Radiology*. 2003/12/03, 230(1), pp. 77–87. doi: 10.1148/radiol.2301021640.

Wake, H., Moorhouse, A. J., Miyamoto, A. and Nabekura, J. (2013) 'Microglia: actively surveying and shaping neuronal circuit structure and function', *Trends in Neurosciences*. Elsevier Applied Science Publishing, 36(4), pp. 209–217. Available at: http://linkinghub.elsevier.com/retrieve/pii/S0166223612002044.

Wang, G., Zhang, J., Hu, X., Zhang, L., Mao, L., Jiang, X., Liou, A. K.-F., Leak, R. K., Gao, Y. and Chen, J. (2013) 'Microglia/macrophage polarization dynamics in white matter after traumatic brain injury.', *Journal of cerebral blood flow and metabolism : official journal of the International Society of Cerebral Blood Flow and Metabolism*. United States, 33(12), pp. 1864–1874. doi: 10.1038/jcbfm.2013.146.

Wang, J. Y., Abdi, H., Bakhadirov, K., Diaz-Arrastia, R. and Devous, M. D. (2012) 'A Comprehensive Reliability Assessment of Quantitative Diffusion Tensor Tractography', *NeuroImage*, 60(2), pp. 1127–1138. doi: 10.1016/j.neuroimage.2011.12.062.

Wechsler, D. (1997) *Wechsler Memory Scale- Third Edition: Administration and Scoring Manual*. San Antonio: TX: Psychological Corporation.

Wechsler, D. (1999) *WASI: Wechsler Abbreviated Scale of Intelligence*. San Antonio: TX: The Psychological Corporation.

Wechsler, D. (2001) *Wechsler Test of Adult Reading*. San Antonio: TX: The Psychological Corporation.

Werner, C. and Engelhard, K. (2007) 'Pathophysiology of traumatic brain injury', *British Journal of Anaesthesia*, 99(1), pp. 4–9. doi: 10.1093/bja/aem131.

Whitnall, L., McMillan, T. M., Murray, G. D. and Teasdale, G. M. (2006) 'Disability in young people and adults after head injury: 5-7 year follow up of a prospective cohort study', *JNNP*, 77(5), pp. 640–645. Available at:

http://www.ncbi.nlm.nih.gov/entrez/query.fcgi?cmd=Retrieve&db=PubMed&dopt=Citation&list_uids=16614025.

Wilson, D. H., Rissin, D. M., Kan, C. W., Fournier, D. R., Piech, T., Campbell, T. G., Meyer, R. E., Fishburn, M. W., Cabrera, C., Patel, P. P. and others (2015) 'The Simoa HD-1 Analyzer A Novel Fully Automated Digital Immunoassay Analyzer with Single-Molecule Sensitivity and Multiplexing', *Journal of laboratory automation*. SAGE Publications, p. 2211068215589580.

Wood, R. L. L. and Rutterford, N. A. (2006) 'Demographic and cognitive predictors of long-term psychosocial outcome following traumatic brain injury', *Journal of the International Neuropsychological Society*. Cambridge Univ Press, 12(3), pp. 350–358.

Xiong, Y., Mahmood, A. and Chopp, M. (2013) 'Animal models of traumatic brain injury', *Nat Rev Neurosci*. Nature Publishing Group, a division of Macmillan Publishers Limited. All Rights Reserved., 14(2), pp. 128–142. Available at: http://dx.doi.org/10.1038/nrn3407.

Yong, V. W., Wells, J., Giuliani, F., Casha, S., Power, C. and Metz, L. M. (2004) 'The promise of minocycline in neurology', *The Lancet Neurology*, 3(12), pp. 744–751. doi: 10.1016/s1474-4422(04)00937-8.

Yrjänheikki, J., Keinänen, R., Pellikka, M., Hökfelt, T. and Koistinaho, J. (1998) 'Tetracyclines inhibit microglial activation and are neuroprotective in global brain ischemia', *Proceedings of the National Academy of Sciences*, 95(26), pp. 15769–15774. doi: 10.1073/pnas.95.26.15769.

Zetterberg, H., Smith, D. H. and Blennow, K. (2013) 'Biomarkers of mild traumatic brain injury in cerebrospinal fluid and blood', *Nat Rev Neurol*. Nature Publishing Group, a division of Macmillan Publishers Limited. All Rights Reserved., 9(4), pp. 201–210. doi: 10.1038/nrneurol.2013.9.

Zhang, H., Avants, B. B., Yushkevich, P. A., Woo, J. H., Wang, S., McCluskey, L. F., Elman, L. B., Melhem, E. R. and Gee, J. C. (2007) 'High-Dimensional Spatial Normalization of Diffusion Tensor Images Improves the Detection of White Matter Differences: An Example Study Using Amyotrophic Lateral

Sclerosis', *Medical Imaging, IEEE Transactions on*, pp. 1585–1597. doi: 10.1109/TMI.2007.906784.

Zhang, Y., Metz, L. M., Yong, V. W., Bell, R. B., Yeung, M., Patry, D. G. and Mitchell, J. R. (2008) 'Pilot study of minocycline in relapsing-remitting multiple sclerosis', *The Canadian Journal of Neurological Sciences. Le Journal Canadien Des Sciences Neurologiques*, 35(2), pp. 185–191. Available at: http://www.ncbi.nlm.nih.gov/pubmed/18574932.

Zürcher, N. R., Loggia, M. L., Lawson, R., Chonde, D. B., Izquierdo-Garcia, D., Yasek, J. E., Akeju, O., Catana, C., Rosen, B. R., Cudkowicz, M. E., Hooker, J. M. and Atassi, N. (2015) 'Increased in vivo glial activation in patients with amyotrophic lateral sclerosis: Assessed with [(11)C]-PBR28', *NeuroImage : Clinical*. Elsevier, 7, pp. 409–414. doi: 10.1016/j.nicl.2015.01.009.

# 8. Appendix

## 8.1. Evidence of permissions to reuse material

### Figure 1

**BMJ PUBLISHING GROUP LTD. LICENSE TERMS AND CONDITIONS**

Jun 13, 2016

This Agreement between Gregory Scott ("You") and BMJ Publishing Group Ltd. ("BMJ Publishing Group Ltd.") consists of your license details and the terms and conditions provided by BMJ Publishing Group Ltd. and Copyright Clearance Center.

| | |
|---|---|
| License Number | 3887280549283 |
| License date | Jun 13, 2016 |
| Licensed Content Publisher | BMJ Publishing Group Ltd. |
| Licensed Content Publication | Journal of Neurology, Neurosurgery & Psychiatry |
| Licensed Content Title | Death after head injury: the 13 year outcome of a case control study |
| Licensed Content Author | T M McMillan, G M Teasdale, C J Weir, E Stewart |
| Licensed Content Date | Aug 1, 2011 |
| Licensed Content Volume Number | 82 |
| Licensed Content Issue Number | 8 |
| Volume number | 82 |
| Issue number | 8 |
| Type of Use | Dissertation/Thesis |
| Requestor type | Individual |
| Format | Print and electronic |
| Portion | Figure/table/extract |
| Number of figure/table/extracts | 1 |
| Descriptionof figure/table/extracts | 1 |
| Will you be translating? | No |
| Circulation/distribution | 1 |
| Title of your thesis / dissertation | Exploring Microglial Activation And Neurodegeneration Following Traumatic Brain Injury |
| Expected completion date | Jun 2016 |
| Estimated size(pages) | 150 |
| Requestor Location | Gregory Scott<br>C3NL, Burlington Danes Building<br>Imperial College London<br>Hammersmith Hospital, Du Cane Road<br>London, UK, W120NN<br>United Kingdom<br>Attn: Gregory Scott |

## Figure 2

**NATURE PUBLISHING GROUP LICENSE**
**TERMS AND CONDITIONS**

Jun 13, 2016

This Agreement between Gregory Scott ("You") and Nature Publishing Group ("Nature Publishing Group") consists of your license details and the terms and conditions provided by Nature Publishing Group and Copyright Clearance Center.

| | |
|---|---|
| License Number | 3887280315788 |
| License date | Jun 13, 2016 |
| Licensed Content Publisher | Nature Publishing Group |
| Licensed Content Publication | Nature Neuroscience |
| Licensed Content Title | ATP mediates rapid microglial response to local brain injury in vivo |
| Licensed Content Author | Dimitrios Davalos,Jaime Grutzendler,Guang Yang,Jiyun V Kim,Yi Zuo et al. |
| Licensed Content Date | Jun 1, 2005 |
| Licensed Content Volume Number | 8 |
| Licensed Content Issue Number | 6 |
| Type of Use | reuse in a dissertation / thesis |
| Requestor type | academic/educational |
| Format | print and electronic |
| Portion | figures/tables/illustrations |
| Number of figures/tables/illustrations | 1 |
| High-res required | no |
| Figures | 2 |
| Author of this NPG article | no |
| Your reference number | |
| Title of your thesis / dissertation | Exploring Microglial Activation And Neurodegeneration Following Traumatic Brain Injury |
| Expected completion date | Jun 2016 |
| Estimated size (number of pages) | 150 |
| Requestor Location | Gregory Scott<br>C3NL, Burlington Danes Building<br>Imperial College London<br>Hammersmith Hospital, Du Cane Road<br>London, UK, W120NN<br>United Kingdom<br>Attn: Gregory Scott |
| Billing Type | Invoice |

# Figure 3

**ELSEVIER LICENSE**
**TERMS AND CONDITIONS**

Jun 13, 2016

This Agreement between Gregory Scott ("You") and Elsevier ("Elsevier") consists of your license details and the terms and conditions provided by Elsevier and Copyright Clearance Center.

| | |
|---|---|
| License Number | 3887271434046 |
| License date | Jun 13, 2016 |
| Licensed Content Publisher | Elsevier |
| Licensed Content Publication | Experimental Neurology |
| Licensed Content Title | Time course of cellular pathology after controlled cortical impact injury |
| Licensed Content Author | S Chen,J.D Pickard,N.G Harris |
| Licensed Content Date | July 2003 |
| Licensed Content Volume Number | 182 |
| Licensed Content Issue Number | 1 |
| Licensed Content Pages | 16 |
| Start Page | 87 |
| End Page | 102 |
| Type of Use | reuse in a thesis/dissertation |
| Portion | figures/tables/illustrations |
| Number of figures/tables/illustrations | 1 |
| Format | both print and electronic |
| Are you the author of this Elsevier article? | No |
| Will you be translating? | No |
| Order reference number | |
| Original figure numbers | 2 |
| Title of your thesis/dissertation | Exploring Microglial Activation And Neurodegeneration Following Traumatic Brain Injury |
| Expected completion date | Jun 2016 |
| Estimated size (number of pages) | 150 |
| Elsevier VAT number | GB 494 6272 12 |
| Requestor Location | Gregory Scott<br>C3NL, Burlington Danes Building<br>Imperial College London |

## Figure 4

**OXFORD UNIVERSITY PRESS LICENSE**
**TERMS AND CONDITIONS**

Jun 13, 2016

This Agreement between Gregory Scott ("You") and Oxford University Press ("Oxford University Press") consists of your license details and the terms and conditions provided by Oxford University Press and Copyright Clearance Center.

| | |
|---|---|
| License Number | 3887280716346 |
| License date | Jun 13, 2016 |
| Licensed content publisher | Oxford University Press |
| Licensed content publication | Journal of Neuropathology and Experimental Neurology |
| Licensed content title | Repetitive Closed-Skull Traumatic Brain Injury in Mice Causes Persistent Multifocal Axonal Injury and Microglial Reactivity |
| Licensed content author | Yoshitsugu Shitaka,Hien T. Tran,Rachel E. Bennett,Laura Sanchez,Marilyn A. Levy,Krikor Dikranian,David L. Brody |
| Licensed content date | 2011-07-01 |
| Type of Use | Thesis/Dissertation |
| Institution name | |
| Title of your work | Exploring Microglial Activation And Neurodegeneration Following Traumatic Brain Injury |
| Publisher of your work | n/a |
| Expected publication date | Jun 2016 |
| Permissions cost | 0.00 USD |
| Value added tax | 0.00 USD |
| Total | 0.00 USD |
| Requestor Location | Gregory Scott<br>C3NL, Burlington Danes Building<br>Imperial College London<br>Hammersmith Hospital, Du Cane Road<br>London, UK, W120NN<br>United Kingdom<br>Attn: Gregory Scott |
| Publisher Tax ID | GB125506730 |
| Billing Type | Invoice |
| Billing Address | Gregory Scott<br>C3NL, Burlington Danes Building<br>Imperial College London<br>Hammersmith Hospital, Du Cane Road<br>London, UK, United Kingdom W120NN<br>Attn: Gregory Scott |
| Total | 0.00 USD |
| Terms and Conditions | |

## Figure 5

**OXFORD UNIVERSITY PRESS LICENSE TERMS AND CONDITIONS**

Jun 13, 2016

This Agreement between Gregory Scott ("You") and Oxford University Press ("Oxford University Press") consists of your license details and the terms and conditions provided by Oxford University Press and Copyright Clearance Center.

| | |
|---|---|
| License Number | 3887280818630 |
| License date | Jun 13, 2016 |
| Licensed content publisher | Oxford University Press |
| Licensed content publication | Journal of Neuropathology and Experimental Neurology |
| Licensed content title | Progressive Neurodegeneration After Experimental Brain Trauma: Association With Chronic Microglial Activation |
| Licensed content author | David J. Loane,Alok Kumar,Bogdan A. Stoica,Rainier Cabatbat,Alan I. Faden |
| Licensed content date | 2014-01-01 |
| Type of Use | Thesis/Dissertation |
| Institution name | |
| Title of your work | Exploring Microglial Activation And Neurodegeneration Following Traumatic Brain Injury |
| Publisher of your work | n/a |
| Expected publication date | Jun 2016 |
| Permissions cost | 0.00 USD |
| Value added tax | 0.00 USD |
| Total | 0.00 USD |
| Requestor Location | Gregory Scott<br>C3NL, Burlington Danes Building<br>Imperial College London<br>Hammersmith Hospital, Du Cane Road<br>London, UK, W120NN<br>United Kingdom<br>Attn: Gregory Scott |
| Publisher Tax ID | GB125506730 |
| Billing Type | Invoice |
| Billing Address | Gregory Scott<br>C3NL, Burlington Danes Building<br>Imperial College London<br>Hammersmith Hospital, Du Cane Road<br>London, UK, United Kingdom W120NN<br>Attn: Gregory Scott |
| Total | 0.00 USD |
| Terms and Conditions | |

## Figure 6 & 7

**JOHN WILEY AND SONS LICENSE TERMS AND CONDITIONS**

Jun 13, 2016

This Agreement between Gregory Scott ("You") and John Wiley and Sons ("John Wiley and Sons") consists of your license details and the terms and conditions provided by John Wiley and Sons and Copyright Clearance Center.

| | |
|---|---|
| License Number | 3887281157665 |
| License date | Jun 13, 2016 |
| Licensed Content Publisher | John Wiley and Sons |
| Licensed Content Publication | Neuropathology and Applied Neurobiology |
| Licensed Content Title | The neuroinflammatory response in humans after traumatic brain injury |
| Licensed Content Author | C. Smith,S. M. Gentleman,P. D. Leclercq,L. S. Murray,W. S. T. Griffin,D. I. Graham,J. A. R. Nicoll |
| Licensed Content Date | Sep 9, 2013 |
| Licensed Content Pages | 13 |
| Type of use | Dissertation/Thesis |
| Requestor type | University/Academic |
| Format | Print and electronic |
| Portion | Figure/table |
| Number of figures/tables | 3 |
| Original Wiley figure/table number(s) | Figures 4,5,6 |
| Will you be translating? | No |
| Title of your thesis / dissertation | Exploring Microglial Activation And Neurodegeneration Following Traumatic Brain Injury |
| Expected completion date | Jun 2016 |
| Expected size (number of pages) | 150 |
| Requestor Location | Gregory Scott<br>C3NL, Burlington Danes Building<br>Imperial College London<br>Hammersmith Hospital, Du Cane Road<br>London, UK, W120NN<br>United Kingdom<br>Attn: Gregory Scott |
| Publisher Tax ID | EU826007151 |
| Billing Type | Invoice |
| Billing Address | Gregory Scott<br>C3NL, Burlington Danes Building<br>Imperial College London<br>Hammersmith Hospital, Du Cane Road |

## Figure 8

**NATURE PUBLISHING GROUP LICENSE**
**TERMS AND CONDITIONS**

Jun 13, 2016

This Agreement between Gregory Scott ("You") and Nature Publishing Group ("Nature Publishing Group") consists of your license details and the terms and conditions provided by Nature Publishing Group and Copyright Clearance Center.

| | |
|---|---|
| License Number | 3887280930542 |
| License date | Jun 13, 2016 |
| Licensed Content Publisher | Nature Publishing Group |
| Licensed Content Publication | Nature Reviews Neurology |
| Licensed Content Title | Chronic neuropathologies of single and repetitive TBI: substrates of dementia? |
| Licensed Content Author | Douglas H. Smith, Victoria E. Johnson and William Stewart |
| Licensed Content Date | Apr 1, 2013 |
| Licensed Content Volume Number | 9 |
| Licensed Content Issue Number | 4 |
| Type of Use | reuse in a dissertation / thesis |
| Requestor type | academic/educational |
| Format | print and electronic |
| Portion | figures/tables/illustrations |
| Number of figures/tables/illustrations | 1 |
| High-res required | no |
| Figures | 3 |
| Author of this NPG article | no |
| Your reference number | |
| Title of your thesis / dissertation | Exploring Microglial Activation And Neurodegeneration Following Traumatic Brain Injury |
| Expected completion date | Jun 2016 |
| Estimated size (number of pages) | 150 |
| Requestor Location | Gregory Scott<br>C3NL, Burlington Danes Building<br>Imperial College London<br>Hammersmith Hospital, Du Cane Road<br>London, UK, W120NN<br>United Kingdom<br>Attn: Gregory Scott |
| Billing Type | Invoice |

## Figure 9

**JOHN WILEY AND SONS LICENSE TERMS AND CONDITIONS**

Jun 13, 2016

This Agreement between Gregory Scott ("You") and John Wiley and Sons ("John Wiley and Sons") consists of your license details and the terms and conditions provided by John Wiley and Sons and Copyright Clearance Center.

| | |
|---|---|
| License Number | 3887281415788 |
| License date | Jun 13, 2016 |
| Licensed Content Publisher | John Wiley and Sons |
| Licensed Content Publication | Annals of Neurology |
| Licensed Content Title | Inflammation after trauma: Microglial activation and traumatic brain injury |
| Licensed Content Author | Anil F. Ramlackhansingh,David J. Brooks,Richard J. Greenwood,Subrata K. Bose,Federico E. Turkheimer,Kirsi M. Kinnunen,Steve Gentleman,Rolf A. Heckemann,Karen Gunanayagam,Giorgio Gelosa,David J. Sharp |
| Licensed Content Date | Jun 27, 2011 |
| Licensed Content Pages | 10 |
| Type of use | Dissertation/Thesis |
| Requestor type | University/Academic |
| Format | Print and electronic |
| Portion | Figure/table |
| Number of figures/tables | 1 |
| Original Wiley figure/table number(s) | 3 |
| Will you be translating? | No |
| Title of your thesis / dissertation | Exploring Microglial Activation And Neurodegeneration Following Traumatic Brain Injury |
| Expected completion date | Jun 2016 |
| Expected size (number of pages) | 150 |
| Requestor Location | Gregory Scott<br>C3NL, Burlington Danes Building<br>Imperial College London<br>Hammersmith Hospital, Du Cane Road<br>London, UK, W120NN<br>United Kingdom<br>Attn: Gregory Scott |
| Publisher Tax ID | EU826007151 |
| Billing Type | Invoice |
| Billing Address | Gregory Scott<br>C3NL, Burlington Danes Building |

## Figure 10

**NATURE PUBLISHING GROUP LICENSE TERMS AND CONDITIONS**

Jun 13, 2016

This Agreement between Gregory Scott ("You") and Nature Publishing Group ("Nature Publishing Group") consists of your license details and the terms and conditions provided by Nature Publishing Group and Copyright Clearance Center.

| | |
|---|---|
| License Number | 3887290082725 |
| License date | Jun 13, 2016 |
| Licensed Content Publisher | Nature Publishing Group |
| Licensed Content Publication | Nature Reviews Neuroscience |
| Licensed Content Title | Traumatic brain injury and amyloid-[beta] pathology: a link to Alzheimer's disease? |
| Licensed Content Author | Victoria E. Johnson, William Stewart and Douglas H. Smith |
| Licensed Content Date | May 1, 2010 |
| Licensed Content Volume Number | 11 |
| Licensed Content Issue Number | 5 |
| Type of Use | reuse in a dissertation / thesis |
| Requestor type | academic/educational |
| Format | print and electronic |
| Portion | figures/tables/illustrations |
| Number of figures/tables/illustrations | 1 |
| High-res required | no |
| Figures | 1 |
| Author of this NPG article | no |
| Your reference number | |
| Title of your thesis / dissertation | Exploring Microglial Activation And Neurodegeneration Following Traumatic Brain Injury |
| Expected completion date | Jun 2016 |
| Estimated size (number of pages) | 150 |
| Requestor Location | Gregory Scott<br>C3NL, Burlington Danes Building<br>Imperial College London<br>Hammersmith Hospital, Du Cane Road<br>London, UK, W120NN<br>United Kingdom<br>Attn: Gregory Scott |
| Billing Type | Invoice |

## Chapter 2

Wolters Kluwer

**Title:** Amyloid pathology and axonal injury after brain trauma

**Author:** Gregory Scott, Anil F. Ramlackhansingh, Paul Edison, Peter Hellyer, James Cole, Mattia Veronese, Rob Leech, Richard J. Greenwood, Federico E. Turkheimer, Steve M. Gentleman, Rolf A. Heckemann, Paul M. Matthews, David J. Brooks, David J. Sharp

**Publication:** Neurology

**Publisher:** Wolters Kluwer Health, Inc.

**Date:** Feb 3, 2016

Copyright © 2016, American Academy of Neurology

Logged in as:
Gregory Scott
Account #:
3000735820
LOGOUT

This reuse is free of charge. No permission letter is needed from Wolters Kluwer Health, Lippincott Williams & Wilkins. We require that all authors always include a full acknowledgement. Example: AIDS: 13 November 2013 - Volume 27 - Issue 17 - p 2679-2689. Wolters Kluwer Health Lippincott Williams & Wilkins© No modifications will be permitted.

# Chapter 3

**Jess Ramos Jr <info@biomedcentral.com>** Today at 01:04

To: Gregory Scott

00630925 re:Request to reuse text and figures for PhD thesis

JR

Dear Dr. Scott,

Thank you for contacting BioMed Central.

Reproduction of figures or tables is permitted free of charge and without formal written permission from the publisher or the copyright holder, provided that the figure/table is original, BioMed Central is duly identified as the original publisher, and that proper attribution of authorship and the correct citation details are given as acknowledgement.

If you have any questions please do not hesitate to contact me.

Best wishes,

Neil
Customer Services
info@biomedcentral.com
Phone: +44 (0)203 192 2009
Fax: +44 (0)203 192 2010
www.biomedcentral.com
----------Your Question/Comment ----------

Dear Staff at BioMed Central

I am completing my PhD thesis at Imperial College London, entitled "Exploring Microglial Activation And Neurodegeneration Following Traumatic Brain Injury".

I seek your permission to reprint, in my own thesis the text and figures from the following article, which I was a co-author of:

Scott, G., Hellyer, P.J., Ramlackhansingh, A.F., Brooks, D.J., Matthews, P.M., Sharp, D.J., 2015. Thalamic inflammation after brain trauma is associated with thalamo-cortical white matter damage. Journal of neuroinflammation, 12(1), pp:1-5